Universidade do Minho
Escola de Engenharia

Elizabeth Rosado Balmayor

New applications of particulate materials in tissue engineering strategies: Delivery of bioactive agents and selective cell isolation

Maio de 2009

New applications of particulate materials in tissue engineering strategies: Delivery of bioactive agents and selective cell isolation

Elizabeth Rosado Balmayor

UMinho | 2009

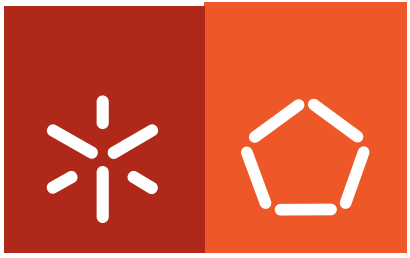

Universidade do Minho
Escola de Engenharia

Elizabeth Rosado Balmayor

New applications of particulate materials in tissue engineering strategies: Delivery of bioactive agents and selective cell isolation

Tese de Doutoramento
Ramo de Ciências e Tecnologia de Materiais
Área de Biomateriais

Trabalho efectuado sob a orientação do
Professor Doutor Rui Luís Gonçalves dos Reis
e da
Doutora Helena Paula de Sousa Sepúlveda Azevedo

Maio de 2009

1. É AUTORIZADA A REPRODUÇÃO PARCIAL DESTA TESE/TRABALHO APENAS PARA EFEITOS DE INVESTIGAÇÃO, MEDIANTE DECLARAÇÃO ESCRITA DO INTERESSADO, QUE A TAL SE COMPROMETE;

Universidade do Minho, ___/___/_____

Assinatura: _____

TO MY PARENTS

“I am among those who think that science has great beauty. A scientist in his laboratory is not only a technician: he is also a child placed before natural phenomena which impress him like a fairy tale”

Marie Curie (1867-1934)

Acknowledgments

Last words to be written… the most difficult for me!. More than three years have passed since I arrived in Portugal to be part of the 3Bs research group as a PhD student. I cannot conclude this relevant stage of my life without expressing my most sincere gratitude to all those people that gave me constant support and encouragement throughout all these years.

I would like to acknowledge my supervisor, Prof. Rui Reis. Opening "this door" for me when doing this phone interview for the Alea Jacta EST position was of huge importance to my career. The opportunities you give me, to perform my research in Europe, to be part of the 3Bs research group, to go for the most important conferences all around the word being able to present my research; always full of confidence in me, was very decisive for my life as a young scientist. I admire your strength of character and perseverance, your capability to overcome any challenge. THANK YOU FOR EVERYTHING! I am also very grateful to you for allowing me the chance of doing this PhD in collaboration with the enthusiastic LBI research group in Vienna. It was a tremendously enriching experience for me.

I will like also to thank to my co-supervisor, Dra. Helena Azevedo. Minha chefinha, all my words of gratitude are just not enough to express my thankfulness to you! I always felt like the most fortunate PhD student at 3Bs, so much support, confidence, and perseverance coming from you. So much knowledge I could acquire from you in each scientific conversation! I always knew that I could count on you for everything. My most sincere thanks to you, Helena, because now I feel that I started with an excellent supervisor and I am finishing with a friend. MUITO OBRIGADA!!!

I would like to thank Prof. Martijn van Griensven for putting so much time, effort, and enthusiasm to the final part of this PhD thesis. For every single correction, even when they were not your papers. Because of teaching me that a good result is always possible! That, even when cells were not reacting to dexamethasone, as we expected …it was interesting, and we needed to understand why!!! ik bewonder je talent, je gave om te werken en je leiderschap in het LBI. Ik bewonder jou als persoon.

I would like to acknowledge the Marie Curie European program for providing me with the PhD scholarship in the Alea Jacta EST project (MEST-CT-2004-008104). The research work described in this thesis was partially supported under the scope of the European network of excellence EXPERTISSUES (NMP3-CT-2004-500283).

I would like to express my most sincere gratitude to Ana Leite and Ricardo Silva, the ALEA JACTA EST "parents". THANK YOU for making possible the existence of all of us: "the *ALEAS"* Your inspiration, help and constant support is something I will keep forever as a valuable experience. Then, I would like to thank my sister and two brothers *ALEAS*, to my Paulinha, to Tom and Wojtek, for helping me to pass through a very hard start; for all friendship, help and support. THANK YOU FOR EVERYTHING!

I would like to dedicate special words to all the colleagues that share with me this trajectory through all my experiments to build up this final result. First of all, to Iva Pashkuleva whose support, scientific advising and endless friendship were constant through all these years and are relevant for many of the achievements described in this thesis. I would like to thank also Kadrus (churrita!) and Erkan, for all their help, support and friendship provided since the very first stage of this research. For the many hours, even weekends, we spend understanding the science behind the nano- and microparticles development. To Xana, for "introducing" me in the amazing world that is a cell culture laboratory. Thank you for all the motivation and availability to help, not only me but all students when we needed you, my most sincere gratitude to you. To MARINA, for all the help with the confocal and for so much friendship and valuable advises. Furthermore, I would like to thank also Paulo Bessa, Paulinho, for all the knowledge and passion transmitted about BMPs. I express thanks to Ana Frias and Mariana, with whom I am enjoying the "ongoing" part of this research. Thank you girls for all help and support. To Roger, the king of the microscopy lab! ☺, Thank you for your valuable help with the fluorescence. To Belinha (big caramelinha!), for a successfully starting of a new project together and for all words of hope and encouragement at this final stage.

Vielen Dank an allen Kollegen in dem LBI, specially to Georg, Daniela and Asmita, Kathi Lang, Sebastian and Gabriel. Special words of thankfulness to Astrid, Tricia and Katrin Reise who made every day easier, nicer and more enjoyable for me. Thank you all for your help and friendship.

Thanks to all my colleagues at 3Bs Research Group. Because each achievement is always the result of help, scientific advises and effort of all colleagues. ALL OF YOU: *THANK YOU!* To the ones that give me a strong support and encouragement in this final moments: especially to Simone (Minha Madrinha!), to Berta, Bruno, and Miguel. Very special thanks to all the 3Bs Guimarães superfamily! (Elisabete (gajona), Sr. Eng. Emanuel and Victor, Muito obrigada!).

My last words are going then to the people that are responsible for making me feel in Portugal at HOME. To my FRIENDS: to Ricardo Pires (coita, your friendship is of inestimable value for me, THANK YOU!), to Iva, Luciano, Paula and Ricardo Silva, to Kadrus Maria, to Ana Aroso (maninha). To my Portuguese FAMILY. To Ana Anselmo and Zé, to Teresa, for always believing in me and providing me with all love and support since the day I arrived in Portugal.

Then to Ivo, whose support, enduring friendship, patience, dedication and valuable advises were essential throughout this journey. Thank you for teaching me that a single problem is not the end of the world. Thank you for making me grow as a person. Obrigada por tanto apoio incondicional, que não é possível descrever com palavras! MUITO OBRIGADA CHIKINHO!

A las personas más importantes en mi vida, a quienes está dedicada esta tesis, a mis padres. No existen palabras de agradecimientos que puedan expresar mis sentimientos hacia los dos. A mi papá por ser el motor impulsor de toda mi formación como profesional. Por ser el más sólido ejemplo que un hijo puede tener. Gracias por ser mi papá. A mi mamá, mi mucarciori, tanto sacrificio por verme llegar hasta aquí! Tanto esfuerzo y desvelo! Tanta dedicación y amor. POR SER UNA MADRE EXCEPCIONAL! Por ser amiga y aliada siempre para mí. A LOS DOS, Valió la pena! Cada logro mío es un logro de ustedes. Los amo profundamente y espero, en este momento, haber logrado que se sientan extremadamente orgullosos de su hijita.

ABSTRACT

During the past few years, researchers working in tissue engineering (TE) have realized that drug delivery is a fundamental part of the TE strategy. Therefore, a large number of technologies have been optimized to guide the potential of drug delivery in those applications. Drug delivery systems (DDS) can be designed to provide controlled release of bioactive molecules to the site of action with minimal side-effects by reducing the exposure of the drug to other tissues. Microparticulate DDS are claimed to have several advantages, such as enhanced bioavailability, possibility for targeting delivery and minimally invasive administration, together with greater efficacy/safety.

This PhD work describes attempts to develop particulate systems with potential application in TE strategies. Microparticles based on natural origin polymers (starch and chitosan and blends thereof) were used. In addition, a synthetic polymer (poly-ε-caprolactone, PCL) was used alone or combined with starch. For the preparation of these particulate systems, emulsion procedures, based on evaporation of solvents or use of crosslinking agents, were optimized. The developed systems were characterized in terms of morphology, physicochemical properties, particle size and size distribution. Their potential as DDS either for antibiotics (gentamicin sulphate, GTM), steroids (Dexamethasone, DEX) or growth factors (bone morphogenetic protein 2, BMP-2) was evaluated with encapsulation efficiencies of 93% for DEX, 67% for GTM and 24% for BMP-2. The release profiles were evaluated in environments mimicking physiological conditions and were characterized by three main phases typical of drug release from biodegradable carriers: i) burst release, ii) period of minimal release, and iii) the release of the remaining active agent while the polymeric matrix is degraded.

The *in vitro* biocompatibility of the developed system was investigated using different cell lines where aspects such as cytotoxicity, cell proliferation and morphology were evaluated. Moreover, the maintenance of the activity/function of all entrapped molecules was investigated. The antibacterial activity of released GTM was assessed by an *in vitro* disc diffusion susceptibility test using Gram positive bacteria (*Staphylococcus aureus*) whereas the bioactivity of DEX and BMP-2 was analyzed by determining their ability to induce osteogenic differentiation of precursor cells. For the tested conditions, all developed microparticles were non-cytotoxic, highly biodegradable and suitable as carriers for sustained delivery purposes.

The ability to isolate living cells is an essential aspect of TE research. Magnetic cell separation methods are among the most efficient methods for cell separation. Therefore, an additional objective of this work was to develop magnetic functionalized particles for cell isolation (e.g.

stem cell subpopulations). Towards this goal, surface functionalized magnetic poly-ε-caprolactone microparticles (m-PCL) were fabricated. 13% of magnetite nanoparticles (core) were effectively entrapped within a poly-ε-caprolactone (shell). Amino and epoxy groups were introduced on the surface of the m-PCL. The m-PCL were characterized for morphology, particle size and size distribution, physicochemical and magnetic properties. Their effectiveness for covalent coupling of protein-like molecules was evaluated by using bovine serum albumin, resulting in coupling efficiency higher than 47% for epoxy and 71% for amino functionalized m-PCL. Additionally, cell viability, proliferation and morphology upon contact with developed microparticles were evaluated. The m-PCL were shown to be non-cytotoxic and their surface functionalization did not show any detrimental influence on cell viability and proliferation.

Overall, the developed microparticulate systems are versatile and very promising to be used in TE strategies.

RESUMO

Durante os últimos anos, tem havido um crescente interesse no desenvolvimento de sistemas de libertação controlada para aplicação em estratégias de engenharia de tecidos (ET) humanos. Os sistemas de libertação controlada podem ser utilizados com a finalidade de melhorar o índice terapêutico de fármacos por alteração da sua distribuição e, consequentemente, aumentar a sua eficácia terapêutica e/ou reduzir a sua toxicidade. Diversas tecnologias têm sido desenvolvidas e optimizadas a fim de direccionar o potencial da libertação controlada em aplicações de ET. Sistemas na forma de micropartículas para libertação de agentes bioactivos apresentam diversas vantagens tais como controlo da sua biodisponibilidade, possiblidade de direccionar a terapia e administração não invasiva.

O presente trabalho de doutoramento pretende avaliar e explorar a potencial de sistemas de micropartículas para libertação controlada de agentes bioactivos em estratégias de ET de osso. Para tal, foram desenvolvidas micropartículas à base de polímeros naturais, nomeadamente misturas de amido e quitosano. Foi também usado o polímero sintético policaprolactona (PCL) isolado ou combinado com amido. As partículas foram produzidas recorrendo a técnicas de emulsão utilizando diferentes agentes reticuladores ou por evaporação de solventes. As propiedades físico-químicas assim como a morfologia e o tamanho das partículas foram avaliados de forma a caracterizar os sistemas desenvolvidos. Como agentes bioactivos foram usados o antibiótico gentamicina (GTM), o corticóide dexametasona (DEX) e o factor de crescimento proteína morfogenética do osso (BMP-2), tendo estes sido incorporados nos sistemas desenvolvidos com eficiências de encapsulamento de 67%, 93% e 24%, respectivamente.

Os perfis de libertação foram estudados de forma a mimetizar condições fisiológicas, tendo-se observado três fases distintas: i) uma fase inicial em que ocorre libertação súbita do agente incorporado, ii) período de libertação mínima e iii) libertação do agente activo remanescente que ocorre com a degradação da matriz polimérica.

A biocompatibilidade dos sistemas desenvolvidos foi testada in vitro usando linhas celulares, sendo avaliados parâmetros como a citotoxicidade, morfologia e proliferação celular. A actividade dos agentes incorporados foi analisada por diferentes métodos. A actividade antibacteriana da gentamicina libertada foi avaliadada pelo método da difusão em agar, que se baseia na determinação dos halos de inibição do crescimento de um dado microorganismo (bactéria Gram positiva Staphylococcus aureus). A actividade osteogénica dos agentes encapsulados DEX e BMP-2 foi analisada através de estudos in vitro com células precursoras,

tendo-se avaliado a sua morfologia, proliferação e viabilidade, bem como a expressão de marcadores da linhagem osteogénica (e.g. ALP, osteocalcina).

Todas as partículas desenvolvidas mostraram ser biodegradáveis e não citotóxicas nas condições testadas. Além disso, apresentam uma libertação controlada do agente incorporado sem comprometer a sua acção, o que as torna adequadas para aplicações em estratégias de ET.

É conhecido que algumas nanopartículas magnéticas apresentam um enorme potencial para diversas aplicações biotecnológicas, nomeadadamente no isolamento de subpopulações de células estaminais/precursoras. Estas partículas podem ser revestidas com um material biocompatível e funcionalizadas com anticorpos específicos para determinado tipo de células. De facto, este trabalho envolveu também o desenvolvimento de partículas magnéticas funcionalizadas para o isolamento de células. Nanopartículas de magnetite foram revestidas com uma solução polimérica de PCL de forma a obter partículas do tipo core-shell. As partículas foram caracterizadas em termos de morfologia, tamanho e distribuição, sendo também avaliadas as suas propriedades fisico-quimicas e magnéticas. Posteriormente foram funcionalizadas com grupos epóxi e amino para ligação de proteínas na superfície. A sua biocompatabilidade foi avaliada em estudos in vitro. As micropartículas magnéticas não apresentaram citoxicidade nem afectaram a viabilidade e proliferação celulares, podendo ser usadas para isolamento de células.

Em geral, pode afirmar-se que os sistemas de micropartículas desenvolvidas neste trabalho são versáteis e apresentam grande potencial para serem aplicadas em estratégias de engenharia de tecidos.

Table of Contents

List of Figures

List of Tables

List of Text Boxes

List of abreviations and nomenclature

Materials and Reagents		**Chapter**
SPCL	Starch-poly-ε-caprolactone	5/6/7
PCL	Poly-ε-caprolactone	5/6/8
ST	Starch	3/4
CHT	Chitosan	3/4
CHT-ST	Starch conjugated chitosan	3/4
DEX	Dexamethasone	5/6/7
GTM	Gentamicin sulfate	3/4
BMP-2	Bone morphogenetic protein 2	7
PVA	Polyvinyl alcohol	5/6/7/8
KBr	Potassium bromide	4/5/6/8
PBS	Phosphate buffered saline solution	3/4/5/6/7/8
DNS	Dinitrosalicylic acid	6
MTS	(3-(4,5-dimethylthiazol-2-yl)-5-(3-carboxymethoxyphenyl)-2-(4-sulfophenyl)-2H-tetrazolium)	4/6/7/8
EtO	Ethylene oxide	4/6/8
DMEM	Dulbecco's Modified Eagle's Medium	4/6/7/8
FBS	Fetal bovine serum	4/6/8
SaOs-2	Human Osteoblast-like cell line	4/6/8
ALP	Alkaline phosphatase	7
C2Cl2	Mouse skeletal myoblast cell line	7
ASCs	Human adipose dserived stem cells	7/8
BMPs	Bone morphogenetic proteins	7
BSA	Bovine serum albumin	7/8
FCS	Fetal calf serum	7
TPP	Sodium Tripolyphosphate	3/4
D	Deuterium	3
DCL	Deuterium chloride	3
HOD, D_2O	Deuterium oxide	3/4
CS	Chitosan-starch microparticles	3
CSG	Gentamicin loaded chitosan-starch microparticles	3
CSGT	Gentamicin loaded chitosan-starch ionically cross linked with TPP	3
GA	Glutaraldehyde	4
pNP	p-Nitrophenol	7
DNS	Dinitrosalicylic acid	4
OM	Osteogenic differentiation culture medium	7
NH_2-m-PCL	Amino functionalized magnetic poly-ε-caprolactone	8
m-PCL	Magnetic poly-ε-caprolactone	8
epoxy-m-PCL	Epoxy functionalized magnetic poly-ε-caprolactone	8
FITC	Fluorescein 5-(6)-isothiocyanate	8
ECH	Epichlorohydrin	8

EDC	*N*-(3-Dimethylaminopropyl)-*N*′-ethylcarbodiimide hydrochloride	8
MES	2-(*N*-morpholino)ethanesulfonic acid	8
DMSO	Dimethyl Sulfoxide	8
FITC-BSA	Bovine serum albumin protein labeled with fluorescein isothiocyanate	8

Methods and Techniques

FTIR	Fourier Transformed Infrared Spectroscopy	4/5/6/8
IR	Infrared	5
UV	Ultraviolet	5/6/8
SEM	Scanning Electron Microscopy	3/4/5/6/7/8
µ-CT	Micro-Computed Tomography	5
XRD	X-Ray Diffraction	5/8
RP-HPLC	Reverse phase high-performance chromatography	5/6
ELISA	Enzyme-linked immunosorbent assay	7
LM	Litgh Transmission Microscopy	3
^{1}H-NMR	Protonic Nuclear Magnetic Resonance	3/4
NMR	Nuclear Magnetic Resonance	3/4
OLT	Optical Light Transmission	8
DLS	Standard sieves meshes and dynamic light scattering	8
TGA	Thermogravimetric análisis	8
VSM	Vibrational Magnetometry	8
XPS	X-Ray Photoelectron Spectroscopy	8
CLSM	Confocal Laser Scanning Microscopy	8

Definitions

TE	Tissue Engineering	5/7
GFs	Grouth Factors	7
p	Statistical level of signbificance	6/7
BMPs	Bone morphogenetic proteins	7
EE	Encapsulation Efficiency	3/5/7
OCN	Osteocalcin	7
O.D.	Optical Density	7/8
Ms	Saturation Magnetization	8
Mr	Remanence Magnetization	8
Hc	Coercive Field	8
Hs	Saturation Field	8
Mr	Relative Saturation Remanence	8
PDI	Polydispersion Index	8
IEP	Isoelectric point	8
Ag	Antigen	8
Ab	Antibody	8

n.d	Not determined	3
n	Difussion Exponent	3
MIC	Minimal Inhibition Concentration	3

Others

v/v	volume-volume	3/5/6
w/w	weight-weight	3/4/5/6
u/L	Enzymatic units per liter	6
EC	Number used for the numerical classification of enzymes e.g. Lipase EC 3.1.1.3	6
MW	Molecular weigth	3/5
s/s	Spherical/smooth	5
r/p	Round/porous	5
HP	Highly/porous	5
HPD	Highly Polydispersity	5
C_i	Initialconcentration of dexamethasone	5
C_r	Concentration of unloaded dexamethasone	5
w/o	Water-in-oil	3

Chapter 1 - Introduction

Drug delivery systems: Limitations, current research and future challenges

1.1 ABSTRACT

During the last few decades, a fair amount of scientific investigations focused on the developing of novel and efficient drug delivery techniques. According to different clinical needs, several specific biopharmaceutical carriers have been proposed. Micro- and nanoparticulated systems, membranes and films, gels and even microelectronic chips have been successfully applied in order to deliver biopharmaceuticals via different anatomical routes. The ultimate goal is to deliver the potential drug to its specific target, where it is needed. Thereby, the bioactive molecule should be protected against environmental degradation and delivery should be achieved in a dose and timely correct manner. Drug delivery systems (DDS) have several advantages, among others they are able to improve the stability, adsorption and therapeutic concentration of the molecules in combination with a long-term and controlled release of the drug. Moreover, the adverse effects related with some drugs can be reduced and thereby patient's compliance could be improved. Currently, an increase on the research efforts and on the generation of novel results regarding DDS is observed. However, most of the developments remain in an investigational state without being successfully transferred to clinical applications. Even though, current research indicates that DDS may have potential advantages in comparison to traditional administration routes in many different applications. In this review, the constraints for successful accreditation of the available DDS in conjunction with their applications in preclinical and clinical investigations will be discussed. Moreover, it is our intention to highlight up-to-date findings in the field of drug delivery research and to envision future developments.

***This chapter is based on the following publication:**

Balmayor, E. R.; Azevedo, H. S.; Reis, R. L. Drug delivery systems: Limitations, current research and future challenges. **2009. Submitted**.

Many different drug delivery systems (DDS) are being developed in distinct institutions. However, and despite significant progress accomplished on pharmaceutical research, the majority of DDS remains on the research stage. This raises the question what are the barriers to bring them from the laboratory bench to approved applied medications? These are two important questions among many that encouraged us to summarize the current limitations, present research and future challenges on the development of DDS.

1.2 DDS: the start

When a drug is administrated to the human body using traditional medication routes, a complex cascade of events is occurring. Depending on the anatomical route, the bioactive molecules are passing through several tissues and organs before reaching the site to perform their therapeutic action. In those organs, drugs can be biodegraded and inactivated due to the highly aggressive environment being either of chemical or biological nature. For instance per os medication encounters digestive enzymes in the upper digestive tract before being exposed to the highly acidic gastric juice [1]. In order to obtain relevant therapeutic levels, high initial concentrations of certain drugs need to be administered.

Nowadays, different and more sophisticated molecules for therapeutic purposes are being developed. In some of those, the traditional administration routes may be problematic. Main typical difficulties encountered are short half-lives within the human body, severe adverse effects, and uncontrollable dosages. DDS can overcome these limitations by means of providing alternative mechanisms to introduce therapeutic agents into the body. The main goals behind the rationale of drug delivery research are represented in Figure 1.1. In addition, some of the well established advantages that offer the use of DDS compared to traditional administration methods of medications are summarized in text box 1.1.

The main goal of DDS at the beginning of development was to *raise the level of bioactive drugs in the blood*. The pioneers' investigations proposed the creation of a matrix or carrier that could control and guide the release of drug molecules. Additionally, this matrix may act as a rate-controlling device to deliver the bioactive drug in a pre-determined pattern, well localized place, and during a desired time period [2]. Therefore, polymers were selected as the most suitable materials. Features like biocompatibility and non-toxicity, hydrophilicity and biodegradability are some of the attractive properties of these materials that allow their selection as carriers for drug delivery [2].

Hydrophilicity and biodegradability are two important properties defining the release mechanism of the contained drug. Hydrophilic matrices release the contained drug by diffusion phenomena due to the swelling of the polymer upon contact with fluids. Similarly for

biodegradable matrices, the rate of degradation in the physiological environment will control the release of the drug. Lately, natural occurring and biodegradable polymers are preferred when selected materials as carriers to conform DDS. They have the important advantages of rapid clearance from the body, being non-toxic, producing degradation products that can easily be metabolized and the absence of surgeries to remove medical devices from the body.

Text box 1.1 Advantages of DDS compared with traditional medication*

- Preservation of the stability and bioactivity of the drugs. Specifically in the case of sensitive drugs with short *in vivo* half-life, the bioactive molecule can be protected from biodegradation and inactivation due to the action of enzymes or environmental conditions (e.g. acidic gastric juice). E.g. proteins and peptides based drugs commonly destroyed after oral intake.
- Improvement of the adsorption and therapeutic concentrations of the medications within the target tissue, organ or diseased part of the body. Hence, allows maintaining bioactive drugs at therapeutically desired range.
- Allows reproducible, controlled and long term administration of the drugs.
- Allows the possibility of deliver drugs at desired place of the body, i.e. site specific treatments and local administration.
- The frequency of drug administration is reduced.
- Harmful/adverse side effects related to systemic administration and over-dosages are eliminated or may be reduced by delivering continuous small amounts of drugs instead of large doses.
- Drug administration may be improved and facilitated in deprived areas where medical supervision may be needed and is not available.
- Improvement of patient compliance and comfort. Patients' negligence in the treatments is avoided since they do not need to remember taking daily doses of long medications routines. Uncomfortable injections and pills can be avoided.
- From an economic perspective, DDS may result in less expensive products, great variability on the market and less waste of drugs. Well established and classical drugs, with expiring patents, can be reformulated with novel administration mechanisms improving their therapeutic action.

*Critically compiled from Refs. [1-4]

The first generation of devices developed as DDS were mainly based on polymeric implants [2, 5, 6]. These implants were extensively used in the field of orthopedics and trauma (mainly bone). However, relative toxicity and inflammation related to these devices, together with the need for repeated surgical interventions for device tests and final removal became were strong disadvantages associated with these implants. Moreover, implants were painful for the patients. Implants used as drug containers bear the difficulty of controling or even stop the drug release without removing the device.

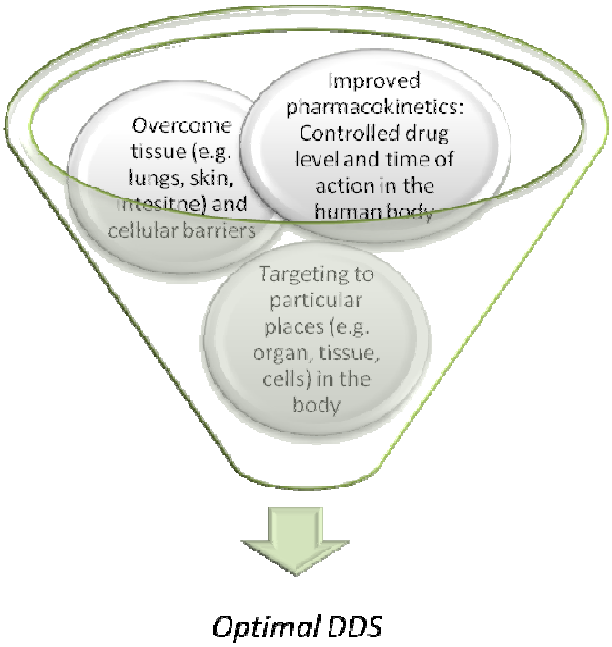

Figure 1.1 Goals in drug delivery (Adapted from Langer and Peppas [7])

Thus, novel devices are being proposed, such as those, where pharmaceutical agents are encapsulated within smart polymers or attached to them [1, 2, 8]. The highest complexity is, however, to move from research to product development, clinical applications, and finally commercial exploitation. This is due to the lack of technological feasibility, reproducibility, control and marketability that characterize most of the proposed DDS at the research level. The idea is to find "the effective formulation" by an optimal combination of a "good" drug and "good" polymeric matrix. This "effective DDS" should have reliable and consistent performance.

Indeed, several new delivery technologies arise each year as result of frontier research. Every part of the body has been studied as potential route of administration. Consequently, transdermal patches [9-12], oral capsules and pills [13-15], injectable gels [16] and drug carrier suspensions [17-19] and novel inhalation systems [19, 20] are among the DDS available to-date with satisfactory results on medical uses. Reviewing their current clinical applications including their advantages and limitations is the objective of this manuscript. In addition, we include our findings and insights on the future challenges that face the development of DDS.

1.3 Transdermal drug delivery

Delivering drugs through the skin is regarded as an alternative to oral delivery or hypodermic injections [9, 10, 12]. The main advantages and drawbacks of transdermal drug

delivery systems are listed in Table 1.1. The fact that by simply removing an external patch applied to the patient's skin immediately stops the administration of the drug highlights the security of this DDS. This advantage, together with their simplicity in use, makes such patches the most available and used DDS nowadays (Table 1.2).

Presently available transdermal patches can be classified into two main categories: reservoir-and-matrix or drug-in-adhesive type [12]. A reservoir system holds the drug in a solution or gel, from which the delivery can be controlled by a rate-controlling film located between the drug reservoir and the skin. By contrast, drug-in-adhesive type combines the drug, adhesive and mechanical backbone of the patch into a simple design. The latter does not involve rate-controlling films or membranes. The skin permeability will control the rate of the drug delivery.

However, the skin normally functions as a barrier to the exterior. This is mainly achieved by the *stratum corneum*, the outermost layer of the epidermis [9, 11, 12]. Nevertheless, possibilities exist to overcome this barrier. Low molecular weight drugs in the range of 100-500 Daltons are one approach to overcome the main limitation of transdermal DDS [9, 12]. However, to limit them only to low molecular weight substances as active compounds, is a drawback for extensive clinical application.

Table 1.1 Advantages and limitations of transdermal DDS*

Advantages	Limitations
• Low dose frequency leading to improved patient safety.	• Thermal drug instability.
• Simple and fast interruption and elimination from the body: By removing the topic patch, the drug delivery can be immediately stopped.	• Chemical reactions of the drug with polymers and excipients.
• Easy accessibility of skin which aids in high patient compliance.	• Difficult to pass the skin natural barrier: stratum corneum
• Easy to administer by the patient him/herself.	
• Induces steady state drug levels in the blood.	
• Avoids gastrointestinal irritation.	
• Avoids first pass effect by liver detoxification step.	
• Ability to achieve sustained release.	

*Critically compiled from Refs. [9-12]

In order to be able to administer higher molecular weight drugs, other ways of circumventing the skin barrier were investigated, e.g. molecular absorption enhancers. These are substances that promote the passage of drugs through the different skin layers [11, 12, 21, 22]. For example, terpene-derived compounds and phenol derivatives seem to improve transdermal absorption [12]. Clinical trials have been performed using this type of substances

such as linalool, alpha terpineneol and carvacrol in order to enhance the absorption of haloperidol [12, 23]. Linalool showed the most satisfactory results by inducing therapeutic levels of haloperidol.

Another possibility of increasing the transport of drugs through the skin is by applying different energy forms [10-12], e.g. an electric field, ultrasound etc. These "active" methods of skin permeation include iontophoresis, which induces a potential difference across the skin [10-12]. Hence, it promotes the transfer of charged ionic drugs or high molecular weight compounds. Current clinical applications include the administration of lidocaine and iontocaine (Phoresor®), local anesthetics [1, 12] and dexamethasone, as well as local anti-inflammatory agents [12]. Besides applying an electric gradient, sonophoresis and electroporation are alternative methods. However, these have been less studied. One final application is the use of low frequency ultrasound that enhanced absorption of mannitol [24].

Table 1.2 Transdermal DDS: current applications and available marketable products*

Applications (Active drug)/Commonly used products
• Menopause symptoms (estradiol)/Esclim®, Vivelle®, Vivelle-Dot®, Climara®
• Smoker's addiction (Nicotine)/Nicoderm CQ®, Nicotrol®
• Chest pain due to heart disease (Nitro-glycerine)/Nitro-Dur®, Nitrodisc®
• Low levels of male sex hormone (Testosterone)/Androderm®
• continuous analgesia (Fentanyl)/Duragesic®, Transdermal System®
• Motion sickness (scopolamine)/Transderm-Scop®
• Contraceptive (ethinyl estradiol-norelgestromin)/Ortho-Evra®

*Critically compiled from Refs. [9-12], and from www.drugs.com

1.3.1 Microfabrication for transdermal drug delivery: microneedles

In addition to the above mentioned chemical and physicochemical procedures, physically disrupting the stratum corneum has been used for improving transdermal drug delivery [2, 9-11, 25]. This technique uses microneedles to create "micro-holes" that allow for transdermal passage of drug molecules [2, 9, 25, 26]. Needles have been fabricated out of silicon, metals and polymeric materials. Moreover, these micro-devices have been coated with different compounds like proteins, DNA or virus particles [2, 10]. Sizes are usually characterized by ranges from sub-micron to millimeter scale [25, 26]. Recently, micron size needles have been used for transdermal drug delivery. These microneedles support delivery of drugs in combination with passive patches through the skin layers (Text box 1.2).

In vitro experiments have shown a remarkable increase in skin permeability for both small (even nanoparticles) and large drug molecules [26, 27]. Animal experiments showed

major increases in transdermal delivery capacity of vaccines, oligonucleotides, insulin, desmopressin and human growth hormone [26, 28-30].

Text box 1.2 Microneedles as transdermal DDS*

Fabrication of small needles in the micron scale offers persuasive possibilities to improve transdermal administration of drugs:

- The outmost layer of the skin can be selectively "pierced" with small needles. The size should be large enough to allow the drug molecules to enter, but small enough to avoid reaching nerve terminations, causing pain or significant damage.
- The *permeability of the skin is increased* (micron-scale pathways can be created into the skin).
- Targeted effect to the stratum corneum layer of the skin.
- Drugs can be delivered into the skin in a *minimal invasive and controlled manner*.
- Greater *device reproducibility and uniformity* due to batch-processing techniques.
- Possibilities of incorporation of different components for *pulsatile release* of drugs in response to physiological requirements.
- Appears to be *safe*, *well tolerated* by patients and allow *rapid skin recovery* post-administration.

*Critically compiled from Refs. [1, 2, 8-11]

Subsequent human trials proved that microneedles are painless, effective and reliable in delivering drugs [31, 32]. Naltrexone, for instance, was transdermally administered to healthy volunteers by using them [33]. Moreover, therapeutic serum concentrations were achieved. Additional transdermal drug delivery systems, based on microneedle technology, in clinical development are the influenza vaccine [34] and osteoporosis treatment [9, 10]. The influenza vaccine has successfully completed a phase III clinical trial. It has currently been submitted for registration in Europe by a collaborative effort of Becton Dickinson and Sanofi-Pasteur [34]. A clinical phase II for the delivery of parathyroid hormone to treat osteoporosis is currently conducted by the company Zosano Pharmaceuticals [9, 10]. During these clinical trials no severe adverse effects have been reported. Furthermore, no infections or bleedings have been diagnosed. Only mild and temporary skin irritations could be observed.

1.4 Oral drug delivery

In addition to the parenteral, transdermal delivery route, the oral route is another preferred method [2, 35-37]. It is non-invasive and constitutes a convenient administration procedure with a good patient compliance. However, there are some limitations related with oral intake of drugs molecules. As eluded above, the destruction or inactivation of drugs, especially proteins and peptides, due to enzymatic degradation and acidity of the

gastrointestinal tract are detrimental for this administration route. Furthermore, the intestinal epithelium may form a barrier, inhibiting the uptake of large molecules [2]. Therefore, DDS may be a solution. Various approaches based on the use of protective coatings, targeted delivery, permeation enhancers, protease inhibitors and bioadhesive agents have been extensively investigated in recent years [2, 38-40]. These methods have shown to increase oral bioavailability of drug molecules.

Nano- and microparticle DDS have been developed for oral administration of agents. Microfabricated devices can be designed with different shapes, sizes and surface morphologies by using a variety of materials [2, 41], maximizing the contact area with the intestinal epithelium. Several additives, like permeation enhancers and enzyme inhibitors, can be added to improve drug uptake and protect them from biodegradation.

Unfortunately, these DDS display side effects, associated with the release kinetics (peaks) of the drugs. Therefore, strategies to improve drug delivery profiles are investigated [3]. Controlled release *osmotic delivery systems*, or push-pull systems, were successfully used to reformulate nifedipine based products [42, 43]. Extended bioavailability leading to an optimized blood pressure control with concomitant reduced side effects was observed. Similarly, oxybutynin chloride and methylphenidate were successfully reformulated [44]. Moreover, this technology allows for the delivery of hydrophobic and low permeability drugs.

In addition to osmotic technology, *multilayer matrices* [45, 46] have been developed with different rates of swelling and biodegradation. This ensures controlling the rate of drug release through dissolution, diffusion and degradation of the matrix. The core of the multilayer matrix contains the drug(s). The additional layers regulate the diffusion of the drug(s) out of the device. This multilayer technology has been used to reformulate several immediate release formulations, such as diltiazem, paroxetine and diclofenac sodium [3].

1.5 Inhalation drug delivery

Inhalative drugs utilize the huge surface area of the lungs to improve absorption. Inhalation represents a comfortable means for drug administration. Devices with dose counter and functional status indicator are already available in the market, especially for the treatment of asthma [4]. However, the efficacy of the traditional oral inhalers could be improved by using chitosan microspheres as nasal DDS for salbutamol administration [47]. Mainly, the controlled release of the drug was prolonged.

Unfortunately, nasal mucosa presents a physical and metabolic barrier for drug permeation. Polar drug molecules and additive compounds have a poor absorption when using the nasal route [2]. To eliminate this limitation, the use of cyclodextrins as molecular carriers

seems to be promising. Chemically defined as cyclic oligosaccharides, cyclodextrins have the possibility of forming highly stable molecular inclusion complexes with a wide range of drug molecules both in solution or solid state [2, 48, 49]. The molecule of interest occupies the cyclodextrin hydrophobic cavity. The hydrophilic exterior allows dissolution in water. Thus, the drug molecules are protected from the environment and the hydrophilicity of the entire system is enhanced (Text box 1.3). Further absorption enhancers such as poly-L-arginine and lipids are also under investigation [1, 49]. Besides salbutamol administration, clinical trials have been conducted for testosterone, insulin, morphine and interferon among others [50-53].

Text box 1.3 Cyclodextrins as molecular carrier for traditional drugs formulations and DDS*

The utilization of cyclodextrins in drug formulations design is based on *I)* enhanced solubility in water of poorly soluble drugs, *II)* stabilization of labile agents against biodegradation, *III)* taste modification by covering with flavors and *IV)* masking unpleasant odors. Particularly for DDS, cyclodextrins can control the release of encapsulated drugs. For example, in inhalation drug delivery formulations, cyclodextrins are able to reduce or minimize the enzymatic activity of nasal mucosa. Also, they can largely improve the permeation of various lipophilic drugs, and the fraction that is not absorbed is easily removed by the nasal mucociliary clearance system. These facts allow their selection to-date as a worldwide used preservation agent for nasal DDS.

*Critically compiled from Refs. [1, 2, 48, 49, 54]

1.6 Injectable drug delivery

Modern technology tries to avoid the use of injections for drug administration. Usually as a result of pain and fear, patients are typically reluctant to use frequent injections. Additionally, drug toxicity related to transiently high plasma concentrations when administrated intravenously, needs to be avoided especially during chronic treatments. For example, some chemotherapeutics, steroids or antibiotics are potent drugs that may evoke severe adverse effects. The toxicity of these drugs limits their dosing and hence their drug efficacy. Therefore, it is desirable to develop systems that have a high efficiency, an accelerated onset in action and being minimally invasive or reduce the number of repeated injections. Injection systems are sometimes inevitable.

The combination of a DDS with a therapeutic implant by means of using an injectable formulation has become increasingly attractive. The possibility of using biodegradable materials (avoid the need of surgical removal after therapeutic function) that can be injected (minimal invasive administration) and composed by drug delivery vehicles (local administration of therapeutic drugs) is a novel means in medical care. Hydrogels comprise an important matrix system for their application in such DDS [54, 55]. Their benefits and limitations while

being components of DDS are summarized in Table 1.3. At the same time, nano- or microcapsules can be added to the injectable implant to provide suitable mechanical properties and control release of antibiotics or anti-inflammatory drugs [54].

Table 1.3 Hydrogels: Benefits and limitations for their application in drug delivery*

Hydrogels: three dimensional, cross-linked networks of water soluble polymers, with particular interest as DDS due to their unique physical properties: highly porous and hydrophilic structure.	
Benefits	Limitations
• Optimal pharmacokinetics: drugs can elute slowly maintaining high local concentration in the surrounding tissues for an extended period. • Highly biocompatible, promoted by high water content and their physicochemical similarity to native extracellular matrix. • Biodegradability and/or matrix dissolution via enzymatic, hydrolytic and environmental means. • Smart matrices responding to physiological stimuli. • Relatively deformable, adjusting to the shape of the surface to which they are applied. • Can be designed with muco/bioadhesive properties.	• Low tensile strength. • Limited quantity and homogeneity of the drug loaded. • Rapid drug release (High water content and porosity). • Some hydrogels may need surgical implantation and are not injectable.

*Critically compiled from Refs. [54-56]

1.7 Nanoparticles suspension as DDS

Currently, nanoparticle suspensions are used as DDS for a variety of administration routes as it has partially been outlined above. A common advantage is *their small size and particulated shapes*, which increases the surface area and thereby enhances the dissolution rate and bioavailability [57].

When used as components of *oral* formulations, nanosuspensions can overcome the main limitation of bioavailability described for the oral administration route. By means of decreasing size and increasing the surface area leads to enhancement of the concentration of the released drug. Furthermore, mucosa-adhesion is also improved, which can accelerate the gastrointestinal transit [57-59]. As a result, bioavailability of the medication is improved. Animal studies indicated that an improved pharmacokinetic profile (optimal drug concentration in plasma for a prolonged time period) and bioavailability was obtained by the nanoparticulated formulation of danazol suspension [59]. Additionally, nanoparticulated systems can reduce the gastric irritation associated with oral intake. Experiments in rats showed that by reducing naproxen particle size from micro- to nanometers scale resulted in faster absorption, decreased gastric residence time and produced local high and prolonged concentrations of the drug [60].

Injectable nano-formulations provide the possibility of administering hydrophobic drugs without using solvents, additives or other additional compounds. Generally, the use of nanosuspensions as injectable solutions can reduce the toxicity and adverse effects usually related with the high concentration of drugs administrated by this route [57].

As the main component of *inhalation* DDS, nanoparticles not only improve bioavailability and drug adsorption, but are also beneficial with respect to homogeneity. Moreover, a significant higher fraction can be administrated in each dose, lowering the need for systemic uptake. Clinical trials with budesonide nanoparticulated suspension indicated a two-fold drug concentration in plasma for longer periods of time and increased drug absorption, compared with the traditional inhalation product [61].

Nanosuspensions were initially developed to solve limitations related with poor drug solubility. To-date, they have been proven to be very efficient to optimize pharamacokinetics, drug bioavailability, safety and efficacy in all types of DDS and for different administration routes [57, 59]. Additionally, the protection of sensitive drugs molecules can be achieved by the combination of this technology and specific materials, resulting in the fabrication of nanosized devices for drug encapsulation [1, 2, 8]. Thus, this technology may be beneficial for the delivery of proteins, growth factors and peptides [3, 55, 62]. Moreover, this technology may be used in the future for cell encapsulation or targeting and gene delivery [1].

1.8 Novel findings and challenges facing DDS

Nowadays, numerous medical equipments, rehabilitation techniques, drugs and minimal invasive chirurgical procedures have been constantly improved for the most diverse injuries. However, due to the limited capacity of some tissues to regenerate, the treatment of complicated and comminuted injuries is difficult and may fail. To generate new possibilities for tissue repair and regeneration, DDS can assist new emerging technologies (e.g. tissue engineering [55, 63]) based on the delivery of therapeutic proteins and peptides. Additionally, highly complex and sensitive proteins, like growth factors display a specific therapeutic action within narrow borders. This creates the need for DDS to provide more sophisticated and efficient devices. The efficient delivery of those therapeutic molecules to the injured site is necessary. Thereby, a high bioavailability and controlled release is of eminent importance.

1.8.1 Growth factor delivery

Nowadays, numerous growth factors have been identified and produced using recombinant technology [64]. Growth factors are naturally occurring proteins capable of stimulating cellular proliferation, migration and/or differentiation into a specialized phenotype

(e.g. osteoblast for bone or chondrocytes for cartilage regeneration). Thus, being involved in the regulation of several cellular functions, they can enhance the healing and regeneration process of diverse tissues [62, 65].

Traditional delivery strategies of growth factors have clear limitations. Therefore, only a limited number of those proteins have been approved and commercialized for therapeutic purposes. The lack of protection against biodegradation and the subsequent low local bioavailability are some of the disadvantages related with the delivery of growth factors by the traditional means. To overcome these limitations, several technologies have been explored for the better control of growth factors release. These technologies vary in their use of nano- and microfabricated systems in the form of fibers, capsules and particles, three dimensional porous scaffolds and injectable gels. All of them based on the use of biomaterials as the main component of their matrices. Fibrin hydrogel releasing IGF-I, for example, has been investigated to repair articular cartilage defects in an animal model [66]. Similarly, an alginate hydrogel carrying VEGF has been applied for treating ischemic disease in mice [67]. Moreover, in the same model, a mixture of VEGF and PDGF loaded in a polymeric scaffold was investigated [68]. Nano- and microparticles made of poly(glycolic) and poly(lactic) acid [69], silk fibroin [70], and gelatin [71, 72] have also been extensively investigated for the loading and release of growth factors in different applications.

Polymers as DDS for growth factors achieve a localized and controlled release to yield a desirable concentration over a period of time. The release profile can be optimized to the desired clinical application by tailoring either the properties of the polymeric matrix or the features of the developed device during their processing (e.g. vehicle size, porosity and pore size and distribution, crosslinking, and degradation rate) [73].

Biomaterials have proven to be highly useful in delivering growth factors in a controllable manner and by providing protection against non-friendly environments maintaining the bioactivity of those molecules. In the past few years, novel and sophisticated technologies have been developed besides the use of polymeric matrices creating new possibilities for the delivery of growth factors. Cell and gene therapy are further examples of application of these technologies. These investigations will lead to a future development where growth factors will be delivered/expressed/produced at the site of interest and only at the levels and time at which they are required.

1.8.2 Cell encapsulation

As stated above, there are still limitations to currently available DDS. Moreover, it is difficult to deliver peptides and proteins such as growth factors. Therefore, the need exist to

find alternative approaches for drug delivery. Cells can be considered as "biological factories". They can continuously produce and release therapeutic agents. Delivery can be performed by cell encapsulation or immobilization within a semipermeable membrane [74]. This ensures protection against the immune system and diminishes mechanical stress. The membrane should allow diffusion of nutrients and oxygen towards the cells and waste products as well as the therapeutic agent in the opposite direction (Figure 1.2).

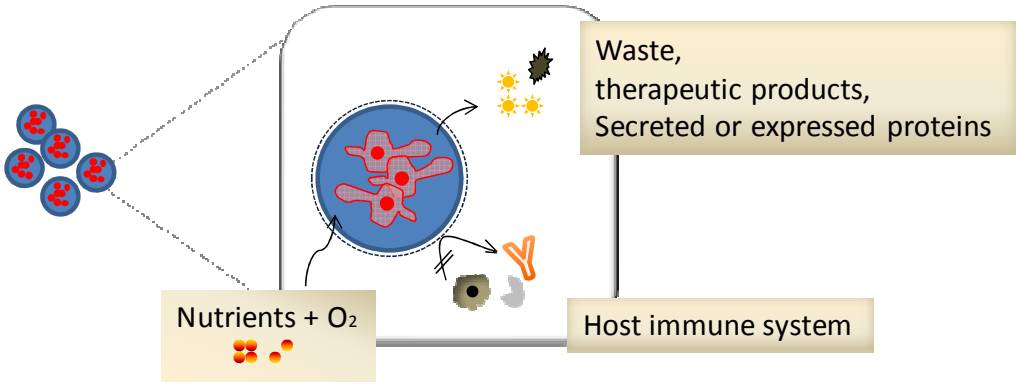

Figure 1.2 Function of the semipermeable membrane in cell encapsulation technology (Adapted from Orive, G. et al. [74])

Advantages of cell encapsulation technology as DDS are [74-77]: *I*) no need for immunosuppression, *II*) fully biocompatible materials are used for the capsules that do not interfere with cellular function or exert toxicity. The capsules can be tailored to obtain the optimal properties for cell encapsulation such as permeability of the membrane, *III*) therapeutic products can be released in a sustained and controlled way for continuously long time periods, *IV*) bioactivity of the therapeutic agent is guaranteed since they are produced by the cells, *V*) cells can easily be genetically modified to express any desired protein for therapy, *VI*) safety. When the capsule degrades, the foreign cells will be eliminated immediately by the immune system. VII) Finally, the common toxicity due to the high drug concentrations is not present.

Capsules have small sizes and can therefore be easily administrated into the blood circulation. Furthermore, the ratio between capsule surface and volume is improved in comparison to other devices geometries allowing transfer of oxygen and nutrients into the capsules ensuring high cell viability [78]. Capsules can be easily produced due to established processing methods (e.g. emulsions, ionic complexations, spray drying, etc). Additionally, so called core-shell capsules entrap cells inside a free empty core surrounded by a semipermeable shell. Usually, the diffusion is controlled by size-exclusion phenomena and

diffusion rate. Therefore, the material that composes this semipermeable shell is of eminent importance. The optimum size for these devices is 100-500 μm [77].

Several biomaterials can be used for cell encapsulation. They are biocompatible and do not interfere with cellular function. Alginate seems to be the most studied for cell encapsulation. It shows biocompatibility and biodegradability, although some immune reactions may occur. Alginate creates three dimensional structures by the formation of interchain bridges upon reaction with multivalent ions. Thereby, it forms a gel-like structure.

A wide range of *cell types* and sources have been used for encapsulation such as genetically modified cells expressing desired proteins, therapeutic stem cells or disease specific cell types (table 1.4). For the latter, pancreatic islets cells have been encapsulated to treat diabetes in both animal studies [79, 80] and pilot clinical trials [81, 82].

Table 1.4 Cells encapsulation systems recently employed*

Factors to consider for a suitable cells: I) allogenic vs. xenogenic source, II) controlled proliferation once encapsulated, III) possibility for genetic modification.	
Developed systems	Application
Alginate-Kidney cells	Hemophilia, neurotrophic factors
-Parathyroid cells	Artificial organs
-chondrocytes	Bone-cartilage regeneration
-Leydig cells	Hormone replacement
-Adrenal chromatin cells	e.g. Parkinson´s disease
-Stem cells	e.g. bone regeneration
-Myeloma cells	Hepatic growth factor release
Alginate/HEMA-MMA-Fibroblast	Epilepsy, metabolic deficiencies
-Myoblast	Cancer, metabolic deficiencies
-Ovary cells	Fabry disease
-Hepatocytes	Liver related diseases and transplantation
-PC12 pheochromocytoma cells	Neurotrophic and neurotransmitters factors
Alginate/Chitosan-Tumor cells	Cancer vaccine, interleukins
Chitosan-Fibroblast	*In vitro* study: tissue engineering
-Chondrocytes	
Collagen-Myoblast	*In vitro* study
Hyaluronic acid-Chondrocytes	*In vitro* study: cartilage formation
Dextran/RGD-Human embryonic stem cells	*In vitro* study: vascular differentiation
Agarose-Murine embryonic stem cells and kidney cells	*In vitro* study: tissue engineering
Agarose/Gelatin-Feline kidney cells	*In vitro* study: Increase in metabolic activity

*Critically compiled from Refs. [74-77, 83-89]

Another example are choroid plexus cells, that encapsulated in an alginate based system released neurotrophic factors to the brain in a primate model to prevent degeneration of neurons in Huntington´s disease [90]. Entrapped bone marrow stromal cells in poly lactic glycolic acid capsules enhanced bone regeneration in an animal model [91].

1.8.3 Gene therapy

Gene therapy is another example of a new emerging technology that facilitates the delivery of growth factors, as high and sustained levels of growth factors at the site of injured cannot be achieved by administration as a protein. The most suitable approach to accomplish satisfactory results is to combine this novel and emerging technology with the well established achievements from the drug delivery and tissue engineering field.

The gene encoding the desired growth factor can be transferred into a cell by the use of viral or non-viral vectors (figure 1.3). The transfected cell subsequently secretes the desired protein (Figure 1.3 A). In addition, the transfected cell can differentiate into a desired phenotype (osteoblast for bone or chondrocyte for cartilage regeneration) (Figure 1.3 B).

Local gene delivery can be achieved by either *in vivo* or *ex vivo* approaches [92-95]. Basically, the *in vivo* approach [93] simply directly administers the vector into the injured tissue. However, serious safety concerns exist for this approach due to lack of control of the virus. On the other hand, the *ex vivo* strategy [92] provides more control over each step. This strategy is based on the *in vitro* genetic modification of cells, where the growth and transfection can be carefully controlled. Of note, the cells can be harvested in an autologous way. Finally, the modified cells can be re-injected or transplanted into site of injury. Numerous advantages are claimed [92-95] for the *ex vivo* strategy: *I)* the patient's cells can be cryopreserved at any stage of the process to be used in subsequent therapies, *II)* the concentration of the expressed protein can be controlled by controlling the amount of vector during transfection, thereby diminishing systemic adverse effects or toxicity.

Several studies on the use of gene therapy have been reported recently. Studies on gene therapy of urological dysfunction [92], bone and cartilage injuries [93-97] and cardiovascular dysfunction [98] have been reported (Huard et al.). An adenovirus expressing BMP-2 has been used to induce bone formation [99]. A polyhedron promoter of baculovirus encoding BMP-2 loaded onto collagen sponges induced ectopic bone formation in rats after 4 weeks (Hosseinkhani et al.) [100]. Inducible nitric oxide synthase adenovirus transduced cells were more effective to treat erectile dysfunction when injected to the corpus cavernosum of adult rats in comparison with plasmid or adenoviral solutions [101].

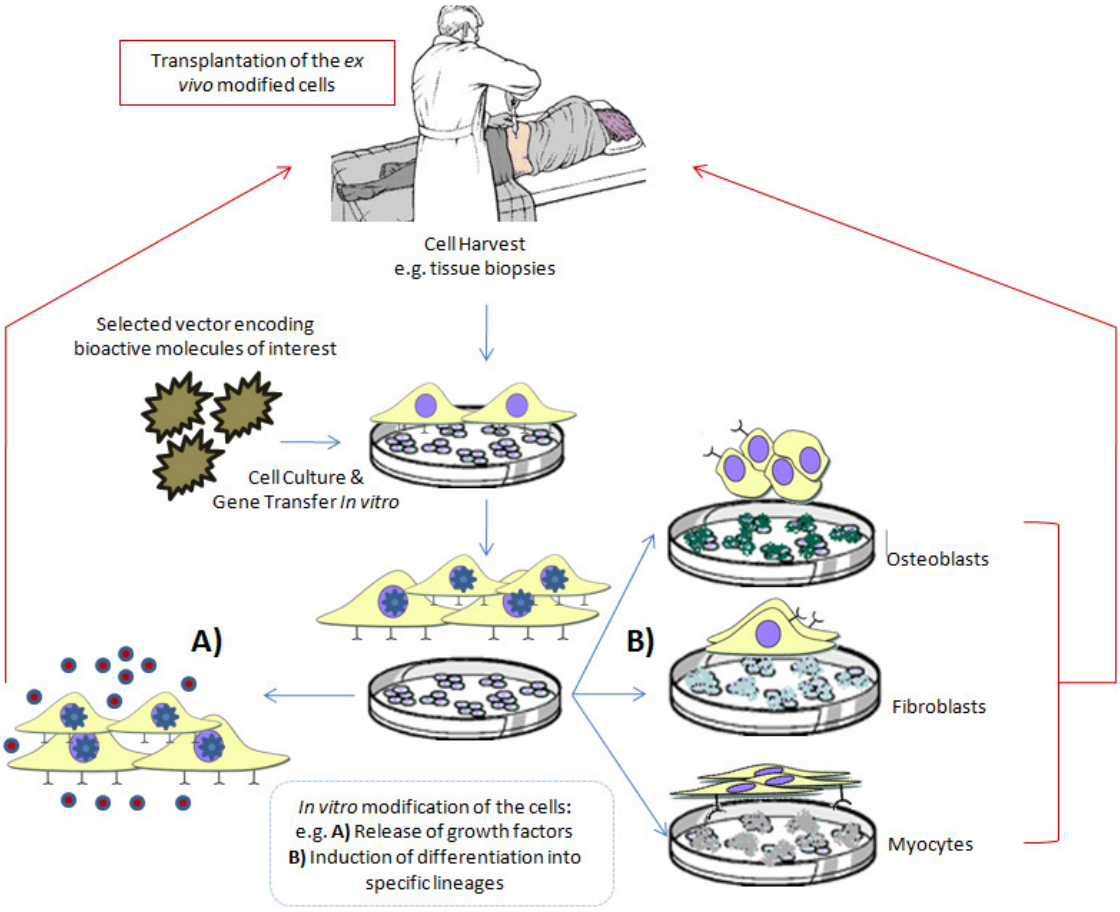

Figure 1.3 Representation of an autologous *ex vivo* gene therapy. The cells are isolated, grown and transfected *in vitro* in a controllable fashion before re-administration into the injured site. Two examples are represented, the transfected cells can sustained release therapeutic entities **A)** and can be induced to differentiated into different phenotypes for tissue regeneration **B)**

Despite the fact that a significant portion of gene-therapy research is conducted for bone and cartilage regeneration, only few have been tested in clinical trials for human joint diseases. Viruses such as retrovirus, adenovirus and lentivirus, are still the preferred vectors due to their potential efficiency [93, 95, 102]. However, they have safety concerns related to their intrinsic cytotoxicity, immunogenicity and possible mutagenesis that prevent them from being transferred to clinical applications Therefore, numerous efforts are still required in order to increase the transfection efficiency of non-viral vectors.

1.9 CONCLUDING REMARKS: envisioning the future of DDS

As stated before, the main aim of DDS at the beginning was to *raise the serum level of therapeutic agents*. This evolved *to locally deliver cells, anticancer drugs, growth factors and therapeutic genes*. DDS has become, therefore, a powerful tool in health care.

Transdermal DDS are currently the most employed products. Drug delivery devices for the transdermal route have passed successfully through *in vitro*, *in vivo* and human studies. They show a combination of safety and efficacy in use. Indeed, the skin seems to remain an excellent route for DDS. These DDS are even under constant improvement today, as it can be observed by developed microneedles. DDS for oral, inhalation, injection will need additional efforts to increase reproducibility, control of drug concentrations and release profiles. The possibility of overcoming their limitations and successfully enter human clinical trials seems to be close to reality.

New challenges for the future, besides the improvement of known DDS, are the delivery of therapeutic entities using "biological devices". E.g. cells are recognized as a source for potential delivery of therapeutics. Cell and gene therapy concepts are already introduced into the clinical arena. Although they are not yet established as approved therapeutic techniques, remarkable results have been obtained, mainly in the field of bone and cartilage regeneration. At the experimental level many studies have been reported with success to prove the feasibility of these therapies for tissue healing. A fair amount of research is still needed to successfully transfer cell and gene based technologies to the medical practice. The unavailability of safe vectors carrying therapeutic genes appears to be the main obstacle in these technologies. Therefore, in our opinion, the optimization of the use of non-viral vectors is of major importance in the future of cell and gene related therapies.

1.10 ACKNOWLEDGEMENTS

E. R. Balmayor thanks the Marie Curie Host Fellowships for Early Stage Research Training (EST) "Alea Jacta EST" (MEST-CT-2004-008104) for providing her with a PhD Fellowship. This work was partially supported by the European NoE EXPERTISSUES (NMP3-CT-2004-500283).

1.11 REFERENCES

1. Orive, G.; Hernández, R. M.; Gascón, A. R.; Domínguez-Gil, A.; Pedraz, J. L. *Current Opinion in Biotechnology* **2003**, 14 (6): 659-664.
2. Paolino, D.; Fresta, M.; Sinha, P.; Ferrari, M. In *Encyclopedia of Medical Devices and Instrumentation*, 2nd ed.; Webster, J. G., Ed. John Wiley & Sons, Inc.: New York, **2006**; pp 437-495.
3. Rosen, H.; Abribat, T. *Nature Reviews Drug Discovery* **2005**, 4: 381-385.
4. Jain, K. K. *Trends in Pharmacological Sciences* **1998**, 19 (5): 155-157.
5. Ranade, W. *The Journal of Clinical Pharmacology* **1990**, 30: 871-889.
6. Nitsch, M. J.; Banakar, U. V. *Journal of Biomaterials Applications* **1994**, 8 (3): 247-284.
7. Langer, R.; Peppas, N. A. *AIChE Journal* **2003**, 49 (12): 2990-3006.

8. Orive, G.; Gascon, A. R.; Hernandez, R. M.; Dominguez-Gil, A.; Pedraz, J. L. *Trends in Pharmacological Sciences* **2004**, 25 (7): 382-387.
9. Arora, A.; Prausnitz, M. R.; Mitragotri, S. *International Journal of Pharmaceutics* **2008**, 364 (2): 227-236.
10. Prausnitz, M. R.; Langer, R. *Nature Biotechnology* **2008**, 26 (11): 1261-1268.
11. Prausnitz, M. R.; Mitragotri, S.; Langer, R. *Nature Reviews Drug Discovery* **2004**, 3 (2): 115-124.
12. Scheindlin, S. *Molecular Interventions* **2004**, 4 (6): 308-312.
13. Vilivalam, V. D.; Illum, L.; Iqbal, K. *Pharmaceutical Science & Technology Today* **2000**, 3 (2): 64-69.
14. Majuru, S. *Drug Delivery Technology* **2004**, 4 (8): 9-14.
15. Hosny, E. A.; Al-Shora, H. I.; Elmazar, M. M. *International Journal of Pharmaceutics* **2002**, 237 (1-2): 71-76.
16. Rosenblatt, J. S.; Berg, R. A. Collagen-based injectable drug delivery system and its use. US Patent Specification 5807581, **1998**.
17. Bernstein, G. *Expert Opinion on Drug Delivery* **2008**, 5 (9): 1047-1055.
18. Rogueda, P. *Expert Opinion on Drug Delivery* **2005**, 2 (4): 625-638.
19. Yang, J. Z.; Young, A. L.; Chiang, P.-C.; Thurston, A.; Pretzer, D. K. *Journal of Pharmaceutical Sciences* **2008**, 97 (11): 4869-4878.
20. Engstrom, J. D.; Tam, J. M.; Miller, M. A.; Williams, R. O.; Johnston, K. P. *Pharmaceutical Research* **2008**, 26 (1): 101-117.
21. Williams, A. C.; Barry, B. W. *Advanced Drug Delivery Reviews* **2004**, 56 (5): 603-618.
22. Smith, E. W.; Maibach, H. I. In *Percutaneous Penetration Enhancers*, 2nd ed.; Smith, E. W.; Maibach, H. I., Eds. CRC Press. Taylor & Francis Group: Boca Raton, FL, **2006**; pp 4-14.
23. Vaddi, H. K.; Ho, P. C.; Chan, S. Y. *Journal of Pharmaceutical Sciences* **2002**, 91 (7): 1639-1651.
24. Tang, H.; Blankschtein, D.; Langer, R. *Journal of Pharmaceutical Sciences* **2002**, 91 (8): 1776-1794.
25. McAllister, D. V.; Allen, M. G.; Prausnitz, M. R. *Annual Review of Biomedical Engineering* **2000**, 2: 289-313.
26. McAllister, D. V.; Wang, P. M.; Davis, S. P.; Park, J. H.; Canatella, P. J.; Allen, M. G.; Prausnitz, M. R. *Proceedings of the National Academy of Sciences of the United States of America* **2003**, 100 (24): 13755-60.
27. Henry, S.; McAllister, D. V.; Allen, M. G.; Prausnitz, M. R. *Journal of Pharmaceutical Sciences* **1998**, 87 (8): 922-925.
28. Lin, W.; Cormier, M.; Samiee, A.; Griffin, A.; Johnson, B.; Teng, C. L.; Hardee, G. E.; Daddona, P. E. *Pharmaceutical Research* **2001**, 18 (12): 1789-93.
29. Martanto, W.; Davis, S. P.; Holiday, N. R.; Wang, J.; Gill, H. S.; Prausnitz, M. R. *Pharmaceutical Research* **2004**, 21 (6): 947-52.
30. Cormier, M.; Daddona, P. E. In *Modified-Release Drug Delivery Technology*, Rathbone, M. J.; Hadgraft, J.; Roberts, M. S., Eds. Marcel Dekker, Inc.: New York, **2003**; pp 589-598.
31. Kaushik, S.; Hord, A. H.; Denson, D. D.; McAllister, D. V.; Smitra, S.; Allen, M. G.; Prausnitz, M. R. *Anesthesia and Analgesia* **2001**, 92 (2): 502-4.
32. Laurent, P. E.; Bonnet, S.; Alchas, P.; Regolini, P.; Mikszta, J. A.; Pettis, R.; Harvey, N. G. *Vaccine* **2007**, 25 (52): 8833-42.
33. Wermeling, D. P.; Banks, S. L.; Hudson, D. A.; Gill, H. S.; Gupta, J.; Prausnitz, M. R.; Stinchcomb, A. L. *Proceedings of the National Academy of Sciences of the United States of America* **2008**, 105 (6): 2058-63.
34. Dean, C. H.; Alarcon, J. B.; Waterston, A. M.; Draper, K.; Early, R.; Guirakhoo, F.; Monath, T. P.; Mikszta, J. A. *Human Vaccines* **2005**, 1 (3): 106-11.
35. Mutwiri, G.; Bowersock, T. L.; Babiuk, L. A. *Expert Opinion on Drug Delivery* **2005**, 2 (5): 791-806.

36. Lavelle, E. C.; O'Hagan, D. T. *Expert Opinion on Drug Delivery* **2006**, 3 (6): 747-762.
37. Maroni, A.; Zema, L.; Cerea, M.; Sangalli, M. E. *Expert Opinion on Drug Delivery* **2005**, 2 (5): 855-871.
38. Rhodes, C. T.; Porter, S. C. *Drug Development and Industrial Pharmacy* **1998**, 24 (12): 1139-1154.
39. Lambkin, I.; Pinilla, C. *Expert Opinion on Biological Therapy* **2002**, 2 (1): 67-73.
40. Peppas, N. A.; Robinson, J. R. *Journal of Drug Targeting* **1995**, 3 (3): 183-184.
41. Simone, E. A.; Dziubla, T. D.; Muzykantov, V. R. *Expert Opinion on Drug Delivery* **2008**, 5 (12): 1283-1300.
42. Anderson, R. U.; Mobley, D.; Blank, B.; Saltzstein, D.; Susset, J.; Brown, J. S. *The Journal of Urology* **1999**, 161 (6): 1809-12.
43. Versi, E.; Appell, R.; Mobley, D.; Patton, W.; Saltzstein, D. *Obstetrics and Gynecology* **2000**, 95 (5): 718-21.
44. Swanson, J.; Gupta, S.; Lam, A.; Shoulson, I.; Lerner, M.; Modi, N.; Lindemulder, E.; Wigal, S. *Archives of General Psychiatry* **2003**, 60 (2): 204-11.
45. Conte, U.; Maggi, L.; Colombo, P.; Lamanna, A. *Journal of Controlled Release* **1993**, 26 (1): 39-47.
46. Conte, U.; Maggi, L. *Biomaterials* **1996**, 17 (9): 889-96.
47. Jain, S. K.; Chourasia, M. K.; Jain, A. K.; Jain, R. K.; Shrivastava, A. K. *Drug Delivery* **2004**, 11 (2): 113-22.
48. Loftsson, T.; Brewster, M. E. *Journal of Pharmaceutical Sciences* **1996**, 85 (10): 1017-25.
49. Merkus, F. W. H. M.; Verhoef, J. C.; Marttin, E.; Romeijn, S. G.; van der Kuy, P. H. M.; Hermens, W. A. J. J.; Schipper, N. G. M. *Advanced Drug Delivery Reviews* **1999**, 36 (1): 41-57.
50. Hayes, R. P.; Muchmore, D.; Schmitke, J. *Current Medical Research and Opinion* **2007**, 23 (2): 435-442.
51. Otulana, B.; Okikawa, J.; Linn, L.; Morishige, R.; Thipphawong, J. *International Journal of Clinical Pharmacology, Therapy, & Toxicology* **2004**, 42 (8): 456-462.
52. Davison S; Thipphawong J; Blanchard J; Liu K; Morishige R; Gonda I; Okikawa J; Adams J; Evans A; Otulana B; S., D. *The Journal of Clinical Pharmacology* **2005**, 45 (2): 177-184.
53. Jiang, R. G.; Pan, W. S.; Wang, C. L.; Liu, H. *Pharmazie* **2005**, 60 (8): 632-633.
54. Hoare, T. R.; Kohane, D. S. *Polymer* **2008**, 49 (8): 1993-2007.
55. Malafaya, P. B.; Silva, G. A.; Baran, E. T.; Reis, R. L. *Current Opinion in Solid State and Materials Science* **2002**, 6 (4): 297-312.
56. Lee, K. Y.; Mooney, D. J. *Chemical Reviews* **2001**, 101 (7): 1869-1879.
57. Rabinow, B. E. *Nature Reviews Drug Discovery* **2004**, 3 (9): 785-796.
58. Jia, L.; Wong, H.; Cerna, C.; Weitman, S. D. *Pharmaceutical Research* **2002**, 19 (8): 1091-1096.
59. Liversidge, G. G.; Cundy, K. C. *International Journal of Pharmaceutics* **1995**, 125 (1): 91-97.
60. Liversidge, G. G.; Conzentino, P. *International Journal of Pharmaceutics* **1995**, 125 (2): 309-313.
61. Kraft, W. K.; Steiger, B.; Beussink, D.; Quiring, J. N.; Fitzgerald, N.; Greenberg, H. E.; Waldman, S. A. *Journal of Clinical Pharmacology* **2004**, 44 (1): 67-72.
62. Anitua, E.; Sanchez, M.; Orive, G.; Andia, I. *Trends in Pharmacological Sciences* **2008**, 29 (1): 37-41.
63. Silva, G. A.; Ducheyne, P.; Reis, R. L. *Journal of Tissue Engineering and Regenerative Medicine* **2007**, 1 (1): 4-24.
64. Bessa, P. C.; Casal, M.; Reis, R. L. *J Tissue Eng Regen Med* **2008**, 2 (1): 1-13.
65. Werner, S.; Grose, R. *Physiological Reviews* **2003**, 83 (3): 835-70.
66. Fortier, L. A.; Mohammed, H. O.; Lust, G.; Nixon, A. J. *The Journal of Bone and Joint Surgery* **2002**, 84 (2): 276-88.
67. Silva, E. A.; Mooney, D. J. *Journal of Thrombosis and Haemostasis* **2007**, 5 (3): 590-598.

68. Chen, R. R.; Silva, E. A.; Yuen, W. W.; Mooney, D. J. *Pharmaceutical Research* **2007**, 24 (2): 258-64.
69. Meinel, L.; Zoidis, E.; Zapf, J.; Hassa, P.; Hottiger, M. O.; Auer, J. A.; Schneider, R.; Gander, B.; Luginbuehl, V.; Bettschart-Wolfisberger, R.; Illi, O. E.; Merkle, H. P.; von Rechenberg, B. *Bone* **2003**, 33 (4): 660-72.
70. Wenk, E.; Wandrey, A. J.; Merkle, H. P.; Meinel, L. *Journal of Controlled Release* **2008**, 132 (1): 26-34.
71. Patel, Z. S.; Young, S.; Tabata, Y.; Jansen, J. A.; Wong, M. E.; Mikos, A. G. *Bone* **2008**, 43 (5): 931-40.
72. Holland, T. A.; Tabata, Y.; Mikos, A. G. *Journal of Controlled Release* **2003**, 91 (3): 299-313.
73. Langer, R.; Tirrell, D. A. *Nature* **2004**, 428 (6982): 487-492.
74. Orive, G.; Gascon, A. R.; Hernandez, R. M.; Igartua, M.; Pedraz, J. L. *Trends in Pharmacological Sciences* **2003**, 24 (5): 207-210.
75. Orive, G.; Hernandez, R. M.; Gascon, A. R.; Igartua, M.; Pedraz, J. L. *Trends in Biotechnology* **2002**, 20 (9): 382-387.
76. Orive, G.; Hernandez, R. M.; Gascon, A. R.; Calafiore, R.; Chang, T. M. S.; de Vos, P.; Hortelano, G.; Hunkeler, D.; Lacik, I.; Pedraz, J. L. *Trends in Biotechnology* **2004**, 22 (2): 87-92.
77. Murua, A.; Portero, A.; Orive, G.; Hernandez, R. M.; de Castro, M.; Pedraz, J. L. *Journal of Controlled Release* **2008**, 132 (2): 76-83.
78. de Vos, P.; Andersson, A.; Tam, S. K.; Faas, M. M.; Hallé, J. P. *Immunology, Endocrine & Metabolic Agents in Medicinal Chemistry* **2006**, 6 (2): 139-153.
79. Black, S. P.; Constantinidis, I.; Cui, H.; Tucker-Burden, C.; Weber, C. J.; Safley, S. A. *Biochemical and Biophysical Research Communications* **2006**, 340 (1): 236-43.
80. Dufrane, D.; Goebbels, R. M.; Saliez, A.; Guiot, Y.; Gianello, P. *Transplantation* **2006**, 81 (9): 1345-1353.
81. Calafiore, R.; Basta, G.; Luca, G.; Lemmi, A.; Racanicchi, L.; Mancuso, F.; Montanucci, M. P.; Brunetti, P. *Transplantation Proceedings* **2006**, 38 (4): 1156-1157.
82. Calafiore, R.; Basta, G.; Luca, G.; Lemmi, A.; Montanucci, M. P.; Calabrese, G.; Racanicchi, L.; Mancuso, F.; Brunetti, P. *Diabetes Care* **2006**, 29 (1): 137-138.
83. Hong, Y.; Song, H. Q.; Gong, Y. H.; Mao, Z. W.; Gao, C. Y.; Shen, J. C. *Acta Biomaterialia* **2007**, 3 (1): 23-31.
84. Inanc, B.; Elcin, A. E.; Koc, A.; Balos, K.; Parlar, A.; Elcin, Y. M. *Journal of Biomedical Materials Research Part A* **2007**, 82A (4): 917-926.
85. Wu, T. J.; Huang, H. H.; Hsu, Y. M.; Lyu, S. R.; Wang, Y. J. *Biotechnology and Bioengineering* **2007**, 98 (3): 578-85.
86. Chung, C.; Mesa, J.; Miller, G. J.; Randolph, M. A.; Gill, T. J.; Burdick, J. A. *Tissue Engineering* **2006**, 12 (9): 2665-73.
87. Ferreira, L. S.; Gerecht, S.; Fuller, J.; Shieh, H. F.; Vunjak-Novakovic, G.; Langer, R. *Biomaterials* **2007**, 28 (17): 2706-17.
88. Sakai, S.; Hashimoto, I.; Kawakami, K. *Biotechnology and Bioengineering* **2008**, 99 (1): 235-243.
89. Sakai, S.; Hashimoto, I.; Kawakami, K. *Biotechnology Letters* **2007**, 29 (5): 731-735.
90. Emerich, D. F.; Thanos, C. G.; Goddard, M.; Skinner, S. J. M.; Geany, M. S.; Bell, W. J.; Bintz, B.; Schneider, P.; Chu, Y. P.; Babu, R. S.; Borlongan, C. V.; Boekelheide, K.; Hall, S.; Bryant, B.; Kordower, J. H. *Neurobiology of Disease* **2006**, 23 (2): 471-480.
91. Kaigler, D.; Krebsbach, P. H.; Wang, Z.; West, E. R.; Horger, K.; Mooney, D. J. *Journal of Dental Research* **2006**, 85 (7): 633-637.
92. Chancellor, M. B.; Yoshimura, N.; Pruchnic, R.; Huard, J. *Trends in Molecular Medicine* **2001**, 7 (7): 301-306.
93. Adachi, N.; Pelinkovic, D.; Lee, C. W.; Fu, F. H.; Huard, J. *Operative Techniques in Orthopaedics* **2001**, 11 (2): 138-144.

94. Wright, V. J.; Peng, H. R.; Huard, J. *Drug Discovery Today* **2001**, 6 (14): 728-733.
95. Huard, J.; Li, Y.; Peng, H. R.; Fu, F. H. *Journal of Gene Medicine* **2003**, 5 (2): 93-108.
96. Kimelman, N.; Pelled, G.; Helm, G. A.; Huard, J.; Schwarz, E. M.; Gazit, D. *Tissue Engineering* **2007**, 13 (6): 1135-1150.
97. Usas, A.; Huard, J. *Biomaterials* **2007**, 28 (36): 5401-6.
98. Sakai, T.; Ling, Y.; Payne, T. R.; Huard, J. *Trends in Cardiovascular Medicine* **2002**, 12 (3): 115-20.
99. Meinel, L.; Hofmann, S.; Betz, O.; Fajardo, R.; Merkle, H. P.; Langer, R.; Evans, C. H.; Vunjak-Novakovic, G.; Kaplan, D. L. *Biomaterials* **2006**, 27 (28): 4993-5002.
100. Hosseinkhani, H.; Yamamoto, M.; Inatsugu, Y.; Hiraoka, Y.; Inoue, S.; Shimokawa, H.; Tabata, Y. *Biomaterials* **2006**, 27 (8): 1387-98.
101. Tirney, S.; Mattes, C. E.; Yoshimura, N.; Yokayama, T.; Ozawa, H.; Tzeng, E.; Birder, L. A.; Kanai, A. J.; Huard, J.; de Groat, W. C.; Chancellor, M. B. *Molecular Urology* **2001**, 5 (1): 37-43.
102. Jo, J.; Tabata, Y. *European Journal of Pharmaceutics and Biopharmaceutics* **2008**, 68 (1): 90-104.

Chapter 2 – Materials and Methods

2.1 Hypotheses and experimental approach

This PhD work attempts to shed light on several key factors regarding the development and characterization of novel microparticle systems for molecular delivery in bone regeneration strategies. The specific aims for this work include:

- Develop and characterize particulate systems based on different materials and exhibiting diverse properties;

- Evaluate the carrier potential of the developed systems for the controlled release of biologically relevant molecules;

- Evaluate *in vitro* the biocompatibility of the developed carrier systems and their ability to foster osteogenesis.

- Develop an optimize methods to prepare magnetic particles with uniform and adequate size and functionalized surfaces for cell isolation applications.

The hypotheses used in this work include:

- Non-toxic and biodegradable microparticles with adequate properties can be used for the incorporation and release of a wide group of bioactive agents, including antibiotics, steroids and growth factors.

- Selected bioactive agents can be encapsulated within the microparticle systems by adequate methods, and incorporated molecules remain active after encapsulation and release.

- Microparticles based on starch combinations provide sustained release for incorporated bioactive agents.

- Loaded microparticles are biocompatible and promote desired biological responses (e.g. cell differentiation).

- Functionalized magnetic-poly-ε-caprolactone microparticles can be used to covalently bind protein-like molecules (e.g. antibodies) and separated by the application of an external magnetic field.

The work described in this dissertation can be divided into three main parts. The first two sections include the development of particulate delivery systems for the controlled release of bioactive agents relevant in bone repair strategies: *i)* antibiotics (gentamicin sulphate) to combat bone infection and *ii)* osteoinductive agents (bone morphogenetic protein 2 and dexamethasone) for enhancing bone regeneration. The final research topic addressed in

this thesis, presented in chapter 8, is entirely dedicated to the development of particulate materials for cell isolation purposes, to be further applied in cell research and therapy. The overall experimental approach was to create microparticulate materials for the efficient and controlled delivery of bioactive molecules. The materials were characterized from a materials science perspective and tested *in vitro* to assess their potential as delivery carriers and biological performance. Each of these parts is related, yet scientifically independent. Several experiments were carried out to understand the fundamental aspects of their formulation on their resulting functionality and biocompatibility, which can be sub-divided as follows:

i) Preparation of microparticulate systems with different properties using three different polymeric materials namely a blend of starch with poly-ε-caprolactone (SPCL), chitosan-starch conjugate (CHT-ST), poly-ε-caprolactone (PCL);

ii) Incorporation and *in vitro* release of bioactive molecules (gentamicin sulphate, bone morphogenetic protein-2, and dexamethasone) using the developed microparticle systems;

iii) Characterization of the developed microparticles and drug loaded microparticles regarding morphology, size distribution and chemical structure. Surface characterization of the functionalized particles was performed for the poly-ε-caprolactone system;

iv) In vitro enzymatic degradation studies of the microparticles, including evaluation of the release profile of the entrapped bioactive drugs in an enzymatic environment;

v) Protein binding studies on surface functionalized particles (poly-ε-caprolactone system only);

vi) Biocompatibility of the obtained microparticles (cell viability, proliferation and morphology as a result of the contact of the microparticles with different cell types).

vii) Determination of the bioactivity of entrapped/*in vitro* released bioactive molecules: antibacterial activity of released gentamicin sulphate and biological activity of released bone morphogenetic protein-2 and dexamethasone towards osteogenesis.

2.2 Materials

The majority of the chemical reagents, unless otherwise noted, was purchased from Sigma-Aldrich (St. Louis, MO, USA) and used as provided. Reagents and solvents for high-performance liquid chromatography (HPLC) were of HPLC grade and obtained from LABSCAN (CITY, Ireland). Similarly, reagents for spectroscopic analysis (e.g. potassium bromide (KBr) for FTIR and deuterated solvents for ^{1}H-NMR) were obtained with the adequate requirements for each technique. Details are presented for each chemical or material when used for the first time in this chapter.

Further details are provided in this chapter for the materials used in the cell culture studies (e.g. cell lines and primary cells, culture medium components and cell culture supplies).

All the chemicals were stored and manipulated following the manufacturer's instructions and safety practices.

2.2.1 Corn starch-poly-ε-caprolactone blend

A polymeric blend of corn starch with poly-ε-caprolactone (SPCL, 30-70 wt %) was used for the production of the starch-based microparticles (*Chapters 5, 6 and 7*). This blended material was supplied by Novamont (Italy) in granular form and processed by conventional injection moulding under optimized conditions [1] in a Klockner-Ferromatik Desma FM20 machine to produce compact discs (Ø=1 cm). More details about the thermal properties of this polymeric blend have been described elsewhere [2].

SPCL is both biodegradable and biocompatible material and combines the properties of each polymer in a single composition. The hydrophilic and biodegradability nature of starch, associated with a synthetic hydrophobic polymer (PCL) suggested the potential of this material to develop microparticle systems for drug delivery applications.

SPCL discs were used without further treatment. Before the preparation of the microparticles, the discs were manually cut in small pieces and subsequently dissolved in methylene chloride under vigorous stirring to form the microparticles.

2.2.2 Poly-ε-caprolactone

Poly-ε-caprolactone (TONE^{TM} PCL-787) was obtained from Union Carbide Chemicals and Plastics Division (USA). The average molecular weight, reported by the manufacturer, was 125 kDa.

The PCL was obtained in a granular form and used as received for the core-shell microparticles preparation (*Chapter 8*). In detail, this polymer was used for the entrapment of magnetite content into a polymeric shell for the development of the magnetic particulate system. PCL was selected for this study due to its well known biocompatibility and its semicrystalline nature that makes this polymer very easy to process by a variety of techniques. Furthermore, its surface can be easily functionalized.

2.2.3 Chitosan

Chitosan (from crab shells, medium molecular weight) was purchased from Sigma-Aldrich (USA). Molecular weight and degree of N-deacetylation were determined prior use. The determination of chitosan molecular weight (MW) was conducted by a viscosimetric

method [3], using 0.3 M acetic acid/ 0.2 M sodium acetate as a solvent mixture. The viscosity average molecular weight (MW) was calculated based on the Mark-Houwink equation [4, 5]. The MW of the chitosan was found to be 385 kDa. The degree of N-deacetylation of the chitosan was determined by ^{1}H-NMR sprectroscopy method [6], and was found to be 81.25%.

Chitosan was used, without further treatment, to obtain a conjugation complex with oxidized starch. Subsequently, a microparticulated system was developed by the use of the chitosan-starch complex (*Chapter 3 and 4*).

2.2.4 Soluble potato starch

Starch from potato origin was supplied as powder by ATO (The Netherlands). This polysaccharide was modified to make it water soluble (designated as Paselli 2 by the manufacturer). Before using this polymer, an oxidation treatment was performed.

2.3 Preparation of different microparticulated systems

A variety of methods have been reported for the preparation of both nano- and microparticulated systems. The most widely used techniques are methods based on emulsions (e.g. suspension polymerization, water-in-oil single and double emulsions), solvent evaporation, organic phase separation or coacervation, and spray-drying methods [7-13]. In the presented studies, we have selected water-in-oil emulsions and solvent evaporation as the more suitable methods to employ in the preparation of the microparticles, mainly based on the physicochemical properties of the materials used.

2.3.1 Microparticles for the controlled delivery of bioactive agents

2.3.1.1 Corn starch-poly-ε-caprolactone blend microparticles (SPCL): Dexamethasone and bone morphogenetic protein-2 loading

The selected method to produce the SPCL microparticles was based on an emulsion solvent extraction/evaporation technique [14]. Once SPCL has been dissolved in methylene chloride, this solution was dropped into a 200 mL polyvinyl alcohol (PVA) solution and emulsified for 4 h under constant mechanical stirring in order to evaporate the organic solvent providing structural integrity to the microparticles. Different experimental conditions were evaluated, namely different polymeric concentrations (SPCL, 5-20%), stirring rates (400-20000 rpm), PVA concentrations and molecular weights (0.5-5%, 30 000-100 000 g/mol). The resulting microparticles where then collected by filtration, thoroughly washed with distilled water and vacuum dried in a desiccators and/or freeze-dried. For the microparticles

loaded with the growth factor (BMP-2) a lyophilization process was performed due to the sensitivity of those molecules to high temperatures.

After selection of the proper condition, dexamethasone (DEX) (97%, cell culture tested, Sigma-Aldrich, USA) was loaded by mixing the SPCL solution in methylene chloride with the steroid at different percentages (5, 10 and 15% (w/w), relatively to polymer weight). The same procedure was performed as described for unloaded microparticles. The reaction medium was stored at 4 ^{o}C for later quantification of unloaded DEX.

For the microparticles to be loaded with bone morphogenetic protein-2 (BMP-2) (Recombinant human BMP-2, > 95%, R&D systems, USA), a co-encapsulation process was performed using bovine serum albumin (BSA) (≥96%, Sigma-Aldrich, USA). BSA protects bioactive molecules from inactivation in presence of harsh organic solvents. 200 mg of BSA and 10 µg of BMP-2 were mixed and added to the SPCL solution before the addition to the stirring PVA emulsification medium. After formation of the microparticles, the reaction medium was collected and stored at 4 ^{o}C for quantification of unloaded proteins (please see section 2.6.2).

All experiments using DEX and BMP-2 loaded microparticles were carried out in triplicate.

2.3.1.2 Starch-conjugated chitosan microparticles (CHT-ST): Gentamicin sulfate loading

Hydrated polymers, like chitosan, usually need crosslinking to provide them with structural stability. Conjugation of chitosan with oxidized starch can lead to a more stable complex. The most common crosslinker agents for chitosan are glutaldehyde [15] and formaldehyde [16]. They are capable of forming highly stable products. However, their toxicity and the possibility of impairing the biocompatibility of their crosslinked products are considered major drawbacks [15, 17]. Moreover, natural origin polysaccharides with free aldehyde groups like starch or cellulose have been investigated for possible conjugation with chitosan [18-20]. As a result, a polysaccharide complex is obtained with the needed structural integrity together with an enhancement of biocompatibility, biodegradability and hydrophilicity of the resulting systems.

Sodium periodate oxidation of soluble starch. Starch was oxidized to generate a polyaldehyde able to react with the primary amino groups of chitosan by means of imine conjugation (highly unstable conjugate) [21]. Subsequently, a reduction process is needed to stabilize the final conjugate. Briefly, soluble starch was dissolved in distilled water (0.02 g/mL) in a light protected glass vessel. Subsequently, sodium iodate (10 mg/mL) was added dropwise into the starch solution, allowing the reaction to proceed for 30 minutes at room temperature under slow magnetic stirring. Finally, in order to quench the reaction, glycerin (0.1 mL/mL

solution) was added and stirred for additional 10 minutes. The resulting solution was dialyzed (Dialysis tubing cellulose membrane, MWCO 12 kDa, Sigma-Aldrich, USA) against distilled water for two days with several daily changes. The oxidized starch solution was concentrated by using an ultra-concentrator Amicon® stirred cell 8010 (Millipore, USA) and stored at 4 ^{o}C in a light protected glass vessel until further use.

Starch-conjugated chitosan complex formation. Chitosan solution was prepared by dissolving the polymer in 1% acetic acid solution. The same volume (e.g. 10 mL) of chitosan (1.5% (w/v)) and oxidized starch (2% (w/v)) solutions were mixed thoroughly and the pH adjusted to 5.5. The gel-like solution formed was further used for the formation of the starch-conjugated chitosan microparticles (CHT-ST).

Starch-conjugated chitosan microparticles. CHT-ST microparticles were prepared by water-in-oil emulsification methods using reductive alkylation crosslinking procedure [22]. In this case, both chitosan and oxidized starch are soluble in water and non-soluble in oil. Therefore, an emulsion of the aqueous solution of these polymers is easily formed using oil as the non-soluble phase. Additionally, any further modification to the technique like crosslinking or drug loading is feasible whenever they are soluble in the polymeric solution (aqueous phase).

The previously formed CHT-ST polymeric solution (gel-like, pH=5.5) was added dropwise into a glass reactor containing mineral oil (1% of Tween 80). The oleic phase was continuously emulsified with a mechanical stirrer at 600 rpm for 30 minutes to allow the formation of a stable emulsion. Subsequently, a suitable volume of cold acetone was slowly added and allowed to proceed for two hours. The microparticles were removed from the reaction medium by filtration and washed with distilled water/acetone mixture (1:1) to remove the oil adhering to their surface. After drying at room temperature, the microparticles were incubated for three hours with 0.5 M sodium carbonate buffer solution (pH 8.5) to allow the conjugation between reactive aldehyde groups (Starch) and primary amino groups (Chitosan). After repeatedly washing with distilled water, the microparticles were incubated in sodium borohydride solution (0.05%, w/v) for one hour to reduce excess of reactive aldehyde groups, and to confer stabilization to the imine conjugation (CHT-ST) into covalent bonds. Finally, the resulting microparticles were washed with distilled water and allowed to dry at room temperature.

Three variations were subsequently introduced to the standard procedure described above (starch-conjugated chitosan microparticles without using external crosslinking agents): *i)* two different crosslinking agents were employed: sodium tripolyphosphate (TPP) and glutaraldehyde (GA), at concentrations in the range 0.5-2%. Crosslinking was achieved by

immersing the obtained samples for 3 hours into the crosslinker agent solution, *ii)* the amount of starch in the composition of the CHT-ST conjugate polymer solution used for the microparticles preparation was varied (1-4%), *iii)* the stirring rate employed to form the emulsion was increased from 400 to 800 rpm aiming at producing smaller sizes microparticles.

For the microparticles to be loaded with gentamicin (GTM) (puriss. p.a., Fluka-Bio Chem. Co., Switzerland) the drug was directly added to the starch-conjugated chitosan polymeric solution and carefully dissolved (GTM initial concentrations: 5, 10, and 15 mg/mL of polymer solution). The subsequent procedure used for the formation of the CHT-ST microparticles loaded with GTM was the standard procedure described above without any of the described modifications. However, the effect of external ionic crosslinking on the drug loading and *in vitro* release was investigated by the use of TPP. Hence, the GTM loaded microparticles were immersed into three different concentrations of sodium tripolyphosphate (TPP) solution (0.5, 1, and 2% w/v) for 30 minutes. The initial concentration of GTM used for this study was 15 mg/mL. The reaction medium and washing solutions were stored at 4 ^{o}C until further quantification for unloaded GTM. All the encapsulation procedures described for GTM were performed in triplicate.

2.3.2 Magnetic microparticles for the immunomagnetic separation of cells

2.3.2.1 Magnetic poly-ε-caprolactone microparticles (m-PCL). Entrapment of magnetite core within a polymeric shell

Magnetite nanoparticles. The magnetite nanoparticles were synthesized by a co-precipitation method [23-26]. For that purpose, two different chloride salts were used as iron source (Fe^{3+}/Fe^{2+}) and a concentrated solution of ammonium hydroxide to cause co-precipitation. Briefly, $FeCl_3.6H_2O$ (1.80 M) and $FeCl_2.4H_2O$ (1.20 M) were dissolved in distilled water (previously degassed by N_2 bubbling). Under a N_2 atmosphere and vigorous mechanical stirring, the mixture was heated to 80 ^{o}C. Subsequently, 40 mL of ammonium hydroxide solution (25% in water) were rapidly added, maintaining the reaction conditions for the following 30 minutes. Temperatures in the range of 70-80 ^{o}C and the constant N_2 atmosphere used reduce the oxygen content of the precipitation medium. This minimizes the oxidation of the formed magnetite (Fe_3O_4) to ferromagnetic oxides (Fe_2O_3). After the formation of the magnetite particles, oleic acid was added and the mixture was heated to 80 ^{o}C for 30 minutes. At this time, the mixture changed to a deep black lump indicating the formation of the magnetite particles. The precipitate was separated by the use of an external magnetic field and then extensively washed using a mixture of distilled water and acetone (1:1). The particles are attracted towards the external magnet within a few minutes allowing discarding the

supernatants. At the end of this procedure, a fine black precipitate with superparamagnetic behavior was obtained and dried using a vacuum desiccator at room temperature.

Magnetite nanoparticles entrapment into PCL shell. Core-shell magnetic poly-ε-caprolactone microparticles (m-PCL) have been prepared by emulsion solvent extraction/evaporation method [14]. The synthesized magnetite nanoparticles were included inside the polymeric shell. In brief, PCL was completely dissolved in methylene chloride under vigorous stirring with the subsequent addition of the magnetite nanoparticles. The mixture was sonicated for 10 minutes using an ultrasonic bath, to ensure a good dispersion of the magnetite nanoparticles in the polymeric solution. Subsequently, the suspension was dropped into a continuously stirred PVA medium (100 mL), and emulsified for 4 hours. Different experimental conditions, such us magnetite to polymer ratio (0.005-0.15%), PVA concentration (0.5-2%) and stirring rate (11000-24000 rpm) were tested. The m-PCL microparticles were then collected by magnetic decantation, washed with distilled water and lyophilized to obtain a fine brownish powder.

2.3.2.2 Surface functionalization of the m-PCL core-shell microparticles

Amino groups. The functionalization of the surface of the m-PCL microparticles with amino groups (-NH_2) was achieved by an aminolysis process [27]. For that purpose, dried m-PCL microparticles were immersed in a mixture of 1,6-hexanediamine/2-propanol using different experimental conditions. The microparticles were chemically functionalized in 1,6-hexanediamine at concentrations in the range of 2-20% and at two different temperatures (25 and 37 ^{o}C) for a time period varying from 30 to 90 minutes. The reaction vessel was maintained under constant agitation placed inside a shaking bath (100 rpm). At the end of each treatment period, the amino functionalized m-PCL (NH_2-m-PCL) microparticles were collected by magnetic decantation, and extensively dialyzed (Dialysis tubing cellulose membrane, MWCO 12 kDa, Sigma-Aldrich, USA) using deionized distilled water to remove the free 1,6-hexanediamine. Subsequently, the particles were dried in a vacuum desiccator at room temperature.

Epoxy groups. Epoxy groups were introduced on the surface of the m-PCL microparticles by adapting a previously reported method [28]. The procedure is based on the use of a plasma activation step followed by a chemical reaction. Both plasma activation and chemical functionalization were carried out in a radio frequency plasma reactor “PlasmaPrep5” (Gala Instruments, Germany). Before the experiments, the plasma chamber was thoroughly purged with a continuous flow of the gas (O_2) used during the treatment to reduce trace amounts of air and moisture. The m-PCL microparticles were exposed to oxygen plasma to

activate the surface by peroxy and hydroxyl functional groups. The gas flow (O_2) was adjusted in order to keep a constant pressure of 0.18 mbar inside the chamber. A power of 90 W was applied. The duration of the surface activation was 2 min. Subsequently, vapors of epichlorohydrin (ECH) were introduced inside the chamber (vapor pressure 13.8 mmHg at 21.1 ^{o}C) and allowed to react with the particles for 30 minutes.

Both, amino and epoxy functionalized m-PCL microparticles were then stored under controlled dry conditions, using a vacuum desiccator to preserve their surface activity for further characterization and use.

2.3.2.3 Protein binding studies

Immunomagnetic cell isolation usually involves specific interactions between antigens or antibodies bound onto the surface of the particles, and the counterparts in or on the surface of the cells. Hence, antigens and antibodies determine the efficacy of the isolation process. Aiming to demonstrate the potential of the developed magnetic microparticles for covalent binding of protein molecules, we have selected bovine serum albumin (BSA) as a model protein to study the binding ability of the functionalized m-PCL microparticles.

NH_2-m-PCL microparticles. A typical carbodiimide (*N*-(3-Dimethylaminopropyl)-*N*′-ethylcarbodiimide hydrochloride (EDC) (commercial grade, Sigma-Aldrich, USA) activation-adsorption experiment was carried out [21]. Briefly, 10 mg of dried NH_2-m-PCL microparticles were resuspended in 0.05 M MES buffer followed by the addition of a freshly prepared EDC solution (40 mg/mL). The suspension was carefully mixed at room temperature. Subsequently, the BSA (≥96%, Sigma-Aldrich, USA) was dissolved in MES buffer and added to the microparticle suspension. The suspension was mixed on an orbital shaker for two different time periods (5 hours and overnight), and at two different temperatures (25 and 37 ^{o}C). Subsequently, the supernatants were collected and filtered (Low protein binding Durapore® (PVDF) syringe filter unit, 0.22 µm pore size, Millipore, USA). BSA concentration was determined by UV spectrophotometry at 280 nm. The microparticles were washed and resuspended in MES buffer and stored at 4 ^{o}C for further analysis.

Epoxy-m-PCL microparticles. These particles were used without previous activation of the surface of the microparticles. The dried particles were washed in MES buffer and subsequently mixed with BSA. The experimental procedure was identical to the previously described for NH_2-m-PCL microparticles.

The effect of several experimental parameters on the covalent binding of BSA was studied, i.e. pH (3.5-7, MES buffer, 0.05 M) and ionic strength (concentrations of NaCl: 0.1, 0.5 and 1.5 M). In addition, the efficiency of the covalent BSA binding to the surface groups of the

m-PCL functionalized microparticles was investigated. Thus, the BSA-microparticles complexes were immersed in buffer medium containing 1% Tween 20, which removes only the physically adsorbed protein [29, 30]. After elution, the released BSA was measured at 280 nm.

Aiming to visualize the BSA covalently bound to the surface of functionalized microparticles, confocal laser scanning microscopy (CLSM) (Olympus IX81, Japan) was performed. BSA was labeled with fluorescein isothiocyanate (FITC) prior the binding experiments [31]. Briefly, FITC dissolved in DMSO (10 mg/mL) was slowly added to a 10 mg/mL BSA solution in 0.1 M carbonate buffer (pH 9), under moderate and continuous agitation at room temperature. The mixture was allowed to react overnight at 4 ^{o}C in a light protected vessel. The labelled protein solution was then extensively dialysed (Dialysis tubing cellulose membrane, MWCO 12 kDa, Sigma-Aldrich, USA) against PBS buffer (0.01 M, pH 7.4) at 4 ^{o}C and stored as lyophilized powder in a light protected container for further use.

The subsequent binding experiments were carried out following the procedure described above, but using the labeled FITC-BSA as protein. After elution of the physically adsorbed FITC-BSA, the labeled protein-microparticles complexes were washed with distilled water, mounted using “Vectashield” mounting medium (Vector Laboratories, USA) and visualized by CLSM.

2.4 Physicochemical characterization of the developed microparticles.

The characterization of the developed microparticles was divided into three major categories: morphological analysis, particle size and size distribution, and structural characterization.

2.4.1 Morphological analysis

Optical microscopy (OM/OLT). Examination of the shape and stability of the suspensions of the different particles produced was accomplished by mounting a sample suspension (5 mg of micro/nanoparticles per mL in distilled water) onto a glass slide. The samples were observed by an optical microscope with a polarized light source (Olympus BH2, Japan). The samples were photographed using a high-resolution Leica camera for image acquisition (Leica Microsystems GmbH, Germany). This observation was particularly relevant to assess the stability of the magnetite nanoparticles suspensions.

Scanning electron microscopy (SEM). To analyze the obtained microparticles for their shape and surface morphology, together with their morphology after drug loading and *in vitro* release, all employed samples were analyzed by scanning electron microscopy (SEM). Additionally, this technique was applied to study changes in the morphology of the

microparticles after being subjected to *in vitro* enzymatic degradation (please see section 2.7). A portion of dried microparticles was mounted onto aluminium stubs with a carbon tape and gold sputter-coated (Fisons Instruments, Sputter Coater SC502, UK). All images were collected with a Leica Cambridge S-360 model (UK) scanning electron microscope.

Micro-computed tomography (μ-CT). A representative sample of the porous SPCL microparticles was scanned by micro-computed tomography (μ-CT) using a μ-CT 20 equipment (SCANCO Medicals, Switzerland). The energy of the scanner used was 100 kV/ 98 μA intensity. A threshold range of values of 141-255 was used to estimate the porosity of the samples. Approximately 40 slices of the sample were obtained. Mimics (Materialise, Belgium), CT Analyser and CT Vol Realistic 3D Visualization (SkyScan, Belgium) software were used for image processing and to create and visualize the three-dimensional structure.

2.4.2 Size distribution: Sieves meshes and dynamic light scattering (DLS)

To determine the size distribution of the different microparticles obtained, the samples were separated through a series of standard sieves (20, 60, 100, 125, 150, 250, 450, 500, 650, 900 and 1000 μm; Linker Industrie-Technik, Germany). The microparticle fraction that passed through a sieve and was retained on the sieve with a certain pore size was collected and weighed, and finally correlated with the total mass of the microparticles sample analyzed. These series of standard sieves were also used to separate the particles by size and to obtain microparticle samples with uniform size to be used in further experiments.

In the case of the produced magnetite nanoparticles, the Nano ZS ZEN3600 equipment (dynamic light scattering) (Malvern Instruments, UK) was used to determine the particle size and size distribution. For sample preparation, 1 mg of dried magnetite nanoparticles was resuspended in a mixture of glycerol and ultrapure distilled water (1:1).

2.4.3 Fourier transformed infrared spectroscopy (FTIR)

The chemical structure of the microparticles was analyzed by fourier transformed infrared spectroscopy (FTIR) (IRPrestige-21 FRIT-8400S, Shimadzu, Japan) in transmission mode. Unloaded microparticles, after drug loading and release, and during *in vitro* degradation process were analyzed by FTIR. Weighed samples (1 mg) were mixed with spectroscopic KBr (40 mg) and then formed into a disc in a manual press (161-1100 hand press, PIKE Technologies, USA). Transmission spectra were recorded using at least 32 scans with 4 cm^{-1} resolution, in the spectral range of 4000-500 cm^{-1}.

2.4.4 Nuclear magnetic resonance spectroscopy (^{1}H-NMR)

In the particular case of CHT-ST microparticles, when FTIR spectroscopy could not be used, due to the similarity of the spectra of both polysaccharides, nuclear magnetic resonance spectroscopy (^{1}H-NMR) was selected. ^{1}H-NMR spectra were acquired on a Varian Unit Plus 300 MHz spectrometer (USA). For all samples, the following experimental parameters were used: 256 scans recorded, 5200 Hz filter width, 90^o pulse corresponding to a pulse width of 11 μs, 4 s relaxation delay, and a temperature of 60 ^{o}C. For quantification purposes, the peak area method was used after the start and end points of the integration of each peak had been manually selected. For sample preparation, 10 mg of each sample were put into an NMR tube (ϕ=0.3 mm) and 1 mL of deuterated solvent was added. Chitosan is soluble in moderately acid conditions. Hence, chitosan and CHT-ST microparticles were dissolved in 0.98 mL of D_2O and 0.02 mL of DCL, waiting for complete dissolution. On the other hand, starch and GTM were dissolved in D_2O. The samples were briefly sonicated at room temperature to ensure complete dissolution and homogenization of the sample.

2.4.5 X-ray diffraction (XRD)

In order to confirm the encapsulation into and the *in vitro* release of DEX from the SPCL microparticles, as well as to determine the physical state of the entrapped molecule, X-ray diffraction patterns of DEX loaded SPCL microparticles were obtained in a X-ray diffractometer (X'Pert MPD, Philips, The Netherlands). In addition, during the preparation of the magnetic PCL microparticles, the formation of magnetite (Fe_3O_4) and their presence into the m-PCL microparticles was similarly confirmed. The data collection was performed with a Cu anode and monochromator used at a voltage of 40 kV. The samples were analyzed over the angle range (2θ) of 2^o-60^o.

2.4.6 Thermogravimetric analysis (TGA)

For the magnetic particulated system, m-PCL, different magnetite contents were encapsulated within the polymeric shell by the use of different magnetite to polymer ratios. Hence, to determine the magnetite content entrapped inside the polymeric shell a thermogravimetric analyzer (Q500, TA Instruments, USA) was used. Dried samples were analyzed in closed alumina cups at a temperature range of 30-700 ^{o}C. The used heating rate was 10 ^{o}C/minute. All the experiments were carried out under nitrogen atmosphere. PCL microparticles without iron content were used as controls.

2.4.7 Vibrational magnetometry (VSM)

Aiming to study the magnetic properties of both magnetite nanoparticles and m-PCL microparticles, a vibrating sample magnetometer (VSM, LakeShore, USA) was used. Two different temperatures were used for sample analysis (5 and 300 K). The applied magnetic field was varied from 60 000 to - 60 000 Oe. Values of saturation magnetization (M_s) and remanence magnetization (M_r) as well as coercive field (H_c) and saturation field (H_s) were determined.

2.5 Surface characterization of the functionalized m-PCL microparticles

To confirm and quantify the presence of both amino and epoxy groups on the surface of the m-PCL microparticles as a result of the functionalization treatments, two different analyses were performed.

2.5.1 Amino groups: *ninhydrin colorimetric assay*

2,2-Dihydroxyindane-1,3-dione, commonly known as ninhydrin, is a chemical used to detect ammonia or primary and secondary amines. The principle behind the use of ninhydrin as main component of a quantitative colorimetric assay relies in the formation of a deep blue or purple color product (Ruhemann's purple) when reacting with free amines. This colored product is characterized by a strong absorbance at a wavelength of 570 nm in the ultraviolet spectrum. Therefore, the ninhydrin reaction product can be by quantified by UV spectroscopy [32]. Among the several applications of this method, ninhydrin can also be used to monitor solid phase peptide synthesis and in amino acid analysis of proteins [32].

In our study, in which amino groups are being introduced to functionalize a polymeric surface, this assay is particularly useful for their detection and quantification. Ninhydrin binds to amino groups present on the surface of the polymer producing a purple pigment that can be detected using a spectrophotometer (570 nm) [33-35]. Based on that principle, the $-NH_2$ surface functionalized microparticles (10 mg) were immersed in 1.0 M ninhydrin solution prepared in ethanol for at least 1 minute. The container vessel was then heated to 80 ^{o}C to accelerate the reaction of the ninhydrin with the amino groups present on the surface of the microparticles. After discarding the supernatant and allowing the complete evaporation of the ethanol, 5 mL of 1,4-dioxane was added to dissolve the ninhydrin-treated microparticles. After complete dissolution of the samples, 5 mL of isopropanol were added to stabilize the formed blue compound. The sample was filtered to remove any insoluble material, and the absorbance of the final solution was measured (570 nm). For quantification purposes, a

calibration curve was prepared using solutions of known concentration of 1,6-hexanediamine in a mixture of 1,4-dioxane/ isopropanol (1:1).

The ninhydrin assay is sensitive to the presence of free amino groups from any source. Therefore, solvents or chemicals with amino groups should not be used in order to avoid the interferences.

2.5.2 Epoxy groups: X-ray photoelectron spectroscopy (XPS)

X-ray photoelectron spectroscopy (XPS) is a quantitative spectroscopic technique that measures the surface elemental composition. In this thesis, XPS was used to confirm the success of the surface functionalization after the different treatments.

The analyses were performed (ESCALAB 250iXL" spectroscope, VG Scientific, UK) with PISCES software for data acquisition and analysis. XPS measurements were carried out using monochromatic Al (Kα) radiation (1486.92 eV). Photoelectrons were collected from a take-off angle of 90^{o} relative to the sample surface. The measurement was performed in constant analyzer energy mode (CAE) with 100 eV for survey spectra and 20 eV for high-resolution spectra. Charge referencing was carried out by setting the lower binding energy C 1s photopeak at 285.0 eV. The identity of the chemical functional groups was determined from the high-resolution peak analysis of carbon-1s (C1s) and oxygen-1s (O1s). For sample preparation, a suspension of dried microparticles was prepared in ethanol and dripped onto a silicon wafer surface. After the complete ethanol evaporation, the sample was introduced in the XPS pre-chamber for the measurements.

2.6 *In vitro* experiments to study the release of bioactive molecules

Microparticles loaded with the different bioactive molecules selected in this thesis were employed to determine the percentages of drug loading and encapsulation efficiencies, together with the studies of the profiles of the *in vitro* release of the respective encapsulated molecules. As described before, the microparticles used for these studies are the following: DEX loaded SPCL, BMP-2 loaded SPCL and GTM loaded CHT-ST microparticles.

For each of these systems, pre-weighed microparticles were suspended in phosphate buffered saline (PBS) solution (pH 7.4, 0.01 M) at a concentration of 2.5 mg/mL, except for the BMP-2 loaded SPCL microparticles that were used at 30 mg/mL in PBS. The microparticles were maintained at 37 ^{o}C under constant agitation (50 or 100 rpm) in a shaking water bath. The incubation time for DEX and GTM loaded microparticles was 30 days, whereas for BMP-2 loaded microparticles was 10 days. At predetermined time points, 1 mL aliquots of the supernatants were collected and replaced with the same volume of fresh PBS solution. The

supernatants were then stored at -80 ^{o}C for drug quantification. All the release experiments were carried out in triplicate. Results are reported as average ± standard deviation.

2.6.1 Quantification of DEX by reverse-phase high-performance liquid chromatography (RP-HPLC)

The collected samples during the preparation of the DEX loaded particles (reaction medium) and from the *in vitro* release study were prepared for high-performance liquid chromatography (HPLC) quantification. Samples from the reaction medium were extracted three times with a 1:1 mixture of hexane and ethyl acetate solvents. The final extract was collected and the solvent mixture allowed evaporating under nitrogen flow. The dry extract was reconstituted in a mixture of acetonitrile/water in the same proportions (mobile phase) prior to the analysis. On the other hand, the aliquots from the release medium (PBS solution containing released DEX) were directly analyzed.

DEX was quantified by reverse-phase (RP) HPLC. HPLC was performed on a Jasco PU-2080 Plus system using a RP-18 column (LiChrospher, 5 µm, Merck, Germany) with acetonitrile/water (50:50 v/v) as mobile phase at a flow rate of 0.5 mL/min. Absorbance was monitored at 254 nm (UV detector Jasco 870-UV). The column was eluted under isocratic conditions during 20 min. Data acquisition and peak areas were determined with Shimadzu C-R6A Chromatopac software (Figure 2.1). The concentration of DEX was calculated by using a calibration curve (y = 8697.18 + (1.65 X 10^{7})x, R^2= 0.9995). Triamcinolone was used as an internal standard (Figure 2.1).

2.6.2 Quantification of BMP-2 by an enzyme-linked immunosorbent assay (ELISA)

BMP-2 present in the reaction medium in which the BMP-2 loaded microparticles were obtained and in the aliquots from the *in vitro* release study were quantified using an enzyme-linked immunosorbent assay (ELISA) (Human BMP-2 Quantikine® ELISA Kit, R&D Systems, USA) according to the manufacturer's instructions. The samples stored at -80 ^{o}C were thawed at room temperature without any further heating before analysis. Several samples were included as controls, including plain PBS, unloaded SPCL microparticles and BSA loaded SPCL microparticles. BMP-2 was quantified using a calibration curve of recombinant BMP-2 from human origin included in the original kit.

All the quantification analyses were performed in duplicate assays by the use of triplicate samples.

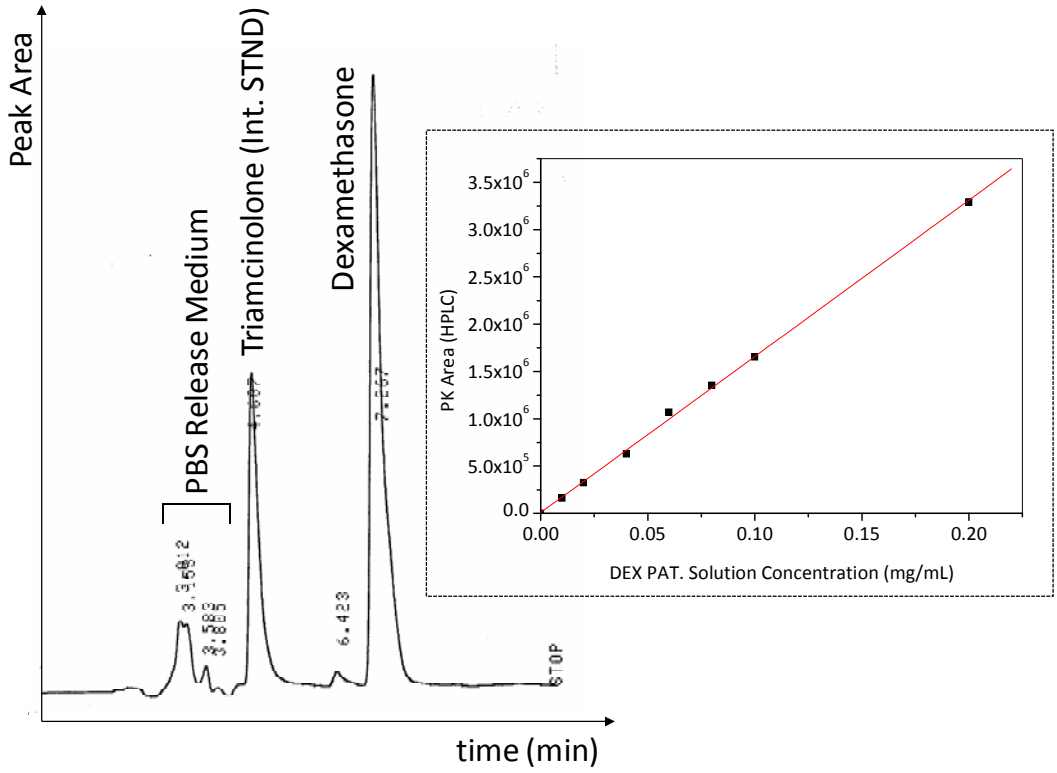

Figure 2.1 Illustrative chromatogram and calibration curve obtained as a result of the quantitative analysis of the aliquots from the *in vitro* release study of DEX from SPCL microparticles in PBS medium

2.6.3 Quantification of GTM by indirect spectrophotometric methodology

A wide variety of methods can be used to quantify aminoglycoside antibiotics (e.g. gentamicin), namely fluorescence polarization immunoassay, enzyme-linked immunosorbent assay (ELISA), microbiologic assay, chromatographic and spectrophotometric methods [36]. Among all of them, spectrophotometric methods are preferable. They are usually rapid, very sensitive and relatively cheap when compared with the ones mentioned above. The main requirement for this method is the absorbance of light in the UV-visible spectrum region by the analyzed compounds. Since GTM does not absorb ultraviolet nor visible light, an indirect method is required for its spectrophotometric assay. Similarly to already mentioned ninhydrin (please see section 2.5.1) several derivatizing agents are reported to react with primary and secondary amines present in the GTM molecule to yield chromophoric products [36]. In this previously reported study, where a comparative quantitative analysis was performed, the best results were obtained when *o*-phtaldialdehyde was used [36].

Therefore, in this thesis an indirect spectrophotometric method was used for the quantification of GTM, using o-phtaldialdehyde as derivatizing agent. Briefly, the *o*-phtaldialdehyde reagent was formulated by dissolving 0.25 g of o-phtaldialdehyde in a

mixture of methanol (6.25 mL) and 2-mercaptoethanol (0.3 mL). Subsequently this solution was added to 56 mL of sodium borate (0.04 M, pH 8) buffer solution to formulate derivatizing reagent. The reagent was maintained in a brown bottle protected from the light for at least 24 h before use. For the colorimetric measurement, GTM solution, o-phtaldialdehyde reagent and isopropanol were mixed in an equal volume ratio, and incubated for 30 minutes at room temperature. The absorbance was subsequently measured at 332 nm. The concentration of GTM was calculated using a calibration curve (y = 0.02 + 9.55 x, R^2= 0.9996) (Figure 2.2).

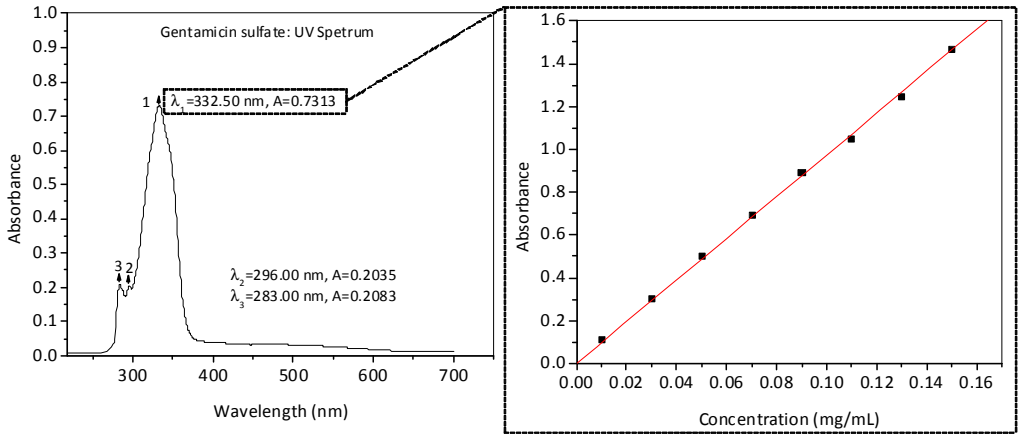

Figure 2.2 Absorption spectra of gentamicin sulphate sample **(a)**. Calibration curve for absorbance versus concentration obtained by the use of a gentamicin solution of known concentration **(b)**

2.6.4 Drug loading and Encapsulation efficiency percentages

The drug loading and encapsulation efficiency are two important parameters to be determined during the encapsulation of bioactive molecules. Usually those two parameters are used indistinctly, and several research studies tend to confuse their meaning. The drug loading is the relation between the weight of the drug partition loaded into the microparticles and the total weight of the loaded microparticles. The encapsulation efficiency is defined as the relation between the difference of the total weight of the drug to be loaded or added and the remaining drug partition in the reaction medium after encapsulation process; and the total weight of the drug to be loaded or added. In order to clarify, both parameters establish a relation of the weight of the drug partition loaded into the microparticles and: *i)* drug loading with the total weight of the microparticles and *ii)* encapsulation efficiency with the total weight to be loaded or initially added.

In all experiments, knowing the initial concentration of drugs added (DEX, BMP-2 and GTM), and the concentration of unloaded drug (remaining in the reaction medium where loaded microparticles were produced) quantified by the different techniques described above, it was possible to determine both parameters according to known equations [37].

$$\%\, DL = [W_1 / W_2] \times 100 \quad (2.1)$$

$$\%\, EE = [(W_3 - W_4)/W_3] \times 100 \quad (2.2)$$

Where DL = drug loaded, EE = encapsulation efficiency, W_1 is the weight of drug in the microparticles, W_2 is the total weight of microparticles, W_3 is the total weight of drug added, and W_4 is the weight of drug that remained in the reaction medium after encapsulation.

2.7 *In vitro* enzymatic degradation studies

Two of the developed systems in this thesis aimed to be used as carriers of important bioactive molecules as part of drug delivery systems: SPCL microparticles for DEX and BMP-2 and CHT-ST microparticles for GTM. One important and desired property is biodegradation when designing drug delivery systems. Biodegradable polymers are able to release the entrapped drug as their degradation take places. Thus, by controlling the degradation rate of polymeric materials the drug release can be identically monitored.

The enzymatic degradation of the developed carrier systems was investigated by incubating the microparticles in PBS (0.01 M, pH 7.4) and PBS containing selected enzymes. In the case that SPCL microparticles, α-amylase (150.5 U/L), lipase (102 U/L) and their mixture were used to mimicking an enzymatic environment. For CHT-ST microparticles, only α-amylase (150.5 U/L) was used. The microparticles were incubated in a ratio of 1:10 with the selected degradation solution at 37 ^{o}C under constant shaking (50-60 rpm). The incubation period amounts up to 8 weeks for the CHT-ST microparticles and up to 12 weeks for the SPCL microparticles. The PBS solutions containing the enzymes were changed weekly to maintain the desired level of enzyme activity throughout the experiment. Meanwhile, sodium azide (0.02%) was added to the degradation solution to avoid possible microbial growth. At the end of the pre-selected degradation times, the supernatants were removed and stored at -80 ^{o}C until further analysis. The microparticles were then thoroughly washed with distilled water. The excess of solution was carefully removed with filter paper and the samples were carefully weighed for the determination of water uptake [38]. Subsequently, the samples were allowed

to dry at room temperature until constant weight. The final weight of the samples was used for the calculation of the weight loss [38]. The supernatant solutions were used to determine the concentration of released DEX or GTM (when loaded microparticles were used) as well as the concentration of reducing sugars released into the solution as a result of starch degradation. The amount of reducing sugars was estimated by the dinitrosalicylic acid (DNS) method [39].

Experiments were performed in triplicate for all the conditions: triplicates were performed for each sample at each time period and the results are shown as mean ± standard deviation.

The weight loss and water uptake were calculated by the use of the equations 2.3 and 2.4.

$$\%\,Weight\ loss = \left[\left(W_f - W_i\right)/W_i\right] \times 100 \quad (2.3)$$

$$\%\,Water\ uptake = \left[\left(W_w - W_i\right)/W_i\right] \times 100 \quad (2.4)$$

Where W_i is the initial weight of the sample, W_w is the wet weight of the sample (water uptake) and W_f is the final weight of the dry sample (weight loss).

Samples were analyzed for their morphology changes and eventual modifications in the chemical composition at each time point of analysis (by SEM, FTIR and ^{1}H-NMR as described in section 2.4.1, 2.4.3 and 2.4.4 respectively).

2.8 Biological evaluation of the obtained microparticles

In order to evaluate the effect of the produced microparticles (SPCL, CHT-ST and m-PCL) on cells, three different types of cells where used: human osteoblast-like cell line (SaOs-2) (ECACC, UK), mouse skeletal myoblast cell line (C2C12) obtained from the German Collection of Microorganisms and Cell Cultures DSMZ-ACC565 (Germany) and human adipose-derived stem cells (ASC) from the Blood Bank of the upper Austrian Red Cross (Austria).

The microparticles used for the studies in contact with the cells were sterilized by ethylene oxide (EtO) using pre-optimized conditions [40]. For that purpose, pre-weighed microparticles were put into 1 mL vials with pierced caps allowing the gas to enter into the closed container. Subsequently, the *in vitro* experiments were performed to investigate the effects on cell viability, proliferation and morphology.

2.8.1 Cytotoxicity

Polymeric materials to be used in medical applications should be characterized by two relevant features: biofunctionality and biocompatibility. Cytotoxicity, as initial phase in testing biocompatibility, detects cell death or other negative effect of materials on cellular functions. Several methodologies for cytotoxicity assay are described nowadays as standardized procedures. Assessing cell membrane integrity is one of the most common procedure to measure cell viability and cytotoxic effects and can be performed by the use of vital dyes, such as trypan blue or propidium iodide. Alternatively, the passage of substances (e.g. lactate dehydrogenase (LDH)) that are normally inside cells to the outside can be monitored. Cytotoxicity can also be monitored using the MTT or MTS assay. This assay measures the reducing potential of the cell using a colorimetric reaction. Viable cells will reduce both, MTT and MTS reagent to a colored formazan product that can be quantified spectrophotometrically at 490 nm [41].

In order to test the possible cytotoxicity of the developed microparticles, the effect of: *i)* the different processing conditions employed to produce the samples, *ii)* the earlier degradation of the samples with subsequent release of degradation products and *iii)* direct contact over the cells, was evaluated by performing a standard MTS (3-(4,5-dimethylthiazol-2-yl)-5-(3-carboxymethoxyphenyl)-2-(4-sulfophenyl)-2H-tetrazolium) assay [42, 43].

Different experiments, based on the use of different samples, were performed to assess the cell viability by using SaOs-2 and C2C12 cells. Initially, the microparticles were incubated in Dulbecco's Modified Eagle's Medium without phenol red (DMEM, Sigma-Aldrich, USA) (0.5 mg/mL) supplemented with 10% heat-inactivated fetal bovine serum (FBS; Biochrom AG, Germany) and 1% of antibiotic/antimycotic (Gibco, USA), for 24, 48, and 72 hours at 37 ^{o}C and 60 rpm. The microparticles may release potential toxic leachables (from the microparticles processing) and early degradation products to the medium. In another experiment, the microparticles from the different production conditions were incubated in direct contact with the cells or indirectly placed in transwell inserts (12 mm, 0.4 μm pore size). This allowed us to evaluate any differences on cell behavior as a result of direct or indirect contact of the samples to the cells.

To perform the MTS assay, SaOs-2 and C2C12 cells in DMEM medium without phenol red (supplemented as described above) were plated at appropriated cell number depending on the type of sample used. The plates were then incubated at 37 ^{o}C in a humidified atmosphere containing 5% CO_2 for 24 hours to achieve approximately 80% confluence. After this seeding period, the culture medium was replaced by DMEM supplemented with the different samples (filtered material extracts (0.45 μm pore size), microparticles (1 mg/mL) and

transwells containing 1 mg microparticles). The plates were incubated for 24 hours in the case of the extract samples and from 1 to 7 days in the case of the particular samples (transwells or directly added). The MTS test was performed according to the CellTiter 96 One Solution Proliferation Assay Kit (Pormega, USA) manufacturer's instructions and as described previously [43, 44]. The absorbance was determined in a microplate reader (EL 312e Biokinetics reader, Biotek Instruments, USA) at 490 nm. The results are expressed as the percentage (%) of cell viability in comparison with the 100% proliferation attributed to the positive control (fresh complete culture medium). Latex rubber extracts, produced by identical methodology as for the sample extracts, was used as negative control for the experiments where the extracts of the particles were analyzed. The samples were tested at least in triplicates per three independent experiments.

2.8.2 Cell proliferation

Cell morphology and proliferation changes as a result of the contact of the microparticles with the cells, were used to evaluate the biocompatibility and feasibility of the m-PCL microparticles. Two cell types were used in contact with the m-PCL particles, SaOs-2 and ASC. ASC are used because of the potential impact of isolating this cell type by this method as it is frequently used in regenerative medicine applications. Hence, the evaluation of the ASCs response to the m-PCL microparticles was of importance for their future application.

Cell proliferation is the measurement of the number of cells that are dividing in a culture over time. One way of measuring this parameter is by performing clonogenic assays, in which a defined number of cells are plated onto the appropriate matrix and the number of colonies that are formed after a period of growth are enumerated. In addition, some techniques also evaluating cell proliferation are based in the use of more indirect parameters, in which molecules that regulate the cell cycle are measured (e.g. CDK kinase assays). However, the measurement of DNA synthesis as a marker for proliferation is the most common used methodology. In this assay, labeled DNA precursors (e.g. 3H-thymidine or bromodeoxyuridine) are added to cells and their incorporation into DNA is quantified after incubation. The amount of labeled precursor incorporated into DNA is quantified either by measuring the total amount of labeled DNA in a population, or by detecting the labeled nuclei microscopically. Incorporation of the labeled precursor into DNA is directly proportional to the amount of cell division occurring in the culture [45]. During the course of this thesis, DNA based assay was selected to be use for cell proliferation studies.

Following the culture conditions already described for cell viability, a SaOs-2 and ASC cells suspensions were plated in 12-well plates (1 X 10^5 cells/mL, 1.5 mL per well). Twenty-four

hours after cell seeding, the culture medium was replaced by a 1 mg/mL suspension of the m-PCL microparticles. After different incubation time (1, 3 and 7 days), supernatants were removed and further analyses performed.

Cell proliferation was evaluated by quantifying the DNA content using PicoGreen ("dsDNA" quantification kit, Molecular Probes, USA) according to the manufacturer's instructions. This assay is based in the use of a fluorescent dye, PicoGreen, sensitive and specific for double-stranded DNA (dsDNA). Briefly, the cell monolayer was carefully washed with PBS buffer (0.01M, pH 7.4). The cells were then lysed by osmotic and thermal shock. The obtained supernatant was subjected to the DNA analysis. Fluorescence was measured (485 nm excitation and 528 nm emission) in a microplate reader and the DNA amounts calculated according to a standard curve. The samples were tested in triplicate in three independent assays.

2.8.3 Cell morphology

Changes in cell morphology constitute a strong indication of the cell responses to, either the contact with biomaterials or the stimulus by bioactive molecules. During the course of a cell culture experiments, the cell morphology is being constantly evaluated by visual observation indicating the status of the cells. A variety of dyes like methylene blue, trypan blue and neutral red are frequently used to visualize specific cellular components.

In this thesis, the morphology of ASCs was analyzed by microscopic observation after incubation with the m-PCL microparticles for 3 and 7 days. Prior observation, each well was washed with 0.1 M PBS and fixed with 2.5% glutaraldehyde solution in PBS (careful was taken to avoid the aspiration of the particles from the well). The cells were stained with 0.4% methylene blue and examined by light-microscopy (Axioplan imager Z1, Carl Zeiss, Germany). Methylene blue staining was used to better visualize the cells and to make the nuclei more visible. The analyzed samples were photographed using a high-resolution camera for image acquisition (Leica Microsystems GmbH, Germany).

2.9 Determination of the bioactivity of the encapsulated and released bioactive molecules

To evaluate the capability of developed carriers for the controlled release of biologically active agents, three different molecules were incorporated into microparticles: DEX and BMP-2 as osteogenic agents into SPCL microparticles; and GTM as an antibiotic into CHT-ST microparticles. Several parameters were evaluated to prove their feasibility as drug delivery systems as described earlier in this chapter (e.g. drug loading and encapsulation efficiency, release profile in different environment). Maintaining the activity of the bioactive

molecules upon the encapsulation process, during storage time, and during the *in vitro* release period is important.

2.9.1 DEX and BMP-2 release from SPCL microparticles: in vitro evaluation of their biological activity towards osteogenesis

Osteocalcin promotor activation assay. This experiment was performed to indirectly assess osteogenic differentiation. Cells were transfected using a vector expressing the osteocalcin (OCN) promoter coupled to a secretable metridia-luciferase. Activation of the OCN-promotor as a result of the release of DEX or BMP-2 results in luminescence that is indicative for osteogenesis.

In detail, 0.5 X 10^5 C2C12 cells/mL were plated in 24-well plates and incubated at 37 ^oC in a humidified environment containing 5% CO_2 for 24 hours. Subsequently, cells were transfected by standard lipofectamine transient transfection, using a vector expressing the osteocalcin (OCN) promotor driving the luciferase reportergene. Briefly, 1 µg of reporter vector DNA was used together with 2 µg of lipofectamine (Invitrogen, Germany) per well. The DNA was mixed with the lipofectamine transfection agent under serum free conditions following the manufacturer´s instructions. The cells were incubated with the transfection solution (37 ^oC, 5% of CO_2 humidified atmosphere) by using DMEM containing 5% FCS for 4 hours. Following transfection, the culture medium was replaced with DMEM supplemented with 1% FCS, 50 µM ascorbic acid and 10 mM β-glycerophosphate (osteogenic differentiation medium=OM). The cells were cultivated for another 24 hours. Finally, the culture medium was exchanged with different samples for bioactivity testing: *i)* collected supernatants from BMP-2 and DEX *in vitro* release, *ii)* a suspension of BMP-2 and DEX loaded microparticles in DMEM (1% FCS, OM) and *iii)* transwell inserts containing BMP-2 and DEX loaded microparticles. The amounts of microparticles used vary in the range of 1-10 mg/mL culture medium. During the following five days' observation period, the medium was not refreshed. At the end, both supernatants and cells were individually collected and stored at -80 ^oC for further analysis. The activation of the OCN-promotor was measured in the collected supernatants using luminescence imaging (Xenogen, USA) upon administration of luciferin (Figure 2.3). The amount of photons was measured and established a relative measure of OCN-promotor activity.

Alkaline phosphatase assay (ALP). Alkaline phosphatase is an enzyme involved in the initial process of bone extracellular matrix mineralization. Thus, during the occurrence of osteogenesis, ALP is expressed by cells which are in a more osteoblast differentiated stage. Consequently, it is regarded as an indicator of an osteoblastic phenotype. In our studies, the effect of the released DEX and BMP-2 on ALP activity was evaluated in C2C12 cells after five

days of incubation by the use of a p-nitrophenol (pNP) assay [46, 47]. This assay is based on the occurrence of hydrolysis of p-nitrophenyl phosphate (colorless compound) in the presence of alkaline phosphatase enzymes to yield free p-nitrophenol product (yellow). This product can be spectrophotometrically measured at 405 nm [47]. Briefly, cells were lysed by osmotic (0.25% Triton-X-100 in PBS) and heat shock. Subsequently, 50 µL substrate solution was added per well (containing p-nitrophenyl phosphate disodium salt) for 30 minutes at room temperature. The optical density was determined at 405 nm in a microplate reader and the activity of ALP calculated according to a standard curve. The standard curve was constructed by the use of pNP solutions of known concentrations.

In addition, the collected supernatants from the DEX release, as well as DEX loaded microparticles were tested in human ASCs for ALP activity to determine DEX bioactivity in primary stem cells.

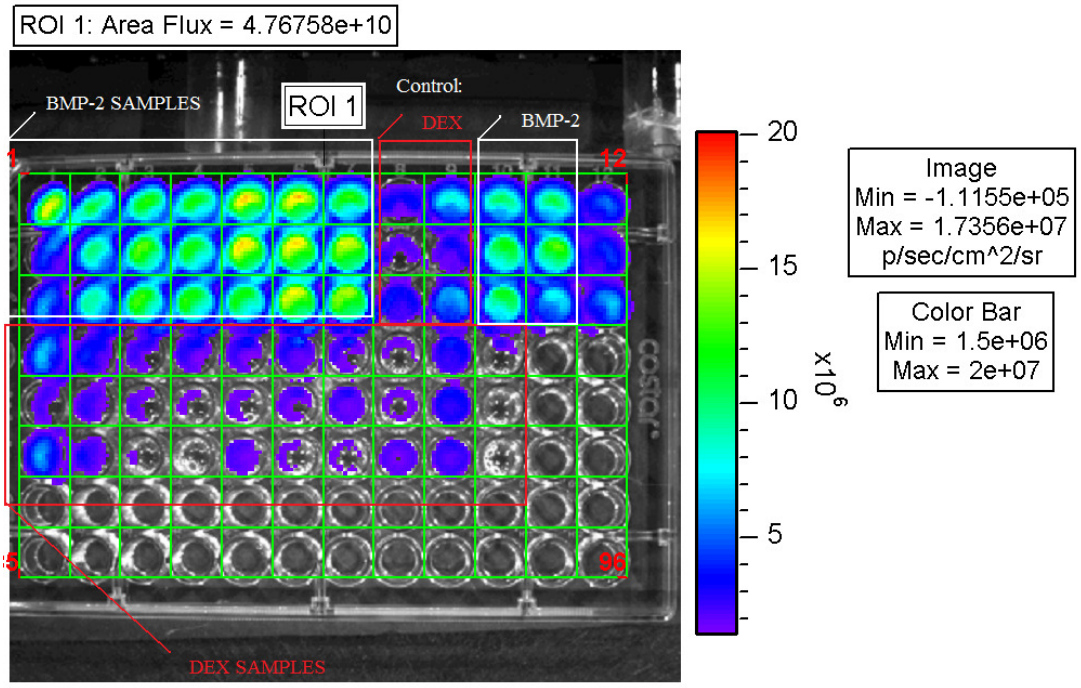

Figure 2.3 Representative luminescence image of analyzed samples

Mineralization assay. Mineralized matrix and calcium deposits were simultaneously evaluated by the use of von Kossa and Alizarin red staining as an indication of late osteogenic differentiation. Staining with the von Kossa method is a qualitative assay for mineralization. A positive reaction is manifested by brown or black staining, which in general can be identified together with the presence of bone nodules formation [47]. On the other hand, Alizarin red is

used to determine qualitatively and quantitatively, the presence of calcific deposition by cells of an osteogenic lineage.

C2C12 cells were seeded at a density of 0.5 X 10^4 cell/mL using OM supplemented with the DEX and BMP-2 loaded microparticles (1 mg/mL) up to 14 days. After 3, 7, 14 days of incubation, the cells were washed twice with PBS solution (without calcium and magnesium) and fixed with 4% formaldehyde solution in PBS. Von Kossa staining was performed to visualize the presence of mineralized deposits. The fixed cells were consecutively incubated with 5% silver nitrate solution in distilled water, 5% sodium carbonate solution in 25% formaldehyde and 5% sodium thiosulphate solution in distilled water. After washing the cells with distilled water, the staining was observed by phase contrast microscopy (Zeiss, Germany).

Alizarin red staining for detection of calcium deposits was performed by incubating fixed cells for 5 minutes in a 0.05% Alizarin red solution in PBS at room temperature. The stained cells were washed with distilled water prior microscopic observation.

2.9.2 GTM released from CHT-ST microparticles: in vitro evaluation of bioactivity

Aminoglycosidic antibiotics (e.g. gentamicin) are often administered clinically, alone or combined with other antimicrobial agents, for the treatment of severe bacterial infections. Therefore, in our study, we selected *Staphylococcus aureus*, a gram-positive bacterium, to test the bactericidal activity of released GTM. The standard antibiotic disc diffusion method [48] in LB-Agar was employed. Following this method, it is possible to determine the inhibition zones of the bacteria as a result of the released GTM from impregnated paper discs placed in the growth plates.

The strain used, *S. aureus* ATCC 25923, was obtained from the Biology Department, University of Minho, Braga, Portugal. Fresh isolates were cultured by plating a bacterial suspension (1.5 X 10^8 CFU/mL) on LB Agar in sterile Petri dishes for 24 hours at 37 ^oC (Luria-Bertani Agar, Lennox, Difco Laboratories, USA), immediately before each experiment. All collected samples from the GTM *in vitro* release experiments up to 30 days were diluted to 0.25 mg/mL with sterile PBS buffer. Subsequently, 13 mm sterile absorption discs (BBL™ Taxo™ PM Discs, BD Co., USA) were placed on the agar plates and 20 µL of each sample was directly pipetted onto each disc. A PBS impregnated disc was used as a negative control sample. A standard solution of gentamicin sulphate 0.25 mg/mL was applied as positive control. All agar plates were incubated at 37 ^oC for 16-18 h. Each sample was tested in triplicate, using different plates. After incubation, the diameters of the inhibition zone were measured using a micrometer.

From the relation between the diameter of inhibition zones of the samples (released GTM) and a standard GTM solution (considered standard for the maximum inhibition zone), the relative activity (%) can be determined [49].

$$\%\ \ Relative\,Activity = \left[\mathrm{IZ_s} / IZ_m\right] \times 100 \qquad (2.5)$$

Where IZ_s is the diameter of sample inhibition zone and IZ_m is the diameter of maximum inhibition correspondent to the standard GTM solution (0.25 mg/mL).

The stability of the GTM loaded CHT-ST microparticles upon storage was tested in well closed containers at 4 ^{o}C and 25 ^{o}C for different periods of time (2-12 weeks). Subsequently, samples were resuspended in sterile PBS and the *in vitro* release of GTM was analyzed, as well as the antibacterial activity of the released antibiotic.

2.10 REFERENCES

1. Reis, R. L.; Cunha, A. M. *Journal of Materials Science-Materials in Medicine* **1995**, 6 (12): 786-792.
2. Mano, J. F.; Koniarova, D.; Reis, R. L. *Journal of Materials Science-Materials in Medicine* **2003**, 14 (2): 127-135.
3. Mathew, S.; Brahmakumar, M.; Abraham, T. E. *Biopolymers* **2006**, 82 (2): 176-187.
4. Terbojevich, M.; Cosani, A.; Muzzarelli, R. A. A. *Carbohydrate Polymers* **1996**, 29 (1): 63-68.
5. Terbojevich, M.; Cosani, A. In *Chitin Handbook. European Chitin Society.*, Muzzarelli, R. A. A.; Peter, M., Eds. Atec Edizioni: Grottammare, Italy, **1997**; pp 87-108.
6. Lavertu, M.; Xia, Z.; Serreqi, A. N.; Berrada, M.; Rodrigues, A.; Wang, D.; Buschmann, M. D.; Gupta, A. *Journal of Pharmaceutical and Biomedical Analysis* **2003**, 32 (6): 1149-1158.
7. Kreuter, J. *Journal of Controlled Release* **1991**, 16 (1-2): 169-176.
8. Gref, R.; Minamitake, Y.; Peracchia, M. T.; Trubetskoy, V.; Torchilin, V.; Langer, R. *Science* **1994**, 263 (5153): 1600-1603.
9. Tuncel, A.; Ecevit, K.; Kesenci, K.; Piskin, E. *Journal of Polymer Science Part a-Polymer Chemistry* **1996**, 34 (1): 45-55.
10. Madan, T.; Munshi, N.; De, T. K.; Maitra, A.; Sarma, P. U.; Aggarwal, S. S. *International Journal of Pharmaceutics* **1997**, 159 (2): 135-147.
11. O'Donnell, P. B.; McGinity, J. W. *Advanced Drug Delivery Reviews* **1997**, 28 (1): 25-42.
12. Lin, W. J.; Yu, C. C. *Journal of Microencapsulation* **2001**, 18 (5): 585-592.
13. Soppimath, K. S.; Aminabhavi, T. M.; Kulkarni, A. R.; Rudzinski, W. E. *Journal of Controlled Release* **2001**, 70 (1-2): 1-20.
14. Lewis, D. H. In *Biodegradable Polymers as Drug Delivery Systems.*, Chasin, M.; Langer, R., Eds. Marcel Dekker, Inc.: New York, **1990**; pp 1-42.
15. Mi, F. L.; Tan, Y. C.; Liang, H. F.; Sung, H. W. *Biomaterials* **2002**, 23 (1): 181-191.
16. He, P.; Davis, S. S.; Illum, L. *International Journal of Pharmaceutics* **1999**, 187 (1): 53-65.
17. Speer, D. P.; Chvapil, M.; Eskelson, C. D.; Ulreich, J. *Journal of Biomedical Materials Research* **1980**, 14 (6): 753-764.
18. Mulhbacher, J.; Ispas-Szabo, P.; Lenaerts, V.; Mateescu, M. A. *Journal of Controlled Release* **2001**, 76 (1-2): 51-58.

19. Lim, S. T.; Martin, G. P.; Berry, D. J.; Brown, M. B. *Journal of Controlled Release* **2000**, 66 (2-3): 281-292.
20. Ehrenfreund-Kleinman, T.; Gazit, Z.; Gazit, D.; Azzam, T.; Golenser, J.; Domb, A. J. *Biomaterials* **2002**, 23 (23): PII S0142-9612(02)00209-0.
21. Hermanson, G. In *Bioconjugate Techniques*, 1st ed.; Academic Press, Inc.: San Diego, CA, **1996**; pp 114-116.
22. Baran, E. T.; Mano, J. F.; Reis, R. L. *Journal of Materials Science-Materials in Medicine* **2004**, 15 (7): 759-765.
23. Hamoudeh, M.; Fessi, H. *Journal of Colloid and Interface Science* **2006**, 300 (2): 584-590.
24. Yang, J.; Park, S. B.; Yoon, H. G.; Huh, Y. M.; Haam, S. *International Journal of Pharmaceutics* **2006**, 324 (2): 185-190.
25. Ramirez, L. P.; Landfester, K. *Macromolecular Chemistry and Physics* **2003**, 204 (1): 22-31.
26. Landfester, K.; Ramirez, L. P. *Journal of Physics-Condensed Matter* **2003**, 15 (15): S1345-S1361.
27. Zhu, Y. B.; Gao, C. Y.; Liu, X. Y.; Shen, J. C. *Biomacromolecules* **2002**, 3 (6): 1312-1319.
28. Larson, B. J.; Helgren, J. M.; Manolache, S. O.; Lau, A. Y.; Lagally, M. G.; Denes, F. S. *Biosensors & Bioelectronics* **2005**, 21 (5): 796-801.
29. Ortega-Vinuesa, J. L.; Bastos-González, D.; Hidalgo-Álvarez, R. *Journal of Colloid and Interface Science* **1995**, 176 (1): 240-247.
30. Peula, J. M.; Hidalgo-Alvarez, R.; Nieves, F. J. D. *Journal of Colloid and Interface Science* **1998**, 201 (2): 132-138.
31. Hungerford, G.; Benesch, J.; Mano, J. F.; Reis, R. L. *Photochemical & Photobiological Sciences* **2007**, 6 (2): 152-158.
32. Kaiser, E.; Colescott, R. L.; Bossinger, C. D.; Cook, P. I. *Analytical Biochemistry* **1970**, 34 (2): 595-598.
33. Moore, S.; Stein, W. H. *The Journal of Biological Chemistry* **1948**, 176 (1): 367-88.
34. Sun, S. W.; Lin, Y. C.; Weng, Y. M.; Chen, M. J. *Journal of Food Composition and Analysis* **2006**, 19 (2-3): 112-117.
35. Santiago, L. Y.; Nowak, R. W.; Rubin, J. P.; Marra, K. G. *Biomaterials* **2006**, 27 (15): 2962-2969.
36. Cabanillas, P. F.; Pena, E. D.; Barrales-Rienda, J. M.; Frutos, G. *International Journal of Pharmaceutics* **2000**, 209 (1-2): 15-26.
37. Wang, S. B.; Chen, A. Z.; Weng, L. J.; Chen, M. Y.; Xie, X. L. *Macromolecular Bioscience* **2004**, 4 (1): 27-30.
38. Silva, G. A.; Costa, F. J.; Neves, N. M.; Coutinho, O. P.; Dias, A. C. P.; Reis, R. L. *Journal of Biomedical Materials Research Part A* **2005**, 73A (2): 234-243.
39. Ghose, T. K. *Pure and Applied Chemistry* **1987**, 59 (2): 257-268.
40. Reis, R. L.; Mendes, S. C.; Cunha, A. M.; Bevis, M. J. *Polymer International* **1997**, 43 (4): 347-352.
41. Silva, G. A.; Marques, A. P.; Gomes, M. E.; Coutinho, O. P.; Reis, R. L. In *Biodegradable Systems in Tissue Engineering and Regenerative Medicine*, Reis, R. L.; San Roman, J., Eds. CRC Press: Boca Raton, FL, **2005**; pp 339-353.
42. Zeltinger, J.; Sherwood, J. K.; Graham, D. A.; Mueller, R.; Griffith, L. G. *Tissue Engineering* **2001**, 7 (5): 557-572.
43. Salgado, A. J.; Coutinho, O. P.; Reis, R. L. *Tissue Engineering* **2004**, 10 (3-4): 465-474.
44. Marques, A. P.; Reis, R. L.; Hunt, J. A. *Biomaterials* **2002**, 23 (6): 1471-1478.
45. Roche-Applied-Science. In *Apoptosis, cell death, and cell proliferation manual*, 3rd edition ed.; Rode, H.-J.; Eisel, D.; Frost, I., Eds. Roche Diagnostics GmbH, Roche Applied Science: Mannheim, Germany, **2004**; pp 78-108.
46. Lian, J. B.; Stein, G. S. *Critical Reviews in Oral Biology & Medicine* **1992**, 3 (3): 269-305.

47. Lennon, D. P.; Caplan, A. I. In *Culture of cells for tissue engineering*, Vunjak-Novakovic, G.; Freshney, R. I., Eds. John Wiley & Sons, Inc.: New Jersey, **2006**; pp 23-59.
48. *Performance Standards for Antimicrobial Disk Susceptibility Tests; Approved Standard-Tenth Edition*; M02-A10; Clinical and Laboratory Standards Institute (CLSI) or NCCLS document: V29, No.1, **2008**; pp 3-27.
49. Liu, S. J.; Chi, P. S.; Lin, S. S.; Ueng, S. W. N.; Chan, E. C.; Chen, J. K. *International Journal of Pharmaceutics* **2007**, 330 (1-2): 45-53.

Chapter 3

Highly biodegradable starch-conjugated chitosan microparticles as carrier for the controlled release of antibiotic drugs: Preparation, characterization and *in vitro* release study

3.1 ABSTRACT

Starch-conjugated chitosan microparticles (CHT-ST) were produced aimed to be used as a carrier for the long term sustained/controlled release of antibiotic drugs. The microparticles were prepared by a reductive alkylation crosslinking method, starting with the oxidation of soluble starch to produce the polyaldehyde, followed by a water-in-oil (w/o) emulsion crosslinking technique. The morphology of the microparticles was examined by light transmission microscopy (LM) and scanning electron microscopy (SEM). The obtained microparticles showed a spherical shape, with a slightly rough and porous surface, and a size range of 80-150 µm. Gentamicin (GTM), an aminoglycosidic antibiotic with a broad spectrum, was entrapped into the CHT-ST microparticles and its release profile was studied *in vitro*. ^{1}H-NMR spectroscopic technique was performed to characterize the system and the possible changes in the microparticles chemical structure upon GTM encapsulation. Increasing concentrations of GTM (from 50 to 150 mg/mL), led to a decrease in the encapsulation efficiency (from 67 to 55%), while drug loading increased from 4 to 27%. A sustained release of GTM was observed over a period of 30 days. The release kinetics could be controlled using an ionic crosslinker agent. For instance, the drug release can be prolonged by increasing the ionic crosslinking density. In addition, a bacterial inhibition test on *Staphylococcus aureus* was conducted to determine the relative bactericidal activity of the released GTM. The diameter of the sample inhibition zone ranged from 12 to 17 mm, which is corresponding with 70 to 100% of relative activity. The released concentration of GTM was found to be well above the literature reported minimal inhibition concentration (MIC).

***This chapter is based on the following publication:**

Balmayor, *E. R.;* Baran, E. T.; Azevedo, H. S.; Reis, R. L. Highly biodegradable starch-conjugated chitosan microparticles as carrier for the controlled release of antibiotic drugs: Preparation, characterization and *in vitro* release study. **2009. Submitted.**

3.2 INTRODUCTION

Polysaccharides are very attractive materials for biomedical applications due to their unique properties. They are usually abundant in nature, being obtained from renewable sources, and have been shown to be non toxic and biocompatible [1, 2].

Chitin and starch are among the most widespread polysaccharides in nature [3]. Chitin (poly β-(1-4) N-acetyl-D-glucosamine), is synthesized by a diverse number of living organisms from arthropods, crustaceans (crab and shrimp shells), to cell walls of fungi [4]. Chitosan is a product of partial chitin deacetylation and can be defined as a copolymer of D-glucosamine and N-Acetyl-D-glucosamine [5, 6]. It is one of the biomaterials most studied and proposed to be used in a broad range of biomedical applications [7, 8] because of its biocompatible, biodegradable and non toxic well demonstrated properties [8, 9]. Starch is cheap, abundant and edible polysaccharide, with interesting biodegradable properties [10-12]. It contains a mixture of two molecules: amylose and amylopectin. Depending on the starch source, the relative weight percentages of those molecules varies between 72-82% amylopectin, and 18-33% amylose [13, 14]. Amylose is responsible for the film forming capability of starches [15]. The use of those natural macromolecules has been proposed for microencapsulation of bioactive materials [16] and as a carrier in drug delivery systems [17-19].

Blends of natural polysaccharides are promising systems for the production of films, sponges, hydrogels, micro- and nanoparticles for the encapsulation of drugs, enzymes or cells [20]. Furthermore, in most cases the presence of natural polysaccharides in blend compositions enhances biocompatibility and biodegradability, and confers hydrophilicity to the resulting systems. A highly desired property for a biomaterial proposed for biomedical and a drug delivery application is biodegradability within body fluids [21].

The use of medical drugs in a safe manner for treating diseased parts of the human body requires the development of new carrier systems capable of improving their release profile, while maximizing its therapeutic effect. Aminoglycoside antibiotic drugs have shown low effectiveness when administered orally [22]. Typically the human body deals reasonably well with this type of drugs, allowing their rapid clearance from the body. They are absorbed from the small intestine and inactivated very fast in the liver [23]. Therefore, the route of their administration can only be done intravenously, intramuscularly or topically [22], with the inconvenience of fast elimination and the need for repetitive dosages. Consequently, the development of novel drug compositions for the sustained release of this type of drugs is thus of great interest.

One member of the group of aminoglycoside antibiotics is Gentamicin (GTM). Besides its wide antibacterial spectrum, GTM is one of the few heat stable antibiotics that remains active even after heating [24]. This fact makes GTM a very useful antibiotic for drug formulations that requires the use of high temperatures during the manufacturing/ encapsulation process.

In the present study, a novel injectable long term drug delivery system with increased biodegradation has been developed based on the conjugation of starch with chitosan. In addition, the developed system was shown to be capable of releasing initially a large dose of antibiotic and then sustain its release, therefore providing an effective method to treat locally bacterial infections.

3.3 EXPERIMENTAL

3.3.1 Materials

Chitosan (medium molecular weight), sodium tripolyphosphate (TPP) (technical grade, 85%), mineral oil (puriss. p.a.), sodium periodate (ACS reagent, > 99.8%), deuterium oxide (D_2O) (99.9% D) and deuterium chloride (DCL) (35 wt %, 99% D) were obtained from Sigma-Aldrich (USA). Soluble potato starch was supplied by ATO (The Netherlands). Gentamicin sulfate from *Micromonospora purpurea* (GTM, puriss. p.a.) was purchased from Fluka-Bio Chem. (Switzerland). All other chemicals were of analytical grade and used as received.

The determination of chitosan molecular weight (MW) was conducted by viscosimetric method [15], using 0.3 M acetic acid/ 0.2 M sodium acetate as a solvent mixture. The viscosity average molecular weight (MW) was calculated based on the Mark-Houwink equation [25, 26]. The MW of the chitosan was found to be 385 kDa. The degree of N-deacetylation of the chitosan was determined by ^{1}H-NMR sprectroscopy method [27], and was found to be 81.25%.

3.3.2 Preparation of CHT-ST microparticles

3.3.2.1 Sodium periodate oxidation of soluble starch

The oxidation reaction of soluble starch was performed according to a procedure previously described [28]. Briefly, soluble starch was dissolved in distilled water (0.02 g/mL) in a light protected glass vessel. 0.125 mL of sodium iodate (10 mg/mL) was added per mL of starch solution, allowing the reaction to proceed for 30 minutes at room temperature under slow magnetic stirring. Finally, glycerin (0.1 mL/mL solution) was added and stirred for additional 10 minutes. The solution was transferred into a dialysis tube (Dialysis tubing cellulose membrane, MWCO 12 kDa, Sigma-Aldrich, USA) and dialyzed against distilled water for two days with several daily changes. The oxidized starch solution was concentrated by

using an ultra-concentrator Amicon® stirred cell 8010 (Millipore, USA) and stored at 4 °C in a light protected glass vessel until further use.

3.3.2.2 CHT-ST microparticles preparation

CHT-ST microparticles were prepared by water-in-oil emulsification methods, using reductive alkylation crosslinking procedure [29]. The preparation procedure is illustrated in Figure 3.1. Chitosan solution 1.5% (w/v) was prepared by dissolving the polymer in aqueous acetic acid solution (1%). Chitosan (1.5%, 10 mL) and oxidized starch (2% (w/v), 10 mL) solutions were mixed throughly using magnetic stirring, and the pH adjusted to 5.5 by using 0.5 M NaOH. The polymer solution was put dropwise into a glass reactor containing mineral oil with 1% of Tween 80 and emulsified with a top stirrer at 600 rpm for 30 minutes. After emulsion formation, 30 mL of cold acetone was added slowly and allowed to proceed for two hours. The microparticles were removed from the reaction medium by filtration and washed with distilled water/acetone mixture (1:1 v/v). After drying at room temperature, the microparticles were transfered to a 0.5 M sodium carbonate buffer solution (pH 8.5) and incubated for three hours to allow the conjugation between reactive aldehyde groups (Starch) and primary amino groups (Chitosan). After repeatedly washing with distilled water, the microparticles were incubated in sodium borohydride solution (0.05% w/v) for one hour to reduce excess of reactive aldehyde groups, and to confer stabilization to the imine conjugation (ST-CHT) into covalent bonds.

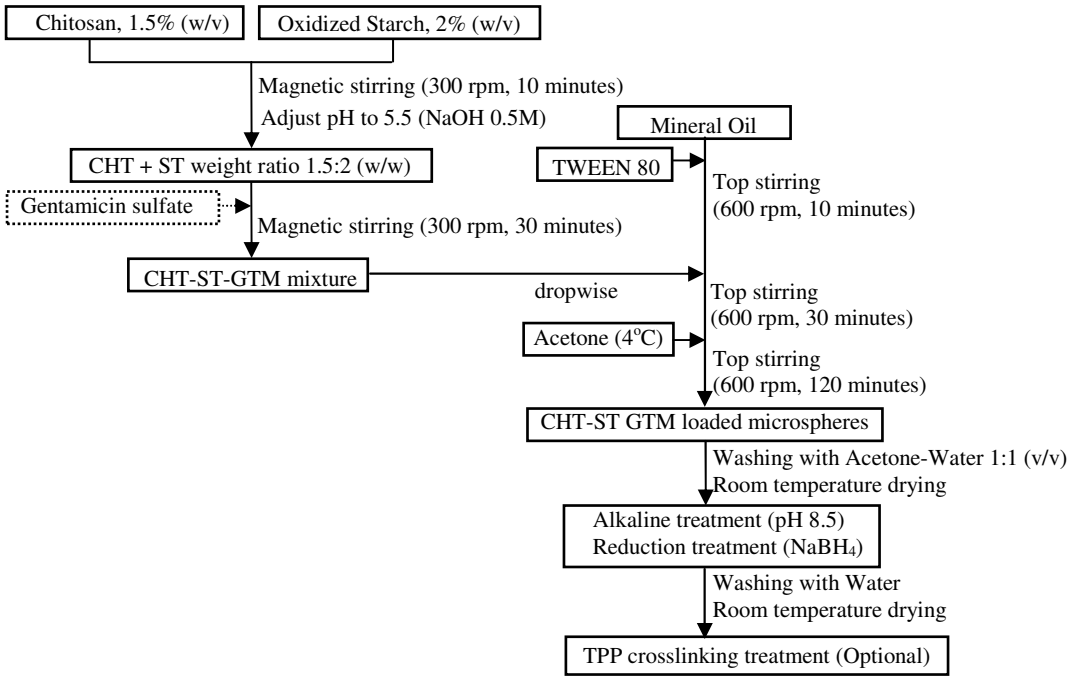

Figure 3.1 Schematic diagram showing the developed preparation procedure of chitosan-starch microparticles

3.3.3 Physicochemical characterization

3.3.3.1 Light transmission (LM) and scanning electron microscopy (SEM)

The morphology and size of the dried microparticles were analyzed by light transmission microscopy (LM) and scanning electron microscopy (SEM). A microparticles suspension (5 mg/mL) was photographed using an optical microscopy Olympus BH2 with polarized light source (Olympus, Japan), using a high-resolution Leica camera for image acquisition (Leica Microsystems GmbH, Germany). For SEM observation, the microparticles were mounted onto metal stubs with a carbon tape and gold sputter-coated (Sputter Coater SC502, Fisons Instruments, UK). The size, shape and surface morphology of the microparticles were analysed with SEM (Leica Cambridge S-360, UK).

3.3.3.2 Size distribution

In order to determine the size distribution of the microparticles obtained under the different experimental conditions, a dry sample was weighed and then separated through a series of standard sieves (20, 60, 100, 125, 150, 250, 450, 500, 650, 900 and 1000 μm, Linker Industrie-Technik, Germany). The microparticle fraction that has been retained on sieve with certain porous size was collected and weighed, and finally correlated with the total mass of the microparticles.

3.3.3.3 Nuclear magnetic resonance spectroscopy (^{1}H-NMR)

^{1}H-NMR spectra were acquired on a Varian Unit Plus 300 MHz spectrometer (USA). For all the samples the following experimental parameters were used: 256 scans were recorded, 5200 Hz filter width, 90^o pulse corresponding to a pulse width of 11 μs, 4 s relaxation delay. The experiments were run at 60 ^{o}C. For quantitative analysis, the peak area method was used and the start and end points of the integration of each peak were selected manually. For the sample preparation, 10 mg of each sample were exactly weighed into a NMR tube (ϕ=0.3 mm) and 1 mL of deuterated solvent was added. Chitosan and CHT-ST microparticles were dissolved in 0.98 mL of D_2O and 0.02 mL of DCL, waiting for complete dissolution, and starch and GTM were dissolved in D_2O. The sample was sonicated at room temperature for 30 min and used for ^{1}H-NMR measurement.

3.3.4 Gentamicin loading

For drug encapsulation, GTM was directly added to the polymer solution using various initial concentrations of GTM (5, 10 and 15 mg/mL of polymer solution) to determine the

influence of drug concentration in the encapsulation efficiency (EE). The preparation of the GTM loaded microparticles was performed as described in section 3.3.2.2 (Figure 3.1). Furthermore, the effect of ionic crosslinking on the drug loading/release was investigated. In order to allow microparticles to be further ionic crosslinked, the GTM loaded microparticles were immersed into three different concentrations of sodium tripolyphosphate (TPP) solution (0.5, 1, 2% w/v) for 30 minutes. The microparticles were then removed by filtration and washed several times with distilled water and allowed to dry at room temperature. The reaction medium and washing solutions were stored at 4 ^{o}C until further quantification for unloaded GTM. The initial concentration of GTM used for the crosslinking studies was 15 mg/mL. Encapsulation procedures for each employed GTM initial concentration were performed in triplicate.

3.3.5 *In vitro* drug release studies

Pre-weighed GTM loaded CHT-ST microparticles were suspended in 0.01 M PBS (pH 7.4) using a solid:liquid weight ratio of 2.5:1 (mg/mL). The microparticles were maintained at 37 ^{o}C under constant agitation (50 rpm) for 30 days in a shaking water bath. At predetermined time points, 1 mL aliquots were taken and replaced with same volume of fresh PBS solution. All the release experiments were carried out in triplicate, using unloaded CHT-ST microparticles as control.

3.3.5.1 Quantitative analysis of the released GTM

An indirect spectrophotometric method was used for the quantification of GTM, using o-phtaldialdehyde as derivatizing agent [24]. The procedure can be described as follows: o-phtaldialdehyde (0.25 g) was dissolved in a mixture of methanol (6.25 mL) and 2-mercaptoethanol (0.3 mL). The resulting solution was mixed with 0.04 M sodium borate (56 mL, pH 8) buffer solution. For the colorimetric measurement, GTM solution, o-phtaldialdehyde reagent and isopropanol were mixed in an equal volume ratio, and incubated for 30 minutes at room temperature. The absorbance was then measured at 332 nm. The concentration of GTM was calculated by using a calibration curve.

For the determination of the encapsulation efficiency and GTM loading into the microparticles, the amount of the drug remaining in the reaction medium during the loading process was quantified according to known equations [30].

3.3.6 Microbiological determination of the activity of released GTM: *in vitro* evaluation

The GTM released from the CHT-ST microparticles was tested for bactericidal activity using *Staphylococcus aureus* as a pathogenic microorganism. Standard strain of *S. aureus* ATCC 25923 (American Type Culture Collection) was obtained from the Department of Biology, University of Minho, Braga, Portugal.

Fresh isolates were cultured for 24 hours at 37 ^{o}C in LB-Agar (Luria-Bertani Agar, Lennox, Difco Laboratories, USA), immediately before each experiment.

3.3.6.1 Susceptibility study: Determination of inhibition zones

The standard antibiotic disc diffusion method [31] in LB-Agar was employed for the assessment of the *in vitro* activity of the released GTM against the selected bacteria, by determination of the inhibition zones. For this, a bacteria suspension with concentration in the range of 1.5 X 10^{8} UFC/mL was seeded in LB Agar sterile Petri dishes. All samples (released GTM solutions from the microparticles up to 30 days) were diluted to 0.25 mg/mL with sterile PBS buffer. Subsequently, 13 mm sterile absorption discs (BBL^{TM} Taxo^{TM} PM Discs, BD, USA) were placed on the agar plates and 20 µL of each sample was directly pipetted onto each disc. A disc impregnated with a solution of sterile PBS was used as control sample, and a standard solution of gentamicin sulfate 0.25 mg/mL was also tested. All agar plates were incubated at 37 ^{o}C for 16-18 h. Each sample was tested in triplicate, using different plates. After incubation, the diameters of the inhibition zone were measured using a micrometer.

From the relation between the samples diameter of inhibition zones (GTM released) and a standard GTM solution (considered standard for the maximum inhibition zone), the relative activity (%) can be determined [32].

3.3.6.2 Short term stability testing: encapsulated GTM activity

For the stability tests, GTM loaded CHT-ST microparticles were stored in a well closed container at 4 ^{o}C and 25 ^{o}C for different periods of time (2, 4, 8 and 12 weeks). After each time point, samples were resuspended in sterile PBS and the *in vitro* release of GTM was analyzed, as well as the microbiological activity of the released antibiotic following the described techniques above.

3.4 RESULTS AND DISCUSSION

3.4.1 Preparation and characterization of CHT-ST GTM loaded microparticles

In this study, CHT-ST microparticles were developed by means of combining two natural origin biodegradable polymers in order to enhance biodegradability of the carrier

system under physiological conditions. In addition, other important properties for their use as delivery vehicles for aminoglycoside antibiotics were investigated, namely adequate microparticle size and morphology (suitability to be used as injectable system), encapsulation efficiencies, controlled release and satisfactory activity of the released drug.

The morphology, shape and size of unloaded and GTM loaded microparticles were analyzed by LM and SEM (Figure 3.2).

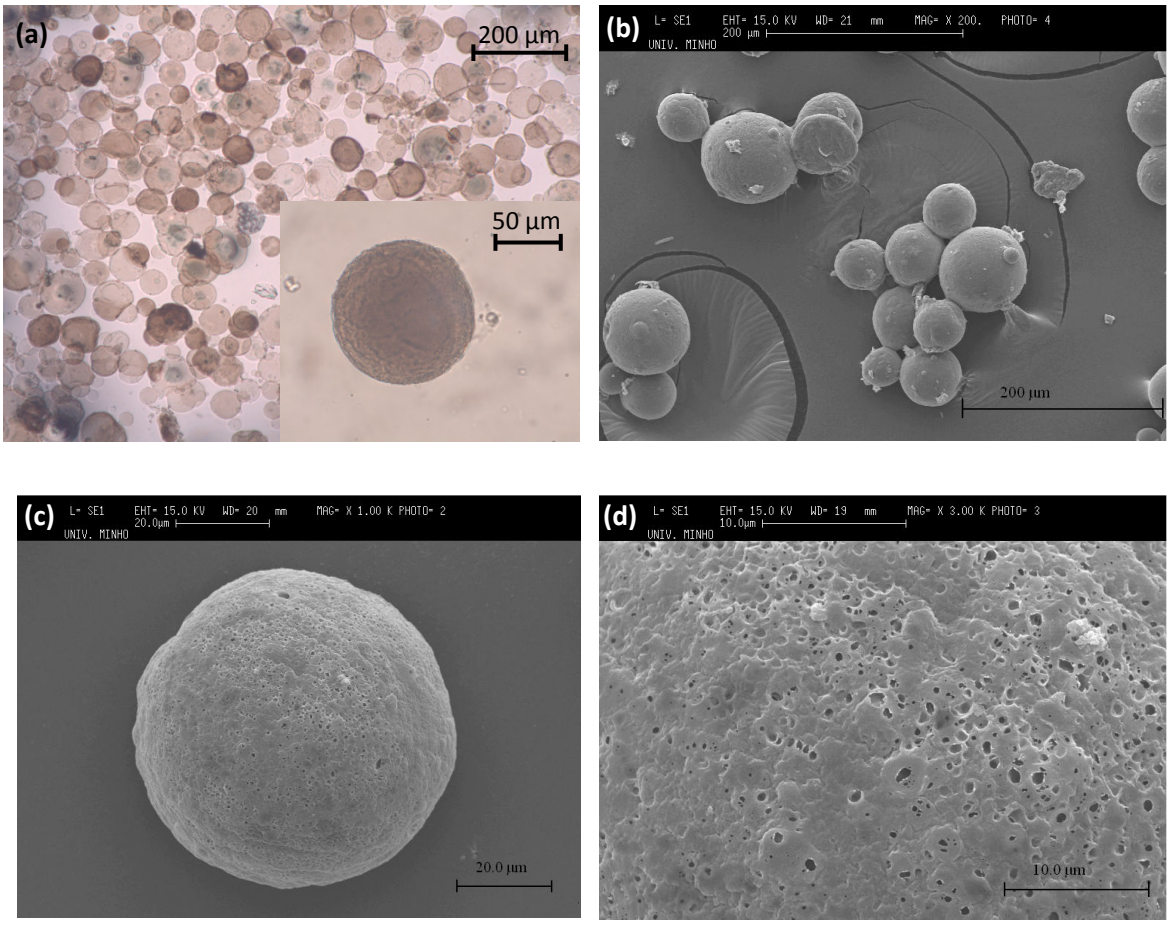

Figure 3.2 Morphological characterization of the chitosan-starch microparticles. Polarized LM images of the obtained microparticles **(a)**. SEM micrographs of gentamicin loaded microparticles: magnifications 200X **(b)**, 1000X **(c)**, 3000X **(d)**

The general features of the obtained CHT-ST microparticles can be observed in Figure 3.2 (a). In this general view, it can be observed the spherical shape presented by the obtained microparticles, which was further confirmed by SEM analysis. In addition, at higher magnification is possible to observe in more detail a single microparticle with a diameter of about 100 µm (Figure 3.2 (c)) showing a slightly rough surface and the presence of small pores (around 1 µm size, Figure 3.2 (d)). No evident differences were observed between unloaded

and GTM loaded microparticles. GTM loaded microparticles maintained the initial spherical shape and morphological characteristics of unloaded microparticles.

The particles have a narrow size distribution (Figure 3.3). Almost 60% of the microparticles are smaller than 100 µm, around 15% are in the range 100-150 µm, and less than 7% are smaller than 60 µm. Thus, a highly homogeneous microparticular system was obtained.

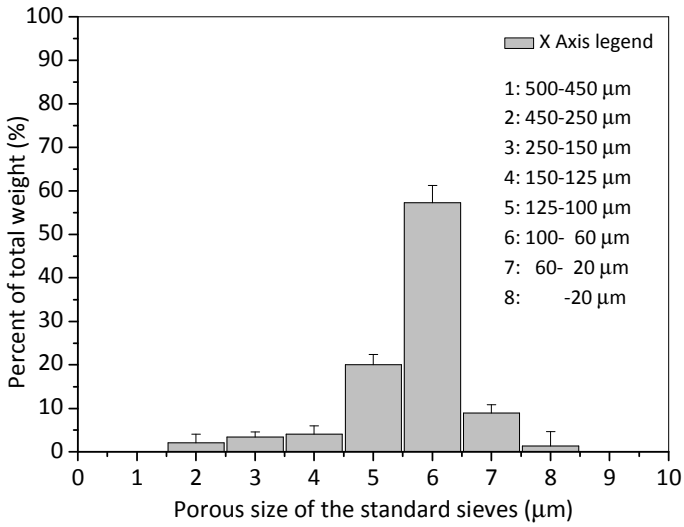

Figure 3.3 Chitosan-starch particle size distribution. The graph shows the results for the unloaded microparticle sample (CS, Table 3.1)

3.4.2 Spectroscopic characterization of CHT-ST GTM loaded microparticles

^{1}H-NMR spectroscopy was performed to confirm the presence of both polysaccharides in the obtained microparticles and analyze their chemical structure in the formulation. At the same time, the presence of GTM into the microparticles and possible chemical interactions between polymers and drug were also analyzed.

GTM can be identified in the spectrum of loaded microparticles (Figure 3.4 (a) and (b)). GTM, as a complex mixture of several compounds [33, 34], gives a very complex ^{1}H-NMR spectrum but exhibiting characteristic peaks (Figure 3.4 (b)) [35, 36]. From the obtained spectrum, it is possible to identify the main signals as a result of the presence of GTM in the developed microparticles. The presence of both polysaccharides (chitosan and starch) as components of the polymeric matrix was also identified in the microparticles spectrum. For chitosan (Figure 3.4 (c)) a typical doublet peak, as result of the presence of the deacetylated

unit at 5.04 ppm, and a peak (singlet) at 2.18 ppm from the acetylated residue, can be found in the resulting microparticles spectrum (Figure 3.4 (a)) [37, 38]. Finally, as result of the presence of the starch in the composition of the microparticles, an intense signal at 5.6 ppm can be assigned to the anomeric proton from the α(1→4) linkages of the amylose molecules in the starch structure [39-41].

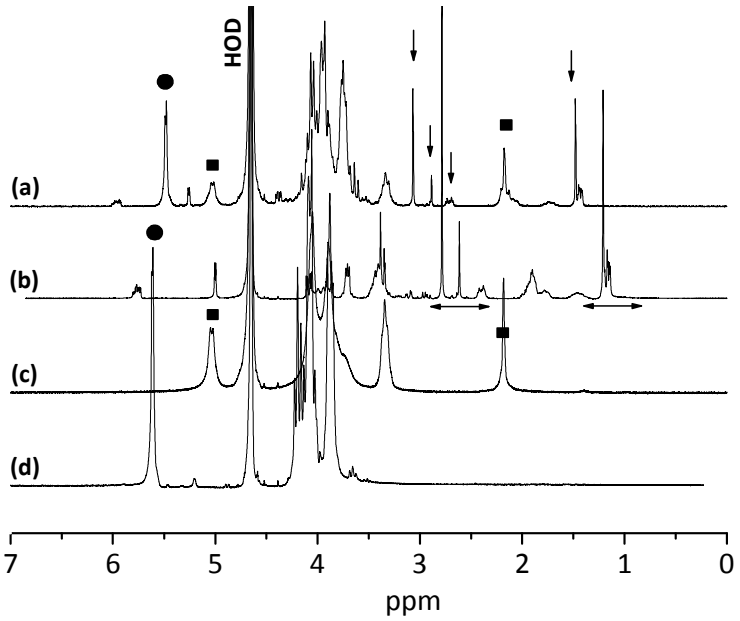

Figure 3.4 ^{1}H-NMR spectra of gentamicin loaded microspheres ↓ **(a)**, Gentamicin sulfate ↔ **(b)**, Chitosan ■ **(c)** and Starch ● **(d)**. Assigned to gentamicin sulfate the signals at 2.7 and 2.6 ppm, singlets resulting from the protons in the amino methyl groups present in the garosamine and purpurosamine components of gentamicin and a very intense peak at 1.2 ppm assigned to the methyl groups of garosamine molecules [32-36]

Obviously, the chemical shifts do not match exactly with the shift of the GTM and starch in aqueous solution, due to the pH of the solvent used (D_2O with 2% of DCL). There were no changes on the signals in the loaded microparticles spectra. Moreover, no new peaks have appeared in the spectra when comparing with the polymers used and drug to be loaded spectrum, indicating that no noticeable interaction between the drug encapsulated with the polymeric matrix had occurred. This may indicate that the drug loading and *in vitro* release is not expected to be affected by any possible chemical interaction between drug and polymer chemical groups.

3.4.3 GTM loading into microparticles

3.4.3.1 Determination of drug loading and encapsulation efficiency of GTM. Effect of the initial drug concentration

The drug loading and encapsulation efficiency (EE) are very important determinations to be made when developing systems for the controlled release of drugs [30]. Higher values of EE are desirable, from the economical point of view and also because lower amounts of microparticles will be necessary, minimizing the amount of foreign material introduced into the patients. In order to maximize EE, several approaches have been used, including different methods for drug loading [42, 43], the use of charged groups in the polymer [44], increasing drug solubility and its initial concentration [45, 46], among others.

As expected, the drug loading increased significantly (from 4.8 to 27.1%) when GTM concentration increases from 5 to 15 mg/mL in the polymer solution, leading to a decrease in the EE (from 67.2 to 55%) (Table 3.1, Figure 3.5).

Table 3.1 Experimental conditions for the preparation of gentamicin loaded chitosan-starch microparticles. Values of encapsulation efficiency (EE, %), drug loading (%) and kinetic parameters obtained for the developed microparticular system

Sample	GTM (mg/mL)	TPP (%)	Size (μm)	GTM loading (%)	EE (%)	Diffusion exponent *n* (r)
CS[a]	-	-	96.1±12.4	-	-	-
CSG[b]-1	15	**-**	119.4±8.3	n.d.	n.d.	0.68 (0.9998)
CSG-2	**5**	-	103.7±22.9	4.86±1.74	67.24±3.11	n.d.
CSG-3	**10**	-	111.5±18.5	11.14±2.21	60.97±2.08	n.d.
CSG-4	**15**	-	116.6±31.8	27.14±1.98	55.01±2.65	n.d.
CSGT[c]-5	15	**0.5**	89.3±28.6	n.d.	n.d.	0.60 (0.9980)
CSGT-6	15	**1**	80.4±22.3	n.d.	n.d.	0.59 (0.9812)
CSGT-7	15	**2**	81.1±17.9	n.d.	n.d.	0.54 (0.9971)

Common experimental conditions for all experiments:
CHT-ST: 1.5:2 (w/w). Volume of polymer solution: 10 mL
Mineral Oil 70 mL (1% Tween 80, (v/v))
Stirring rate: 600 rpm
[a]CS-chitosan-starch microparticles
[b]CSG-gentamicin loaded chitosan-starch microparticles
[c]CSGT- gentamicin loaded chitosan-starch microparticles ionically crosslinked with TPP
n.d.- not determined

This is a predictable consequence of the increment of the initial amount of drug, which causes a gradual increment of the drug loading until a saturation level is achieved. Moreover, increasing the initial amount of the drug into the polymer solution, the partition of hydrophilic drug molecules solubilized in surrounding aqueous solution increases, which can explain the resulting decrease on the EE. Finally, it must be considered that during encapsulation processes, and when using polymeric microparticles, there is a saturation level for the drug to

be entrapped within the polymer droplets during the emulsion formation, and as a result the encapsulation becomes more difficult with the increments on the initial drug concentration.

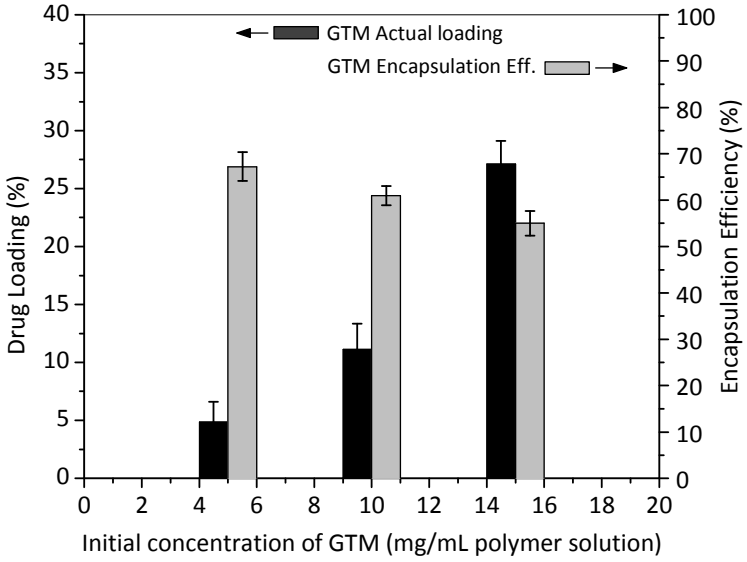

Figure 3.5 Effect of initial gentamicin concentration on encapsulation efficiency and drug loading

3.4.4 GTM release study

3.4.4.1 Release profiles and TPP concentration effect

Generally, three main stages are observed in a typical release pattern of bioactive compounds from biodegradable polymeric matrices [47]. The first stage is characterized by a burst release, due to the rapid diffusion of the bioactive agent located closer to the surface of the polymeric matrix and desorption of closely bound drug. The contact of the polymeric matrix with the release medium results in the swelling of the matrix (which strongly depends on the hydrophilic groups of polymer and crosslinking degree), allowing the drug encapsulated inside to start to diffuse through the polymer into the external environment (second stage). Finally, the polymer degradation starts to control the release process allowing the initial solubilization of the matrix and the release of the remaining bioactive agent occurs as the polymer is eroded. Consequently, two important properties of the system play a significant role in the release kinetics: the solubility of the bioactive agent into the surrounding medium, and the rate of polymer degradation. These release stages have been previously observed by other authors [48-50].

In this case, GTM is highly soluble in aqueous solutions and, as a result, the entrapped GTM molecules diffused rapidly into the external aqueous solution (Figure 3.6 (b)). About 54%

of the encapsulated drug is released in the first 24 hours. The burst release was observed to be followed by two sustained release stages. During the first nine days, 73% of the total entrapped GTM was released, being the remaining drug slowly released in the subsequent days. The second stage may be controlled by the swelling of the polymeric matrix (highly hydrophilic in this case) allowing aqueous solution to penetrate through the polymer, resulting in the diffusion of the GTM to the medium. Lastly, as result of the extended contact of the polymeric matrix with the surrounding medium, the polymer degradation (by hydrolysis mainly) starts to takes place, allowing the remaining drug to be released. After 30 days, 82% of drug was released (Figure 3.6 (b)).

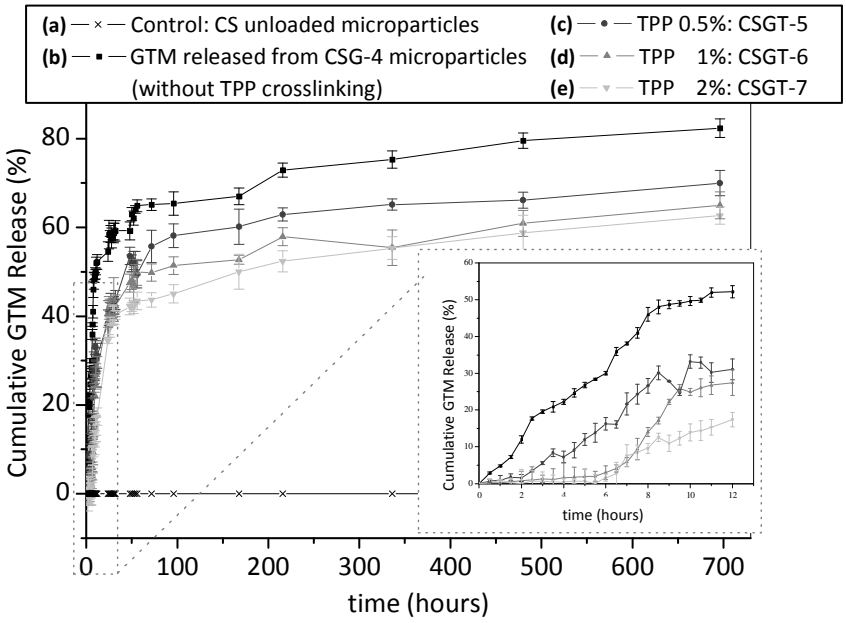

Figure 3.6 Release profiles of gentamicin from chitosan-starch microparticles. Influence of tripolyphosphate crosslinking concentrations on the gentamicin release profiles **(c), (d), (e)**. The first 24 hours of release is enlarged for all the conditions (please see Table 3.1 for samples abbreviations description).

Although the initial burst release is considered an undesirable behavior when developing sustained release systems, for delivering antibiotics a high dose is normally required at initial days to combat bacterial infections effectively and then slowly prolong the release for longer time periods to complete the treatment. Various chemical modifications of the polymeric matrix provide prolonged release times of entrapped antibiotics. In this study, we proposed the use of a non-toxic ionic crosslinker (sodium tripolyphosphate, TPP) to adjust the release of the GTM from CHT-ST microparticles by controlling the crosslinking density.

It is clear that the GTM release was significantly slowed down as the CHT-ST crosslinking density was increased. Moreover, increasing TPP concentrations, the initial burst release is retarded (Figure 3.6 (b), (c) and (d)). The microparticles produced using higher TPP concentrations were more rigid, decreased size (Table 3.1) and showing less swelling in PBS, thus resulting in a slower diffusion of the GTM molecules through the CHT-ST matrix into the PBS medium, with the consequent slowed down of the initial burst release. Under these conditions, the swelling and subsequent matrix degradation is also retarded, resulting in a smaller percentage of GTM released at the end of 30 days incubation. As a final result, a more sustained and slow release of GTM from the CHT-ST microparticles can be achieved for higher degree of crosslinking. Although the fastest release rate was observed from microparticles without ionic crosslinking, this system was still quite effective to ensure a sustained release of GTM after the initial burst stage.

3.4.4.2 Analysis of drug release mechanism

A number of mathematical models have been proposed to describe the mechanisms of drug release from polymeric devices. The Higuchi [51], Korsmeyer [52] and Peppas [53, 54] equations can be mentioned as the most widely used to date and are mainly based on the Fickian diffusion equation [55, 56]. In order to analyze the release mechanism of the GTM from CHT-ST microparticles, and the effect of the TPP crosslinking over the release behavior, the obtained data was processed using of the empirical expression proposed by Ritger-Peppas [53].

Table 3.1 summarizes the values obtained for the diffusion exponent (*n*) considering the CHT-ST microparticles with and without TPP crosslinking treatment. The results show that CHT-ST microparticles prepared with 2% TPP crosslinking exhibited a lower GTM diffusion exponent, *n*. Values of *n* were calculated and found to be 0.68 for microparticles without TPP, and 0.54 for the samples obtained with the highest TPP crosslinking density. The drug transport mechanism obtained for all experimental conditions was *Non-Fickian diffusion or Anomalous* (indication of the *superposition of both extreme phenomena: drug diffusion and macromolecular chain relaxation*) [53, 54]. This result indicates that neither absolute Fickian diffusion (as result of pure drug diffusion) nor Case II-zero order (because of polymer chain relaxation) was the predominant mechanism in this case, since an Anomalous drug transport was obtained. This can be understood as a close combination of contributions of polymer relaxation and drug diffusion factors that determine the drug release mechanism. In the case of various concentration of TPP (0.5, 1 and 2%) the GTM release was clearly slowed down by the increase of the TPP concentration. Analysing the values obtained for *n* the result shows in

all cases an anomalous drug transport mechanism (Table 3.1), from which it can be concluded that the crosslinking density does not show a significant influence in the drug transport mechanism (anomalous in all the cases), affecting solely the diffusion coefficient value.

3.4.4.3 Activity of released GTM

One very important factor when designing drug delivery systems is the maintenance of the activity or function of the bioactive molecules entrapped in the polymeric matrix. In the present study, the relative activity of the released GTM from the microparticles was screened *in vitro* against *S. aureus* (following standard procedures approved by NCCLS) [31].

The obtained results, in values of relative activity (%) and inhibition zones diameters (mm), are shown in Figure 3.7.

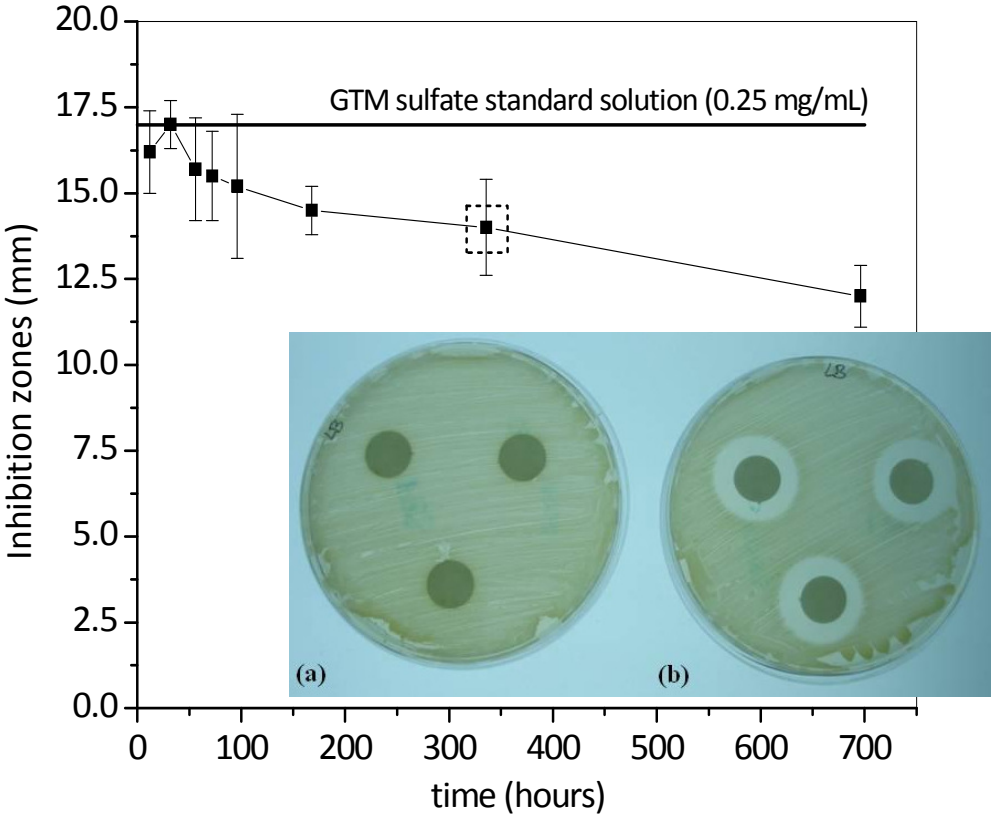

Figure 3.7 Inhibition zone of released gentamicin from chitosan-starch microparticles. The inserted picture represents a photographic observation of the antimicrobial activities against *Staphylococus aureus*. PBS solution without GTM (used as negative control) resulted in no inhibition zone around the impregnated disc **(a).** Disc impregnated with gentamicin released after 15 days, as shown in the line graph (360 hours) **(b)**

The diameters of inhibition zones vary from 17 mm for the standard GTM solution to 12 mm for the GTM released after 30 days of incubation, and the corresponding relative activities change from 100% to 70% (Table 3.2). It can be seen that released GTM have inhibition zones values similar to the one obtained for the standard solution of this antibiotic. Moreover, the obtained results, in terms of diameter inhibition zone (mm) and relative antibactericidal activities (%) are in the same range to the ones reported in the literature for gentamicin sulfate against *S. aureus* [57, 58]. These results indicated that GTM was not affected in terms of stability and antibactericidal activities after the encapsulation process and microparticles processing, neither during the release experiments performed for 30 days in PBS at 37 ^{o}C.

Table 3.2 Diameter of the inhibition zones and relative activities of the released gentamicin against *Staphylococcus aureus*

Sample[a]/Release Day	Diameter inhibition zone (mm)	Relative Activity (%)
GTM CTRL	17.0±1.9	100
CSG-1/1	16.2±1.2	95.29
CSG-1/2	17.0±0.7	100
CSG-1/3	15.7±1.5	92.35
CSG-1/4	15.5±1.3	91.18
CSG-1/5	15.2±2.1	89.41
CSG-1/7	14.5±0.7	85.29
CSG-1/14	14.0±1.4	82.35
CSG-1/30	12.0±0.9	70.59

[a]*CSG: Chitosan-Starch GTM loaded sample/GTM release day (Related experimental conditions in Table 3.1)*

3.4.4.4 Effect of storage temperature and time on the release profile and activity of entrapped GTM

A slightly faster initial burst release was observed during the first 12 hours, with the increasing storage time and temperature (Figure 3.8). The plateau obtained as result of a sustained release up of 4 days remains unchanged. This result was more pronounced for the samples stored at 25 ^{o}C. The released GTM remains active against *S. aureus,* but a decrease in the relative activity was found with increasing storage time.

From the obtained results, the sustained release of GTM from the CHT-ST microparticles does not seem to be significantly impaired. The activity of the GTM remains up to 50% for all the samples tested after 30 days of release. It can be concluded that the developed system allows its storage in a controlled environment for at least 30 days. Samples stored for more than 4 weeks maintained a sustained release of GTM, and the released antibiotic remains active against *S. aureus*.

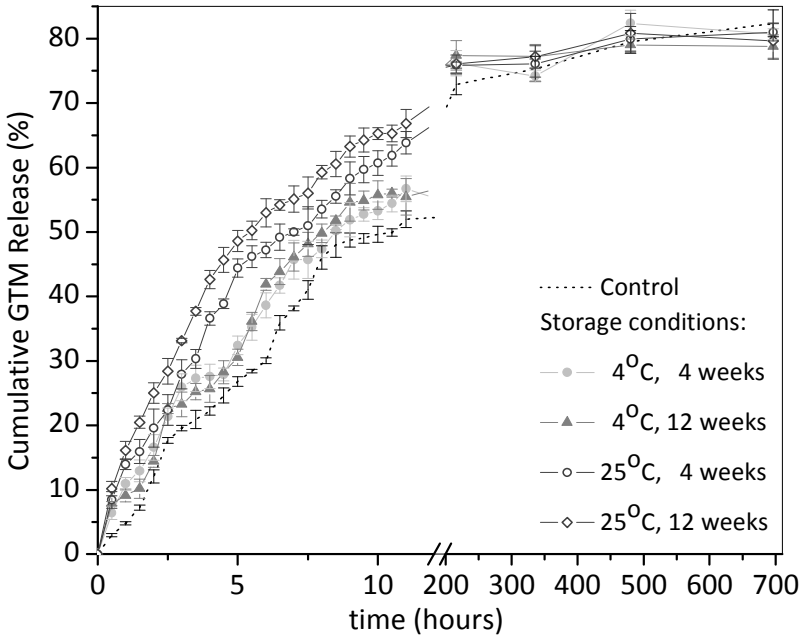

Figure 3.8 Release profiles of gentamicin from chitosan-starch microparticles after being stored for different conditions of time (4 and 12 weeks) and temperature (4 ^{o}C and 25 ^{o}C)

3.5 CONCLUSION

In this work, microparticles with spherical shape and uniform size distribution were produced using a water-in-oil emulsion crosslinking method. The emulsion method is a very simple and effective technique for the production of spherical microparticles for chitosan and similar hydrogel-like polymers, on which the microparticles properties can be tailored by adjusting the experimental conditions. A successful conjugation of chitosan to starch was achieved by means of a reductive alkylation procedure. This method provides several advantages namely the use of natural crosslinkers, avoiding the use of toxic crosslinkers agents like the extensively employed glutaraldehyde, and also an enhancement of the chitosan biodegradation by the presence of physiological enzymes such as α-amylase, due to the starch conjugation (a subsequent publication shows biodegradability results). The potential of the developed CHT-ST microparticles for the sustained release applications was evaluated by studying the loading and release of aminoglycosides, like Gentamicin sulphate. Important parameters, such as initial GTM concentration, showed a noticeable influence on the encapsulation efficiency and drug loading, resulting in an increase in the drug loading when the initial GTM concentration was increased. The encapsulation efficiencies decreased,

however, with increasing percentages of drug loading. The release studies of entrapped GTM in PBS medium showed a long term sustained release during 30 days following an anomalous drug transport mechanism. The release kinetics can be retarded by further ionic crosslinking the polymer conjugate with sodium tripolyphosphate, reducing the burst release. The bacterial inhibition test performed against S*taphylococus aureus* showed that biodegradable CHT-ST microparticles are able to release GTM with a high bactericidal activity, for a 30 days period, time necessary for effective treatment of infections by this bacteria. Studies on the stability of encapsulated GTM showed that samples stored under controlled conditions for periods up to 12 weeks maintain a sustained release pattern of GTM, and the released antibiotic remains active against *S. aureus*. Biodegradable microparticles loaded with important antibiotics can provide effective treatments for persistent infections.

Further studies will be focused on the enzymatic degradation behaviour of the developed microparticles, to demonstrate the initial hypothesis of enhanced biodegradability of the proposed system.

3.6 ACKNOWLEDGEMENTS

This work was supported by Marie Curie Host Fellowships under the Early Stage Research Training (EST) “Alea Jacta EST” (MEST-CT-2004-008104) project, providing E. R. Balmayor a PhD Fellowship, and also partially supported by the European NoE EXPERTISSUES (NMP3-CT-2004-500283). E. R. Balmayor would like to thanks to the Department of Biology, University of Minho, Braga, Portugal for generously providing access to the standard strain of *S. aureus* ATCC 25923 from, and to Bruno Ferreira, B.Sc. for the assistance with the microbiological assays.

3.7 REFERENCES

1. Coviello, T.; Matricardi, P.; Alhaique, F. *Expert Opinion on Drug Delivery* **2006**, 3 (3): 395-404.
2. Pawar, R.; Jadhav, W.; Bhusare, S.; Borade, R.; Farber, S.; Itzkowitz, D.; Domb, A. In *Natural-based Polymers for Biomedical Applications*, Reis, R. L.; Neves, N. M.; Mano, J. F.; Gomes, M. E.; Marques, A. P.; Azevedo, H. S., Eds. Woodhead Publishing Limited, CRC Press LLC: Cambridge, **2008**; pp 3-53.
3. Wang, W.; Liu, X. D.; Xie, Y. B.; Zhang, H.; Yu, W. T.; Xiong, Y.; Xie, W. Y.; Ma, X. J. *Journal of Materials Chemistry* **2006**, 16 (32): 3252-3267.
4. Sinha, V. R.; Singla, A. K.; Wadhawan, S.; Kaushik, R.; Kumria, R.; Bansal, K.; Dhawan, S. *International Journal of Pharmaceutics* **2004**, 274 (1-2): 1-33.
5. Kas, H. S. *Journal of Microencapsulation* **1997**, 14 (6): 689-711.

6. Singla, A. K.; Chawla, M. *Journal of Pharmacy and Pharmacology* **2001**, 53 (8): 1047-1067.
7. Illum, L. *Pharmaceutical Research* **1998**, 15 (9): 1326-1331.
8. Rinaudo, M. *Progress in Polymer Science* **2006**, 31 (7): 603-632.
9. Janes, K. A.; Calvo, P.; Alonso, M. J. *Advanced Drug Delivery Reviews* **2001**, 47 (1): 83-97.
10. Gross, R. A.; Kalra, B. *Science* **2002**, 297 (5582): 803-807.
11. Azevedo, H. S.; Gama, F. M.; Reis, R. L. *Biomacromolecules* **2003**, 4 (6): 1703-1712.
12. Azevedo, H. S.; Reis, R. L. In *Biodegradable Systems in Tissue Engineering and Regenerative Medicine*, Reis, R. L.; San Roman, J., Eds. CRC Press: Boca Raton, FL, **2005**; pp 177-201.
13. Tharanathan, R. N. *Trends in Food Science & Technology* **2003**, 14 (3): 71-78.
14. Sousa, R. A.; Correlo, V. M.; Chung, S.; Neves, N. M.; Mano, J. F.; Reis, R. L. In *Natural-based Polymers for Biomedical Applications*, Reis, R. L.; Neves, N. M.; Mano, J. F.; Gomes, M. E.; Marques, A. P.; Azevedo, H. S., Eds. Woodhead Publishing Limited, CRC Press LLC: Cambridge, **2008**; pp 85-105.
15. Mathew, S.; Brahmakumar, M.; Abraham, T. E. *Biopolymers* **2006**, 82 (2): 176-187.
16. Lim, F.; Sun, A. M. *Science* **1980**, 210 (4472): 908-910.
17. Hari, P. R.; Chandy, T.; Sharma, C. P. *Journal of Applied Polymer Science* **1996**, 59 (11): 1795-1801.
18. Chandy, T.; Mooradian, D. L.; Rao, G. H. R. *Journal of Applied Polymer Science* **1998**, 70 (11): 2143-2153.
19. Ramadas, M.; Paul, W.; Dileep, K. J.; Anitha, Y.; Sharma, C. P. *Journal of Microencapsulation* **2000**, 17 (4): 405-411.
20. Rogovina, S. Z.; Vikhoreva, G. A. *Glycoconjugate Journal* **2006**, 23 (7-8): 611-618.
21. Averous, L. *Journal of Macromolecular Science-Polymer Reviews* **2004**, C44 (3): 231-274.
22. Jana, S.; Deb, J. K. *Applied Microbiology and Biotechnology* **2006**, 70 (2): 140-150.
23. Touw, D. J. *Pharmacy World & Science* **1998**, 20 (4): 149-160.
24. Cabanillas, P. F.; Pena, E. D.; Barrales-Rienda, J. M.; Frutos, G. *International Journal of Pharmaceutics* **2000**, 209 (1-2): 15-26.
25. Terbojevich, M.; Cosani, A.; Muzzarelli, R. A. A. *Carbohydrate Polymers* **1996**, 29 (1): 63-68.
26. Terbojevich, M.; Cosani, A. In *Chitin Handbook. European Chitin Society.*, Muzzarelli, R. A. A.; Peter, M., Eds. Atec Edizioni: Grottammare, Italy, **1997**; pp 87-108.
27. Lavertu, M.; Xia, Z.; Serreqi, A. N.; Berrada, M.; Rodrigues, A.; Wang, D.; Buschmann, M. D.; Gupta, A. *Journal of Pharmaceutical and Biomedical Analysis* **2003**, 32 (6): 1149-1158.
28. Hermanson, G. In *Bioconjugate Techniques*, 1st ed.; Academic Press, Inc.: San Diego, CA, **1996**; pp 114-116.
29. Baran, E. T.; Mano, J. F.; Reis, R. L. *Journal of Materials Science-Materials in Medicine* **2004**, 15 (7): 759-765.
30. Wang, C.; Ye, W.; Zheng, Y.; Liu, X.; Tong, Z. *International Journal of Pharmaceutics* **2007**, 338 (1-2): 165-173.
31. *Performance Standards for Antimicrobial Disk Susceptibility Tests; Approved Standard-Tenth Edition*; M02-A10; Clinical and Laboratory Standards Institute (CLSI) or NCCLS document: V29, No.1, **2008**; pp 3-27.
32. Liu, S. J.; Chi, P. S.; Lin, S. S.; Ueng, S. W. N.; Chan, E. C.; Chen, J. K. *International Journal of Pharmaceutics* **2007**, 330 (1-2): 45-53.
33. Hartke, K.; Hartke, H.; Mutschler, E.; Rucker, G.; Wichtl, M.; Eds. In *Kommentar zum Europaischen Arzneibuch (Comments to the European Pharmacopoeia)*, Wissenschaftliche Verlagsgesellschaft (WVG mbH): Stuttgart, **1998**.
34. Wienen, F.; Deubner, R.; Holzgrabe, U. *Pharmeuropa* **2003**, 15: 273–279.

35. Deubner, R.; Schollmayer, C.; Wienen, F.; Holzgrabe, U. *Magnetic Resonance in Chemistry* **2003**, 41 (8): 589-598.
36. Winter, W.; Deubner, R.; Holzgrabe, U. *Journal of Pharmaceutical and Biomedical Analysis* **2005**, 38 (5): 833-839.
37. Hirai, A.; Odani, H.; Nakajima, A. *Polymer Bulletin* **1991**, 26 (1): 87-94.
38. Varum, K. M.; Anthonsen, M. W.; Grasdalen, H.; Smidsrod, O. *Carbohydrate Research* **1991**, 211 (1): 17-23.
39. McIntyre, D. D.; Ho, C.; Vogel, H. J. *Starch-Starke* **1990**, 42 (7): 260-267.
40. McIntyre, D. D.; Vogel, H. J. *Starch-Starke* **1991**, 43 (2): 69-76.
41. Zang, L. H.; Howseman, A. M.; Shulman, R. G. *Carbohydrate Research* **1991**, 220: 1-9.
42. Yang, Y. Y.; Chung, T. S.; Ng, N. P. *Biomaterials* **2001**, 22 (3): 231-241.
43. Wang, S. B.; Chen, A. Z.; Weng, L. J.; Chen, M. Y.; Xie, X. L. *Macromolecular Bioscience* **2004**, 4 (1): 27-30.
44. Gaspar, M. M.; Blanco, D.; Cruz, M. E. M.; Alonso, M. J. *Journal of Controlled Release* **1998**, 52 (1-2): 53-62.
45. Song, C. X.; Labhasetwar, V.; Murphy, H.; Qu, X.; Humphrey, W. R.; Shebuski, R. J.; Levy, R. J. *Journal of Controlled Release* **1997**, 43 (2-3): 197-212.
46. Baran, E. T.; Ozer, N.; Hasirci, V. *Journal of Microencapsulation* **2002**, 19 (3): 363-376.
47. Silva, G. A.; Ducheyne, P.; Reis, R. L. *Journal of Tissue Engineering and Regenerative Medicine* **2007**, 1 (1): 4-24.
48. Rothen-Weinhold, A.; Besseghir, K.; De Zelicourt, Y.; Gurny, R. *Journal of Controlled Release* **1998**, 52 (1-2): 205–213.
49. Grassi, M.; Colombo, I.; Lapasin, R. *Journal of Controlled Release* **2001**, 76 (1-2): 93-105.
50. Berkland, C.; King, M.; Cox, A.; Kim, K.; Pack, D. W. *Journal of Controlled Release* **2002**, 82 (1): 137-147.
51. Higuchi, T. *Journal of Pharmaceutical Sciences* **1961**, 50 (10): 874-875.
52. Korsmeyer, R. W.; Gurny, R.; Doelker, E.; Buri, P.; Peppas, N. A. *International Journal of Pharmaceutics* **1983**, 15 (1): 25-35.
53. Ritger, P. L.; Peppas, N. A. *Journal of Controlled Release* **1987**, 5 (1): 23-36.
54. Siepmann, J.; Peppas, N. A. *Advanced Drug Delivery Reviews* **2001**, 48 (2-3): 139-157.
55. Crank, J. In *The Mathematics of Diffusion*, 2nd ed.; Oxford University Press, Inc.: New York, **1975**; pp 1-11.
56. Fick, A. *Philippine Magazine and Journal of Science* **1855**, 10: 31-39.
57. Stigtera, M.; Bezemera, J.; de Grootb, K.; Layrollec, P. *Journal of Controlled Release* **2004**, 99: 127–137.
58. Tam, V. H.; Kabbara, S.; Vo, G.; Schilling, A. N.; Coyle, E. A. *Antimicrobial Agents and Chemotherapy* **2006**, 50 (8): 2626–2631.

Chapter 4

Highly biodegradable starch-conjugated chitosan microparticles as carrier for the controlled release of antibiotic drugs: *In vitro* enzymatic degradation and cytotoxicity evaluation

4.1 ABSTRACT

The effect of enzymatic degradation on the release behavior of gentamicin (GTM) from starch-conjugated chitosan microparticles (CHT-ST) was investigated upon exposure to an α-amylase containing solution up to 8 weeks. The degradation of the microparticles was followed by gravimetric measurements, scanning electron microscopy (SEM) and spectroscopic techniques (FTIR/^{1}H-NMR). SEM observations showed an increase in the porosity and surface roughness of the microparticles as well as a reduction in their diameters, indicative of the degradation process. These morphological observations were confirmed by weight lost measurements that showed that about 70% of the microparticles weight was lost in the presence of α-amylase. With prolonged degradation time, a highly porous matrix was obtained leading to an increased permeability. This resulted in increased water penetration with possible diffusion of the entrapped drug. A faster release of GTM from the CHT-ST microparticles was observed in the presence of α-amylase. In addition, an initial evaluation of the cell behavior in the presence of the differently produced CHT-ST microparticles samples was studied using an osteoblast-like cell line (SaOs-2). Its cytotoxic effect over SaOs-2 cells was dependent on the crosslinking agent used and on the amount of starch. Glutaraldehyde (GA) crosslinked microparticles caused some cytotoxicity that was dependent on its concentration. On the contrary, a higher percentage of starch clearly improved the cell viability. Thus, the developed CHT-ST microparticles are biodegradable and non toxic under physiological conditions where degrading enzymes are present. Thus, may be used as a sustained/controlled delivery carrier.

***This chapter is based on the following publication:**

Balmayor, *E. R.;* Baran, E. T.; Marques, A. P.; Azevedo, H. S.; Reis, R. L. Highly biodegradable starch-conjugated chitosan microparticles as carrier for the controlled release of antibiotic drugs: *In vitro* enzymatic degradation and cytotoxicity evaluation. **2009. Submitted.**

4.2 INTRODUCTION

Biomaterials with the ability to perform certain medical functions and subsequently degrade, under a controlled mechanism, into easily metabolized products are of great importance [1-3]. Among the well known advantages of using biodegradable materials, are the elimination of the long term presence of foreign materials and the consequent need for a second surgery for implant removal [2, 4].

Several definitions for biodegradability have been proposed [1, 2, 5-7]. In the context of biomedical applications, biodegradation may be defined as the "gradual breakdown of a material mediated by a specific biological activity" [5, 7]. When in contact with tissues, biomaterials start to degradade as a result of their interaction with biological environments, and its stability will define its application in clinics. In drug delivery applications, it is well known that biodegradability of the carrier system affects and finally controls the release kinetics of the encapsulated drugs [2, 4, 8]. Thus, the polymeric carriers should degrade under physiological conditions allowing for the gradual release of the entrapped drug as well as facilitate repeating dosages to ensure successful treatments [9, 10]. Another important issue related with the use of biodegradable polymers in drug delivery, is the possible toxicity of the leachable molecules and degradation products derived from the material processing and degradation [11, 12]. Thus, the nature of the materials to be selected as drug delivery carriers is also a rather important factor to consider. Polysaccharides are very attractive in this respect as the degradation process results in non-toxic end products such as glucose, maltose and oligosaccharides. These end products may even be incorporated in the normal metabolic pathways of the human body [2, 13-15].

In a previous study [16], we have described the preparation and characterization of starch-chitosan microparticles and analyzed the release of antibiotic drugs from the polymeric carrier *in vitro*. For the present work, we have investigated the susceptibility of starch-chitosan microparticles (CHT-ST) [16] to enzymatic degradation by the hydrolytic enzyme α-amylase. Moreover, the effect of the α-amylase degradation on the release kinetics of entrapped gentamicin (GTM) from the CHT-ST microparticles was also studied. The extent of degradation was evaluated by measuring the weight loss and the presence of reducing sugars in the degradation medium. Changes in the chemical structure as well as in their morphological features were also analyzed. The cytotoxicity of CHT-ST microparticles produced under different processing conditions was assessed over an osteoblast-like cell line.

4.3 EXPERIMENTAL

4.3.1 Materials

The materials studied in this work were chitosan (the viscosity-average MW was found to be 385 kDa and the deacetylation degree 81.25%, [16]) from Sigma-Aldrich (USA) and soluble potato starch, supplied by ATO (The Netherlands). Both materials were used as received. α-amylase (EC 3.2.1.1) from *Aspergillus Oryzae*, 215 U/mg protein, was obtained from Sigma-Aldrich (USA). Other chemicals were analytical grade, from Sigma-Aldrich (USA) and were used as received.

4.3.2 CHT-ST microparticles preparation: variation on the experimental conditions

CHT-ST conjugate was prepared by an initial reductive alkylation cross-linking method [17]. Briefly, starch was oxidized to produce a polyaldehyde that reacts with the amino group of chitosan in the presence of a reducing agent. The production of the CHT-ST microparticles was then carried out using a water-in-oil emulsion technique, as described previously [16]. In brief, equal volumes of chitosan (1.5%, w/v) and oxidized starch (2%, w/v) solutions were mixed, and the pH adjusted to 5.5 by using 0.5 M NaOH. The polymeric solution was added dropwise into a glass reactor containing mineral oil with 1% of Tween 80 and emulsified with a top stirrer at 600 rpm for 30 minutes. After emulsion formation, 30 mL of cold acetone was added slowly. The microparticles were then removed from the reaction medium by filtration and washed with distilled water/acetone mixture (1:1 v/v). After alkaline (sodium carbonate buffer solution, 0.5 M) and reduction (sodium borohydride solution, 0.05%) treatments, the microparticles were washed with distilled water and allowed to dry at room temperature.

Three variations were however introduced to the standard procedure previously described (starch-conjugated chitosan microparticles without crosslinking) [16]: i) two different crosslinking agents, sodium tripolyphosphate (TPP) and glutaraldehyde (GA), at different concentrations (0.5, 1 and 2%) were employed. Crosslinking was achieved by immersing the obtained samples for 3 hours into the crosslinker agent solution, ii) the amount of starch in the composition of the CHT-ST conjugate polymer solution used for the microparticles preparation was varied (1, 2 and 4%), iii) the stirring rate employed to form the emulsion was increased from 400 to 800 rpm aiming at producing smaller sizes microparticles and to evaluate the influence of the particles sizes over the cytotoxicity of the resulting particular biomaterial (Table 4.1).

4.3.3 Enzymatic degradation study. *In vitro* release of GTM in enzymatic environment

Pre-weighed samples (unloaded and GTM loaded CHT-ST microparticles) were incubated in a 1:10 ratio in 0.01 M phosphate buffered saline solution (PBS, pH 7.4) containing α-amylase 150.5 U/L, at 37 ^{o}C and under constant shaking (50 rpm) up to 8 weeks. The buffered enzyme solution was changed weekly to maintain the desired level of enzyme activity throughout the experiment. For the preservation of the degradation solution, sodium azide (0.02%) was added to the buffered enzyme solution (stored at 4 ^{o}C for further use). As a control, the samples were incubated in the presence of PBS only. At the end of each degradation time (1, 2, 3, 7, 14, 30 and 60 days), the supernatants were removed and stored at -80 ^{o}C for further analysis. The excess of solution was carefully removed with filter paper and the samples were weighed using an analytical balance (±0.01 mg accuracy) for the determination of water uptake [18]. Subsequently, the samples were thoroughly washed with distilled water and allowed to dry at room temperature until presenting constant weight. The final weight of the samples was used for the calculation of the weight loss in relation to the initial weight [18]. The supernatants from the degradation solutions were used to quantify the amount of released GTM and to determine the concentration of reducing sugars released into the solution as a product of the degradation process.

Table 4.1 Experimental conditions used during the preparation of chitosan-starch microparticles. Effect of processing conditions over the resulted cytotoxicity, expressed as percentage of cell viability in comparison to control (100% viability)

Sample[a]	GA[b] (%)	TPP[c] (%)	Starch (%)	Stirring rate (rpm)	Size (μm)	Cell viability (% Control)[d]
CHT-ST 1	**0.5**				79.6±6.3	73.21±8.6
CHT-ST 2	**1**	-			75.3±13.4	65.83±5.9
CHT-ST 3	**2**		2		74.3±11.7	55.87±9.1
CHT-ST 4		**0.5**		600	82.9±9.5	79.21±4.0
CHT-ST 5		**1**			70.4±10.4	76.78±7.2
CHT-ST 6		**2**			71.3±24.8	78.81±3.8
CHT-ST 7	-		**1**		87.7±29.1	71.18±9.1
CHT-ST 8*			**2**	**600**	**96.1±12.4**	77.12±6.2
CHT-ST 9		-	**4**	600	91.3±9.8	91.24±1.8
CHT-ST 10			2	**400**	**207.1±11.6**	74.70±8.9
CHT-ST 11				**800**	**60±7.4**	76.27±6.6

Common experimental conditions for all experiments:
Volume of polymer solution: 10 mL
Mineral Oil 70 mL (1% Tween 80, (v/v))

[a]CHT-ST: chitosan-starch microparticles
[b]GA: glutaraldehyde
[c]TPP: sodium tripolyphosphate
[d]percentages of viable cell compared to positive control(100%-DMEM culture medium) as result of the direct contact with chitosan-starch microparticles
* standard condition [16]

The quantification of the released GTM was performed by an indirect spectrophotometric method, as previously described [16]. The amount of reducing sugars in the supernatants was estimated by the dinitrosalicylic acid (DNS) method [19], using a calibration curve obtained with glucose solutions of known concentrations. Briefly, a DNS reagent solution was prepared based on a mixture of 3,5-dinitrosalicylic acid and Rochelle salt, under alkaline conditions. Subsequently, standard solutions and samples were mixed with the DNS reagent under the appropriate conditions and allowed to react at 100 ^{o}C for 5 minutes. Finally, the absorbance was determined using a microplate reader at 540 nm (EL 312e Biokinetics, BioTek Instruments, USA). The amount of reducing sugars was reported as the average concentration of three replicate determinations.

4.3.4 Chemical and Physical characterization

4.3.4.1 Morphological evaluation: scanning electron microscopy (SEM)

The morphology and surface characteristics of the microparticles were evaluated by SEM after the different degradation time points (mentioned in section 4.3.3), to assess the changes resulting from the degradation process. Following standard procedures for the preparation of the samples [16], the samples were analysed by scanning electron microscopy (SEM) (Leica Cambridge S-360 model, UK).

4.3.4.2 Chemical changes: fourier transformed infrared spectroscopy (FTIR)

To assess eventual changes in the chemical composition of the microparticles as result of the enzymatic degradation, the samples were analyzed by fourier transformed infrared spectroscopy (FTIR) spectroscopy in a transmission mode (IRPrestige-21 FTIR-8400S, Shimadzu, Japan) before and after the degradation process. For the preparation of the samples for FTIR analysis, 1 mg of sample was mixed with 40 mg of spectroscopic KBr, and then processed into a disc using a manual press (161-1100 hand press, PIKE Technologies, USA). Transmission spectra were recorded using at least 32 scans with 4 cm^{-1} resolution and in the spectral range 4000-600 cm^{-1}.

4.3.4.3 Nuclear magnetic resonance spectroscopy (^{1}H-NMR)

Proton nuclear magnetic resonance (^{1}H-NMR) spectra were obtained (Varian Unit Plus 300 MHz spectrometer, USA) under the following experimental parameters: 256 scans, 5200 Hz filter width, 90^{o} pulse corresponding to a pulse width of 11 μs and 4 s relaxation delay. The experiments were run at 60 ^{o}C. For the sample preparation, 10 mg of each sample were

dissolved into a mixture of deuterated solvents, 0.98 mL of deuterium oxide (D_2O) and 0.02 mL of deuterium chloride (DCL), until complete dissolution, and transferred into a NMR tube (ϕ=0.3 mm).

4.3.5 Evaluation of cytotoxicity

The human osteoblast-like cell line SaOs-2 (ECACC, UK) was used to evaluate the effect of processing conditions over cell viability. The cytotoxicity of both, the extract of the particles produced under the standard conditions [16] and the different particles developed in this work, was assessed by performing a standard MTS (3-(4,5-dimethylthiazol-2-yl)-5-(3-carboxymethoxyphenyl)-2-(4-sulfophenyl)-2H-tetrazolium) assay [20, 21].

1.3 X 10^4 cells/well were plated in a 96-well plate in Dulbecco's Modified Eagle's Medium (DMEM) without phenol red (Sigma-Aldrich, USA), supplemented with 10% heat-inactivated fetal bovine serum FBS (Biochrom AG, Germany) and 1% antibiotic/antimycotic (Gibco™, Invitrogen, CA). Cells were incubated for 24 hours at 37 ^oC in a humidified atmosphere containing 5% of CO_2 and let to achieve approximately 80% confluence.

In order to test the cytotoxic potential of the CHT-ST microparticles, the standard material was incubated in complete cell culture medium for 24, 48 and 72 hours at 37 ^oC under constant shaking (100 rpm). This incubation was performed using 0.5 mg microparticles per mL of complete culture medium. Subsequently to the incubation period, the extraction medium containing potential toxic leachable and degradation products was filtered (0.45 µm pore size) and added to the 80% confluence cell layer. The cells were incubated for further 24 hours with this medium at 37 ^oC and in a humidified environment containing 5% of CO_2. Latex rubber extract and fresh complete culture medium were used respectively as negative and positive controls for cell viability assay [18].

In a separated experiment, the microparticles obtained from the different experimental conditions, and sterilized by ethylene oxide (EtO) using pre-optimized conditions [22], were directly added to the 80% cell monolayer in a concentration of 1 mg/mL, and incubated for further 72 hours.

The MTS test was performed for both experiments according to the manufacture instructions provided in the CellTiter 96 One Solution Proliferation Assay Kit (Promega, USA), and as described previously [13, 21]. Briefly, after the incubation periods, the cell monolayer was treated with 200 µL/well of MTS reagent solution (5:1 ratio in serum-free DMEM culture medium without phenol red) and incubated for further 3 hours at 37 ^oC and in a humidified environment containing 5% of CO_2. 100 µL of each well were then filtered (0.45 µm pore size) to eliminate the possible presence of solid particles, and transferred to a new 96-well plate.

The absorbance was determined in a microplate reader (EL 312e Biokinetics, BioTek Instruments, USA) at 490 nm. The results are expressed as the percentage of cell viability in comparison with the 100% viability attributed to the positive control. The samples were tested in triplicate in three independent assays.

4.4 RESULTS AND DISCUSSION

4.4.1 Enzymatic degradation

4.4.1.1 Physicochemical characterization: water uptake and weight loss

A biomaterial designed for biomedical applications will for sure interact with human tissues and fluids after implantation, which might initiate their degradation process. Chemical and enzymatic oxidations, non-enzymatic hydrolysis (catalyzed by acids, bases or salts) and enzymatic hydrolysis caused by the action of enzymes are some of the routes for degradation to occur [2, 23]. α-amylase is a glycosidic hydrolase that acts on the α (1-4) glycosidic bond of starch molecules reducing its molecular weight, and yielding maltose, glucose and other small sugars molecules. This enzyme is present in many tissues in the human body, including the human blood [2], although most prominent in exogenic pancreatic secretions and saliva [24]. Therefore, is expected that this enzyme will participate on the degradation of starch-based biomaterials that perform their function in contact with human fluids, tissues and organs. In this study, the degradation of a previously proposed CHT-ST microparticular system [16] was carried out in the presence of α-amylase at a physiological concentration. Weight loss and water uptake percentage was followed over time up to 8 weeks of incubation (Figures 4.1 and 4.2). In comparison to PBS, higher values of water uptake (160.1±5.6 %) were obtained after incubation in α-amylase solution (Figure 4.1). This behavior can be related with the presence of both polysaccharides (chitosan and starch) in the composition of the blend, providing hydrophilic characteristics to the microparticular system. Moreover, it may be also associated with the presence of α-amylase in the solution that promotes water absorption, which is in accordance with previous reported data [23]. The enhanced permeability of the material over the time, caused by the partial degradation resulting from the enzymatic hydrolysis, leads to increased water absorption.

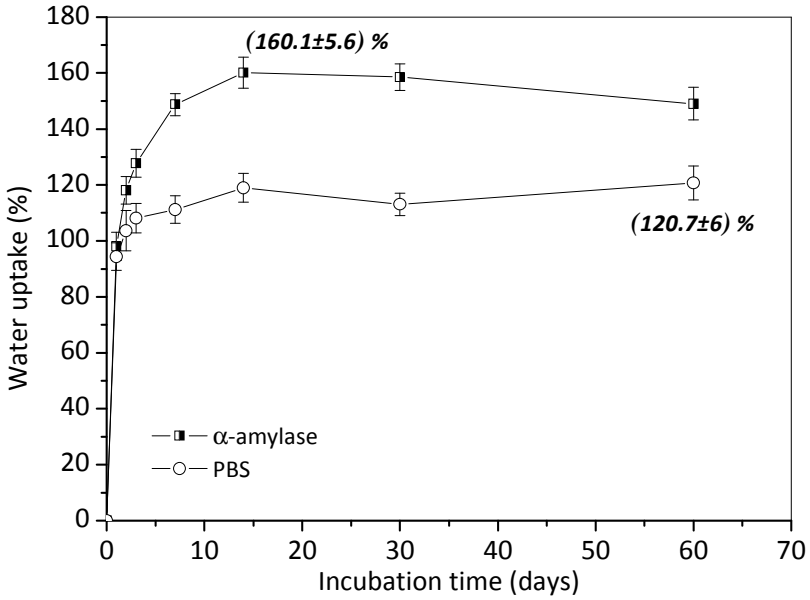

Figure 4.1 Water uptake profile of chitosan-starch microparticles in PBS, and PBS containing α-amylase (37 °C, 100 rpm). The data points in the figure represent the mean of three replicates (n=3) and the error bars the standard deviation

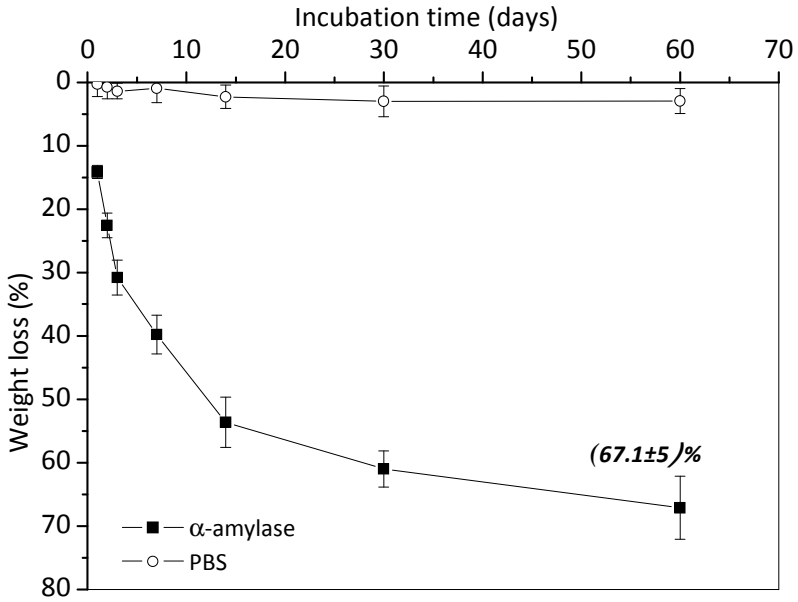

Figure 4.2 Degradation profiles of chitosan-starch microparticles, expressed as weight loss percentage, after incubation in PBS, and PBS containing α-amylase (37 °C, 100 rpm). Error bars represent standard deviations (n=3)

The results of weight loss confirmed the degradation of the CHT-ST microparticles after incubation with α-amylase (Figure 4.2). At initial stages of degradation, considerable increase in weight loss was observed. On the contrary, when the microparticles were incubated in PBS only, the variation of weight loss over time was not significant. At the end of the studied time period, CHT-ST microparticles lost 67.1±5 % of their original weight in presence of α-amylase. This clearly indicates a high degree of degradation of the microparticles in the presence of this enzyme.

4.4.1.2 Determination of reducing sugars in the supernatants

It is well known that enzymatic hydrolysis of polysaccharides is accompanied by the release of glucose and several other soluble sugar molecules to the degradation media [2, 23]. Therefore, the amount of reducing sugars released by the material into the media over time will give an indication of the extent of the material degradation. Figure 4.3 shows the concentration of reducing sugars released into the solution, after incubation of the CHT-ST microparticles with α-amylase. Reducing sugars were found in the supernatants where the microparticles were incubated in the presence of the enzyme, but not in the control supernatants (PBS only). As expected, prolongation of the incubation time led to increasing amounts of reducing sugars. In fact, after 60 days of degradation, the concentration of reducing sugars quantified was 18.02±0.86 mg/mL. The absence of α-(1-4) glycosidic linkages in chitosan leads to assume that the amount of the quantified reducing sugars correspond to the degradation of the starch in the blend.

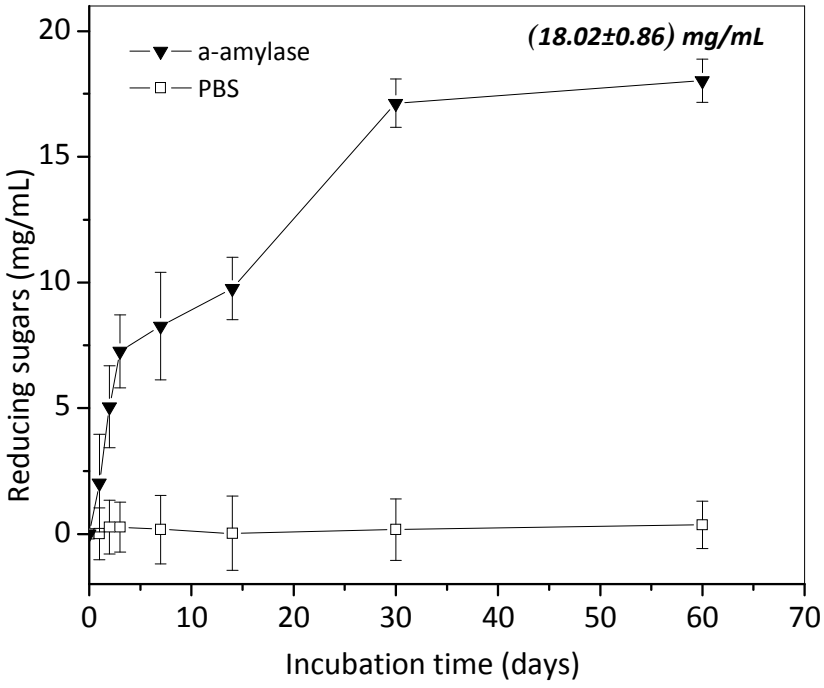

Figure 4.3 Concentration of reducing sugars released from the chitosan-starch microparticles into the solution after incubation in PBS, and PBS containing α-amylase (37 °C, 100 rpm). Error bars represent standard deviations (n=3)

4.4.1.3 Morphological evaluation of degradation process: scanning electron microscopy (SEM)

SEM micrographs presented in Figure 4.4 show the morphology of CHT-ST microparticles before and after incubation with the enzymatic degradation solution in which it is possible to observe the extent of the degradation process in the microparticles when they are immersed in the enzymatic solution. The particle size decreases, there is the appearance of pores at the surface and the particles lose their spherical shape (Figure 4.4 (e) and (f), (g) and (h)) when comparing with the non-degraded control sample (Figure 4.4 (a) and (b)). As a result of the degradation process, the material starts to disintegrate leading to the appearance of fractures which contribute to the loss of the spherical shape and to a decrease in the size of the particles. At higher magnifications, it was possible to observe in detail the surfaces of the samples after enzymatic degradation. In that case, a highly porous matrix was obtained (Figure 4.4 (f) and (h)).

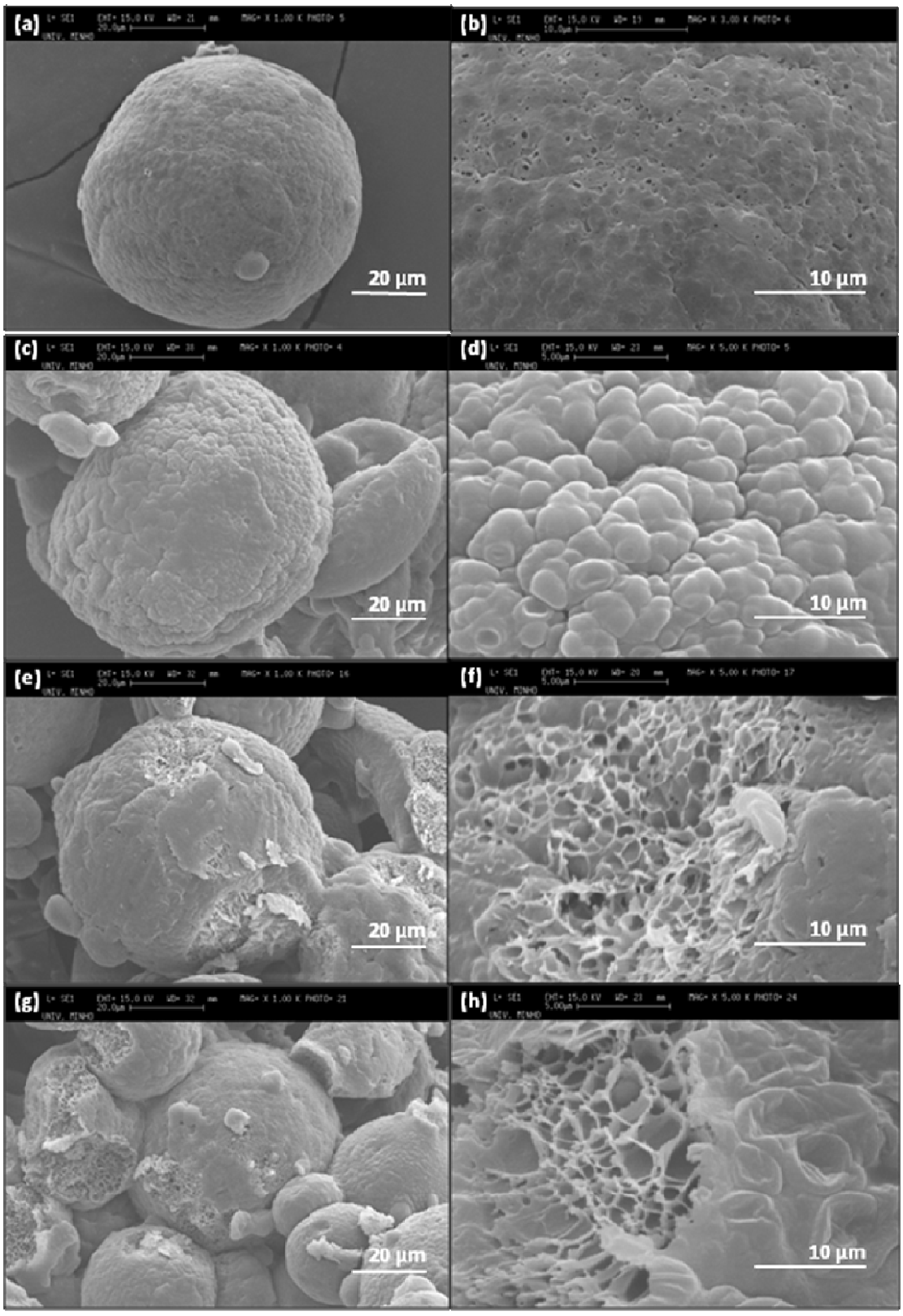

Figure 4.4 SEM micrographs showing the morphology of surfaces and the shape of chitosan-starch microparticles before **(a)**, **(b)** and after enzymatic degradation: 8 weeks of incubation in PBS solution **(c)**, **(d)**; after 2 weeks of incubation in α-amylase solution **(e)**, **(f)**; after 8 weeks of incubation in α-amylase solution **(g)**, **(h)**

After 8 weeks of incubation in PBS, the roughness of the surface of the microparticles clearly increased (Figure 4.4 (d)), but no pore formation or any evidence of degradation, such as changes in the size or shape of the particles, was observed when compared to the enzymatic degraded ones. That roughness on the surface can be a result of the swelling process which causes irreversible changes in the surfaces morphology.

4.4.1.4 Chemical evaluation of degradation process: Fourier transformed infrared (FTIR)-Nuclear magnetic resonance (^{1}H-NMR)

Figure 4.5 shows the FTIR spectra obtained for CHT-ST microparticles before and after 8 weeks of α-amylase degradation.

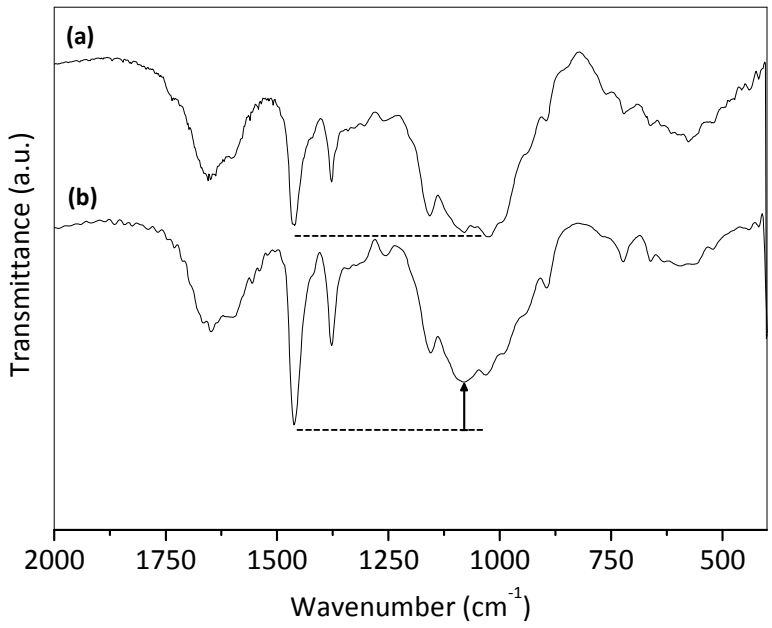

Figure 4.5 FTIR spectra of chitosan-starch microparticles before **(a)** and after **(b)** enzymatic degradation with α-amylase for 8 weeks. *Symbols*: ↥ -indicating a decrease in the intensity of the bands as result of the action of α-amylase cleaving the C-O-C glycosidic linkages of starch

Relevant bands assigned to both polysaccharides, chitosan and starch, can be clearly identified. In the range of 900-1200 cm^{-1}, the carbohydrate fingerprint region, the three major starch specific bands, 1030 cm^{-1}, 1080 cm^{-1} and 1150 cm^{-1} for the C-O-C stretching, can be clearly identified (triplet, broad band). After the enzymatic hydrolysis, a clear decrease in the intensity of those bands can be observed, indicating the action of α-amylase in cleaving the

C-O-C glycosidic linkages of starch. This FTIR evidence of the enzymatic degradation of starch by α-amylase is in concordance with the literature [23, 25-28], where some authors found also evidence of an increasing tendency in the so called "water band" that appears at 1640 cm^{-1} as an indication of the absorbed water in the starch matrix, rather than any structural change in the polymer composition [25]. When CHT-ST microparticles were incubated in PBS only, no notorious changes in chemical composition were observed. FTIR technique proved to be useful to quantify the biodegradation of polymer mixtures [29-32], and more specifically when starch is analyzed due to the presence of very strong absorption in the carbohydrate fingerprint region (900-1200 cm^{-1}), as any loss in starch content results in a decrease in the absorbance in this region.

The proton NMR spectrum of starch has been widely studied in the literature [33-35]. This polysaccharide has a well defined pattern of signals that allows the use of this technique for its study and characterization. Figure 4.6 shows the ^{1}H-NMR spectrum of CHT-ST microparticles before and after α-amylase degradation. The spectrum of chitosan raw material is presented for comparison.

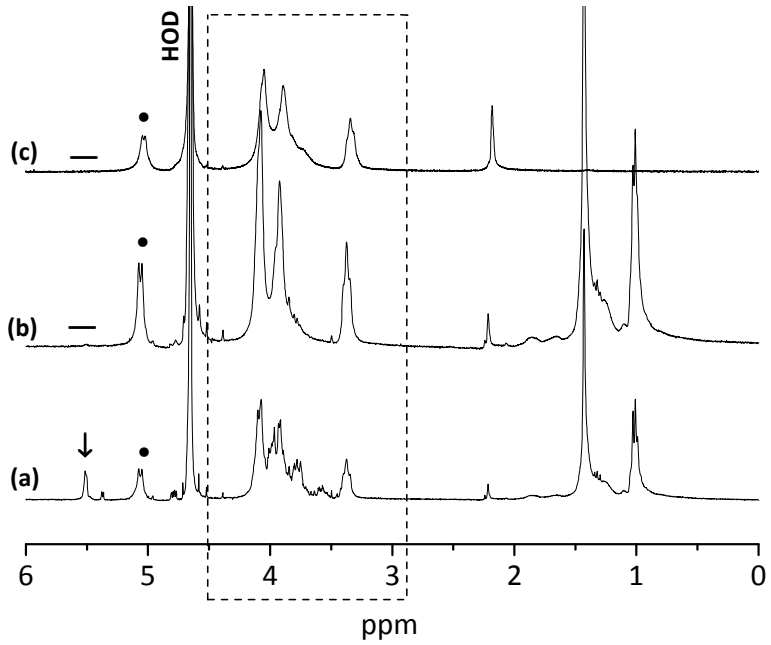

Figure 4.6 ^{1}H-NMR spectra of chitosan-starch microparticles before **(a)** and after 8 weeks of degradation in presence of α-amylase **(b)**. Chitosan raw materials used to produce the microparticles **(c)**. *Symbols*: ↓-Starch (α (1→4) glycosidic linkages, singlet), ● -Chitosan (deacetylated unit, doblet), --- Starch (internal protons, multiplets)

The typical peaks of starch can be identified in the spectrum of the CHT-ST microparticles before degradation. A signal at 5.5 ppm can be observed, due to the anomeric proton associated with α (1→4) linkages of the molecules. After 8 weeks of α-amylase degradation this peak at 5.5 ppm disappears (Figure 4.6) as an indication of the action of the enzyme cleaving the α (1→4) glycosidic linkages in starch. Moreover, the multiplet signal at 4 ppm assigned to the internal protons of starch disappear after α-amylase degradation. This provokes changes in the signal structure/shape leading to the clarification of the chitosan characteristic peaks that were overlapped with the starch multiplets in the same region of the spectrum. At the end of the enzymatic degradation study, the chitosan ^{1}H-NMR characteristic spectrum was observed (3-4.5 ppm) (Figure 4.6). As a result of the analysis of the obtained ^{1}H-NMR spectra before and after degradation, it can be concluded that the starch molecules present in the microparticles composition are being degraded by α-amylase by cleaving its α (1→4) linkages.

4.4.1.5 Effect of α-amylase degradation on the release kinetics of GTM from CHT-ST microparticles

Being the produced CHT-ST microparticles susceptible to enzymatic degradation by α-amylase at physiological concentrations, the effect of enzymatic degradation of CHT-ST microparticles on the GTM release kinetics was studied. It was expected a significant role of the degradation of the polymeric matrix in the release behavior of the entrapped GTM.

In a previously study [16] we have described the GTM release from the CHT-ST microparticles in PBS environment. The data showed that the majority of the released GTM (higher than 72% at the end of 9 days) is mainly controlled by diffusion and swelling processes and that matrix degradation phenomenon does not play a significant role. This is an expected result, since the degradation of the CHT-ST microparticles by spontaneous hydrolysis (PBS) is notably slow during short periods of incubation, and as a consequence should not significantly affect the release behavior. Figure 4.7 shows the release profiles of GTM from CHT-ST microparticles in PBS containing α-amylase, compared to PBS only. The initial burst release (up to 12 hours) of the GTM was unaffected by the presence of the enzyme. However, from that time point on, the GTM was released faster when α-amylase was present. This effect was more pronounced during the diffusion stage, from the second day on, where 71% GTM was released from the CHT-ST microparticles in the presence of the enzyme, whereas only 59% was released from the sample incubated in PBS only. This indicates that the polymer degradation can affect and control the release rate of encapsulated drugs. In fact, from the obtained results it can be concluded that the GTM is released by diffusion phenomena mainly at the beginning (as result

of the swelling of the highly hydrophilic polysaccharide matrix). Thereafter, the degradation of the polymeric microparticles starts to take place accelerated by the presence of enzymes. Thus, at later stages the release rate of encapsulated drug is controlled by the enzymatic degradation process.

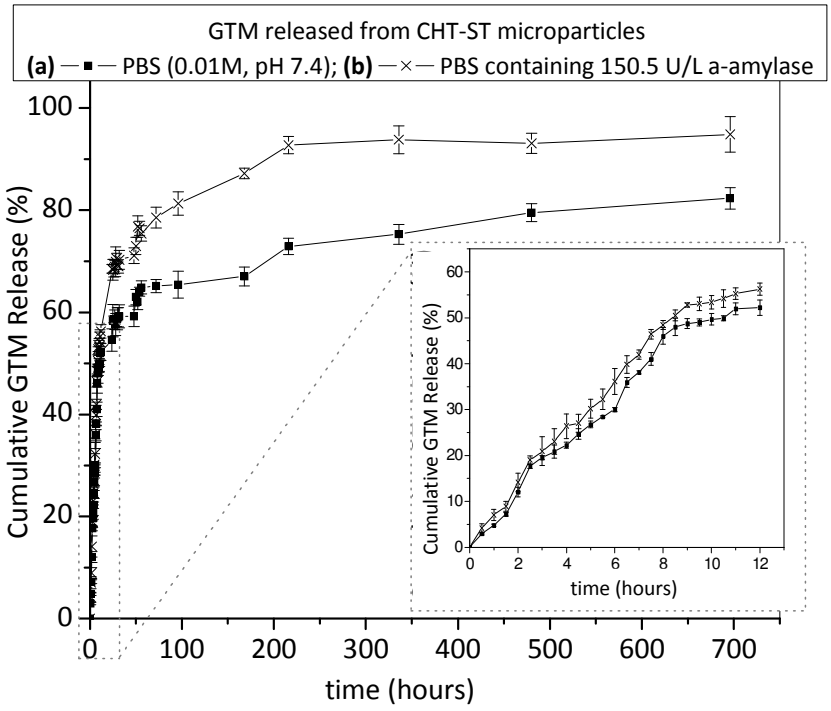

Figure 4.7 Release profiles of gentamicin from chitosan-starch microparticles in PBS **(a)** and α-amylase solutions **(b)**

4.4.2 Cytotoxicity evaluation

4.4.2.1 Effect of material extracts

One of the main concerns related to the use of biodegradable polymers is the potential toxicity of the leachable molecules or degradation products that are released from the material as result of its degradation. Therefore, a first cytotoxicity evaluation was conducted using extracts of the CHT-ST microparticles produced under the standard conditions [16], by incubating the samples in complete DMEM culture medium. Figure 4.8 (a) shows that the extraction time does not significantly influence cell viability which was found to be above 70%, when compared to positive control (100%). The obtained results are in agreement with previous reported cytotoxicity evaluation of chitosan, starch and other polysaccharides based microparticles [36-38]. However, it should be taken into consideration that the

biocompatibility of biomaterials depends on the processing techniques and conditions used to develop the final device, rather than the selected polymer to be used. Therefore, the effect of the new processing conditions was further investigated.

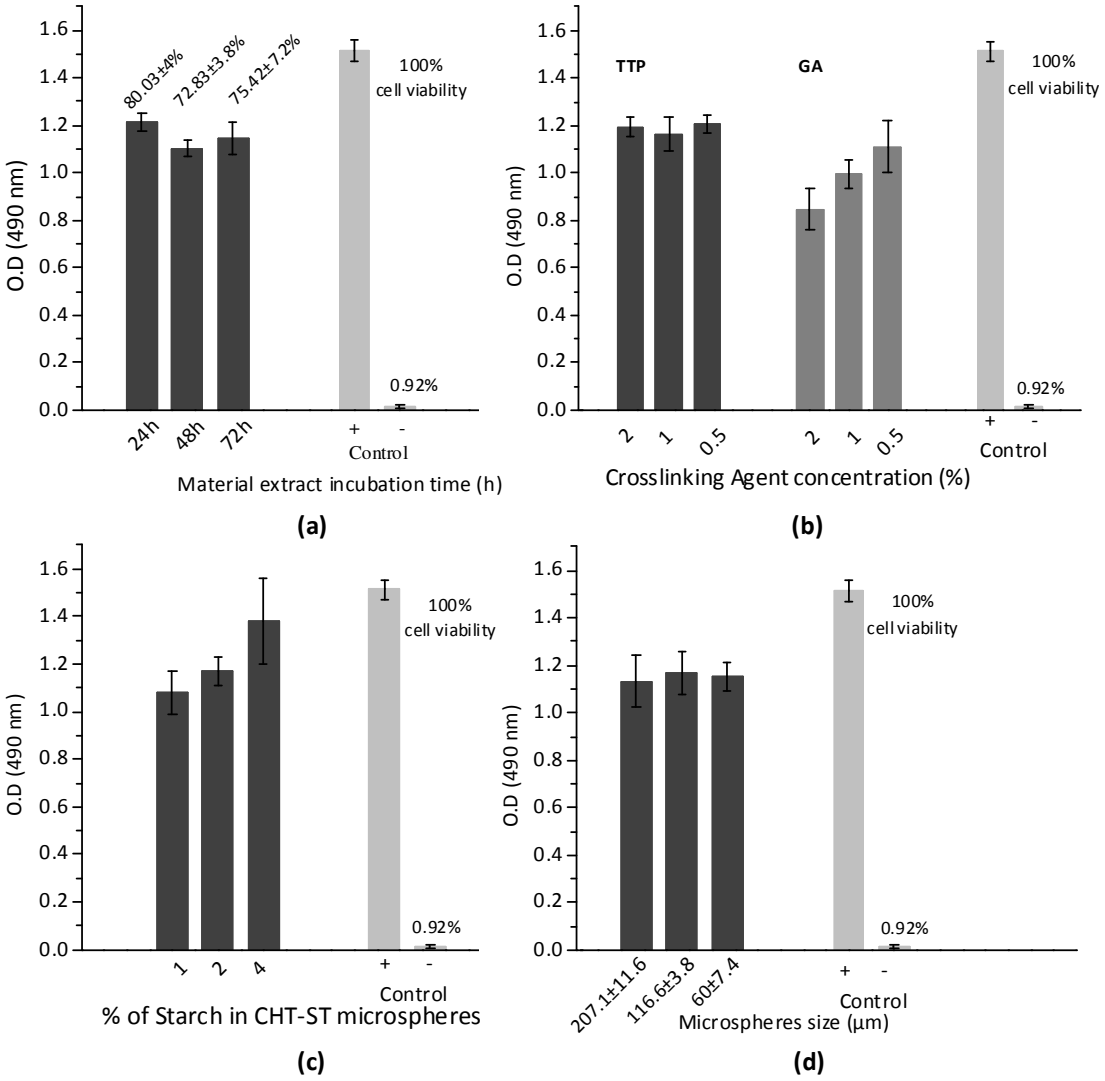

Figure 4.8 Optical density of the MTS solutions after incubation with SaOs2, grown for 24 h in the presence of chitosan-starch microparticles extracts obtained in culture medium for 24, 48 and 72 h **(a)**; grown for 72 h in direct contact with chitosan-starch microparticles obtained by the use of different concentrations of glutaraldehyde and tripolyphosphate as crosslinking agents **(b)**; grown for 72 h in direct contact with chitosan-starch microparticles obtained by the use of different percentages of starch in the composition of the microparticles **(c)**; grown for 72 h in direct contact with chitosan-starch microparticles with different sizes **(d)**

4.4.2.2 Effect of the crosslinking agent and its concentration

Although chitosan is a relatively easy to process, its stability is generally low as result of hydrophilic character and pH sensitivity. To control both their mechanical and chemical properties, various techniques have been used to crosslink chitosan. Chemical reagents such glutaraldehyde (GA), known as excellent crosslinking agent for chitosan, is being widely used during the processing of this polymer [39]. However, during the last decade its cytotoxicity and the possibility of impairing the biocompatibility of its crosslinked products have been considered as major concerns [40, 41]. Recently, chitosan materials were obtained by treatment with multivalent anions such as sodium tripolyphosphate (TPP). TPP has been reported to have no intrinsic cytotoxicity as well as its resulting crosslinked products [42, 43].

Therefore, in this study a comparative cytotoxicity analysis was carried out with CHT-ST microparticles produced using GA and TPP, at three different concentrations. Table 4.1 summarizes the percentage of cell viability depending on the concentration and on the crosslinking agent. Higher cytotoxicity (55.87% cell viability) was obtained for GA, which confirms the previous reported observations [36, 40, 41]. However, a considerable improvement in cell viability was observed when decreasing GA concentration (Table 4.1, Figure 4.8 (b)). Thus, lowering GA content to 0.5% resulted in more than 70% of cell viability. Using the smaller concentration of GA reduces the cytotoxicity of the crosslinked product without compromising the structural stability of the developed material. Given that, GA is a very effective crosslinker agent even at low concentrations. Similarly, the use of GA vapors to crosslink polysaccharide structures, followed by glycine immersion treatment, has been reported to reduce the toxicity of crosslinked products [44]. When TPP is used as a crosslinking agent, values higher than 75% were obtained for cell viability, independent of the concentration used. In fact, the cell viability results are in the same range as the ones obtained when no crosslinking agent was used following the previously reported standard procedure (chitosan-oxidized starch microparticles) [16].

4.4.2.3 Effect of the amount of starch in the composition of the CHT-ST microparticles

Figure 4.8 (c) illustrates the influence of the starch amount in the composition of the microparticles on the cell viability. It can be observed that the presence of starch in the CHT-ST microparticles does not induce any toxic effect on SaOs-2 cells. Moreover, it is possible to observe an enhancement on the cell viability that increased, from 71 to 91%, when the concentration of starch was raised from 1 to 4% (Table 4.1). This result demonstrates that the use of polysaccharide blends in biomaterial design is an effective strategy to improve their

biocompatibility. Furthermore, starch is confirmed as a highly biocompatible natural polymer that can be selected to be used alone, as well as a blend component to improve the tissue and cell behavior [45].

4.4.2.4 Effect of the size of the CHT-ST microparticles

One of the most important experimental parameters for microparticles processing using emulsion techniques is the stirring rate, which mainly controls the size of the resulting particles. By increasing the stirring speeds higher energy is provided to disperse the two immiscible phases (emulsion formation), thus producing smaller drops of the polymeric solution in the dispersed phase. As a result, particles with smaller size are obtained. We have shown that varying the stirring rate from 100 to 1000 rpm, it is possible to produce particles from the micro- to the nano scale range [46].

Increasing the stirring speed from 400 to 800 rpm, microparticles with sizes from 207.1±11.6 µm to 60±7.4 µm were obtained. These smaller microparticles, in comparison to the standard conditions, did not induce a significant difference in cell viability.

As final outcome, it can be summarized that all the produced CHT-ST microparticles would be suitable as delivery vehicles since they did not exhibit a detrimental effect on SaOs-2 cells, thus not compromising their application as drug delivery devices. When GA is used as a crosslinker agent, it is highly recommended to use the lowest concentration or vapors of this chemical to preserve the biocompatibility of the final biomaterial.

4.5 CONCLUSION

The combination of chitosan and oxidized starch have resulted in very hydrophilic microparticles exhibiting high values of water uptake (160%). The *in vitro* enzymatic degradation of the developed CHT-ST microparticles was found to be characterized by an increased initial weight loss, resulting in a loss of 67% of their original weight at the end of the degradation period (60 days). As a result of matrix degradation, increasing amounts of soluble sugars were released to the media. These sugars consist of glucose and other maltooligosaccharide which are innocuous, being easily metabolized in the human body. The occurrence and extent of the degradation was confirmed by morphological observations (SEM), and spectroscopic techniques (FTIR/^{1}H-NMR).

Due to the high hydrophilicity and susceptibility to enzymatic degradation, a highly porous microparticular matrix was obtained after degradation. As a consequence, there is an increase in matrix permeability, leading to increased water penetration and the diffusion of

the entrapped drug being completely released. Thus, the initial stage of drug release is controlled by diffusion, where the hydrophilicity of the matrix plays an important role. At a certain point, when the degradation process is taking place, the remaining amount of entrapped drug is released accordingly. Therefore, the use of the developed biodegradable CHT-ST system, as a vehicle for controlled delivery applications, will allow the degradation process to control the rate of drug release from the biodegradable carriers.

The cell viability studies indicated that the CHT-ST microparticles had a negligible effect over SaOs-2 cells. The obtained percentages of cell viability indicated that microparticles produced using GA as crosslinking agent, caused a significant decrease in cell viability. Therefore, it is highly recommended to use the lowest GA concentrations during the microparticles formation. Moreover, the best results were obtained when increasing amounts of starch in the blend composition were used. This could be especially observed, when no crosslinking is used (chitosan-oxidized starch microparticles). The developed CHT-ST materials are clearly suitable to be used as drug delivery vehicles.

4.6 ACKNOWLEDGEMENTS

E. R. Balmayor thanks the Marie Curie Host Fellowships for Early Stage Research Training (EST) “Alea Jacta EST” (MEST-CT-2004-008104) for providing her a PhD Fellowship. This work was partially supported by the European NoE EXPERTISSUES (NMP3-CT-2004-500283).

4.7 REFERENCES

1. Averous, L. *Journal of Macromolecular Science-Polymer Reviews* **2004**, C44 (3): 231-274.
2. Azevedo, H. S.; Reis, R. L. In *Biodegradable Systems in Tissue Engineering and Regenerative Medicine*, Reis, R. L.; San Roman, J., Eds. CRC Press: Boca Raton, FL, **2005**; pp 177-201.
3. Coviello, T.; Matricardi, P.; Marianecci, C.; Alhaique, F. *Journal of Controlled Release* **2007**, 119 (1): 5-24.
4. Baldwin, S. P.; Saltzman, W. M. *Advanced Drug Delivery Reviews* **1998**, 33 (1-2): 71-86.
5. Williams, D. F.; Zhong, S. P. *International Biodeterioration & Biodegradation* **1994**, 34 (2): 95-130.
6. *Standard Terminology of Environmental Labeling of Packaging Materials and Packages (Withdrawn 2002) D5488-94de1*; ASTM International Standards: DOI: 10.1520/D5488-94DE01, **1994**.
7. Ali, S. A. M.; Doherty, P. J.; Williams, D. F. *Journal of Applied Polymer Science* **1994**, 51 (8): 1389-1398.

8. Silva, G. A.; Ducheyne, P.; Reis, R. L. *Journal of Tissue Engineering and Regenerative Medicine* **2007**, 1 (1): 4-24.
9. Azevedo, H. S.; Santos, T. C.; Reis, R. L. In *Natural-based Polymers for Biomedical Applications*, Reis, R. L.; Neves, N. M.; Mano, J. F.; Gomes, M. E.; Marques, A. P.; Azevedo, H. S., Eds. Woodhead Publishing Limited, CRC Press LLC: Cambridge, **2008**; pp 106-128.
10. Goldbart, R.; Traitel, T.; Lapidot, S. A.; Kost, J. *Polymers for Advanced Technologies* **2002**, 13 (10-12): 1006-1018.
11. Marques, A. P.; Reis, R. L.; Hunt, J. A. *Biomaterials* **2002**, 23 (6): 1471-1478.
12. Silva, G. A.; Marques, A. P.; Gomes, M. E.; Coutinho, O. P.; Reis, R. L. In *Biodegradable Systems in Tissue Engineering and Regenerative Medicine*, Reis, R. L.; San Roman, J., Eds. CRC Press: Boca Raton, FL, **2005**; pp 339-353.
13. Malafaya, P. B.; Silva, G. A.; Reis, R. L. *Advanced Drug Delivery Reviews* **2007**, 59 (4-5): 207-233.
14. Cascone, M. G.; Barbani, N.; Cristallini, C.; Giusti, P.; Ciardelli, G.; Lazzeri, L. *Journal of Biomaterials Science-Polymer Edition* **2001**, 12 (3): 267-281.
15. Venugopal, J.; Ramakrishna, S. *Applied Biochemistry and Biotechnology* **2005**, 125 (3): 147-157.
16. Balmayor, E. R.; Baran, E. T.; Azevedo, H. S.; Reis, R. L. *Highly biodegradable starch-conjugated chitosan microparticles as carrier for the controlled release of aminoglycosides antibiotic drugs: Preparation, characterization and in vitro release study.* **2009**: Submitted.
17. Baran, E. T.; Mano, J. F.; Reis, R. L. *Journal of Materials Science-Materials in Medicine* **2004**, 15 (7): 759-765.
18. Silva, G. A.; Costa, F. J.; Neves, N. M.; Coutinho, O. P.; Dias, A. C. P.; Reis, R. L. *Journal of Biomedical Materials Research Part A* **2005**, 73A (2): 234-243.
19. Ghose, T. K. *Pure and Applied Chemistry* **1987**, 59 (2): 257-268.
20. Zeltinger, J.; Sherwood, J. K.; Graham, D. A.; Mueller, R.; Griffith, L. G. *Tissue Engineering* **2001**, 7 (5): 557-572.
21. Salgado, A. J.; Coutinho, O. P.; Reis, R. L. *Tissue Engineering* **2004**, 10 (3-4): 465-474.
22. Reis, R. L.; Mendes, S. C.; Cunha, A. M.; Bevis, M. J. *Polymer International* **1997**, 43 (4): 347-352.
23. Azevedo, H. S.; Gama, F. M.; Reis, R. L. *Biomacromolecules* **2003**, 4 (6): 1703-1712.
24. Price, N. C.; Stevens, L. In *Fundamentals of Enzymology: The Cell and Molecular Biology of Catalytic Proteins*, 3rd ed.; Price, N. C.; Stevens, L., Eds. Oxford University Press: New York, **1999**; pp 321-367.
25. Snabe, T.; Petersen, S. B. *Journal of Biotechnology* **2002**, 95 (2): PII S0168-1656(02)00005-6.
26. Krieg, P.; Lendl, B.; Vonach, R.; Kellner, R. *Fresenius Journal of Analytical Chemistry* **1996**, 356 (8): 504-507.
27. Lambert, J. B.; Shurvell, H. F.; Lightner, D. A.; Cooks, R. G. In *Organic Structural Spectroscopy*, Prentice-Hall Inc.: New Jersey, **1998**; p 73.
28. Rutiaga, M. O.; Galan, L. J.; Morales, L. H.; Gordon, S. H.; Imam, S. H.; Orts, W. J.; Glenn, G. M.; Nino, K. A. *Journal of Polymers and the Environment* **2005**, 13 (2): 185-191.
29. Imam, S. H.; Gordon, S. H.; Mao, L. J.; Chen, L. *Polymer Degradation and Stability* **2001**, 73 (3): 529-533.
30. ArevaloNino, K.; Sandoval, C. F.; Galan, L. J.; Imam, S. H.; Gordon, S. H.; Greene, R. V. *Biodegradation* **1996**, 7 (3): 231-237.
31. Imam, S. H.; Gordon, S. H.; Nino, K. A.; Greene, R. V. In *Polymeric Materials Encyclopedia*, Salamone, J. C., Ed. CRC Press: Boca Raton, FL, **1996**; Vol. 10, pp 7892-7901.
32. Imam, S. H.; Gould, J. M. *Applied and Environmental Microbiology* **1990**, 56 (4): 872-876.
33. McIntyre, D. D.; Ho, C.; Vogel, H. J. *Starch-Starke* **1990**, 42 (7): 260-267.
34. McIntyre, D. D.; Vogel, H. J. *Starch-Starke* **1991**, 43 (2): 69-76.

35. Zang, L. H.; Howseman, A. M.; Shulman, R. G. *Carbohydrate Research* **1991**, 220: 1-9.
36. CarrenoGomez, B.; Duncan, R. *International Journal of Pharmaceutics* **1997**, 148 (2): 231-240.
37. Manca, M. L.; Mourtas, S.; Dracopoulos, V.; Fadda, A. M.; Antimisiaris, S. G. *Colloids and Surfaces B-Biointerfaces* **2008**, 62 (2): 220-231.
38. Silva, G. A.; Pedro, A.; Costa, F. J.; Neves, N. M.; Coutinho, O. P.; Reis, R. L. *Materials Science & Engineering C-Biomimetic and Supramolecular Systems* **2005**, 25 (2): 237-246.
39. Monteiro, O. A. C.; Airoldi, C. *International Journal of Biological Macromolecules* **1999**, 26 (2-3): 119-128.
40. Speer, D. P.; Chvapil, M.; Eskelson, C. D.; Ulreich, J. *Journal of Biomedical Materials Research* **1980**, 14 (6): 753-764.
41. Mi, F. L.; Tan, Y. C.; Liang, H. F.; Sung, H. W. *Biomaterials* **2002**, 23 (1): 181-191.
42. Desai, K. G. H.; Park, H. J. *Journal of Microencapsulation* **2005**, 22 (2): 179-192.
43. Lee, S. T.; Mi, F. L.; Shen, Y. J.; Shyu, S. S.; Tang, I. H. In *Advances in chitin science.*, Chen, R. H.; Chen, H. C., Eds. National Taiwan Ocean University: Taiwan, **1998**; Vol. 3, pp 475-480.
44. Zhong, S. P.; Teo, W. E.; Zhu, X.; Beuertnan, R.; Ramakrishna, S.; Yung, L. Y. L. *Materials Science & Engineering C-Biomimetic and Supramolecular Systems* **2007**, 27 (2): 262-266.
45. Ciardelli, G.; Chiono, V.; Vozzi, G.; Pracella, M.; Ahluwalia, A.; Barbani, N.; Cristallini, C.; Giusti, P. *Biomacromolecules* **2005**, 6 (4): 1961-1976.
46. Balmayor, E. R.; Tuzlakoglu, K.; Azevedo, H. S.; Reis, R. L. *Acta Biomaterialia* **2009**, 5 (4): 1035-1045.

Chapter 5

Preparation and characterization of starch-poly-ε-caprolactone microparticles incorporating bioactive agents for drug delivery and tissue engineering applications

5.1 ABSTRACT

One limitation associated with the delivery of bioactive agents concerns the short half-life of these molecules when administered intravenously, which results in their loss from the desired site. Incorporation of bioactive agents into depot vehicles provides a means to increase their persistence at the disease site. Major issues are involved in the development of a proper carrier system able to deliver the correct drug, at the desired dose, place and time. In this work, starch-poly-ε-caprolactone (SPCL) microparticles were developed for use in drug delivery and tissue engineering (TE) applications. SPCL microparticles were prepared by using an emulsion solvent extraction/evaporation technique, which was demonstrated to be a successful procedure to obtain particles with a spherical shape (particle size between 5 and 900 μm) and exhibiting different surface morphologies. Their chemical structure was confirmed by Fourier transformed infrared spectroscopy (FTIR). To evaluate the potential of the developed microparticles as a drug delivery system, dexamethasone (DEX) was used as model drug. DEX, a well known component of osteogenic differentiation media, was entrapped into SPCL microparticles at different percentages up to 93%. The encapsulation efficiency was found to be dependent on the polymer concentration and drug-to-polymer ratio. The initial DEX release seems to be governed mainly by diffusion, and it is expected that the remaining DEX will be released when the polymeric matrix starts to degrade. In this work it was demonstrated that SPCL microparticles containing DEX can be successfully prepared and that these microparticular systems seem to be quite promising for controlled release applications, namely as carriers of important differentiation agents in TE.

***This chapter is based on the following publication:**

Balmayor, *E. R.;* Tuzlakoglu, K.; Azevedo, H. S.; Reis, R. L. Preparation and characterization of starch-poly-ε-caprolactone microparticles incorporating bioactive agents for drug delivery and tissue engineering applications. *Acta Biomaterialia* **2009**, 5: 1035-1045.

5.2 INTRODUCTION

Materials of natural origin have been studied and proposed for a wide range of biomedical applications [1-4]. Materials such as collagen, alginate, hyaluronic acid, silk fibroin, chitosan and starch are among the most studied polymers with numerous advantages depending on the specific applications [5-13]. One of the most relevant benefits of using materials of natural origin is their biodegradability inside the human body. Biodegradable systems have the ability to function satisfactorily for a certain time and subsequently to degrade into products easily cleared from the body, with no need for surgery for their removal. This is a particularly desirable property for the design of carriers for the controlled delivery of therapeutic drugs, since it will permit the entrapped drug to be released slowly, allowing repeating dosages and ensuring the successful effect of the treatments [14] as the polymer carrier degrades.

Starch-based polymers have been studied and proposed in the last decade by Reis and coworkers [13, 15-21] for several biomedical applications, such as drug delivery carrier systems, hydrogels and partially degradable bone cements, materials for bone replacement/fixation or fillers for bone defects, and porous structures to be used as scaffolds in tissue engineering of bone and cartilage. These materials were found to be biocompatible [16, 22, 23], non-cytotoxic, biodegradable [24-27] and have shown a great processing versatility [13]. These blended materials have potential application as carriers for the controlled release of different bioactive agents in the form of microparticular systems. Indeed, biodegradable starch-based microparticles have been widely investigated and proposed as drug delivery systems [28-30]. For instance, starch microparticles using soluble potato starch have been developed and proposed for the release of a non-steroidal anti-inflammatory drug [21]. Moreover, a blend of starch and polylactic acid have been used for the encapsulation of steroids, growth factors and bioactive glass in a microparticle system [31-33]. These studies showed that the starch-polylactic acid microparticles are suitable carriers for the controlled release of bioactive agents for bone tissue engineering applications. In addition, derivatives of starch, such as starch acetate or poly(acryl starch), have been described for the incorporation and release of peptides and proteins [34-36]. However, to our knowledge there has so far been no report in the literature on the development of microparticle systems based on starch-poly-ε-caprolactone blended materials. The combination of a hydrophilic natural material (starch) with a hydrophobic synthetic polymer (poly-ε-caprolactone), both biodegradable and biocompatible, in a single blended material constitutes the major advantage of these microparticles.

Numerous controlled release systems have been developed, ranging from implants [37, 38] to novel osmotically driven pills [38]. The use of non-invasive delivery methods, such as injectable systems in the form of nano and microparticles, will bring substantial benefits when compared with some surgical techniques. It has already been reported that injectable systems made of nano and microparticles could be applied as carriers of different drugs and bioactive agents within the field of tissue engineering (e.g. differentiation agents and growth factors [39, 40]). Dexamethasone (DEX) has been widely used in clinical applications to treat immuno-disorders [41, 42], but a more specific and common use has been the control of the inflammatory response and tissue repair during organ transplantation [43]. In the last years, the use of this corticosteroid as an osteogenic agent has increased considerably in *in vitro* cell culture to induce the differentiation of stem cells into an osteoblastic lineage [41, 44-46].

This study aims to establish experimental conditions for the production of a biodegradable and biocompatible microparticular system with different characteristics (e.g. size, size distribution, surface morphology) that can be used as a potential carrier for the delivery of important bioactive agents. For that, we have used a polymeric blend of starch with poly-ε-caprolactone. The microparticular system was characterized in terms of particle size, size distribution, surface morphology and chemical structure. The carrier potential was evaluated by encapsulating DEX into the microparticles and its release behavior studied *in vitro*.

5.3 EXPERIMENTAL

5.3.1 Materials

A polymeric blend of corn starch with poly-ε-caprolactone (SPCL, 30-70 wt %) was used in this study. More details about the thermal properties of this polymeric blend can be found elsewhere [47]. Methylene chloride and polyvinyl alcohol (PVA) were obtained from Sigma-Aldrich (USA), and used as received. Unless otherwise indicated, the molecular weight (MW) of the PVA used was in the range 30 000-70 000 g/mol. DEX (97%, cell culture tested, Sigma-Aldrich, USA) was used as bioactive molecule for the encapsulation studies. Solvents for high-performance liquid chromatography (HPLC) (acetonitrile and water) were HPLC grade (LABSCAN, Ireland). Triamcinolone was used as internal standard for DEX quantification. Potassium bromide (KBr) for IR spectroscopy (≥99.5%) was obtained from Sigma-Aldrich (USA). Other chemicals were of reagent grade, all from Sigma-Aldrich (USA), and used as received.

5.3.2 Preparation of SPCL microparticles

SPCL microparticles were prepared by using an emulsion solvent extraction/evaporation technique [48]. Briefly, SPCL was dissolved in 5 mL of methylene chloride under vigorous stirring. This solution was dropped into a 200 mL PVA solution, and emulsified for 4 h at different stirring rates. Different experimental conditions were evaluated, and the details of each condition are summarized in Table 5.1. The microparticles where then collected by filtration, washed with distilled water and vacuum dried in a desiccator. For the selected condition to be loaded with DEX, SPCL was mixed with the steroid at different percentages (5, 10 and 15% (w/w), relatively to polymer weight) and dissolved in methylene chloride. The same procedure was performed as described for unloaded microparticles. The reaction medium was stored at 4 ^{o}C for later quantification of unloaded DEX. All experiments were carried out in triplicate.

Table 5.1 Effect of the experimental conditions employed during microparticles production on the size and morphology of the resulting microparticles

Condition	SPCL[a] (%)	Emulsification medium PVA[b] (%) [MW (g/mol)][c]	Stirring rate (rpm)	Reaction time (h)	Particle Size (μm)	Shape/ Surface[d] (SEM)
I	**5**	1	600	4	102.3±4.1	s/s
II	5	0.5	600	4	200.4±3.7	s/s
III	10	**0.5**	600	4	575.1±4.6	r/p
IV	**10**	**1** *[30 000-70 000]*	**600**	4	499.6±4.8	r/p(HP)
V	10	1 *[70 000-100 000]*	600	4	702.1±19.0	r/p(HPD)
VI	10	1	**800**	4	283.0±21.0	r/p(HPD)
VII	10	1	**400**	4	913.7±9.8	r/p(HPD)
VIII	10	**2**	600	4	376.0±3.2	r/p
IX	10	**5**	600	4	324.1±15.3	r/p(HPD)
X	**15**	1	600	4	770.0±8.7	r/p
XI	**20**	1	600	4	810.0±16.2	r/p(HPD)
XII	10	1	**20 000**	4	5.73±8.19	s/s

[a]SPCL: polymeric blend of corn starch with poly-ε-caprolactone
[b]PVA: polyvinyl alcohol
[c]PVA MW: The molecular weight of the PVA used was in the range 30 000-70 000 g/mol for all the experiments, but in the case of the experimental condition V the MW was increased (70 000-100 000 g/mol) for comparison.
[d]s/s: spherical/smooth, r/p: round/porous, HPD: High polidispersity, HP: Highly porous

5.3.3 Physicochemical characterization of SPCL microparticles

5.3.3.1 Morphological analysis: scanning electron microscopy (SEM) and micro-computed tomography (μ-CT)

To analyze the morphology and surface of the microparticles obtained under the different experimental conditions, the samples were mounted onto aluminium stubs with a carbon tape and gold sputter-coated (Fisons Instruments, Sputter Coater SC502, UK). All images were collected with a Leica Cambridge S-360 model (UK) scanning electron microscope.

Microparticle samples with porous surfaces (experimental condition III, Table 5.1) were scanned by micro-computed tomography (μ-CT) using a μ-CT 20 equipment (SCANCO Medicals, Switzerland). The energy of the scanner used was 100 kv/ 98 μA intensity. A threshold range of values of 141-255 was used to estimate the porosity of the samples. Approximately 40 slices of the sample were obtained. Mimics (Materialise, Belgium), CT Analyser and CT Vol Realistic 3D Visualization (SkyScan, Belgium) software were used for image processing and to create and visualize the three-dimensional representation.

5.3.3.2 Size distribution

To determine the size distribution of the microparticles obtained under the different experimental conditions, the microparticles were separated through a series of standard sieves (20, 60, 100, 125, 150, 250, 450, 500, 650, 900 and 1000 μm; Linker Industrie-Technik, Germany). The microparticle fraction that passed through a sieve and was retained on the sieve with a certain pore size was collected and weighed, and finally correlated with the total mass of the microparticles sample analyzed.

5.3.3.3 Fourier transformed infrared spectroscopy (FTIR)

The chemical structure of the microparticles (unloaded, loaded with DEX and after release) was analyzed by fourier transformed infrared spectroscopy (FTIR) (IRPrestige-21 FRIT-8400S, Shimadzu, Japan) in transmission mode. For that, microparticles (1 mg) were mixed with KBr (40 mg) and then formed into a disc in a manual press (161-1100 hand press, PIKE Technologies, USA). Transmission spectra were recorded using at least 32 scans with 4 cm^{-1} resolution, in the spectral range 4000-600 cm^{-1}.

5.3.3.4 X-ray diffraction (XRD)

In order to confirm the encapsulation and release of DEX into and from the SPCL microparticles, and to access the physical state of the entrapped drug, X-ray diffraction

patterns of DEX and SPCL microparticles (unloaded, loaded with DEX and after the release studies) were obtained in a X-ray diffractometer (X'Pert MPD, Philips, The Netherlands). The data collection was performed with a Cu anode and monochromator used at a voltage of 40 kV. The samples were analyzed over the angle range (2θ) 2^{o}-60^{o}.

5.3.4 Determination of DEX encapsulation efficiency and release profile from SPCL microparticles

5.3.4.1 Encapsulation efficiency

The encapsulation efficiency (EE) of DEX into the SPCL microparticles was calculated using the following equation:

$$\%\, EE(DEX) = \left[\left(C_{i-DEX} - C_{r-unloaded\ DEX}\right) / C_{i-DEX}\right] \times 100 \qquad (5.1)$$

Where C_i is the initial concentration of DEX added, and C_r is the concentration of unloaded DEX (remaining in the reaction medium: PVA solution where loaded microparticles were produced). DEX concentration was determined by HPLC (please see section 5.3.5). Determinations were made in triplicate and the average is reported.

5.3.4.2 In vitro release of DEX from SPLC microparticles

Pre-weighed SPCL-DEX-loaded microparticles were suspended in 40 mL of phosphate buffered saline solution (PBS, pH 7.4, 0.01 M) at a concentration of 2.5 mg/mL. The microparticles were maintained at 37 ^{o}C under constant agitation (50 rpm) for 30 days in a shaking bath. At predetermined time points, first each 30 min, then each 1 and 2 h, and 4, 5, 7, 10, 14, 30 days, 1 mL aliquots of the supernatant were taken and replaced with the same volume of fresh PBS solution. DEX concentration was quantified by HPLC. All the release experiments were carried out in triplicate and the average is reported.

5.3.5 Quantification of DEX by HPLC

Before HPLC analysis, samples from the reaction medium were extracted three times with a mixture of hexane and ethyl acetate in the same proportions. The final extract was collected and the solvent allowed to evaporate under nitrogen flow. The dry extract was reconstituted in a mixture of acetonitrile/water (50:50 v/v, mobile phase) before analysis. The aliquots from the release medium (PBS solution containing released DEX) were analyzed directly as taken.

DEX was quantified by reverse-phase (RP) HPLC. HPLC was performed on a Jasco PU-2080 Plus system using a RP-18 column (LiChrospher, 5 µm, Merck, Germany) with acetonitrile/water (50:50 v/v) as mobile phase at a flow rate of 0.5 mL/min. Absorbance was monitored at 254 nm (UV detector Jasco 870-UV). The column was eluted in isocratic conditions over 20 min. Data acquisition and peak areas were determined with a Shimadzu C-R6A Chromatopac software. The concentration of DEX was calculated by using a calibration curve (y = 8697.18 + (1.65 X 10^7)x, R^2= 0.9995). Triamcinolone was used as internal standard.

5.4 RESULTS AND DISCUSSION

5.4.1 Preparation of SPCL microparticles: evaluation of the effect of different experimental conditions on particle size and morphology

In order to optimize the proposed methodology for the production of SPCL microparticles with different morphological characteristics and sizes, several experimental conditions were tested (summarized in Table 5.1).

Four different polymeric (SPCL) concentrations were studied to investigate the effect of this parameter on the size and morphology of the microparticles. Figure 5.1 shows the morphological characteristics of the SPCL microparticles obtained with different polymeric concentrations. The viscosity of the SPCL solution is directly related to the polymeric concentration [49]. Consequently, at higher concentrations of SPCL, there is a rather significant increase in the viscosity of the solution and, as result, the size of the drops in the emulsification medium is higher, which leads to an increase in the microparticle size (experimental conditions I, IV, X, XI: Table 5.1). It was found that at polymer concentrations higher than 10% the polidispersity increases due to the higher particle size obtained in these conditions. It was also observed that at higher polymeric concentrations, the microparticles exhibit a porous surface, as shown in Figure 5.2 (b) and (c), when compared with the smooth morphology of the microparticles obtained at lower polymer concentration (Figure 5.2 (a)). A representative sample (experimental condition IV: Table 5.1) from porous microparticles was analyzed by micro-CT scan (Figure 5.3). As result, 44% porosity was obtained, which indicated that 10% of polymer concentration is adequate for the production of microparticles with a porous structure.

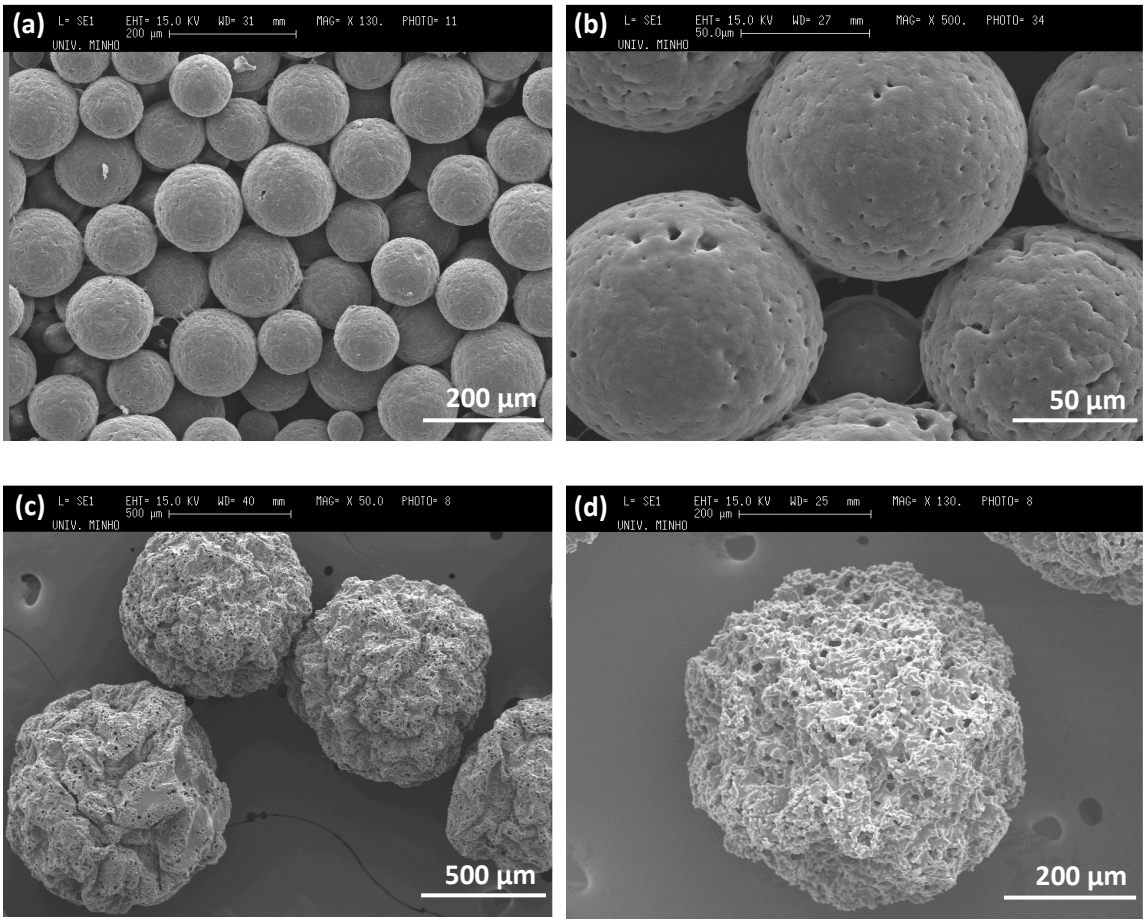

Figure 5.1 SEM micrographs of SPCL microparticles obtained under different experimental conditions: condition I-SPCL 5% **(a), (b)** and condition IV-SPCL 10% **(c), (d)** (Table 5.1)

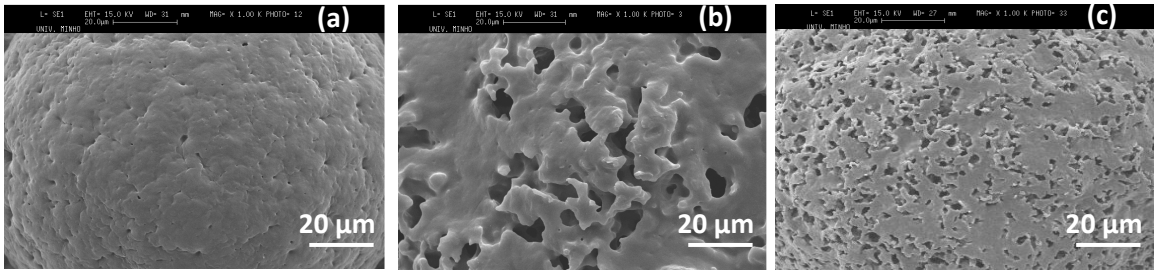

Figure 5.2 SEM micrographs of the surface of SPCL microparticles showing different morphologies when using different polymer concentrations: condition I-SPCL 5% **(a)**, condition IV-SPCL 10% **(b)**, condition XI-SPCL 20% **(c)** (Table 5.1)

By means of selecting the polymer concentration in the range of 5-10%, it is possible to obtain microparticles with a desired size range (100-600 µm), a narrow size distribution as illustrated in Figure 5.4, and different surface morphologies.

The effect of the reaction medium composition was also studied, by the varying the concentration of PVA in the emulsification medium from 0.5 to 5%. The use of PVA as an emulsion stabilizer results in a quite successful preparation of SPCL microparticles. By analyzing the results presented in Table 5.1, it can be observed that the size of the microparticles slightly decreases as the PVA concentration increases (experimental conditions III, IV, VIII, IX: Table 5.1), but this effect was not as significant as the one observed for the polymer concentration. The spherical shape of the microparticles is lost as the concentration of PVA becomes higher than 2%, and the surface of the microparticles becomes more porous. Analyzing the effect of PVA molecular weight (MW), it was found a noticeable increase in the size of the microparticles (experimental conditions IV, V: Table 5.1), when the PVA MW range increased from 30 000-70 000 to 70 000-100 000 g/mol. Therefore, a concentration of 0.5 and 1% of PVA with a MW range 30 000-70 000 g/mol was selected as optimum, avoiding loss of spherical shapes, deformation of particles and uncontrolled particle size.

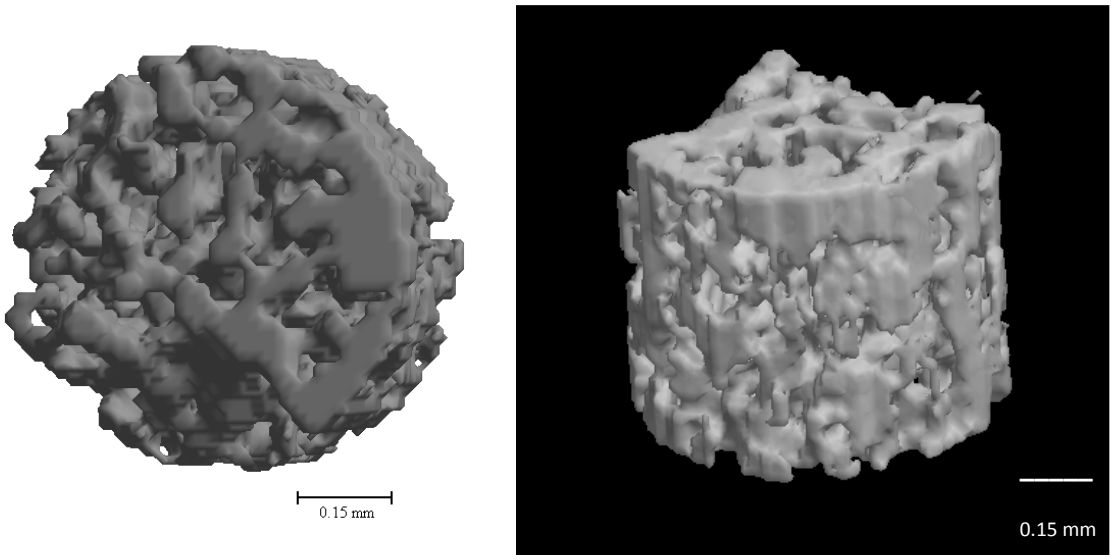

Figure 5.3 Micro-CT three-dimensional reconstruction of the SPCL microparticle illustrating the porosity of the obtained particulate structure (experimental condition IV: Table 5.1)

One of the most important factors affecting the microparticle size is the stirring speed during their preparation [50]. It has been already shown in the literature [51] that by varying the stirring speed from hundreds to thousands of rpm, micro to nanoparticles can be produced. In our experiments, we observed that by increasing the stirring rate, the size of the microparticles drastically decreased (experimental conditions VII (400 rpm), IV (600 rpm), VI (800 rpm) and XII (20 000 rpm): Table 5.1). In fact, an increase in the stirring speeds provides higher energy to disperse two immiscible phases (oil in water phase) and form the emulsion,

producing smaller drops of oil phase in the water (because it is breaking the oil phase into smaller drops) and as a result smaller particles are obtained. Figure 5.5 shows the morphological characteristics and the size of the SPCL microparticles obtained with higher stirring speeds.

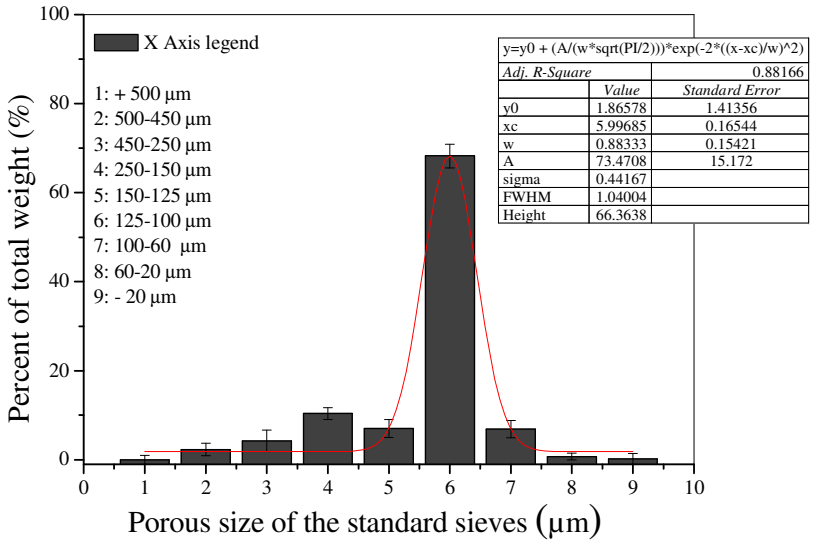

Figure 5.4 Size distribution of the SPCL microparticles (experimental condition I: Table 5.1)

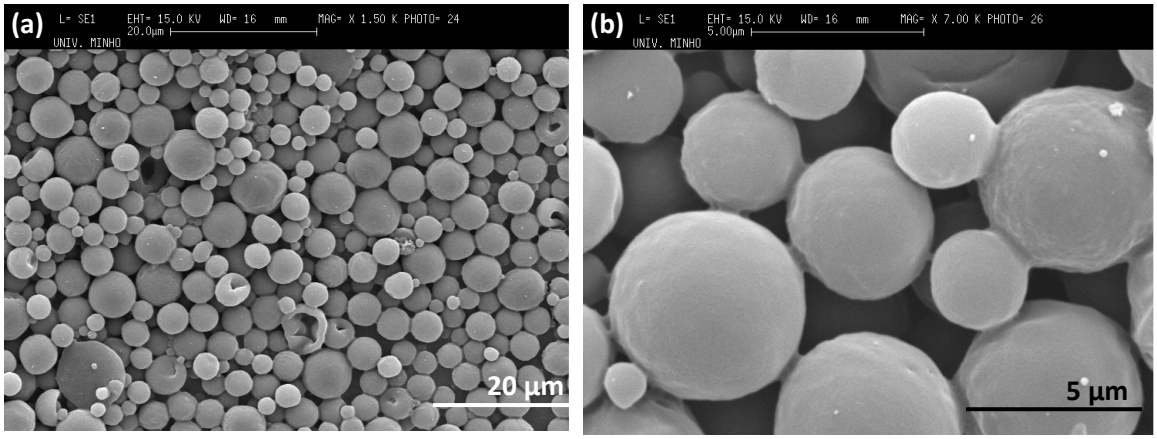

Figure 5.5 SEM micrographs of SPCL microparticles obtained at higher stirring speed, at lower **(a)** and higher **(b)** magnification. Condition XII-20 000 rpm, resulting in a stronger decrease in the size of the resulting microparticles

5.4.2 Physicochemical characterization of unloaded SPCL microparticles

Iodine-potassium solution (Lugol) is a well-known and useful solution for chemically identifying the presence of starch molecules [31]. The amylose present in the starch molecule

has a helical secondary structure [52], where substances such as iodine can lodge, forming a complex as an inclusion compound. This starch-iodine forms a coloured complex (dark blue), and this property can be used to identify the presence and distribution of starch in complex polymeric blends. Staining with Lugol solution was performed for all experimental conditions. These experiments revealed the presence of starch in the microparticles, since a dark blue staining was observed in all conditions. A more intense staining was observed in the microparticles with porous surface. This may due to the diffusion of iodine to the interior of the microparticles in this case, while in the microparticles with smooth surface the iodine is mainly reacting with the starch molecules present at the surface of the microparticles.

The infrared spectrum of SPCL microparticles exhibits the same characteristics peaks of the raw material before processing (the infrared spectrum of SPCL raw material has been described in previous publications [25, 53-55]). The bands from PCL and starch were easily identified. The strongest bands and their assignments are summarized in Table 5.2. This demonstrates that both components of the blend remained present in the chemical structure of the obtained microparticles.

Table 5.2 Characteristics IR bands of the microparticle components (starch and poly-ε-caprolactone) [12, 27]

cm^{-1}	Vibration	Abbreviation
	(from PCL)	
2944/2864	Asymmetric/Symmetric CH_2 stretching	$\upsilon_{as}(CH_2)$, $\upsilon_{s}(CH_2)$
1724	C=O stretching	υ(C=O)
1244	Asymmetric COC stretching	υ_{as}(COC)
1195	OC-C stretching/Symmetric COC stretching	υ(OC-O), υ_{s}(COC)
	(from starch)	
3362	OH stretching	υ(OH)
1021/1048	C-O-C glycosidic bond	υ(COC)

5.4.3 Determination of DEX encapsulation efficiency and *in vitro* release profile

For the loading of DEX and *in vitro* release experiments, conditions I-IV (Table 5.1) were selected for the preparation of SPCL microparticles. Using these conditions, DEX-loaded microparticles were successfully produced. The obtained microparticles exhibited a morphology very similar to unloaded microparticles (Figures 5.1 (d) and 5.6 for morphological comparison). A more compact surface was found and the particle size slightly increased as result of DEX entrapment. The quantification of the DEX, before and after loading, was performed by HPLC.

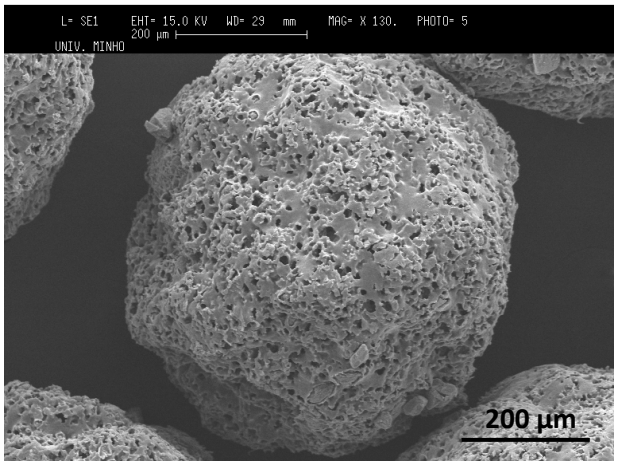

Figure 5.6 SEM micrographs of SPCL-DEX-loaded microparticles (experimental condition IV-DEX: Table 5.3)

5.4.3.1 Encapsulation efficiency

For the determination of the encapsulation efficiency (EE), the amount of DEX remaining in the reaction medium (unloaded DEX) was quantified. Table 5.3 shows the EE values as a function of the initial amount of DEX added to the polymer solution. Higher values were obtained when 15% of DEX was added. There is a notable increase in the EE values when there is an increment from 5 to 10% in the initial DEX amount. However, increasing the initial amount of DEX higher than 10%, yielded no significant increase in EE values. Taking these results into account, 15% was used as the initial amount of DEX (1:5 drug/polymer ratio) for the release studies.

Table 5.3 Effect of the initial amount of DEX on its encapsulation efficiency in the SPCL microparticles

Condition	% SPCL	Particles size (µm)	Drug/polymer ratio (w/w)	Encapsulation efficiency (%)
IV-DEX	10	525.3±7.9	1:20	74.99
			1:10	90.72
			1:5	93.65

5.4.3.2 In vitro release of DEX from SPLC microparticles

Drug release from a polymeric matrix is controlled by a variety of factors, such as the solubility of the drug within the surrounding fluid, the size of the drug molecule and its mobility within the swollen polymeric network, and the dissolution rate of the polymer and polymer-drug interactions. Moreover, several authors have reported that the release kinetic is dependent on different characteristics of the microparticles (e.g. type of polymer, particle size and size distribution, surface morphology) [56-61], and these features can be controlled by the

fabrication conditions. A number of studies in the literature have investigated the effect of fabrication conditions (e.g. interconnected pores and channels, emulsification medium concentration and polymer concentration) on the morphology of obtained microparticles, drug distribution and release kinetics [56-58, 60, 61]. Thus, understanding the influence of microparticles characteristics on the release behavior is important for yielding useful products that can meet different clinical applications.

The release profiles of DEX from SPCL microparticles during 30 days in PBS are illustrated in Figure 5.7. The release in the first day is shown in more detail in the insert graph.

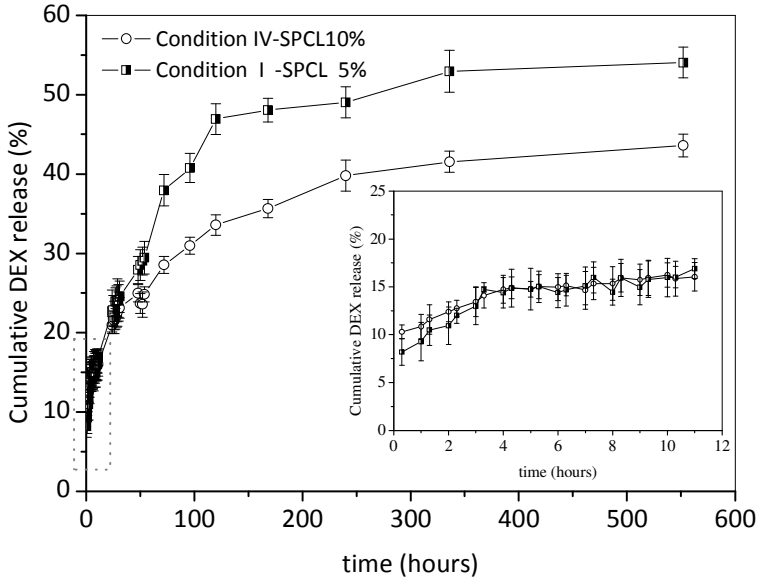

Figure 5.7 *In vitro* release profiles of DEX from SPCL microparticles in PBS (pH 7.4, 0.01 M), at 37 ^{o}C and 50 rpm, for a period of 4 weeks. DEX-loaded SPCL microparticles obtained by the use of different polymer concentrations are compared. The insert graph shows the DEX release for a period of 11 h

The initial burst release is attributable to the release of the drug that is present at the outermost layer of the microparticles and is released quickly [4, 27, 62, 63]. The burst release is then followed by a sustained release stage, which is most likely due to the hydrophobic character of poly-ε-caprolactone (PCL) polymer present in the microparticles and consequently its corresponding low permeability to water. The hydrophobicity of PCL (70% in the blend) can cause a delay in water penetration and, consequently, the diffusion of the drug through the polymeric matrix into the aqueous release medium was retarded. On the other hand, it is necessary to take in consideration that the biodegradation of SPCL in PBS medium is slow [25] when compared with other biodegradable polymers. Therefore, at the initial stages, the

release of DEX from the SPCL microparticles is mainly controlled by diffusion mechanisms, and it is expected that the remaining drug in the polymeric matrix will be released as the degradation process becomes more significant.

When using higher polymer concentrations in the preparation of the microparticles (Figure 5.7) the drug release profile shows a more sustained pattern. This may be due to the fact that as the SPCL concentration increases, the particle size also increases, leading to a decrease in the total surface area of the microparticle system, reducing the area that is in direct contact with the water.

Further evidence of the loading and release of DEX from the SPCL microparticles was shown by FTIR analysis (Figure 5.8). The FTIR spectrum of DEX-loaded SPCL microparticles (Figure 5.8 (b)) shows the characteristics bands of DEX, indicating the successful loading of the drug into the microparticles. After the release studies, it can be observed that there is a reduction in the intensity of the characteristic bands of DEX in the IR spectrum (Figure 5.8 (c)), due to the partial release of the drug from the microparticles. This result further indicates that the DEX present at the outermost layer of the microparticles is released quickly. The release profile obtained in this study, with an initial burst stage followed by a sustained release (typical of first-order release kinetic systems), is in accordance with the release behavior obtained with other delivery systems with similar composition [64].

The structure of the entrapped drug is also an important aspect to take into consideration in drug delivery systems, since it is known that transitions from an amorphous to crystalline structures may occur. These transitions may affect the rate of drug release. For this purpose, XRD studies can show the physical nature of the encapsulated material. In Figure 5.9 XRD diffractograms of DEX, unloaded SPCL microparticles and SPCL microparticles loaded with DEX after 30 days of *in vitro* release are presented. The XRD pattern of DEX shows several crystalline peaks, as marked in Figure 5.9 (d). For the DEX-loaded SPCL microparticles it is possible to see the appearance of the characteristics peaks from the drug at low 2θ, between 10^{o} and 20^{o}, indicating the crystalline state of the DEX entrapped in the SPCL matrix. The maintenance of the crystalline structure may be due to the space available in the polymeric matrix (e.g. pore formation). Another confirmation of the *in vitro* DEX release can be observed in Figure 5.9 (c), where the characteristics peaks of DEX are not observed after 30 days in PBS.

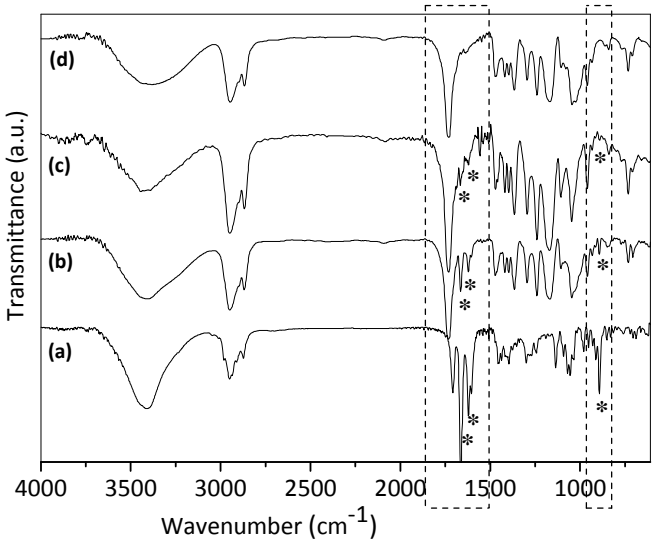

Figure 5.8 FTIR spectra of DEX and SPCL microparticles: DEX **(a)**, DEX-loaded microparticles **(b)**, DEX-loaded microparticles after 30 days of *in vitro* release **(c)**, unloaded SPCL microparticles **(d)**. The characteristics bands of DEX are marked (*)

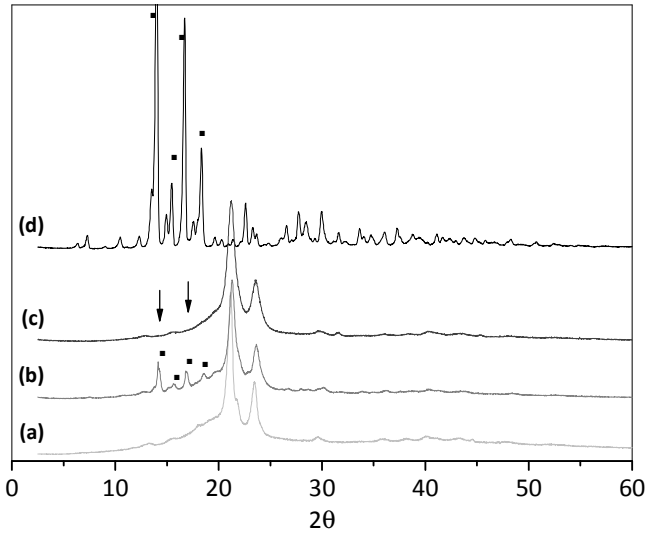

Figure 5.9 XRD diffractograms of SPCL microparticles: unloaded **(a)**, loaded with DEX **(b)**, DEX loaded microparticles after 30 days of release **(c)**, DEX **(d)**. The characteristics peaks of DEX are marked (■)

Several research groups are currently developing controlled release systems in the context of bone tissue engineering with the main goal of inducing *in vitro* the osteogenic differentiation of stem cells. A common problem associated with some of these systems is still in the lack of control over the drug release. Therefore, in this study we propose a very

attractive drug delivery system, consisting of SPCL microparticles that can present diverse characteristics depending on the experimental conditions used during processing. The processing method can be adjusted to obtain particles with different sizes in the micron range, as well as with distinct surface morphologies from smooth to porous. Moreover, the developed SPCL microparticles were found to be biodegradable, non-cytotoxic and biocompatible, as reported in a previous study [27]. The *in vitro* release studies of DEX, a widely used osteogenic agent, showed a sustained release pattern for a period of 30 days, indicating that the developed system might be very useful for the induction of osteoblastic differentiation of stem cells.

Further studies will be carried out in order to study the release behavior of DEX or other bioactive agents in presence of enzymes in order to investigate the effect of matrix degradation on the release kinetics.

5.5 CONCLUSIONS

In this work the production of polymeric microparticles made from a blend of starch with poly-ε-caprolactone (SPCL) by means of an emulsion solvent extraction/evaporation technique was evaluated. Microparticles with different morphologies (smooth and porous) and sizes between 5 and 900 μm could be obtained by using this methodology. Encapsulation of DEX into SPCL microparticles was performed with high encapsulation efficiencies, up to 93%. The *in vitro* release studies showed a sustained release pattern for a period of 30 days, indicating the carrier potential of SPCL microparticles for the delivery of important bioactive agents. The developed system might be very useful in the *in vitro* culturing of stem cells aimed at being committed into the osteoblastic lineage.

5.6 ACKNOWLEDGEMENTS

E. R. Balmayor thanks the Marie Curie Host Fellowships for Early Stage Research Training (EST) “Alea Jacta EST” (MEST-CT-2004-008104) for providing her with a PhD Fellowship. This work was partially supported by the European NoE EXPERTISSUES (NMP3-CT-2004-500283).

5.7 REFERENCES

1. Nair, L. S.; Laurencin, C. T. *Progress in Polymer Science* **2007**, 32 (8-9): 762-798.
2. Elvira, C.; Mano, J. F.; San Roman, J.; Reis, R. L. *Biomaterials* **2002**, 23 (9): PII S0142-9612(01)00322-2.
3. Coviello, T.; Matricardi, P.; Marianecci, C.; Alhaique, F. *Journal of Controlled Release* **2007**, 119 (1): 5-24.

4. Malafaya, P. B.; Silva, G. A.; Reis, R. L. *Advanced Drug Delivery Reviews* **2007**, 59 (4-5): 207-233.
5. Lacerda, S. H. D.; Ingber, B.; Rosenzweig, N. *Biomaterials* **2005**, 26 (34): 7164-7172.
6. George, M.; Abraham, T. E. *Journal of Controlled Release* **2006**, 114 (1): 1-14.
7. Price, R. D.; Berry, M. G.; Navsaria, H. A. *Journal of Plastic Reconstructive and Aesthetic Surgery* **2007**, 60: 1110-1119.
8. Campoccia, D.; Doherty, P.; Radice, M.; Brun, P.; Abatangelo, G.; Williams, D. F. *Biomaterials* **1998**, 19 (23): 2101-2127.
9. MacIntosh, A. C.; Kearns, V. R.; Crawford, A.; Hatton, P. V. *Journal of Tissue Engineering and Regenerative Medicine* **2008**, 2 (2-3): 71-80.
10. Altman, G. H.; Diaz, F.; Jakuba, C.; Calabro, T.; Horan, R. L.; Chen, J. S.; Lu, H.; Richmond, J.; Kaplan, D. L. *Biomaterials* **2003**, 24 (3): 401-416.
11. Ko, J. A.; Park, H. J.; Hwang, S. J.; Park, J. B.; Lee, J. S. *International Journal of Pharmaceutics* **2002**, 249 (1-2): 165-174.
12. Wang, L. Y.; Ma, G. H.; Su, Z. G. *Journal of Controlled Release* **2005**, 106 (1-2): 62-75.
13. Reis, R. L.; Cunha, A. M. In *Encyclopedia of Materials: Science and Technology*, Buschow, K. H. J.; Cahn, R. W.; Flemings, M. C.; Ilschner, B.; Kramer, E. J.; Mahajan, S.; Veyssiere, P., Eds. Elsevier Ltd.: New York, **2001**; Vol. 11, pp 8810-8816.
14. Thomson, R. C.; Wake, M. C.; Yaszemski, M. J.; Mikos, A. G. In *Advances in Polymer Science. Biopolymers II*, Peppas, N. A.; Langer, R. S., Eds. Springer Berlin: Heidelberg, **1995**; Vol. 122, pp 245-274.
15. Pereira, C. S.; Cunha, A. M.; Reis, R. L.; Vazquez, B.; San Roman, J. *Journal of Materials Science-Materials in Medicine* **1998**, 9 (12): 825-833.
16. Mendes, S. C.; Reis, R. L.; Bovell, Y. P.; Cunha, A. M.; van Blitterswijk, C. A.; de Bruijn, J. D. *Biomaterials* **2001**, 22 (14): 2057-2064.
17. Malafaya, P. B.; Elvira, C.; Gallardo, A.; San Roman, J.; Reis, R. L. *Journal of Biomaterials Science-Polymer Edition* **2001**, 12 (11): 1227-1241.
18. Boesel, L. F.; Mano, J. F.; Elvira, C.; San Roman, J.; Reis, R. L. In *Biodegradable Polymers and Plastics*, Chiellini, E.; Solaro, R., Eds. Kluwer Academic/Plenum Publishers: New York, **2003**; pp 243-260.
19. Gomes, M. E.; Sikavitsas, V. I.; Behravesh, E.; Reis, R. L.; Mikos, A. G. *Journal of Biomedical Materials Research Part A* **2003**, 67A (1): 87-95.
20. Gomes, M. E.; Reis, R. L. *International Materials Reviews* **2004**, 49 (5): 261-273.
21. Malafaya, P. B.; Stappers, F.; Reis, R. L. *Journal of Materials Science-Materials in Medicine* **2006**, 17 (4): 371-377.
22. Marques, A. P.; Reis, R. L.; Hunt, J. A. *Biomaterials* **2002**, 23 (6): 1471-1478.
23. Gomes, M. E.; Reis, R. L.; Cunha, A. M.; Blitterswijk, C. A.; de Bruijn, J. D. *Biomaterials* **2001**, 22 (13): 1911-1917.
24. Gomes, M. E.; Godinho, J. S.; Tchalamov, D.; Cunha, A. M.; Reis, R. L. *Materials Science & Engineering C-Biomimetic and Supramolecular Systems* **2002**, 20 (1-2): 19-26.
25. Azevedo, H. S.; Gama, F. M.; Reis, R. L. *Biomacromolecules* **2003**, 4 (6): 1703-1712.
26. Azevedo, H. S.; Reis, R. L. In *Biodegradable Systems in Tissue Engineering and Regenerative Medicine*, Reis, R. L.; San Roman, J., Eds. CRC Press: Boca Raton, FL, **2005**; pp 177-201.
27. Balmayor, E. R.; Tuzlakoglu, K.; Marques, A. P.; Azevedo, H. S.; Reis, R. L. *Journal of Materials Science-Materials in Medicine* **2008**, 19 (4): 1617-1623.
28. Taguchi, T. *Clinical Pharmacokinetics* **1994**, 26 (4): 275-291.
29. Bjork, E.; Edman, P. *International Journal of Pharmaceutics* **1990**, 62 (2-3): 187-192.
30. Fahlvik, A. K.; Holtz, E.; Schroder, U.; Klaveness, J. *Investigative Radiology* **1990**, 25 (7): 793-797.
31. Silva, G. A.; Costa, F. J.; Neves, N. M.; Coutinho, O. P.; Dias, A. C. P.; Reis, R. L. *Journal of Biomedical Materials Research Part A* **2005**, 73A (2): 234-243.

32. Silva, G. A.; Pedro, A.; Costa, F. J.; Neves, N. M.; Coutinho, O. P.; Reis, R. L. *Materials Science & Engineering C-Biomimetic and Supramolecular Systems* **2005**, 25 (2): 237-246.
33. Silva, G. A.; Coutinho, O. P.; Ducheyne, P.; Shapiro, I. M.; Reis, R. L. *Tissue Engineering* **2007**, 13 (6): 1259-1268.
34. Tuovinen, L.; Peltonen, S.; Liikola, M.; Hotakainen, M.; Lahtela-Kakkonen, M.; Poso, A.; Jarvinen, K. *Biomaterials* **2004**, 25 (18): 4355-4362.
35. Wikingsson, L. D.; Sjoholm, I. *Vaccine* **2002**, 20 (27-28): 3355-3363.
36. Rydell, N.; Sjoholm, I. *Vaccine* **2004**, 22 (9-10): 1265-1274.
37. Nitsch, M. J.; Banakar, U. V. *Journal of Biomaterials Applications* **1994**, 8 (3): 247-284.
38. Langer, R.; Peppas, N. A. *Aiche Journal* **2003**, 49 (12): 2990-3006.
39. Meinel, L.; Illi, O. E.; Zapf, J.; Malfanti, M.; Merkle, H. P.; Gander, B. *Journal of Controlled Release* **2001**, 70 (1-2): 193-202.
40. Cleland, J. L.; Duenas, E. T.; Park, A.; Daugherty, A.; Kahn, J.; Kowalski, J.; Cuthbertson, A. *Journal of Controlled Release* **2001**, 72 (1-3): 13-24.
41. Connolly, A. M.; Schierbecker, J.; Renna, R.; Florence, J. *Neuromuscular Disorders* **2002**, 12 (10): 917-925.
42. Kim, H. J.; Zhao, H. B.; Kitaura, H.; Bhattacharyya, S.; Brewer, J. A.; Muglia, L. J.; Ross, F. P.; Teitelbaum, S. L. *Journal of Clinical Investigation* **2006**, 116 (8): 2152-2160.
43. Galeska, I.; Kim, T. K.; Patil, S. D.; Bhardwaj, U.; Chatttopadhyay, D.; Papadimitrakopoulos, F.; Burgess, D. J. *Aaps Journal* **2005**, 7 (1): E231-E240.
44. Silva, G. A.; Coutinho, O. P.; Ducheyne, P.; Reis, R. L. *Journal of Tissue Engineering and Regenerative Medicine* **2007**, 1 (2): 97-109.
45. de Girolamo, L.; Sartori, M. F.; Albisetti, W.; Brini, A. T. *Journal of Tissue Engineering and Regenerative Medicine* **2007**, 1 (2): 154-157.
46. Maxson, S.; Burg, K. J. L. *Journal of Tissue Engineering and Regenerative Medicine* **2008**, 2 (2-3): 147-154.
47. Mano, J. F.; Koniarova, D.; Reis, R. L. *Journal of Materials Science-Materials in Medicine* **2003**, 14 (2): 127-135.
48. Lewis, D. H. In *Biodegradable Polymers as Drug Delivery Systems.*, Chasin, M.; Langer, R., Eds. Marcel Dekker, Inc.: New York, **1990**; pp 1-42.
49. Rodriguez, M.; Vila-Jato, J. L.; Torres, D. *Journal of Controlled Release* **1998**, 55 (1): 67-77.
50. Crotts, G.; Park, T. G. *Journal of Controlled Release* **1995**, 35 (2-3): 91-105.
51. Benoit, M. A.; Baras, B.; Gillard, J. *International Journal of Pharmaceutics* **1999**, 184 (1): 73-84.
52. Averous, L. *Journal of Macromolecular Science-Polymer Reviews* **2004**, C44 (3): 231-274.
53. Elzein, T.; Nasser-Eddine, M.; Delaite, C.; Bistac, S.; Dumas, P. *Journal of Colloid and Interface Science* **2004**, 273 (2): 381-387.
54. Pashkuleva, I.; Marques, A. P.; Vaz, F.; Reis, R. L. *Journal of Materials Science-Materials in Medicine* **2005**, 16 (1): 81-92.
55. Barikani, M.; Mohammadi, M. *Carbohydrate Polymers* **2007**, 68: 773-780.
56. Igartua, M.; Hernandez, R. M.; Esquisabel, A.; Gascon, A. R.; Calvo, M. B.; Pedraz, J. L. *Journal of Microencapsulation* **1997**, 14 (3): 349-356.
57. Ohagan, D. T.; Jeffery, H.; Davis, S. S. *International Journal of Pharmaceutics* **1994**, 103 (1): 37-45.
58. Sah, H. K.; Toddywala, R.; Chien, Y. W. *Journal of Controlled Release* **1994**, 30 (3): 201-211.
59. Giunchedi, P.; Conti, B.; Maggi, L.; Conte, U. *Journal of Microencapsulation* **1994**, 11 (4): 381-393.
60. Embleton, J. K.; Tighe, B. J. *Journal of Microencapsulation* **1993**, 10 (3): 341-352.
61. Yang, Y. Y.; Chung, T. S.; Ng, N. P. *Biomaterials* **2001**, 22 (3): 231-241.

62. Jameela, S. R.; Suma, N.; Jayakrishnan, A. *Journal of Biomaterials Science-Polymer Edition* **1997**, 8 (6): 457-466.
63. Silva, G. A.; Ducheyne, P.; Reis, R. L. *Journal of Tissue Engineering and Regenerative Medicine* **2007**, 1 (1): 4-24.
64. Yoon, J. J.; Kim, J. H.; Park, T. G. *Biomaterials* **2003**, 24 (13): 2323-2329.

Chapter 6

A Novel Enzymatically-Mediated Drug Delivery Carrier for Bone Tissue Engineering Applications: Combining Biodegradable Starch-based Microparticles and Differentiation Agents

6.1 ABSTRACT

In many biomedical applications, the performance of biomaterials depends largely on their degradation behavior. For instance, in drug delivery applications, the polymeric carrier should degrade under physiological conditions slowly releasing the encapsulated drug. The aim of this work was, therefore, to develop an enzymatic-mediated degradation carrier system for the delivery of differentiation agents to be used in bone tissue engineering applications. For that, a polymeric blend of starch with poly-ε-caprolactone (SPCL) was used to produce a microparticle carrier for the controlled release of dexamethasone (DEX). In order to investigate the effect of enzymes on the degradation behavior of the developed system and release profile of the encapsulated osteogenic agent (DEX), the microparticles were incubated in phosphate buffer solution in the presence of α-amylase and/or lipase enzymes (at physiological concentrations), at 37^{o}C for different periods of time. The degradation was followed by gravimetric measurements, scanning electron microscopy (SEM) and Fourier transformed infrared spectroscopy (FTIR) and the release of DEX was monitored by high performance liquid chromatography (HPLC). The developed microparticles were shown to be susceptible to enzymatic degradation, as observed by an increase in weight loss and porosity with degradation time when compared with control samples (incubation in buffer only). For longer degradation times, the diameter of the microparticles decreased significantly and a highly porous matrix was obtained. The *in vitro* release studies showed a sustained release pattern with 48% of the encapsulated drug being released for a period of 30 days. As the degradation proceeds, it is expected that the remaining encapsulated drug will be completely released as a consequence of an increasingly permeable matrix and faster diffusion of the drug. Cytocompatibility results indicated the possibility of the developed microparticles to be used as biomaterial due to their reduced cytotoxic effects.

***This chapter is based on the following publication:**

Balmayor, *E. R.;* Tuzlakoglu, K.; Marques, A. P.; Azevedo, H. S.; Reis, R. L. A Novel Enzymatically-Mediated Drug Delivery Carrier for Bone Tissue Engineering Applications: Combining Biodegradable Starch-based Microparticles and Differentiation Agents. *Journal of Materials Science-Materials in Medicine* **2008**, 19 (4): 1617-1623.

6.2 INTRODUCTION

Development of materials in the particulate form has been a subject of great interest for several decades. In fact, nowadays polymeric microparticles have been used in several applications, including chemical, biological and medical uses [1-4], and more recently in Tissue Engineering research [1, 5-7]. Since the early 80's, the possibility of incorporating different drugs and bioactive agents into small polymeric vehicles, was predicted as a promising approach for the administration of those agents [1, 8-10]. More recently, the use of biodegradable polymers to design controlled drug delivery carriers, having the additional advantage of minimizing the need for device removal after the release of the bioactive agent, has been reported [9].

The fact that the degradation process affects, and ultimately controls the rate of drug release from biodegradable carriers, controlling the degradation rate of polymeric materials has been one of the critical issues in general biomaterials research [11]. A potential disadvantage of using biodegradable polymers in biomedical applications is the eventual toxicity of the degradation products, which are aimed at being non-toxic leachables and easy metabolized molecules [12].

Biodegradable starch-based polymers have been proposed for several biomedical applications such as drug delivery systems [13, 14], bone cements [15] and bone tissue engineering scaffolding [16, 17], due to their great processing versatility [17] and to their promising properties regarding biodegradability [18] and biocompatibility [12, 19].

The aim of this study was to develop an enzymatic-mediated degradation carrier system, based on a blend of starch with poly-ε-caprolactone in microparticulate form, for the controlled release of differentiation agents for bone tissue engineering applications. For this purpose, the degradation behavior of the developed system was investigated in presence of relevant enzymes and the release of dexamethasone was studied under these conditions. The cytotoxicity of the developed system was also assessed by culturing osteoblast-like cells in extracts of the materials after increasing incubation periods in cell culture medium.

6.3 EXPERIMENTAL

6.3.1 Materials

The studied material was a polymeric blend of corn starch with poly-ε-caprolactone (SPCL, 30-70 wt%). The material was originally in a granular form. More details on this material can be found elsewhere [20]. Dexamethasone (DEX, 97%, cell culture tested, Sigma-Aldrich,

USA) was used as a bioactive molecule for the encapsulation studies. Solvents used in HPLC analysis were HPLC grade. Other chemicals were of reagent grade and used as received.

The enzymes selected for this study were α-amylase (EC 3.2.1.1) from Aspergillus Oryzae and lipase (EC 3.1.1.3) from Aspergillus Oryzae, both purchased from Sigma-Aldrich (USA).

6.3.2. Preparation of SPCL microparticles

The SPCL microparticles were prepared as previously described [21]. Briefly, SPCL was dissolved in methylene chloride under vigorous stirring. This solution was dropped into a 200 mL polyvinyl alcohol (PVA) solution, and emulsified under agitation (600 rpm) for 4 hours. The microparticles were then collected by filtration, washed with distilled water and dried under vacuum. For encapsulation of DEX, the drug was directly added to the polymeric solution at 15% (wt%, relatively to polymer weight).

6.3.3 *In vitro* enzymatic degradation study

The enzymatic degradation of the developed carrier system was investigated by incubating the microparticles in a ratio 1:10 with phosphate buffered saline solution (PBS, 0.01 M, pH 7.4) containing α-amylase (150.5 U/L) and/or lipase (102 U/L), at 37 ^{o}C and 60 rpm up to 12 weeks. To avoid microbial growth, sodium azide (0.02%) was added to the degradation solution. As a control, the samples were also incubated in PBS solution without enzymes. At the end of the pre-selected degradation times, the supernatants were removed and stored at -80 ^{o}C until further analysis. The microparticles were then thoroughly washed with distilled water and allowed to dry at room temperature until constant weight. The final weight of the samples was used for the calculation of the weight loss [14]. The supernatant solutions were used to determine the concentration of reducing sugars released into the solution as a result of starch degradation (hydrolysis of glycosidic linkages in starch molecule with the consequent release of soluble oligosaccharides). The amount of reducing sugars was estimated by the dinitrosalicylic acid (DNS) method [22]. Experiments were performed in triplicate for all the conditions.

6.3.4. Physicochemical characterization

The changes on the surface morphology of the microparticles after degradation were analyzed by Scanning electron microscopy (SEM, Leica Cambridge S-360 model, UK). The samples were fixed to the support using a carbon tape and gold sputter-coated (Fisons Instruments, Sputter Coater SC502, UK) prior to observation.

To assess eventual changes in the chemical composition caused by the degradation process, the microparticles were analyzed by Infrared spectroscopy in transmission mode (FTIR - IRPrestige-21 FRIT-8400S, Shimadzu, Japan). Pre-weighed microparticles (1 mg) were mixed with KBr (40 mg) and then formed into a disc in a press. Transmission spectra were recorded using at least 32 scans with 4 cm^{-1} resolution, in the spectral range of 4000-600 cm^{-1}.

6.3.5 *In vitro* release of DEX from SPLC microparticles

The release of DEX encapsulated in the SPCL microparticles was assessed in PBS only and in PBS containing α-amylase and lipase enzymes in order to investigate the effect of enzymatic degradation on the release kinetics of DEX. For that, the microparticles were suspended in the release solution (2.5 mg/mL). Samples were maintained at 37 ^{o}C and 50 rpm up to 4 weeks. At pre-determined time periods, 1 mL aliquots were taken from the supernatant and replaced with the same volume of fresh medium solution. All the release experiments were carried out in triplicate.

Released DEX was quantified by reverse phase high-performance liquid chromatography (RP-HPLC). Before chromatographic analysis, samples were extracted three times with a mixture of hexane and ethyl acetate in the same proportions. HPLC was performed on a Jasco PU-2080 Plus system using a RP-18 column (LiChrospher, 5 µm, Merck, Germany) and acetonitrile-water (50:50 v/v) as mobile phase (0.5 mL/min). Absorbance was monitored at 254 nm (UV detector, Jasco 870-UV). The column was eluted in isocratic conditions over 20 min. Data acquisition and peak areas were determined with the Shimadzu C-R6A Chromatopac software. The concentration of DEX was calculated from a calibration curve of known DEX concentrations and using triamcinolone as internal standard.

6.3.6 Cytotoxicity evaluation on materials extract

The cytotoxicity evaluation of the SPCL microparticles, was conducted by the use of MTS (3-(4,5-dimethylthiazol-2-yl)-5-(3-carboxymethoxyphenyl)-2-(4-sulfophenyl)-2H-tetrazolium) test, which is extensively used to quantify the number of viable cells [23, 24]. SPCL microparticles were sterilized by ethylene oxide (EtO) using pre-optimized conditions [25]. Each sample was incubated in Dulbecco's Modified Eagle's Medium without phenol red (DMEM, Sigma-Aldrich, USA) (0.5 mg/mL) supplemented with 10% of heat-inactivated fetal bovine serum (FBS; Biochrom AG, Germany) and 1% of antibiotic/antimycotic (Gibco, USA), for 24, 48, and 72 hours at 37 ^{o}C and 60 rpm, in order to obtain the extract of the materials containing potential toxic leachables and degradation products. Latex rubber extract and fresh complete culture medium were used respectively as negative and positive controls for cell

viability [24]. A Human Osteoblast-like cell (SaOs-2, ECACC, UK) suspension was plated in 96-well plates, at density of 6.6 X 10^4 cell/mL, 0.2 mL/well, and incubated at 37 ^oC in a humidified atmosphere containing 5% of CO_2 for 24 hours to allow about 80% of confluence. After this period, the culture medium was replaced by the material extract and the plates were incubated for further 24 hours. The MTS test was performed according to the CellTiter 96 One Solution Proliferation Assay Kit (Pormega, USA) manufactures instructions and as described previously [24]. The absorbance was determined in a microplate reader (EL 312e Biokinetics reader, Biotek Instruments, USA) at 490nm. The results are expressed as the percentage (%) of cell viability in comparison with the 100% proliferation attributed to the positive control. The samples were tested in five replicated, and three independent experiments.

6.3.7 Statistical analysis

In order to confirm the difference in the rate of release of DEX in PBS only and in PBS containing α-amylase and lipase enzymes, the release data was analyzed for statistical significant differences. The statistical analysis was performed with the OriginPro® 7.0 (Microcal software, USA), fixing the level of significance at $p < 0.05$. The normality of the data was checked by applying the Shapiro-Wilk test implemented by Origin for this purposes. The statistical analysis (Student´s t-test for two independent samples) was used to test the two different data (DEX release in PBS, and DEX release in enzymatic environment) for the hypotheses of the release rate in the presence of enzymes to be significant higher than the release rate in PBS alone.

6.4 RESULTS

The microcarriers used in this work are shown in Figure 6.3 (a) where microparticles with round shape, porous surface and diameter of about 400 μm can be observed.

The degradation behavior of the developed microparticles was studied by incubating them in different degradation solutions containing relevant enzymes and their weight loss was followed over time (Figure 6.1). It is well known that starch is degraded by α-amylase and that PCL hydrolysis can be catalysed by lipase enzymes [11]. An increase in weight loss was observed at initial stages of degradation for all conditions, which then remains constant for the samples incubated in PBS and α-amylase solution. In the same figure, significant differences in the percentage of weight can be observed, depending on the degradation media. The samples incubated in presence of enzymes show higher percentages of weight loss, when compared with the control (PBS), being this effect more notorious for the degradation solutions

containing lipase enzyme. At the end of the degradation period, the SPCL microparticles lost approximately 15% of their original weight when incubated in PBS, 45% in presence of α-amylase and 70% in the presence of lipase. These results clearly indicate a high degree of degradation of the SPCL microparticles in the presence of the enzymes.

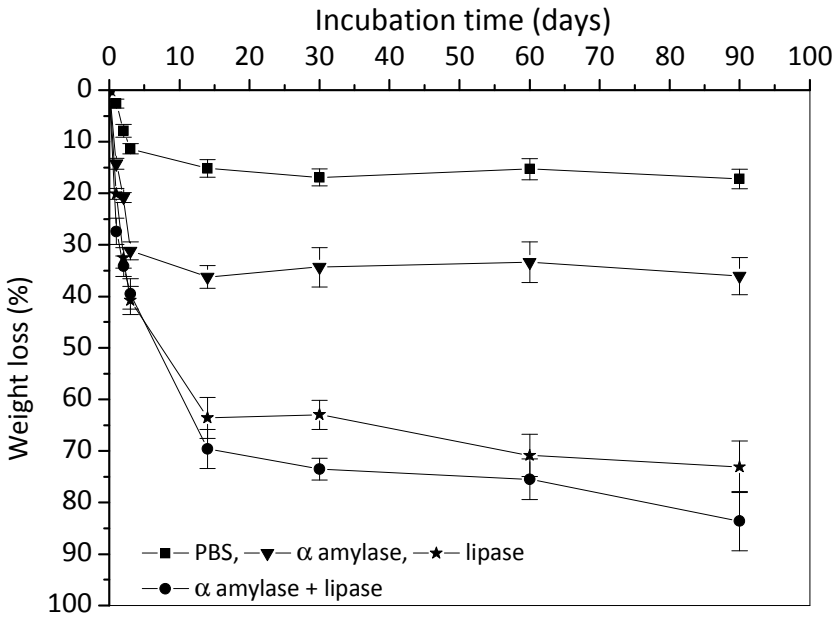

Figure 6.1 Weight loss of SPCL microparticles after incubation in different degradation solutions at 37 ^{o}C. Error bars are standard deviations (n=3)

In order to estimate the degradation of the starch component of the blend in the various degradation conditions, the amount of reducing sugars released in the solutions, as result of starch hydrolysis, was measured (Figure 6.2). The supernatants where the SPCL microparticles were incubated in the presence of α-amylase showed the highest concentration of reducing sugars, whereas a negligible amount of sugars was observed in the control. This result confirms the susceptibility of the starch present in the blend to be hydrolyzed by α-amylase enzyme at physiological concentrations. In the presence of lipase, the amount of detected reducing sugars was very low but a decrease on the solution pH was observed over time (from pH 7.4 at day 0 to pH 5.2 at the end of the degradation period). This drop in the solution pH is due to the release of carboxylic end groups to the solution as consequence of the ester hydrolysis in the PCL chain catalyzed by lipase.

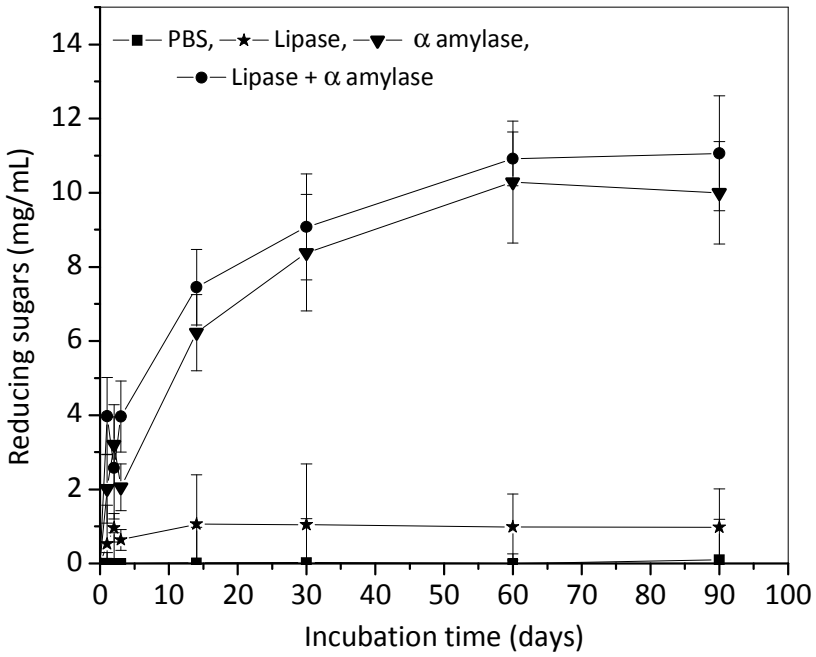

Figure 6.2 Concentration of reducing sugars released from SPCL microparticles when incubated in different degradation solutions at 37 ^{o}C. Error bars are standard deviations (n=3)

The extent of the enzymatic degradation is well illustrated in the SEM micrographs shown in Figure 6.3. After degradation in lipase-containing solution, the diameter of the SPCL microparticles decreased significantly and a highly porous matrix was obtained.

The chemical changes resulting from the enzymatic degradation of the particles were detected by FTIR (Figure 6.4). A decrease of the intensity of the band at 1040-1100 cm^{-1} was detected when samples were incubated with α-amylase, indicating the action of the enzyme in cleaving the glycosidic linkages of starch. A reduction on the intensity of the PCL ester band at 1700-1740 cm^{-1} was observed for the samples incubated with lipase, confirming the lipase activity in hydrolyzing ester bonds. The differences on the bands of starch and PCL demonstrated the degradation of the two components of the material as a consequence of the combination of α-amylase and lipase activities.

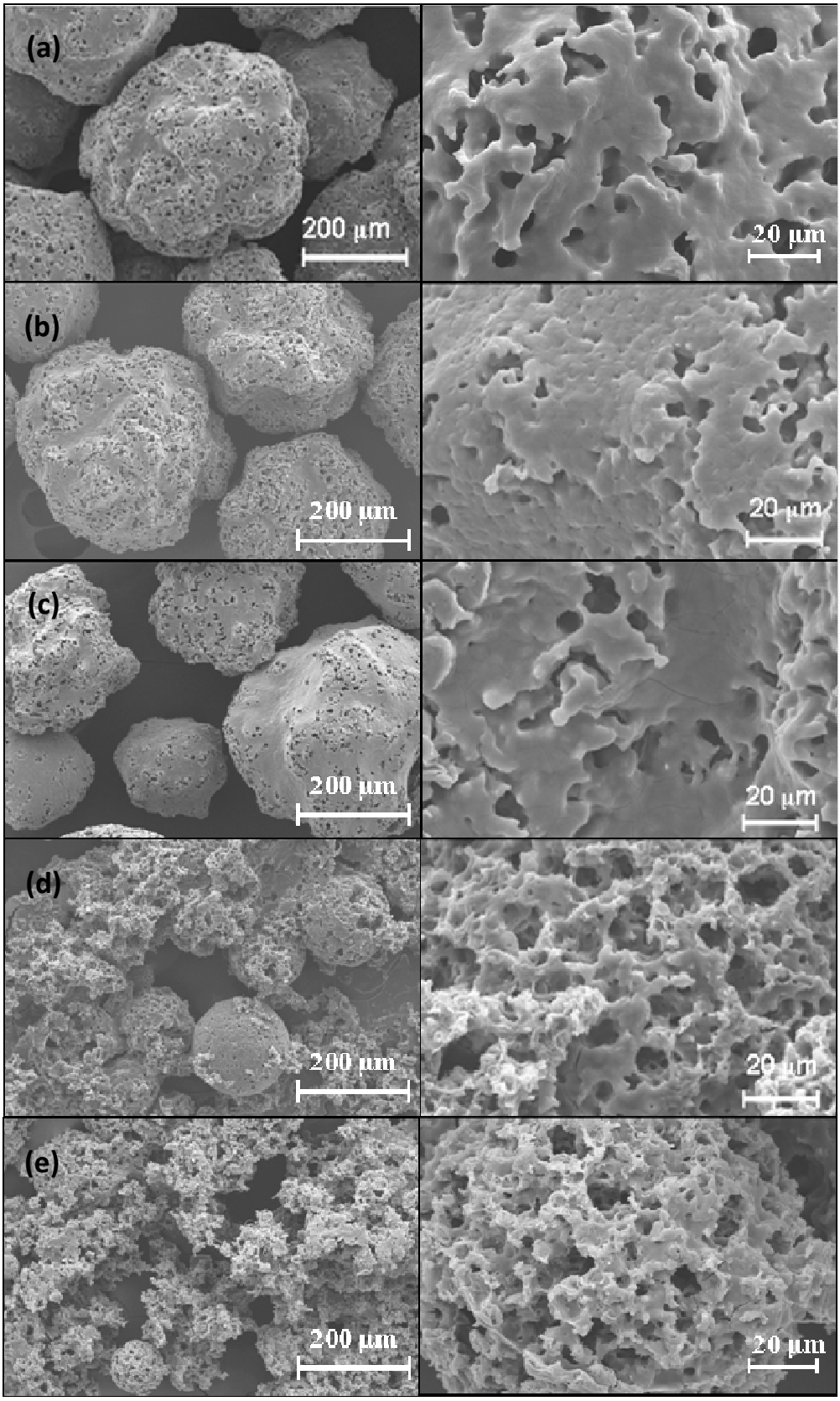

Figure 6.3 SEM micrographs of SPCL microparticles before **(a)** and after degradation for 90 days in PBS **(b)**, α-amylase **(c)**, lipase **(d)**, α-amylase and lipase **(e)** solutions

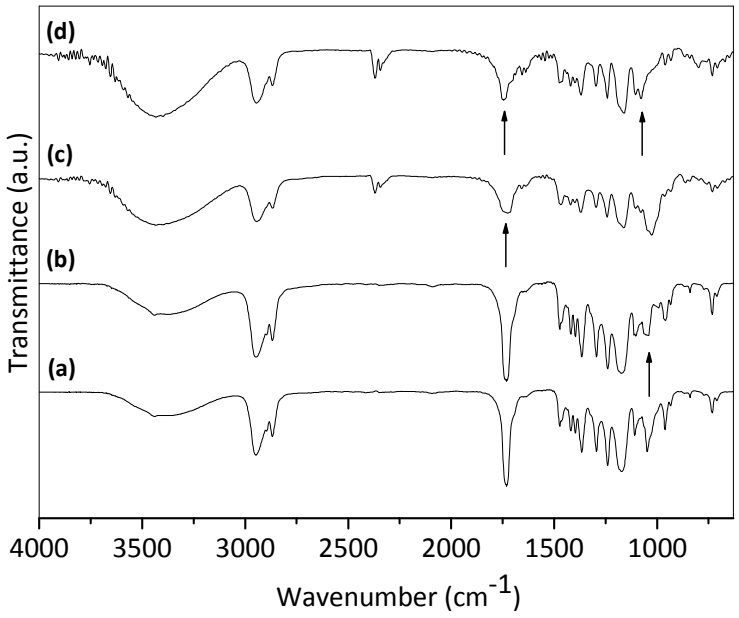

Figure 6.4 FTIR spectra of SPCL microparticles before **(a)** and after degradation in presence of α-amylase **(b)**, lipase **(c)**, and α-amylase and lipase **(d)** solutions

The release profile of DEX from SPCL microparticles for a period of 4 weeks, in PBS and in presence of enzymes (α-amylase+lipase) is illustrated in Figure 6.5. As a general observation, the release profiles are characterized by two main stages: the initial burst release, mainly during the first day where more than 20% of the drug was released, and a sustained release of almost 45% of the DEX at the end of a 4 weeks period. The release profile obtained in an enzymatic environment showed a higher amount of the released DEX into the medium. The statistical analysis of the data reveals no significant differences between the two release conditions (PBS and enzymatic environment) for the first 3 hours (*p* values (0.70) > 0.05). For time periods up to this time (more than 3 hours) and until the end of the release study, the statistical calculations confirm the hypothesis, at the 0.05 level, the release rate of DEX in the presences of enzymes is significantly greater than the release in PBS alone (*p* values (0.018) < 0.05). A confidence interval of 95% was fixed for all the calculations.

The MTS results depicted in Figure 6.6 showed that 48% of the cells remained viable when incubated with the extracts from the SPCL microparticles and the extraction time did not show any influence on the cytotoxicity results. The percentage of cell viability may be related with the presence of residual solvent, used during the preparation of the microparticles, that might be released to the extract solution and causing cell death. Additional washing steps will

be included in the microparticle's preparation to ensure complete removal of solvents or other toxic reagents.

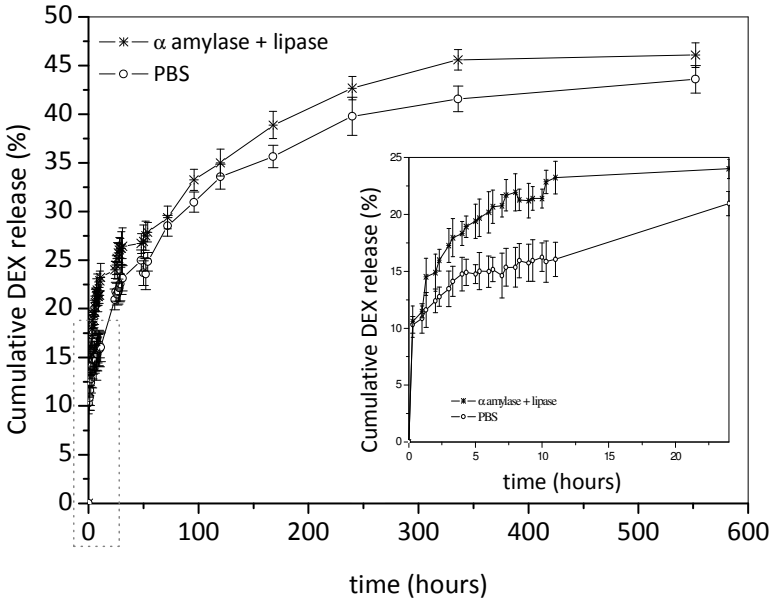

Figure 6.5 Release profiles of dexamethasone from SPCL microparticles in PBS and in presence of enzymatic activity at 37°C for a period of 4 weeks. The insert graph shows the DEX release for a period of 24 hours. The release rate of DEX in the presence of enzymes is significantly greater than the release in PBS alone, for time periods longer than 3 hours ($p < 0.05$). Error bars are standard deviations (n=3)

6.5 DISCUSSION

Polymeric biomaterials when exposed to body fluids or placed in contact with tissues, may undergo several physicochemical changes as result of the most diverse interactions with the surrounding environment [1, 2, 11]. The degradation tests performed in this study showed a higher degradation rate when α-amylase and lipase are present in the degradation solution. The samples incubated with lipase enzyme completely lost their spherical shape at the end of degradation period. The degradation products in the presence of α-amylase are mainly sugars resulting from the cleavage of the glycosidic bonds in the starch structure. On the other hand, lipase acts in the polyester component in the blend, at a specific position on the ester bond of the macromolecule. As result of the degradation process, carboxylic acid units are released to the solution, which explain the observed decrease of the pH. The combination of the two

enzymes resulted in higher values of weight loss and reducing sugars in solution, indicating the degradation of both components of the blend.

The SEM analysis confirmed the results discussed above. The appearance of porosity, cavities and fractures, and the decrease on the diameter of the SPCL microparticles as result of degradation process, was more notorious in the presence of lipase and of both enzymes.

There are two main ways for a drug to be released from a polymeric carrier [26]: i) diffusion through the polymer, which depend on the ability of the aqueous environment to penetrate the drug-containing polymer, inducing the swelling of the matrix and consequently the release of the entrapped drug ; ii) degradation of the material containing the drug, by water, enzymes and acidic or basic conditions . In this case, the drug starts to be released by diffusion until a gradual degradation of the polymer takes place thus controlling the release process. The remaining drug in the polymeric matrix is released as the degradation process becomes more significant. For the developed DEX loaded SPCL microparticles, the initial burst effect was clearly observed in both studied environments, associated with the fast release of the drug located close to the surface of the particles, mainly by the diffusion phenomena. This burst was followed by a period of minimal release due to the hydrophobicity of PCL (major component of the blend: 70%), which causes a barrier for water penetration and consequently preventing the diffusion of the drug through the polymer matrix. At this stage, the drug was released faster from the sample in presence of enzymes, indicating that the enzymatic degradation of the SPCL microparticles increases the release rate of the entrapped DEX. These results indicate that the release of DEX from the SPCL microparticles is firstly controlled by diffusion and then by the degradation of the polymeric matrix. The dependence of the drug release with the degradation of the system along the time makes the SPCL microparticulate system more adequate for sustained rather than controlled drug release.

The main concern of biodegradable polymers when proposed for biomedical applications, is the potential toxicity of their leachables and degradation products. The slightly cytotoxicity of the developed system for osteoblast-like cells, may be due to the presence of residual solvent. Previous studies [12] have attributed similar results to components added and or formed during the processing.

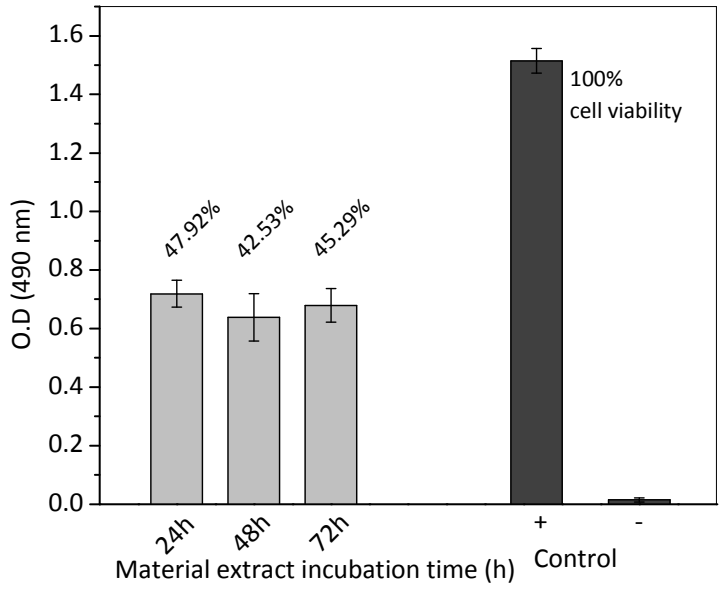

Figure 6.6 Optical density of the MTS solutions after incubation with SaOs-2 grown for 24 hours in the presence of SPCL microparticles extracts obtained in culture medium for 24, 48 and 72 hours. Percentages of viable cells, compared to positive control, are presented

6.6 CONCLUSIONS

Considering the overall results obtained in this study, it is expected that the developed SPCL microparticulate system is a suitable carrier for the sustained release of drugs, with the advantage of being susceptible to enzymatic degradation, thus being ultimately digested in the body, avoiding the surgical removal. These results are indicative of the potential of the developed system to be used in the controlled release of growth and differentiation factors with relevance in the field of bone regeneration.

6.7 ACKNOWLEDGMENTS

E. R. Balmayor is beneficiary of Marie Curie PhD grant under the Alea Jacta EST Project (MEST-CT-2004-008104). This work was partially supported by the European Network of excellence (NoE) EXPERTISSUES (NMP3-CT-2004-500283).

6.8 REFERENCES

1. Silva, G. A.; Ducheyne, P.; Reis, R. L. *Journal of Tissue Engineering and Regenerative Medicine* **2007**, 1 (1): 4-24.
2. Tuncel, A.; Ecevit, K.; Kesenci, K.; Piskin, E. *Journal of Polymer Science Part a-Polymer Chemistry* **1996**, 34 (1): 45-55.
3. Kamyshny, A.; Magdassi, S. *Colloids and Surfaces B-Biointerfaces* **2000**, 18 (1): 13-17.
4. Shinkai, M. *Journal of Bioscience and Bioengineering* **2002**, 94 (6): 606-613.
5. Silva, G. A.; Coutinho, O. P.; Ducheyne, P.; Reis, R. L. *Journal of Tissue Engineering and Regenerative Medicine* **2007**, 1 (2): 97-109.
6. Silva, G. A.; Pedro, A.; Costa, F. J.; Neves, N. M.; Coutinho, O. P.; Reis, R. L. *Materials Science & Engineering C-Biomimetic and Supramolecular Systems* **2005**, 25 (2): 237-246.
7. Malafaya, P. B.; Silva, G. A.; Reis, R. L. *Advanced Drug Delivery Reviews* **2007**, 59 (4-5): 207-233.
8. Bissery, M. C.; Valeriote, F.; Thies, C. In *Microspheres and Drug Therapy: Pharmacautical, Immunological and Medical Aspects.* , Davis, S. S.; Ilium, L.; McVie, J. G.; Tomilson, E., Eds. Elsevier: New York, **1984**; pp 217–227.
9. Baldwin, S. P.; Saltzman, W. M. *Advanced Drug Delivery Reviews* **1998**, 33 (1-2): 71-86.
10. Eliaz, R. E.; Kost, J. *Journal of Biomedical Materials Research* **2000**, 50 (3): 388-396.
11. Azevedo, H. S.; Reis, R. L. In *Biodegradable Systems in Tissue Engineering and Regenerative Medicine*, Reis, R. L.; San Roman, J., Eds. CRC Press: Boca Raton, FL, **2005**; pp 177-201.
12. Marques, A. P.; Reis, R. L.; Hunt, J. A. *Biomaterials* **2002**, 23 (6): 1471-1478.
13. Malafaya, P. B.; Elvira, C.; Gallardo, A.; San Roman, J.; Reis, R. L. *Journal of Biomaterials Science-Polymer Edition* **2001**, 12 (11): 1227-1241.
14. Silva, G. A.; Costa, F. J.; Neves, N. M.; Coutinho, O. P.; Dias, A. C. P.; Reis, R. L. *Journal of Biomedical Materials Research Part A* **2005**, 73A (2): 234-243.
15. Boesel, L. F.; Mano, J. F.; Elvira, C.; San Roman, J.; Reis, R. L. In *Biodegradable Polymers and Plastics*, Chiellini, E.; Solaro, R., Eds. Kluwer Academic/Plenum Publishers: New York, **2003**; pp 243-260.
16. Gomes, M. E.; Sikavitsas, V. I.; Behravesh, E.; Reis, R. L.; Mikos, A. G. *Journal of Biomedical Materials Research Part A* **2003**, 67A (1): 87-95.
17. Reis, R. L.; Cunha, A. M., Starch Polymers. In *Encyclopedia of Materials: Science and Technology*, Buschow, K. H. J.; Cahn, R. W.; Flemings, M. C.; Ilschner, B.; Kramer, E. J.; Mahajan, S.; Veyssiere, P., Eds. Elsevier Ltd.: New York, **2001**; Vol. 11, pp 8810-8816.
18. Azevedo, H. S.; Gama, F. M.; Reis, R. L. *Biomacromolecules* **2003**, 4 (6): 1703-1712.
19. Mendes, S. C.; Reis, R. L.; Bovell, Y. P.; Cunha, A. M.; van Blitterswijk, C. A.; de Bruijn, J. D. *Biomaterials* **2001**, 22 (14): 2057-2064.
20. Neves, N. M.; Kouyumdzhiev, A.; Reis, R. L. *Materials Science & Engineering C-Biomimetic and Supramolecular Systems* **2005**, 25 (2): 195-200.
21. Balmayor, E. R.; Tuzlakoglu, K.; Azevedo, H. S.; Reis, R. L. In *Preparation and characterization of novel starch-poly-ε-caprolactone microparticles incorporaring bioactive agents for drug delivery and tissue engineering applications.*, European Materials Research Society Fall Meeting, Warsaw, Poland., **2006**; Conference Engine pielaszek research: Warsaw, Poland., **2006**; p 219.
22. Ghose, T. K. *Pure and Applied Chemistry* **1987**, 59 (2): 257-268.
23. Zeltinger, J.; Sherwood, J. K.; Graham, D. A.; Mueller, R.; Griffith, L. G. *Tissue Engineering* **2001**, 7 (5): 557-572.
24. Salgado, A. J.; Coutinho, O. P.; Reis, R. L. *Tissue Engineering* **2004**, 10 (3-4): 465-474.
25. Reis, R. L.; Mendes, S. C.; Cunha, A. M.; Bevis, M. J. *Polymer International* **1997**, 43 (4): 347-352.

26. Langer, R.; Peppas, N. A. *Aiche Journal* **2003**, 49 (12): 2990-3006.

Chapter 7

Biodegradable microparticles deliver bioactive Dexamethasone and BMP2 for bone tissue engineering

7.1 ABSTRACT

We have established earlier, a method to produce starch-poly-ε-caprolactone (SPCL) microparticles as biodegradable carriers for the controlled release of dexamethasone (DEX). The present study aims to investigate the potential of the previously developed system to support the delivery of bone morphogenetic protein-2 (BMP-2). The system was characterized regarding morphology and size distribution. BMP-2 encapsulation efficiency as well as the *in vitro* release profile was evaluated by ELISA. BMP-2 was rapidly released during the first 12 hours, followed by a more sustained release for up to 10 days. The osteogenic activity of DEX and BMP-2, after incorporation and during release was evaluated using a myoblast cell line (C2C12). Alkaline phosphatase (ALP) activity was increased by released BMP-2. Alizarin red and von Kossa and staining were used to evaluate mineralization by adherent cells in culture upon stimulation with BMP-2 loaded microparticles, which showed the presence of calcium deposits. A luciferase assay, for osteocalcin promotor activity, showed high levels of activity in C2C12 cells treated with the BMP-2 loaded microparticles. In contrast, no evidence of osteogenesis in C2C12 cells was observed after exposure to DEX loaded microparticles. However, human adipose stem cells exposed to these microparticles were characterized by high values of ALP. The results clearly demonstrate that SPCL microparticles are suitable carriers for the incorporation and controlled release of glucocorticoids and growth factors with relevance in bone related applications.

***This chapter is based on the following publication:**

Balmayor, *E. R.;* Feichtinger, G.; Azevedo, H. S.; van Griensven, M.; Reis, R. L. Biodegradable microparticles deliver bioactive Dexamethasone and BMP-2 for bone tissue engineering. *Clinical Orthopaedics and Related Research (CORR)* **2009**. **Accepted for publication.**

7.2 INTRODUCTION

In general, bone possesses a good healing capacity and the majority of bone defects are spontaneously cured. This requires, however, optimal biological and micro-environmental conditions. Treatment of complex fractures and other bone defects caused by high energy trauma, disease, developmental deformity, revision surgery, and tumor resection, have been improved due to advances in surgical techniques, orthopedic implant and peri-operative management [1-6]. However, detrimental wound healing circumstances (e.g. co-morbidities like diabetes mellitus, infections, improper vascular supply etc.), sub-optimal surgical techniques or biomechanical instability can result in impaired healing capacity (e.g. non-unions, large remaining bone gaps) [7]. Such defects create major surgical and socio-economical challenges [8]. Tissue engineering (TE) has emerged as a possible new alternative to traditional medical technology, improving treatments for human diseases and disorders. TE is a technology based on the development of biological substitutes for repair, reconstruction, regeneration, or replacement of tissues during illness or malfunction [9]. TE involves the culture of living cells, using a support material (e.g. scaffold) in combination with biologically active molecules (e.g. growth factors [GFs]) [10]. To be successful, a three-dimensional supporting biomaterial (construct) is typically required which must be biocompatible, preferably biodegradable, with the ability of entrapping and releasing bioactive molecules capable of stimulating cellular growth, proliferation and differentiation into specialized cell types [11].

GFs are naturally occurring proteins capable of stimulating cellular proliferation, migration, and/or differentiation into a specialized phenotype [12, 13]. During the differentiation process of stem cells, various hormones and cytokines regulate osteoblast differentiation. Among these, bone morphogenetic proteins (BMPs) are probably the most important GFs involved [14-16]. BMPs are local factors that upregulate Cbfa1 expression, an important transcription factor that influences bone development [17, 18]. BMPs regulate osteogenesis at two different levels: (1) the commitment of skeletal progenitor cells and (2) the maturation of osteoblasts in postnatal development [18]. BMPs, and more specifically BMP-2, have potent effects in inducing osteoblast differentiation of different cell sources [19-23]. In conjunction with GFs, certain cell-permeable small molecules have shown to control cell proliferation and to induce the differentiation of various stem cells [24]. One example is dexamethasone (DEX), which in combination with ascorbic acid and β-glycerophosphate, promotes osteogenesis under defined conditions [24-26]. Several studies have demonstrated that DEX can induce terminally differentiated osteoblasts [27-29]. The intimate interaction

between those bioactive molecules plays a crucial role in osteoblast differentiation and bone formation.

Although direct application of these bioactive molecules can be beneficial, repeated administration and high doses are often required due to their short half-lives (i.e. 7 to 16 minutes for BMP-2 (INFUSE product) and 10-15 hours for BMP-7 (Osigraft STRYKER)) [30]. Simultaneously, the difficulty of the proper delivery to the specific injury site, causes the need of controlled delivery techniques that will ensure constant levels of BMP-2 at the desired site for an extended time period. Osteo-inducing factors, such as BMP-2, are needed to be delivered to the site of interest in the suitable concentration. Therefore, their sustained delivery at the site of injury should prolong the bioavailability of these molecules, and therefore, the duration of their therapeutic action. This constitutes an important challenge nowadays for the development of delivery systems for BMP-2. For instance, BMP-2 is currently administered clinically using collagen. But, large amounts of BMP-2 are needed in order to overcome the instability due to its short half life. BMP-2 remains around 8 days in the collagen carrier. Thus, the possibility of developing biodegradable microparticles capable of releasing bioactive BMP-2 in a sustained manner, for longer periods, is highly interesting and has been widely investigated. In this study, we developed and tested a novel injectable drug delivery system consisting of starch-poly-ϵ-caprolactone microparticles for induction of osteogenesis aiming to decrease the amounts of GF used in clinical application. Proper delivery requires controlled release techniques that will ensure constant levels of osteogenic factors at the site of interest at adequate concentrations over an appropriate time period.

Therefore, this study aims to investigate (1) whether biodegradable starch-poly-ϵ-caprolactone (SPCL) microparticles can serve as a carrier for controlled release of BMP-2 and DEX; and if this hypothesis is confirmed, (2) whether the entrapped drugs, i.e., DEX and BMP-2, remain bioactive during encapsulation and upon release; and (3) whether the released DEX and BMP-2 are equally active concerning osteogenesis in an osteo/myo-blast cell line (C2C12).

7.3 EXPERIMENTAL

In order to answer the formulated questions, DEX and BMP-2 were first encapsulated in SPCL microparticles. Subsequently, the encapsulation efficiency and the release kinetics were investigated *in vitro*. Furthermore, the cytotoxicity of the microparticles *per se* was determined. Secondly, the bioactivity of the released molecules was investigated in cell culture experiments. For this, a bone precursor cell line was used in order to observe the osteogenic activity of the system. As DEX was not able to induce osteogenesis in the osteoprecursor cell

line, its osteogenic potential was tested in mesenchymal stem cells derived from adipose tissue.

7.3.1 Preparation of BMP-2 loaded SPCL microparticles

A biodegradable microparticulated system made of a polymeric blend of starch and poly-ϵ-caprolactone (SPCL, 30–70 wt %) [31] containing DEX was produced as described previously [32, 33]. In this study, BMP-2 (Recombinant human BMP-2, > 95%, R&D systems, USA) was loaded in the SPCL microparticles using an emulsion solvent extraction/evaporation technique [32, 34]. Briefly, 0.25 g SPCL was dissolved in 5 mL methylene chloride (Sigma-Aldrich, USA) under vigorous stirring. This solution was dropped into a 200 mL polyvinyl alcohol solution (0.5% v/v, molecular weight: 30 000–70 000 g/mol; Sigma-Aldrich, USA) and emulsified at a speed of 600 rpm for 4 hours at room temperature to evaporate/extract the organic solvent, providing structural integrity to the microparticles. For the microparticles to be loaded with BMP-2, a co-encapsulation process was performed using bovine serum albumin (BSA) (≥ 96%; Sigma-Aldrich, USA). BSA protects bioactive molecules such as growth factors and peptides, from inactivation [35-37], e.g., as a result of exposure to harsh organic solvents. BSA (200 mg) and BMP-2 (10 µg) were mixed and added to the SPCL solution just before addition to the stirring polyvinyl alcohol emulsification medium. At the end of BSA and BMP-2 loading, the reaction medium was collected and stored at 4 °C for quantification of unloaded proteins (please see section 7.3.3). The microparticles were thoroughly washed with distilled water and freeze-dried. The encapsulation efficiency was determined by establishing a relation between the amounts of BMP-2 and BSA remaining in the reaction medium (unloaded) after loading and the initial amount available for incorporation [32, 38].

7.3.2 Characterization of BMP-2 loaded SPCL microparticles: scanning electron microscopy (SEM) and size distribution

A fraction of BMP-2 loaded microparticles was collected and separated through a series of standard sieves (60–450 µm; Linker Industrie-Technik GmbH, Germany) to determine their size distribution. Particles with a size in the range of 100 to 150 µm were selected to study the *in vitro* release of BMP-2 and its effect on cells. Unloaded SPCL microparticles and loaded with BSA alone were also produced to be used as controls. These unloaded SPCL microparticles had an average size distribution of 102.3±4.1 µm [32].

To examine the surface morphology, shape, and size of the obtained microparticles, scanning electron microscopy (SEM; Leica Cambridge S-360 model, UK) was performed. Dry

samples were mounted onto aluminum stubs, gold sputter-coated (Fisons Instruments, UK), and viewed at magnifications of 150X and 400X.

7.3.3 *In vitro* release of entrapped BMP-2

The release of BMP-2 from the loaded SPCL microparticles was assessed *in vitro*. For that purpose, 150 mg BMP-2 loaded microparticles were suspended in 5 mL 0.01 M phosphate buffered saline (PBS; pH 7.4) solution. All the samples were maintained at 37 °C in an orbital shaker under constant agitation at 100 rpm. At predetermined time points, up to 10 days, 1 mL aliquots of the supernatant were taken and replaced with the same volume of fresh PBS solution. Collected supernatants were then stored at −80 °C for BMP-2 quantification. Released BMP-2 was quantified by enzyme-linked immunosorbent assay (ELISA) (Human BMP-2 Quantikine® ELISA Kit, R&D Systems, USA) according to the manufacturer's instructions.

7.3.4 Effect of unloaded SPCL microparticles on C2C12 cell viability

A mouse skeletal osteo/myoblast cell line (C2C12) obtained from the German Collection of Microorganisms and Cell Cultures DSMZ-ACC565 (Germany) was cultured in Dulbecco's Modified Eagle's Medium (DMEM) high glucose (Lonza, Switzerland), supplemented with 5% heat inactivated fetal calf serum (FCS) (Lonza, Switzerland) and 2 mmol/L L-glutamine (Lonza, Switzerland).

Before use in cell culture experiments, the microparticles (unloaded and loaded) were sterilized by ethylene oxide using preoptimized conditions as described by Reis et al. [39].

7.3.4.1 Cell viability

Cell viability was determined by bringing C2C12 cells in contact with unloaded SPCL microparticles. A standard 3-(4,5-dimethylthiazol-2-yl)-5-(3-carboxymethoxyphenyl)-2-(4-sulfophenyl)-2H-tetrazolium (MTS) assay was used. The MTS test was performed according to the manufacturer's instructions (Promega, USA) and modified using protocols previously described [40, 41]. Briefly, C2C12 cells were plated in 24-well plates at 0.5 x 10^5 cells/mL (1 mL/well) and incubated at 37 °C in a humidified environment containing 5% CO_2 for 24 hours. Subsequently, the culture medium was replaced by DMEM supplemented with a suspension of the SPCL microparticles (1 mg/mL). After 1, 3, and 7 days, the supernatants (containing the particles) were removed. Cells were incubated with 200 µL MTS reagent solution (5:1 ratio in serum-free DMEM culture medium without phenol red) per well at 37 °C in a humidified environment containing 5% CO_2 for 3 hours. From each well, 100 µL medium was transferred to a 96-well plate and the absorbance at 490 nm was measured in a

microplate reader (BioTek Instruments, USA). The results are expressed as the percentage of cell viability in comparison to the 100% viability attributed to the complete DMEM culture medium control (positive control).

7.3.5 Effects of BMP-2 and DEX loaded SPCL microparticles on osteogenesis

This study was focused on evaluating the effect of DEX and BMP-2 loaded microparticles on the cells for their potential to induce osteogenesis. For that, different assays were performed namely: Osteocalcin (OCN) promotor activity, alkaline phosphatase (ALP) activity and specific staining assays for the detection of mineralized matrix.

7.3.5.1 Osteocalcin (OCN) promotor activation assay

To determine osteocalcin (OCN) (indirectly via promotor activity), a well known gene expressed during late osteogenesis, C2C12 cells were identically plated in 24-well plates following the same procedure described above (please see section 7.3.4.1) for 24 hours. Subsequently, the cells were transfected by a standard lipofectamine transient transfection, using a vector expressing the OCN promotor driving a luciferase reporter gene. Reporter vector DNA (1 μg) together with lipofectamine (2 μg; Invitrogen, Germany) was used per well. The DNA was mixed with the lipofectamine transfection agent under serum-free conditions following the manufacturer's instructions. The cells were incubated with the transfection solution at 37 °C in a humidified atmosphere containing 5% CO_2 in DMEM containing 5% FCS for 4 hours. After transfection, the FCS content was reduced to 1% and the medium was supplemented with 50 μmol/L ascorbic acid and 10 mmol/L β-glycerophosphate (osteogenic differentiation medium). The cells were further cultivated for 24 hours at 37 °C in a humidified atmosphere containing 5% CO_2. Finally, the culture medium was changed with the different samples to be tested. Two different samples were used for this assay: (samples 1) collected supernatants from the BMP-2 and DEX *in vitro* release study (release time points: 1, 5 and 10 days) and (samples 2) a suspension of BMP-2 and DEX loaded microparticles in osteogenic differentiation medium. For the first mentioned samples (samples 1), aliquots of 1 mL (supernatants) were collected from the *in vitro* release studies and stored (−80 °C) until analyzed. The collected aliquots were freeze dried and resuspended for stimulating the cells using the same volume of osteogenic differentiation medium to maintain the released concentrations for each time point selected (DEX: 4, 9 and 10.5 mg/mL after 1, 5 and 10 days respectively [32]). When the samples were placed in direct contact with the cells (samples 2), the amounts of microparticles used ranged from 1 to 10 mg per mL of osteogenic DMEM culture medium. As controls, BMP-2 (100 ng/mL), BMP-2/BSA (at a ratio of 1:20 000; 100 ng of

BMP-2 and 2 mg of BSA per mL) and DEX (10^{-8} M) solutions were used. Additionally, transwell experiments were carried out in parallel. This experiment aims to evaluate any differences on cell behavior as a result of direct/indirect contact of the microparticles over the cells. In this case, 10 mg/mL loaded particles were added to the transwell inserts, ensuring that the cells were only exposed to soluble factors released from the particles. For this purpose, 12-mm Transwell® inserts (0.4-µm pore size; Corning, USA) were used. The cells were then cultured for 5 days without any medium change. At the end of the 5 days, the activation of the OCN promotor was measured using luminescence imaging (Xenogen, USA) upon administration of luciferin. The amount of photons was measured and established a relative measure of OCN promotor activity. The cell monolayer was washed twice with PBS without calcium (Lonza, Switzerland) and stored at −80 °C with 100 µL PBS for further alkaline phosphatase (ALP) assay.

7.3.5.2 Alkaline phosphatase assay (ALP)

The effect of the released molecules and loaded microparticles on the activity of alkaline phosphatase (ALP), a marker expressed by the cells in a more osteoblast-differentiated stage, was evaluated in C2C12 after 5 days of culture using a p-nitrophenol (pNP) assay [42]. Briefly, cells were lysed by osmotic (0.25% Triton X-100™ solution in PBS) and heat shock. Subsequently, 50 µL substrate solution was added per well (containing p-nitrophenyl phosphate disodium salt) for 30 minutes at room temperature. The optical density was determined at 405 nm in a microplate reader and the activity of ALP calculated according to a standard curve. The standard curve was constructed using pNP solutions of known concentrations.

In addition to the use of C2C12 cells, DEX samples (collected supernatants from the DEX release study and DEX loaded microparticles) were also tested in human adipose-derived stem cells (ASCs) for ALP activity to determine DEX bioactivity *per se* in primary stem cells. For these experiments, human-ASCs were obtained from three different donors from the Blood Bank of the upper Austrian Red Cross (Austria).

7.3.5.3 Mineralization assay

Mineralized matrix and calcium deposition were assessed as an indication of osteogenic differentiation. C2C12 cells were seeded at a density of 0.5 x 10^4 cell/mL (1 mL/well) using osteogenic differentiation medium supplemented with the DEX and BMP-2 loaded microparticles up to 14 days. After different time points (3, 7, 14 days), the supernatant was removed and the cells were washed twice with PBS solution (without calcium and magnesium) and fixed with 4% formaldehyde solution in PBS. Von Kossa staining was

performed to visualize the presence of mineralized deposits. Briefly, fixed cells were incubated with 5% silver nitrate solution for 30 minutes at room temperature. After cells have been washed several times with distilled water, staining was developed using 5% sodium carbonate solution in 25% formaldehyde followed by the a 5% sodium thiosulfate solution in distilled water. After washing the cells with water, the staining was observed by phase-contrast microscopy (Zeiss, Germany). Alizarin red staining was performed for examination of calcium deposition. Briefly, the fixed cells were incubated for 5 minutes in a 0.05% alizarin red solution in PBS at room temperature. The stained cells were washed with distilled water before microscopic observation.

As controls, C2C12 cells were seeded using plain osteogenic differentiation medium (without microparticles) and medium supplemented with the unloaded microparticles.

7.3.6 Statistical analysis

All the experiments were independently performed three times. Each experiment employed three replicates for each condition, sample tested or different time points. Thus, 9 separate measurements were taken into account for each single condition. All the obtained values are reported as mean value ± standard deviation.

The statistical analysis was performed with OriginPro® 7.0 (Microcal software, OriginLab, USA). Normal distribution of the data was analysed by applying the Shapiro-Wilk test implemented by Origin for this purposes. Differences in averaged size of the microparticles between DEX and BMP-2 loaded microparticles were determined using the Student´s t-test for two independent samples. The same statistical analysis was performed to determine differences for encapsulation efficiency between BSA and BMP-2 during BSA/BMP-2 co-encapsulation process; and for OCN (quantified luminescence levels) and ALP activity between DEX and BMP-2 loaded microparticles incubated with C2C12.

7.4 RESULTS

7.4.1 BMP-2 loaded SPCL microparticles

The first goal of the study was to test whether SPCL microparticles are suitable as delivery carrier for the controlled release of BMP-2 and DEX. SPCL microparticles with spherical shapes and smooth surfaces, as confirmed by SEM observations, could be produced (Figure 7.1 (a)). DEX and BMP-2 loaded SPCL microparticles exhibited a surface morphology similar to the unloaded ones (Figure 7.1 (c) and (d)). The microparticles loaded with DEX ($p = 0.0070$) and BMP-2 ($p= 0.0007$) were larger in size than the unloaded SPLC microparticles (102.3 ± 4.1 µm

[32]). Furthermore, the DEX loaded microparticles had a larger (p = 0.0113) average size than the BMP-2 loaded ones (Figure 7.1 (b)).

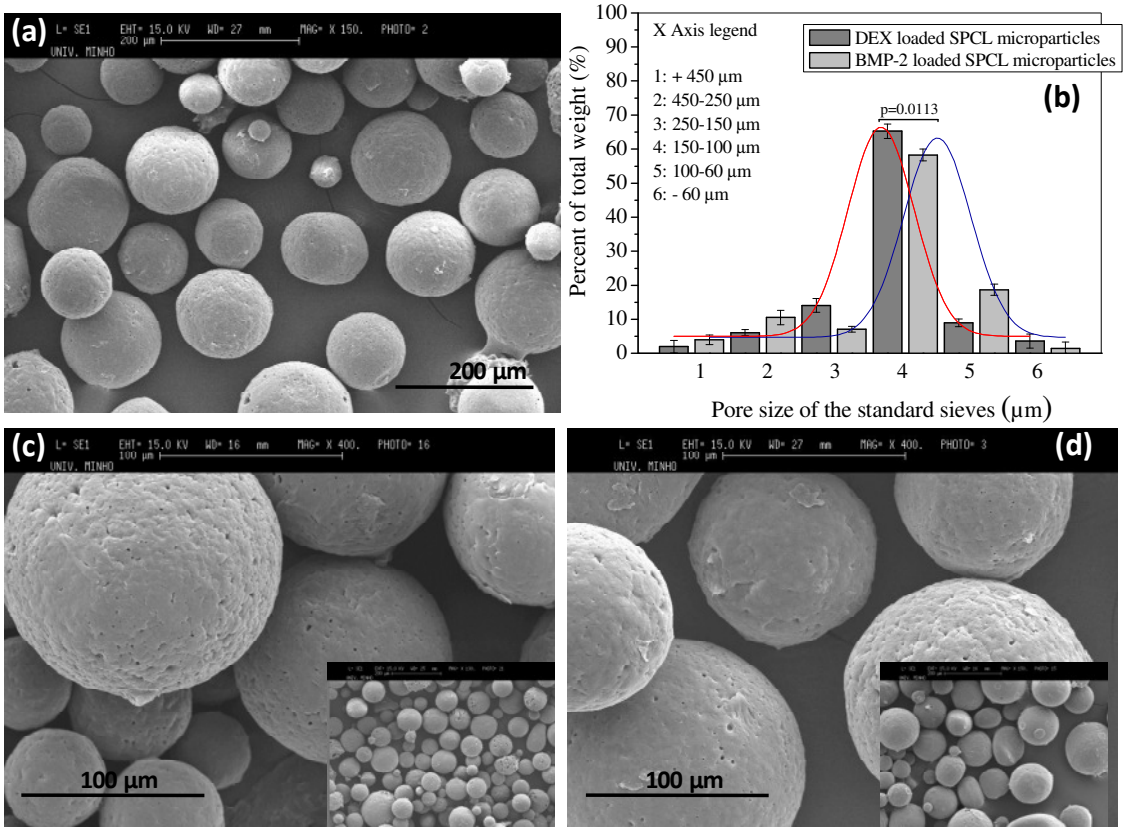

Figure 7.1 Starch-poly-ε-caprolactone (SPCL) microparticles characterized by spherical shapes and smooth surfaces. SEM micrographs of unloaded microparticles **(a)**. Size distribution of the DEX and BMP-2 loaded SPCL microparticles: Pair of values statistically compared is indicated in the graph with the correspondent p value (0.0113) **(b)**. SEM micrographs of DEX loaded **(c)** and BMP-2 loaded **(d)** SPCL microparticles (inserted micrographs at lower magnification, 150X, for general observation)

The encapsulation efficiency (EE) values for BSA and BMP-2 during the co-encapsulation process were relatively low and very similar each, 27.02±3.4 % and 24.86±0.7 %, respectively (p = 0.3418). The *in vitro* release studies indicated the presence of a burst release during the first 12 hours, which continued up to 2 days (Figure 7.2). After this period, a plateau was reached and maintained until the end of the release period. After 10 days, more than 60% of the entrapped BMP-2 was released. Incubating C2C12 cells with the SPCL microparticles maintained cell viability up to 87% (Figure 7.3).

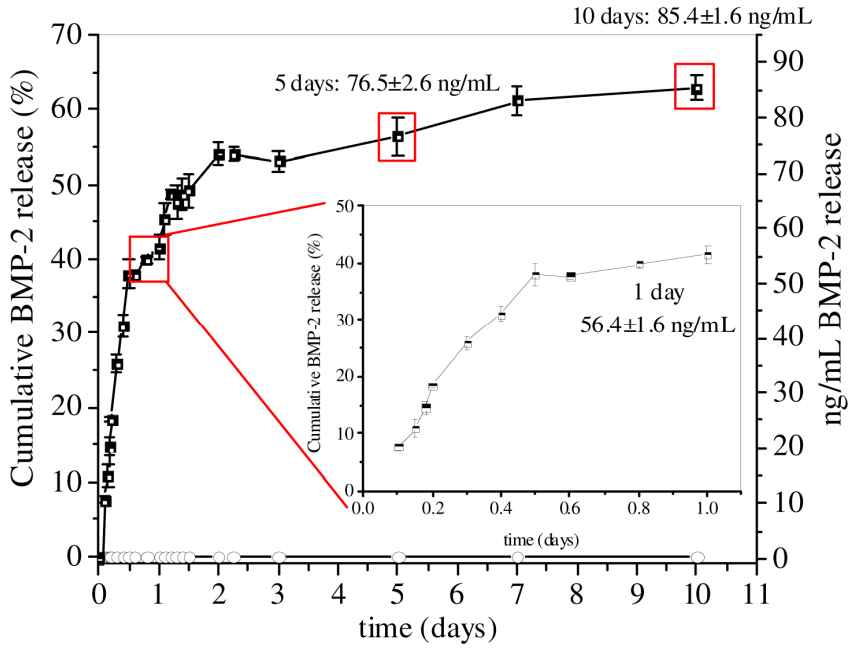

Figure 7.2 BMP-2 released from SPCL microparticles during a 10 days period. The *in vitro* release profiles of BMP-2 is shown after incubation of the loaded particles in PBS medium, as quantified by ELISA assay. The open circles correspond to the SPCL unloaded microparticles used as control sample for this experiment. The insert graph shows the BMP-2 release for a period of 1 day (burst release)

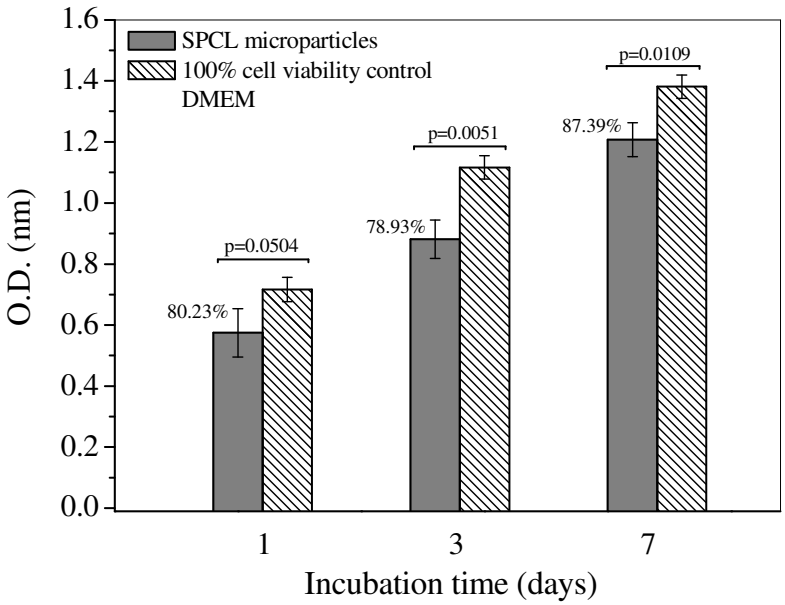

Figure 7.3 Cell viability of C2C12 cells upon exposure to SPCL microparticles as determined by the MTS test. The indicated values refer to the cell viability percentage compared to the values obtained for the cells cultivated in DMEM (used as control), which were set at 100% at each respective time point. Values are mean ± standard deviation (n=3). Pairs of values statistically compared are indicated in the graph with the correspondent p values

7.4.2. Bioactivity of entrapped/released DEX and BMP-2 in/from SPCL microparticles: Osteogenesis

Released BMP-2 was bioactive as shown by activation of the osteocalcin promotor in C2C12 cells. Administration of BMP-2 loaded particles increased ($p = 0.0112$) expression of OCN promotor activity as determined by luminescence measurements (Figure 7.4 (a)). The levels of luminescence for the supernatants collected after 10 days of BMP-2 *in vitro* release (85.4±1.6 ng/mL BMP-2 released) were similar ($p = 0.2771$) to the ones obtained for the BMP-2 control solution (100 ng/mL). These values were lower ($p = 0.0019$) than those obtained for the cells incubated directly with the BMP-2 loaded microparticles. However, increasing the concentration of incubated BMP-2 loaded microparticles did not further enhance ($p = 0.5552$) OCN promotor activity. On the other hand, neither DEX samples nor DEX control solution induced the expression of the OCN promotor in the C2C12 cells (Figure 7.4 (b)). The luminescence levels of DEX related samples were even lower ($p = 0.0104$) than the values for DMEM culture media used as negative control for this assay. In addition, the levels of luminescence quantified for DEX loaded microparticles were very similar ($p = 0.1231$) to those obtained when transwell experiments were performed. Thus, indicating no influence on the DEX action as result of indirect/direct contact of the loaded microparticles over the cells.

Finally, it was shown that BMP-2 is more bioactive than DEX in C2C12 cells. DEX was bioactive as shown by the possibility to induce osteogenic differentiation in ASC. ALP activity of C2C12 cells increased upon incubation with BMP-2 loaded microparticles (Figure 7.5). It can be observed higher levels of ALP activity for cells treated with BMP-2 loaded microparticles than for cells treated with the DEX loaded microparticles ($p = 0.000002$) and unloaded microparticles ($p = 0.000001$). In addition, it was found that the ALP activity in C2C12 cells treated with SPCL unloaded microparticles was similar ($p = 0.2409$) to the levels in DMEM culture media. Similarly, no change in ALP activity was obtained when the cells were treated with BMP-2 compared to BSA/BMP-2 control solutions ($p = 0.4135$). This suggests that the increase in ALP levels results, solely, from the release of bioactive BMP-2 from the SPCL microparticles. Furthermore, this is an indication that BSA did not interfere with the osteogenic potential of BMP-2.

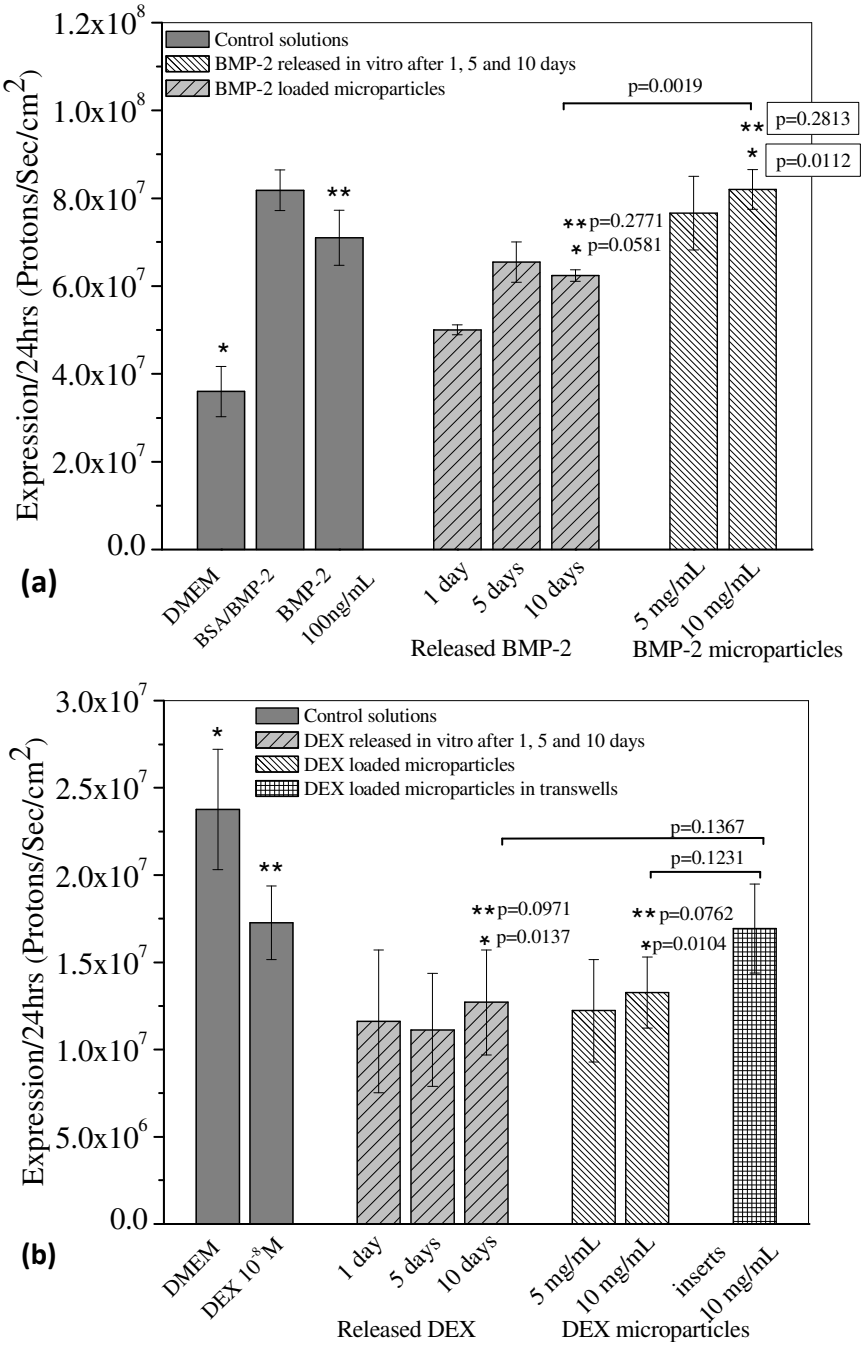

Figure 7.4 OCN promotor activity as determined by luciferase activity in C2C12 cells after administration of: BMP-2 **(a)** or DEX **(b)**. Controls include culture medium only (DMEM), BSA/BMP-2 (2 mg/100 ng per mL), BMP-2 (100 ng/mL) or DEX (10^{-8} M) solutions. Samples include supernatants from the *in vitro* release of BMP-2 and DEX after 1, 5 and 10 days, and BMP-2 and DEX loaded microparticles incubated directly with the cells (5 mg/mL and 10 mg/mL). In addition, transwell experiments using DEX loaded microparticles (10 mg/mL) are represented for comparison. Values are mean ± standard deviation (n=3). Each pair of values compared are indicated: (*) when compared to DMEM control, (**) to BMP-2 or DEX control solutions and (¯) when a comparison was established between the tested samples

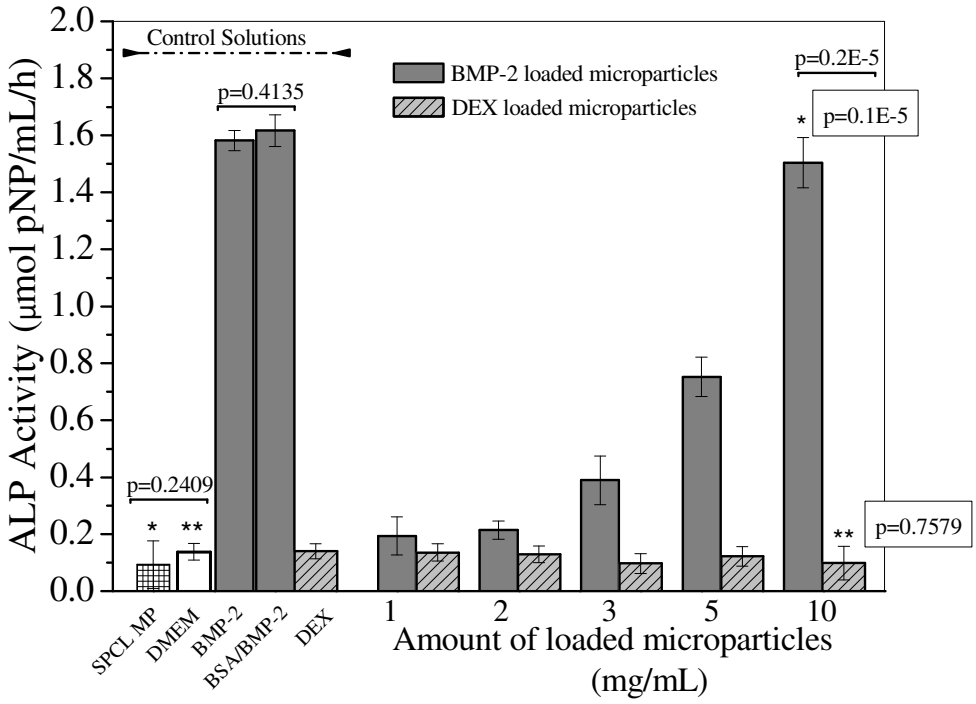

Figure 7.5 Alkaline Phosphatase activity in C2C12 cells as determined using pNP assay. Controls include unloaded SPCL microparticles (SPCL MP), BSA/BMP-2 (2 mg/ 100 ng per mL), and BMP-2 (100 ng/mL) solutions or DEX (10^{-8} M) solution. Samples include BMP-2 and DEX loaded microparticles incubated directly with the cells (1-10 mg/mL). Values are mean ± standard deviation (n=3). Each pair of values compared are indicated: (*) when compared to SPCL unloaded microparticles, (**) to DMEM control and (¯) when a comparison was established between a pair of controls or samples ALP values

von Kossa staining demonstrated the presence of mineralization nodules in C2C12 treated with BMP-2 loaded microparticles (Figure 7.6 (b), (c), (d)). Similarly, alizarin red staining for calcium deposits revealed a higher staining intensity of C2C12 cells that where incubated with BMP-2 loaded microparticles compared to both SPCL unloaded microparticles and DMEM culture medium alone (Figure 7.6 (e), (f), (g)). Furthermore, the intensity of von Kossa and alizarin red stained zones increased with culture time. Moreover, staining was more intense with increasing concentrations of BMP-2 loaded microparticles. In contrast, no mineralization nodules or calcium deposits were detected for C2C12 treated with DEX loaded microparticles. This is in agreement with the observation that C2C12 cells incubated with DEX released supernatants, DEX loaded microparticles, and DEX control solutions do not exhibit activation of the OCN promotor (Figure 7.4 (b)) or ALP activity (Figure 7.5). However, when ASCs were used, DEX was bioactive as shown by a significant increase of ALP activity ($p = 0.000004$) upon incubation of DEX loaded microparticles with these cells (Figure 7.7).

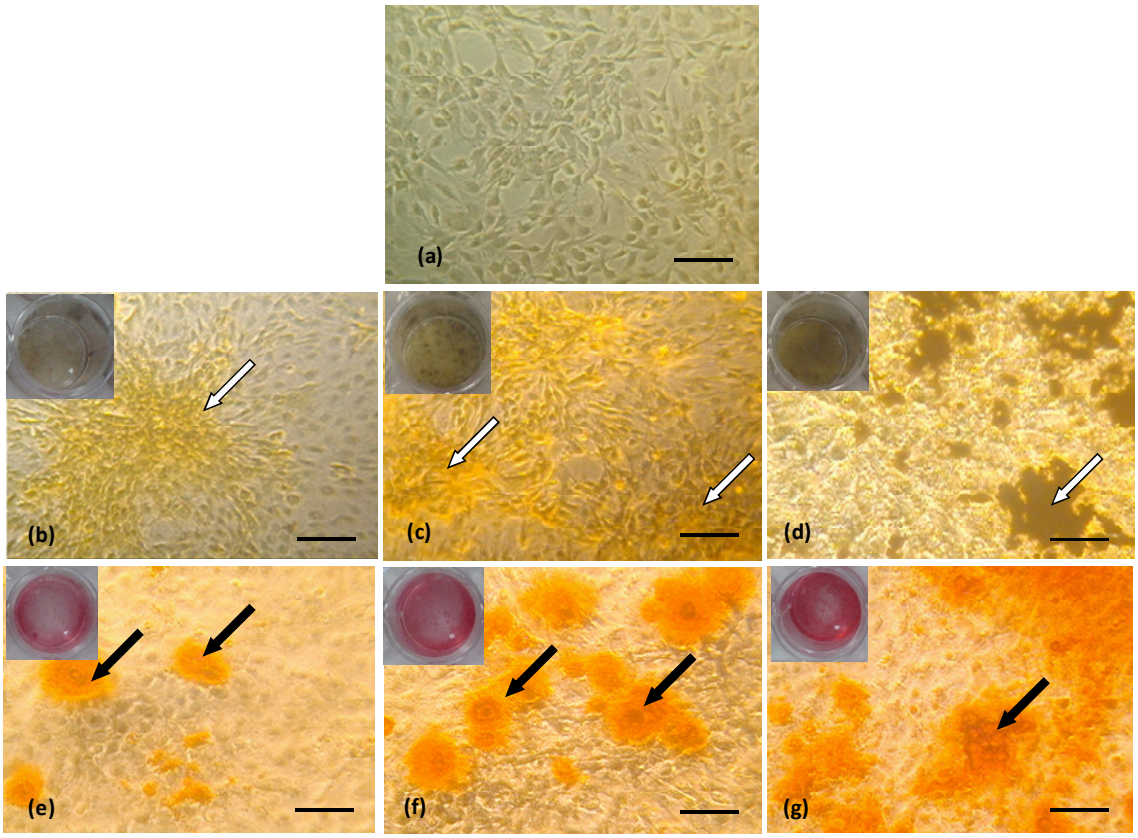

Figure 7.6 Photomicrographs illustrate mineralization and calcium deposits of C2C12 cells upon incubation with BMP-2 loaded microparticles stained with von Kossa (3 days **(b)**, 7 days **(c)** and 14 days of culture**(d)**) and Alizarin red (3 days **(e)**, 7 days **(f)** and 14 days of culture **(g)**). Control cells **(a)**: Bar = 50 µm. Staining zones of mineralization nodules (after 3 days of culture) and mineral deposition (from 14 days of culture further) are indicated with white arrows. Similarly, the presence of calcium, indicated with black arrows, can be observed as early as at 3 days of culture. The inserts images show a general view of the well

Overall, the obtained results indicated the occurrence of osteogenesis in C2C12 cells as result of bioactive BMP-2 released from SPCL microparticles. Furthermore, DEX was found to be not suitable as an osteogenic agent for C2C12 cells, but could induce osteogenesis in ASCs. Both encapsulated drugs (DEX and BMP-2) remained bioactive upon encapsulation and after release in/from the SPCL microparticles.

7.5 DISCUSSION

Clinically, high doses of BMP-2 are needed to exert its effects in non-union tibial fractures or anterior fusion of the lumbar spine that can be detrimental by inducing hyperostosis or heterotopic ossification. Currently, BMP-2 is applied using a bovine collagen

sponge that can only be introduced to the defect using an open surgery and may elicit immune reactions. Hence, the presented study aimed to develop and characterize a novel injectable drug delivery system for BMP-2 by using SPCL microparticles. Therefore, three main aspects have been addressed during this study to provide answers to the initially formulated questions. Thus, whether biodegradable SPCL microparticles can serve as a carrier for controlled release of BMP-2 and DEX; whether the entrapped drugs, i.e., DEX and BMP-2, remain bioactive during encapsulation and upon release; and whether the released DEX and BMP-2 are equally active concerning osteogenesis in an osteo/myo-blast cell line (C2C12).

BMP-2 was successfully encapsulated in the SPCL microparticles. However, the obtained encapsulation efficiency (EE) value was low (≅ 25%). Nevertheless, the released BMP-2 showed satisfactory levels of bioactivity. Therefore, it can be stated that this limitation of low EE does not jeopardize the functionality of the developed delivery system. Indeed, our value of EE for BMP-2 is lower than some other values reported in the literature for GFs [36, 43, 44]. However, many of the reported encapsulation methods include the use of high temperatures and toxic organic solvents without using a carrier protein to protect the GFs. As a result, high values of EE are obtained, but the bioactivity of the GFs is in many cases compromised. Therefore, we used co-encapsulation method with BSA as carrier protein. Moreover, all the processing and encapsulation was performed at room temperature. Although this had resulted in lower encapsulation efficiency, the bioactivity of the GFs was preserved. Therefore, this method was shown to be more efficient, needing less GF for encapsulation purposes. In this study, a starch-poly-ε-caprolactone blend was chosen to encapsulate DEX and BMP-2 because of their known biocompatibility [37, 40, 45] and proven biodegradability [33, 46, 47]. Moreover, the combination of a hydrophilic natural material (starch) with a hydrophobic synthetic polymer (polycaprolactone), in a single material constitutes the major advantage of this system. Therefore, these loaded SPCL microparticles should result in an optimal biodegradable carrier to induce osteogenesis for bone TE. In a previous study [33], it was investigated the release of DEX from the SPCL microparticles in PBS and enzymatically controlled environments. The release mechanism was characterized by diffusion phenomena and at late stages by degradation of the microparticles. As a consequence, the biodegradation of the polymeric matrix controlled the overall DEX release process. The initial burst release observed for BMP-2 in the present work and previously for DEX [32, 33] can be explained as a result of drug entrapment in the proximity of the microparticles' surface. Subsequently, the BMP-2 loaded SPCL microparticles start to take up water from the aqueous environment, with the consequent swelling of the polymeric matrix and diffusion of the BMP-2 through the polymer into the medium [48, 49]. As a result of poly-

ε-caprolactone (PCL) hydrophobicity, the release of BMP-2 from the SPCL microparticles is sustained from 2 up to 10 days. This is an evident advantage of this carrier system, being able to maintain bioactivity and newly BMP-2 being released up to 10 days. The pronounced burst release has been considered a drawback for several control delivery systems [50, 51]. However, for osteogenesis, at early stages high concentrations of BMP-2 are needed. Subsequently, more constant and sustained release is desired. The possibility of more sustained release of BMP-2 for longer time periods represent the most important benefit when compared with other delivery systems that have been proposed for BMP-2 [43, 52]. Thus, in this particular case, this system may be advantageous for bone TE.

Indeed, BMP-2 loaded microparticles were able to induce osteogenesis in C2C12 cells and did not show any cytotoxicity. Moreover, the bioactivity of the released BMP-2 was confirmed since transfected C2C12 showed activation of the OCN promotor as measured by luminescence intensity. Activation of the OCN promotor is indicative of late-stage osteogenic differentiation [53]. This induction was maximal, as increasing concentration of BMP-2 loaded microparticles did not change activity, showing a plateau in luminescence intensity. This means that the BMP-2 induced a maximal cellular response. The BMP-2 receptor is maximally activated due to binding of the BMP-2 and thus no further increase in OCN activity can be found. BMP-2 receptor I and II activity is mainly regulated by downstream signal transduction molecules such as smad1, 5 and 8 all of them phosphorylate smad4. Interactions with RunX2 are possible [54]. This indicates that the concentration of BMP-2 is enough to exert the maximal biological effect.

The results were corroborated by ALP determinations, an early osteogenic marker. It is well known that BMP-2 can upregulate ALP activity [55]. Similar differentiation behavior was observed by the two different assays. Histology results confirmed highly bioactive BMP-2 was released from the SPCL microparticles, inducing mineralization including calcium deposition. As this activity is exerted via an ALP independent pathway, it can be concluded that the released BMP-2 exerts maximal effects as also mineralization is induced [56]. Thus, the BMP-2 loaded microparticles and the BMP-2 released from the microparticles were bioactive and able to induce osteogenesis and maturation. These are two distinct processes known from BMP-2 action as has also been shown in primary myoblasts using BMP-2 gene therapy [57]. In contrast, DEX loaded microparticles were not able to induce osteogenesis, as indicated by absent ALP activity and OCN promotor activation. Interestingly, the same results were obtained with control solutions of plain DEX (without being encapsulated). Thus, the inactivity of the DEX samples was not a result of the encapsulation or inefficient *in vitro* release, but rather dependent on the cell type used (C2C12 cells). It has been shown that glucocorticoids,

among them DEX, inhibit proliferation and differentiation capacity in C2C12 cells [58, 59] but not in other cell types. This was confirmed by the ability of DEX loaded microparticles to induce osteogenesis in ASCs in contrast to C2C12, as observed by increased values of ALP.

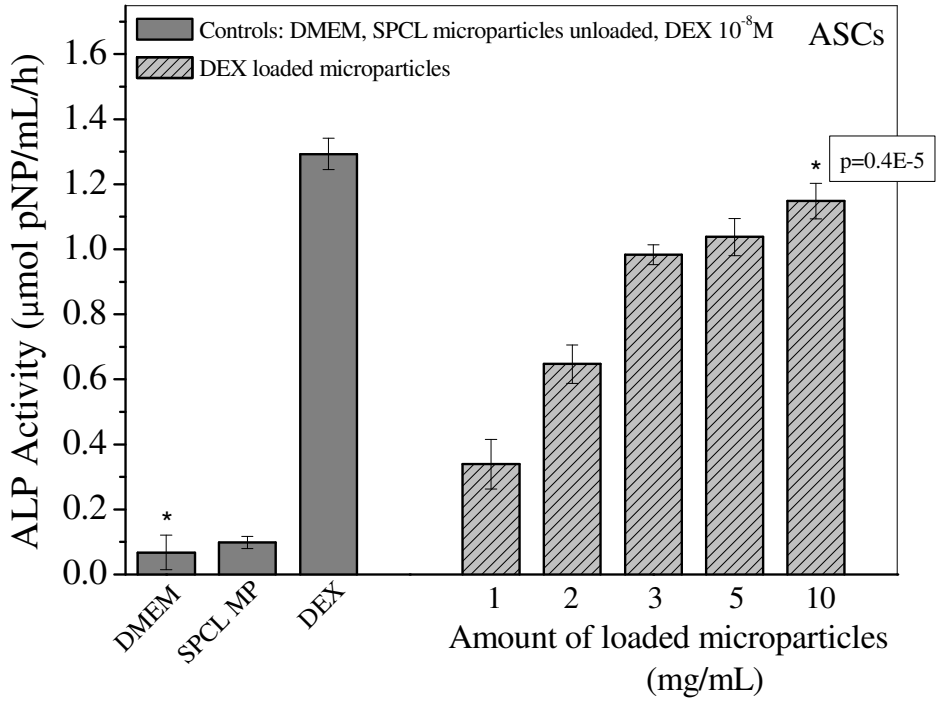

Figure 7.7 Alkaline Phosphatase activity in human Adipose Derived Stem Cells (ASCs) incubated with DEX loaded microparticles as determined using pNP assay. Controls include unloaded SPCL microparticles (SPCL MP) and DEX (10^{-8} M) solution. Samples include DEX loaded microparticles incubated directly with the cells (1-10 mg/mL). Values are mean ± standard deviation (n=3). Pairs of values statistically compared are indicated (*) in the graph with the correspondent p value ($p=0.4x10^{-5}$)

This result indicated the DEX loaded SPCL microparticles were capable of stimulating the development of an osteogenic phenotype in human ASCs by releasing bioactive DEX. Thus, DEX may not be suitable to induce osteogenesis in the C2C12 cell line as it has been described previously [58, 59]. However, ASCs are more clinically relevant in the context of bone TE. Therefore, this line of investigation will be of continued interest in the future. Especially, as DEX is not a protein, it will elicit fewer immunologic reactions. Furthermore, the production of DEX is cheaper than that of BMP-2. However, DEX also contains the drawbacks of glucocorticoids. Therefore, careful investigations are necessary to evaluate its clinical suitability.

This study investigated the potential of a biodegradable microparticle system combined with bioactive molecules to induce osteogenesis. Although the encapsulation efficiency was low for BMP-2, the bioactivity was well preserved upon its release using the encapsulation method proposed in this study (co-encapsulation). DEX was encapsulated with high encapsulation efficiency values and was bioactive in ASCs while inducing osteogenesis. Our data suggest the biodegradability and biocompatibility of starch-based materials, as well as defined release profiles of encapsulated drugs, may allow their successful use as devices for the controlled/sustained delivery of bioactive molecules in bone TE. Especially, our device bears the advantage of requiring lower concentrations of BMP-2 and allowing a sustained release over longer periods of time than the currently available commercial products.

7.6 ACKNOWLEDGMENTS

The authors wish to thank to the Marie Curie Host Fellowships for Early Stage Research Training (EST) "Alea Jacta EST" (MEST-CT-2004-008104) and the European NoE EXPERTISSUES (NMP3-CT-2004-500283) for providing the funding for this work. In addition, the authors thank Ms. Daniela Dopler for expert technical assistance during the *in vitro* cell culture experiments.

7.7 REFERENCES

1. Perka, C.; Schultz, O.; Spitzer, R. S.; Lindenhayn, K.; Burmester, G. R.; Sittinger, M. *Biomaterials* **2000**, 21 (11): 1145-1153.
2. Komaki, H.; Tanaka, T.; Chazono, M.; Kikuchi, T. *Biomaterials* **2006**, 27 (29): 5118-5126.
3. den Boer, F. C.; Wippermann, B. W.; Blokhuis, T. J.; Patka, P.; Bakker, F. C.; Haarman, H. *Journal of Orthopaedic Research* **2003**, 21 (3): 521-528.
4. Gugala, Z.; Gogolewski, S. *Injury* **2002**, 33 (S2): 71-76.
5. Laurencin, C.; Khan, Y.; El-Amin, S. F. *Expert Review of Medical Devices* **2006**, 3 (1): 49-57.
6. Wildemann, B.; Kadow-Romacker, A.; Pruss, A.; Haas, N. P.; Schmidmaier, G. *Cell and Tissue Banking* **2007**, 8: 107–114.
7. Perry, C. R. *Clinical Orthopaedics and Related Research* **1999**, 360: 71-86.
8. DeCoster, T. A.; Gehlert, R.; Mikola, E. A.; Pirela-Cruz, M. A. *Journal of the American Academy of Orthopaedic Surgeons* **2004**, 12 (1): 28-38.
9. Langer, R.; Vacanti, J. P. *Science* **1993**, 260 (5110): 920-926.
10. Gomes, M. E.; Reis, R. L.; Mikos, A. G. In *Biodegradable Systems in Tissue Engineering and Regenerative Medicine*, Reis, R. L.; San Roman, J., Eds. CRC Press: Boca Raton, FL, **2005**; pp 29-38.
11. Laurencin, C. T.; Ambrosio, A. M. A.; Borden, M. D.; Cooper, J. A. *Annual Review of Biomedical Engineering* **1999**, 1: 19-46.
12. Martinek, V.; Huard, J.; Fu, F. H. In *Tendon Injuries: Basic Science and Clinical Medicine*, Maffulli, N.; Renstrom, P.; Leadbetter, W., Eds. Springer: London, **2005**; pp 307-312.

13. Salgado, A. J.; Coutinho, O. P.; Reis, R. L. *Macromolecular Bioscience* **2004**, 4 (8): 743-765.
14. Bessa, P. C.; Casal, M.; Reis, R. L. *Journal of tissue engineering and regenerative medicine* **2008**, 2 (2-3): 81-96.
15. Bessa, P. C.; Casal, M.; Reis, R. L. *Journal of tissue engineering and regenerative medicine* **2008**, 2 (1): 1-13.
16. Urist, M. R.; Silverman, B. F.; Büring, K.; Dubuc, F. L.; Rosenberg, J. M. *Clinical Orthopaedics and Related Research* **1967**, 53: 243-283.
17. Aubin, J. E.; Triffitt, J. T. In *Principles of Bone Biology*, 2nd ed.; Bilezikian, J. P.; Raisz, L. G.; Rodan, G. A., Eds. Academic Press, Inc.: San Diego, CA, **2002**; Vol. 1, pp 59-81.
18. Yamaguchi, A.; Komori, T.; Suda, T. *Endocrine Reviews* **2000**, 21 (4): 393-411.
19. Gitelman, S. E.; Kirk, M.; Ye, J. Q.; Filvaroff, E. H.; Kahn, A. J.; Derynck, R. *Cell growth & differentiation* **1995**, 6 (7): 827-36.
20. Katagiri, T.; Yamaguchi, A.; Ikeda, T.; Yoshiki, S.; Wozney, J. M.; Rosen, V.; Wang, E. A.; Tanaka, H.; Omura, S.; Suda, T. *Biochemical and biophysical research communications* **1990**, 172 (1): 295-9.
21. Katagiri, T.; Yamaguchi, A.; Komaki, M.; Abe, E.; Takahashi, N.; Ikeda, T.; Rosen, V.; Wozney, J. M.; Fujisawa-Sehara, A.; Suda, T. *The Journal of cell biology* **1994**, 127 (6 Pt 1): 1755-66.
22. Sampath, T. K.; Maliakal, J. C.; Hauschka, P. V.; Jones, W. K.; Sasak, H.; Tucker, R. F.; White, K. H.; Coughlin, J. E.; Tucker, M. M.; Pang, R. H.; et al. *The Journal of biological chemistry* **1992**, 267 (28): 20352-62.
23. Yamaguchi, A.; Katagiri, T.; Ikeda, T.; Wozney, J. M.; Rosen, V.; Wang, E. A.; Kahn, A. J.; Suda, T.; Yoshiki, S. *The Journal of cell biology* **1991**, 113 (3): 681-7.
24. Ding, S.; Schultz, P. G. *Nature Biotechnology* **2004**, 22 (7): 833-840.
25. Grigoriadis, A. E.; Heersche, J. N. M.; Aubin, J. E. *Journal of Cell Biology* **1988**, 106 (6): 2139-2151.
26. Jaiswal, N.; Haynesworth, S. E.; Caplan, A. I.; Bruder, S. P. *Journal of Cellular Biochemistry* **1997**, 64 (2): 295-312.
27. Jorgensen, N. R.; Henriksen, Z.; Sorensen, O. H.; Civitelli, R. *Steroids* **2004**, 69 (4): 219-226.
28. Morsczeck, C.; Moehl, C.; Gotz, W.; Heredia, A.; Schaffer, T. E.; Eckstein, N.; Sippel, C.; Hoffmann, K. H. *Cell Biology International* **2005**, 29 (7): 567-575.
29. Rickard, D. J.; Sullivan, T. A.; Shenker, B. J.; Leboy, P. S.; Kazhdan, I. *Developmental Biology* **1994**, 161 (1): 218-228.
30. Keskin, S. D.; Hasirci, V. In *Tissue Engineering, Stem Cells and Gene Therapies*, Elcin, M., Ed. Kluwer Academic/Plenum Publishers: New York, **2003**; pp 279-296.
31. Bastioli, C.; Bellotti, V.; Montino, A.; Tredici, G. D.; Lombi, R.; Ponti, R. Biodegradable polymeric compositions based on starch and thermoplastic polymers. *United States Patent* 5,412,005, **1995**.
32. Balmayor, E. R.; Tuzlakoglu, K.; Azevedo, H. S.; Reis, R. L. *Acta Biomaterialia* **2009**, 5 (4): 1035-1045.
33. Balmayor, E. R.; Tuzlakoglu, K.; Marques, A. P.; Azevedo, H. S.; Reis, R. L. *Journal of Materials Science-Materials in Medicine* **2008**, 19 (4): 1617-1623.
34. Lewis, D. H. In *Biodegradable Polymers as Drug Delivery Systems.*, Chasin, M.; Langer, R., Eds. Marcel Dekker, Inc.: New York, **1990**; pp 1-42.
35. Kim, H. D.; Valentini, R. F. *Biomaterials* **1997**, 18 (17): 1175-1184.
36. Meinel, L.; Illi, O. E.; Zapf, J.; Malfanti, M.; Merkle, H. P.; Gander, B. *Journal of Controlled Release* **2001**, 70 (1-2): 193-202.
37. Silva, G. A.; Coutinho, O. P.; Ducheyne, P.; Shapiro, I. M.; Reis, R. L. *Tissue Engineering* **2007**, 13 (6): 1259-1268.

38. Wang, S. B.; Chen, A. Z.; Weng, L. J.; Chen, M. Y.; Xie, X. L. *Macromolecular Bioscience* **2004**, 4 (1): 27-30.
39. Reis, R. L.; Mendes, S. C.; Cunha, A. M.; Bevis, M. J. *Polymer International* **1997**, 43 (4): 347-352.
40. Marques, A. P.; Reis, R. L.; Hunt, J. A. *Biomaterials* **2002**, 23 (6): 1471-1478.
41. Salgado, A. J.; Coutinho, O. P.; Reis, R. L. *Tissue Engineering* **2004**, 10 (3-4): 465-474.
42. Lian, J. B.; Stein, G. S. *Critical Reviews in Oral Biology & Medicine* **1992**, 3 (3): 269-305.
43. Chen, F. M.; Wu, Z. F.; Sun, H. H.; Wu, H.; Xin, S. N.; Wang, Q. T.; Dong, G. Y.; Ma, Z. W.; Huang, S.; Zhang, J. J.; Jin, Y. *International Journal of Pharmaceutics* **2006**, 307 (1): 23-32.
44. Kim, S. E.; Park, J. H.; Cho, Y. W.; Chung, H.; Jeong, S. Y.; Lee, E. B.; Kwon, I. C. *Journal of Controlled Release* **2003**, 91 (3): 365-374.
45. Mendes, S. C.; Reis, R. L.; Bovell, Y. P.; Cunha, A. M.; van Blitterswijk, C. A.; de Bruijn, J. D. *Biomaterials* **2001**, 22 (14): 2057-2064.
46. Azevedo, H. S.; Gama, F. M.; Reis, R. L. *Biomacromolecules* **2003**, 4 (6): 1703-1712.
47. Azevedo, H. S.; Reis, R. L. In *Biodegradable Systems in Tissue Engineering and Regenerative Medicine*, Reis, R. L.; San Roman, J., Eds. CRC Press: Boca Raton, FL, **2005**; pp 177-201.
48. Demirgoz, D.; Elvira, C.; Mano, J. F.; Cunha, A. M.; Piskin, E.; Reis, R. L. *Polymer Degradation and Stability* **2000**, 70 (2): 161-170.
49. Reis, R. L.; Cunha, A. M. In *Encyclopedia of Materials: Science and Technology*, Buschow, K. H. J.; Cahn, R. W.; Flemings, M. C.; Ilschner, B.; Kramer, E. J.; Mahajan, S.; Veyssiere, P., Eds. Elsevier Ltd.: New York, **2001**; Vol. 11, pp 8810-8816.
50. Huang, X.; Brazel, C. S. *Journal of Controlled Release* **2001**, 73 (2-3): 121-136.
51. Yeo, Y.; Park, K. *Archives of pharmacal research* **2004**, 27 (1): 1-12.
52. Patel, Z. S.; Yamamoto, M.; Ueda, H.; Tabata, Y.; Mikos, A. G. *Acta Biomaterialia* **2008**, 4 (5): 1126-1138.
53. Yamamoto, N.; Furuya, K.; Hanada, K. *Biological & Pharmaceutical Bulletin* **2002**, 25 (4): 509-515.
54. Chen, D.; Zhao, M.; Mundy, G. R. *Growth Factors* **2004**, 22 (4): 233-241.
55. Kim, I. S.; Song, Y. M.; Cho, T. H.; Park, Y. D.; Lee, K. B.; Noh, I.; Weber, F.; Hwang, S. J. *Development Growth & Differentiation* **2008**, 50 (7): 553-564.
56. Luppen, C. A.; Chandler, R. L.; Noh, T.; Mortlock, D. P.; Frenkel, B. *Growth Factors* **2008**, 26 (4): 226-237.
57. Gersbach, C. A.; Guldberg, R. E.; Garcia, A. J. *Journal of Cellular Biochemistry* **2007**, 100 (5): 1324-1336.
58. Salehian, B.; Mahabadi, V.; Bilas, J.; Taylor, W. E.; Ma, K. *Metabolism-Clinical and Experimental* **2006**, 55 (9): 1239-1247.
59. te Pas, M. F. W.; de Jong, P. R.; Verburg, F. J. *Molecular Biology Reports* **2000**, 27 (2): 87-98.

Chapter 8

Synthesis, surface functionalization and characterization of superparamagnetic poly-ε-caprolactone microparticles

8.1 ABSTRACT

Nowadays, there has been a growing interest on developing strategies for cell isolation using magnetic functionalized particles. The basic instrumentation only requires a set of magnets and it has been described by different authors as a very effective technique. The most important factors in this process are the type of magnetic particles and the used ligand. In this study, we have successfully fabricated amino and epoxy surface functionalized magnetic microparticles by using poly-ε-caprolactone as coating material. Particles with size in the range of 4-135 μm, spherical shape and about 13% (wt) of magnetite entrapped inside a poly-ε-caprolactone shell were synthesized. The obtained core-shell microparticles demonstrated a superparamagnetic behavior. The superparamagnetic microparticles were in addition surface functionalized with amino and epoxy groups allowing for the incorporation of target ligands. Activation by O_2 plasma treatment followed by epichlorohydrin reaction was proposed in order to functionalize the particles surface with epoxy groups. To the best of our knowledge, this study constitutes the first report on the application of this process on polymeric particulated systems. Furthermore, we have demonstrated the efficiency of the developed particles for bovine serum albumin (BSA) covalent coupling (covalent efficiency higher than 47% for epoxy and 71% for amino funcionalized particles). A protein coupling protocol for the developed functionalized magnetic microparticles was optimized and it is presented in this work. pH range on the vicinity of the isolectric point of the used ligand and lower ion concentrations buffers have shown to be two very important parameters on the performance of the particles. Moreover, when carbodiimide was used for NH_2-m-PCL microparticles surface activation, the most favorable pH was in the optimal range for this reaction to occur. Finally, a good cell response, in terms of both viability and proliferation, was observed by the use of osteoblastic cell line. Furthermore, characteristic cell morphology and good proliferation resulted from the contact of the amino functionalized particles with human derived adipose stem cells. The overall research described herein may lead to further studies on the synthesis, surface functionalization and characterization of highly biocompatible superparamagnetic microparticles and consequent innovative applications. Furthermore, it

may help to attain a better understanding of the intricate relationship between the material surface functionality and the protein adsorption phenomena. Thus, predicting their behavior and improving the efficiency in forming a highly stable functional particle-protein biocomplex.

***This chapter is based on the following publication:**

Balmayor, *E. R.;* Pashkuleva, I.; Rada, T.; Gomes, M. E.; Azevedo, H. S.; Reis, R. L. Synthesis, surface functionalization and characterization of superparamagnetic poly-ε-caprolactone microparticles. **2009. Submitted.**

8.2 INTRODUCTION

Superparamagnetic nano- and microparticles have attracted much attention in the last decades due to their extensive applications in the biotechnology and medicine fields. The combination of their properties, such as size, shape, morphology, superparamagnetic behavior and ability for surface functionalization, provides a unique potential for further development in biomedical applications. Immunomagnetic separation of enzymes [1-5], proteins [5-7], and cells [8-10] or detection of specific targets in clinical diagnosis [10-13] by magnetic particles are only a few of the examples of their broad application. In addition, they are key components in medical diagnostics [14-16]. However, remaining challenges in particles development is the design and processing of highly specific materials tailored for a certain applications.

Magnetite nanoparticles are defined as iron (II, III) oxide (Fe_3O_4) particles with average size in the nano-scale and presenting superparamagnetic features. Thus, the particles exhibit magnetic behavior only when placed within a magnetic field, showing no residual magnetism when the field is removed [15]. Usually, the particles are handled as a suspension or fluid. The magnetite suspension can be used as it is or the particles can be further coated with organic or inorganic compounds. Lately, polymeric materials have been used for this purpose [9, 17-21]. They present several advantages as coating material: like processing versatility allowing for controlled hydrophilicity/hydrophobicity, reactive surfaces, tailored degradation and low toxicity, among others. In this paper we have chosen poly-ε-caprolactone (PCL) as an example of an aliphatic polyester widely used in biomedical applications. It has been demonstrated that it is biodegradable [22-24] and biocompatible [23-25]. Moreover, this semicrystalline polymer can be easily processed by a variety of techniques [26] and its surface is easily functionalized [27, 28]. Core-shell polymeric particles containing a magnetic core (magnetite) entrapped inside a polymeric shell (PCL) were successfully developed and the procedure is described in this article. Functionalization of the surface targeting specific binding of antigens or antibodies, enzymes, proteins and cells can be further performed. Amino, epoxy and carboxy functional groups are some of the well known surface functionalities that favor covalent binding capabilities of the target ligands [5, 9]. Covalent binding is highly desired because it provides more stable material-biomolecule complexes. Furthermore, it avoids nonspecific reactions between the material surface and the target biomolecule and hence it directs the coupling reaction [29, 30].

The experimental procedure employing functionalized magnetic particles is quite simple (Figure 8.1). When added to a heterogeneous cell suspension, the particles will bind the targeted entities based on the specific interactions, such as covalent coupling [31, 32] or

electrostatic interactions between the material surface and the cell or biomolecule [33, 34]. The resulting complex can be removed from the suspension by placing the system within a magnetic field gradient because of the particles superparamagnetic behavior.

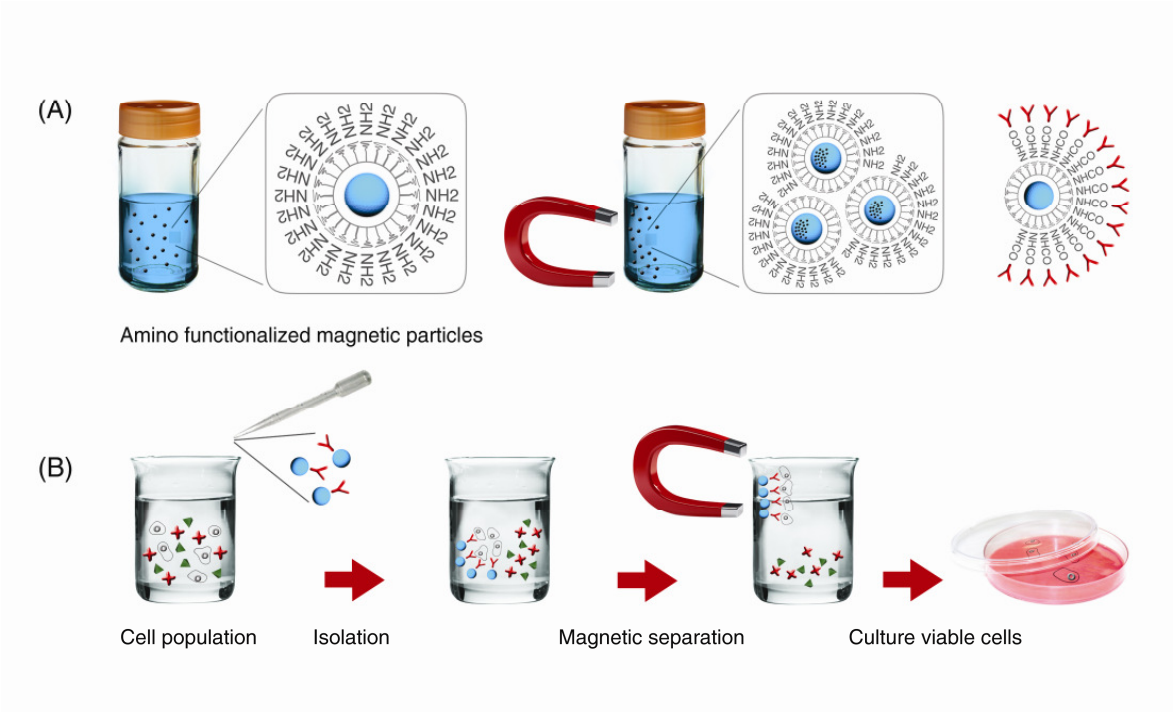

Figure 8.1 Schematic representation of surface functionalized magnetic particles **(A)** and the principle of cell isolation using these particles **(B)**

When developing magnetic particles intended to be used for cell isolation, several features needed to be carefully addressed: For instance, the size of the beads should be in the range of 5-50 µm with narrow size distribution, adequate hydrophobicity and surface functionalization [8]. This work presents the development of superparamagnetic poly-ε-caprolactone microparticles with tailored characteristics for isolation of cells. Superparamagnetic m-PCL microparticles with different size, surface area, iron contents and surface chemistry (-NH_2 and epoxy) were obtained and their capacity to covalent bind protein-like ligands was analyzed. It was found that the protein adsorption can be significantly improved by the alternate surface functionalization. To the best of our knowledge this is the first research work that reports development of a set of different poly-ε-caprolactone core-shell superparamagnetic microparticles with tailored surface functionalities for protein-like covalent binding. Moreover, we were also able to enhance both cell viability and proliferation to the developed microparticles.

8.3 EXPERIMENTAL

8.3.1 Materials

For the magnetite nanoparticles preparation, ferrous chloride tetrahydrate ($FeCl_2.4H_2O$; ≥ 98%) was purchased from Fluka (Switzerland). Ferric chloride hexahydrate ($FeCl_3.6H_2O$; 99%) and ammonium hydroxide solution (30-33% in water) were obtained from Riedel-de Haën (Germany). Oleic acid (99%) was purchased from Sigma-Aldrich (USA).

Poly-ε-caprolactone (Tone™ PCL-787, average molecular weight 125 KDa, reported by the manufacturer) was obtained from Union Carbide Chemicals and Plastics Division (USA) and was used for the core-shell microparticles preparation. Dichloromethane (99.5%, stabilized with amylene) was purchased from Panreac (Spain) and polyvinyl alcohol (PVA, 87-90% hydrolyzed, average molecular weight 30 000-70 000) from Sigma-Aldrich (USA). For surface functionalization, 1,6-hexanediamine (98%) and epichlorohydrin (ECH, ≥ 99%) both purchased from Sigma-Aldrich (USA), were used.

Bovine serum albumin (BSA, ≥96%) and *N*-(3-Dimethylaminopropyl)-*N*'-ethylcarbodiimide hydrochloride (commercial grade), both purchased from Sigma-Aldrich (USA), were used for the binding experiments. Fluorescein 5-(6)-isothiocyanate (≥ 90%) obtained from Fluka (Switzerland) was used to label BSA protein. All the reagents were used as received.

8.3.2 Magnetite nanoparticles synthesis

The superparamagnetic magnetite nanoparticles were prepared by a co-precipitation method using iron chloride salts (Fe^{2+}/Fe^{3+}) as iron source [17-19, 35]. $FeCl_3.6H_2O$ (1.80 M) and $FeCl_2.4H_2O$ (1.20 M) were dissolved in distilled water previously degassed by bubbling N_2 for 30 minutes. Under a N_2 atmosphere and vigorous mechanical stirring, the mixture was heated to 80 ^oC. Subsequently, 40 mL of ammonium hydroxide solution (25% in water) were rapidly added, maintaining the reaction conditions for the following 30 minutes. In order to minimize the oxidation of the formed magnetite (Fe_3O_4) to ferromagnetic oxides (Fe_2O_3), the oxygen content of the precipitation medium was stabilized at the lowest level by continuous N_2 bubbling. After precipitation of magnetite particles, 15 mL of oleic acid was added dropwise (within a 10 minutes period). The mixture was heated for 30 minutes. At this time, the color of the mixture changed to a deep black lump indicating the formation of the magnetite particles. The precipitate was separated and then extensively washed using a mixture of distilled water and acetone (1:1, v:v). As a result of the external magnetic field, the particles were attracted

towards the magnet within a few minutes allowing to discard the supernatants after each washing step. A homogeneous and fine black precipitate was obtained that was further dried in a vacuum desiccator at room temperature for 24 hours.

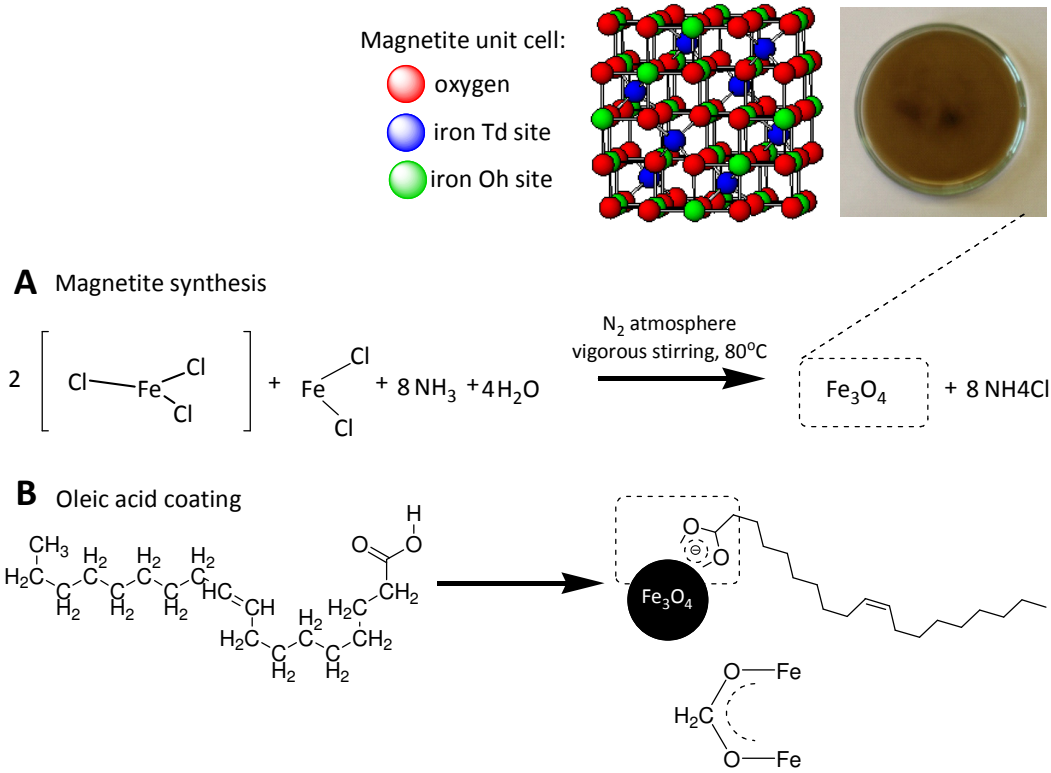

Figure 8.2 Synthesis of magnetite nanoparticles **A)**. Magnetite stabilized by the interaction of the polar ends of the oleic acid molecules with the magnetite nanoparticles **B)**

8.3.3 m-PCL core-shell microparticles preparation

Core-shell magnetic poly-ε-caprolactone microparticles (m-PCL) were prepared by an emulsion solvent extraction/evaporation method [36], in which magnetite nanoparticles were included inside the polymeric shell. Briefly, PCL was dissolved in 5 mL of dichloromethane under vigorous stirring. After complete dissolution of the polymer, the magnetite nanoparticles were added. The mixture was sonicated for 10 minutes at 100 W using an ultrasonic bath "Ultrasons 3001208" (J.P.Selecta, Spain), to ensure a good dispersion of the magnetite nanoparticles in the polymeric solution. Subsequently, the suspension was dropped into a continuously stirred PVA medium (100 mL), and emulsified for 4 hours at different stirring rates using the dispersing device "Ultra-Turrax Yellow line DI 18 basic", (IKA Werke GmbH & Co. KG, Germany). Different experimental conditions, such as magnetite to polymer ratio, PVA concentration and stirring rate were used (Table 8.1). The m-PCL microparticles were then collected by magnetic decantation, washed with distilled water and lyophilized to obtain a fine brownish powder.

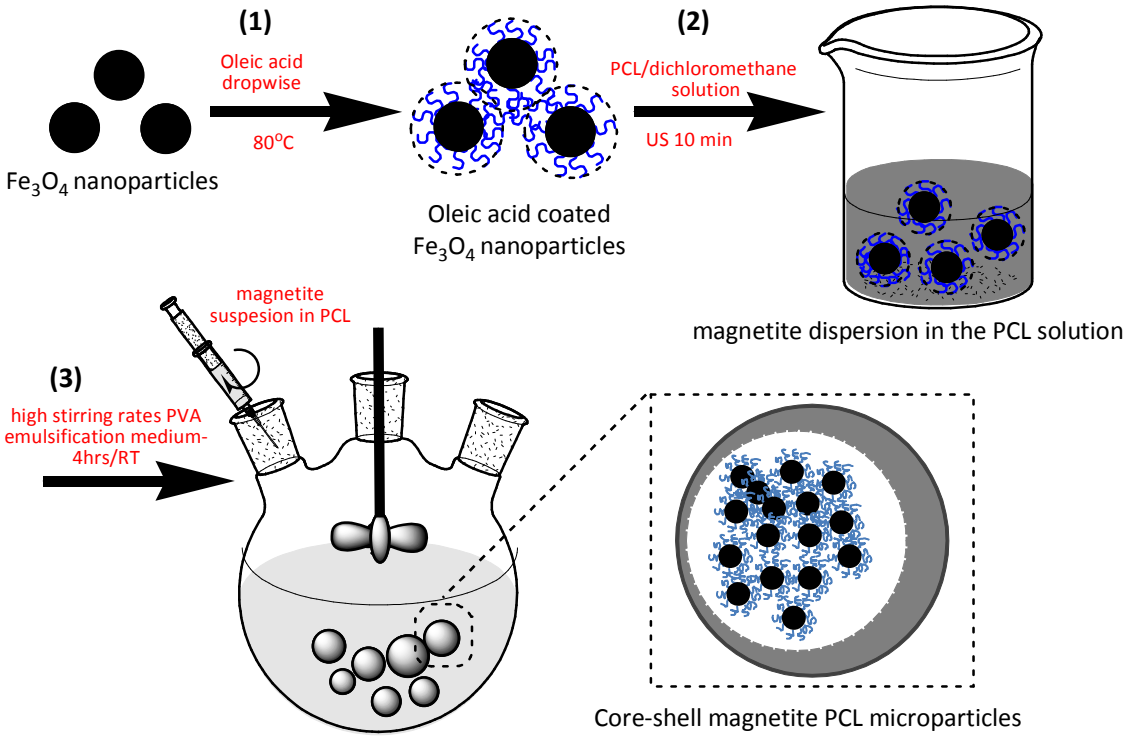

Figure 8.3 Core-shell m-PCL microparticles formation

8.3.4 Surface functionalization of the m-PCL core-shell microparticles

8.3.4.1 Amino groups: aminolysis of m-PCL microparticles [37]

Dried m-PCL microparticles were immersed in a 1,6-hexanediamine/2-propanol solution. The microparticles were chemically functionalized at two different temperatures (25 and 37 °C) for a time period varying from 30 to 90 minutes, maintaining the reaction vessel under constant agitation (100 rpm). The effect of several reaction conditions on the microparticles functionalization was investigated and the obtained results are presented in Table 8.2. At the end of each treatment period, the amino functionalized m-PCL (NH_2-m-PCL) microparticles were collected by magnetic decantation, and extensively dialyzed using deionized distilled water to remove the free 1,6-hexanediamine. Finally, NH_2-m-PCL microparticles were dried in a vacuum desiccator at room temperature until constant weight.

Table 8.1 Experimental conditions used for the production of m-PCL microparticles and their effect on the particle size, magnetite content and magnetic properties for the obtained samples

Samples	Magnetite /polymer ratio	PVA (%)	Stirring rate (rpm)	Particle Size (μm) ± S.D.	Magnetite content[a] (%)	M_s/300K (emu/g)	m_r /300K
m-PCL 1	**0.005**	1	11 000	93.7 ± 8.3	0.59	3.8	0.2849
m-PCL 2	**0.05**			97.4 ± 10.3	4.19	4.2	0.2530
m-PCL 3	**0.10**			107.0 ± 9.2	10.34	4	0.3103
m-PCL 4	**0.15**			134.1 ± 7.5	13.13	4.6	0.3007
m-PCL 5	0.10	**0.5**		112.0 ± 4.8	n.a.	n.a.	
m-PCL 6		**1**		97.2 ± 11.0			
m-PCL 7		**2**		82.6 ± 8.3			
m-PCL 8		1	**11 000**	104.0 ± 5.2			
m-PCL 9			**20 000**	52.1 ± 6.9			
m-PCL 10			**24 000**	4.2 ± 2.1			

[a]Determined by Thermogravimetric analysis (TGA)
M_s: Saturation magnetization
m_r: Magnetic remanence

Table 8.2 NH_2 density (ninhydrin assay) as a function of the conditions employed for surface functionalization of m-PCL microparticles

Samples	Aminolysis time (min)	1,6-hexanediamine (%)	Aminolysis temperature (^oC)	NH_2 density ($X10^{-7}$ mol/mg)
m-PCL	-	-	-	0.007 ± 0.19
NH_2-m-PCL 1	**30**	10	37	5.59 ± 0.43
NH_2-m-PCL 2[a]	**60**	**10**	**37**	6.27 ± 0.33
NH_2-m-PCL 3	**90**	10	37	5.54 ± 0.56
NH_2-m-PCL 4	60	**2**	37	3.69 ± 0.40
NH_2-m-PCL 5	60	**5**	37	4.06 ± 0.27
NH_2-m-PCL 6	60	**20**	37	4.08 ± 0.59
NH_2-m-PCL 7	60	10	**25**	5.84 ± 0.83

[a]NH_2-m-PCL microparticles with the highest amount of NH_2 surface groups, thus selected for BSA adsorption experiments

8.3.4.2 Epoxide groups: cold plasma and epichlorohydrin reaction

Epoxide groups were introduced on the surface of the m-PCL microparticles by using an adapted methodology, earlier proposed by Larson et al. [38] for oxide surfaces of films. The procedure is based on the use of a plasma activation step followed by chemical reaction. Both plasma activation and chemical functionalization were carried out in a radio frequency plasma reactor "PlasmaPrep5" (Gala Instruments, Germany).

Before the experiments, the plasma chamber was thoroughly purged with a continuous flow of the gas (O_2) used during the treatment to reduce trace amounts of air and

moisture. The m-PCL microparticles were exposed to oxygen plasma to activate the surface by peroxy and hydroxyl functional groups. The gas flow (O_2) was adjusted in order to keep a constant pressure of 0.18 mbar inside the chamber. A power of 90 W was applied. The duration of the surface activation was 2 min. Subsequently, vapors of epichlorohydrin (ECH) were introduced inside the chamber (vapor pressure 21.1 ^{o}C at 13.8 mmHg) and allowed to react with the particles for 30 minutes (Figure 8.4).

The epoxy functionalized m-PCL (epoxy-m-PCL) microparticles were then stored under dry controlled conditions, using a vacuum desiccator to preserve their full surface activity.

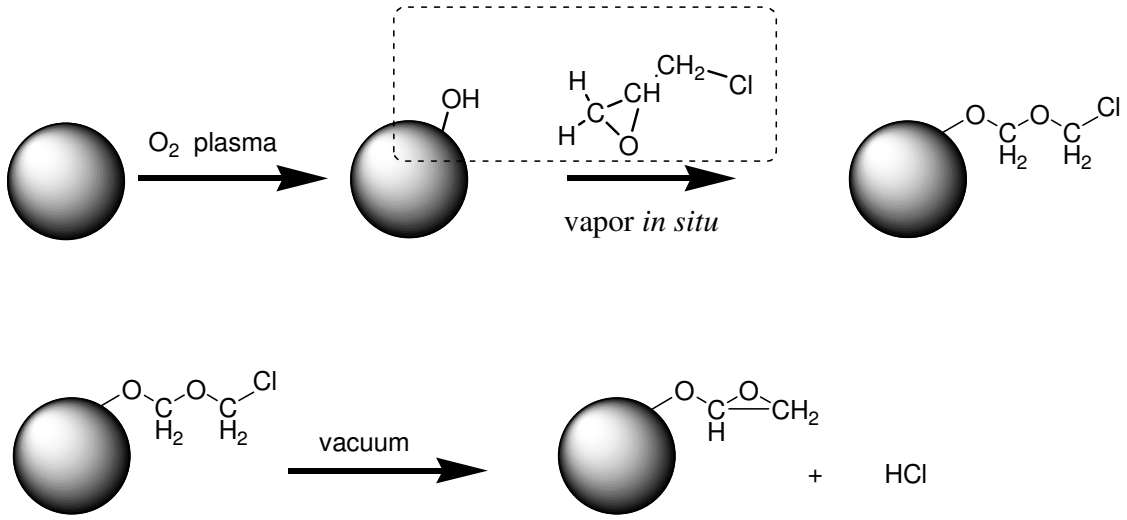

Figure 8.4 Reaction mechanism for epoxy surface functionalization of the core-shell m-PCL microparticles

8.3.5 Physicochemical characterization of magnetite nanoparticles and m-PCL core-shell microparticles

8.3.5.1 Morphological analysis: optical light transmission (OLT) and scanning electron microscopy (SEM)

To investigate the morphology, shape and stability of the magnetite nanoparticles and m-PCL microparticles, a sample suspension (5 mg/mL in distilled water) was mounted onto a glass slide and observed in an optical microscope with polarized light source (Olympus BH2, Japan). The analyzed sample was photographed using a high-resolution Leica camera for image acquisition (Leica Microsystems GmbH, Germany).

m-PCL microparticles were also analyzed by scanning electron microscopy (SEM), in order to characterize the surface morphology, shape and size. Dry m-PCL microparticles were mounted onto metal stubs with a carbon tape and then gold sputter-coated (Sputter Coater

SC502, Fisons Instruments, UK). Images were taken using a scanning electron microscope (Leica Cambridge S-360, UK).

8.3.5.2 Size distribution: standard sieves meshes and dynamic light scattering (DLS)

Particle size and size distribution for the magnetite were analyzed by dynamic light scattering (DLS) (Nano ZS ZEN3600, Malvern Instruments, UK). For the sample preparation, 1 mg of dried magnetite nanoparticles was resuspended in a mixture of glycerol and ultrapure distilled water (1:1, v:v).

The size distribution of the m-PCL microparticles obtained at different experimental conditions was determined through a separation process using series of standard sieves (20, 60, 100, 125, 150, 250 µm: Linker Industrie-Technik GmbH, Germany). Each fraction was weighed out and correlated with the total mass of the analyzed microparticle sample.

8.3.5.3 Fourier transformed infrared spectroscopy (FTIR)

The chemical structure of the obtained particles was analyzed by fourier transformed infrared spectroscopy (FTIR) (IRPrestige-21, Shimadzu, Japan) in the transmission mode. Equal amounts of each sample (magnetite nanoparticles, PCL microparticles, and m-PCL microparticles) were mixed with KBr and then pressed into pellets. Transmission spectra were recorded using 32 scans with 4 cm^{-1} resolution, in the spectral range 4000-600 cm^{-1}.

8.3.5.4 X-ray diffraction analysis (XRD)

The identification of the magnetite into the m-PCL microparticles, as well as the analysis of the obtained magnetite chemical structure was investigated by X-ray diffraction (XRD). X-ray diffraction patterns of magnetite nanoparticles, PCL microparticles (control sample without magnetite content) and m-PCL core-shell microparticles were determined in an X-ray diffractometer (Philips Analytical X'Pert MPD, The Netherlands). The data collection was performed using Cu^{2+} as anode material and monochromator used at a voltage of 40 kV. The samples were analyzed at an angle range (2θ) of 2-60^{o}. Magnetite phases were identified by matching the diffraction peaks to the Joint Committee on Powder Diffraction Standars (JCPDS) files.

8.3.5.5 Thermogravimetric analysis (TGA)

The magnetite content entrapped inside the polymeric shell was determined using a thermogravimetric analyzer (TGA) (Q500, TA Instruments, USA). Dried samples (magnetite nanoparticles, PCL microparticles (without magnetite content) and m-PCL core-shell

microparticles) were analyzed in closed alumina cups in a temperature range 30-700^{o}C. The used heating rate was 10^{o}C/minute. All the experiments were carried out in a nitrogen atmosphere.

8.3.5.6 Superparamagnetic properties: vibrational magnetometry (VSM)

A vibrating sample magnetometer (VSM, LakeShore, USA) was used to study the magnetic properties of the obtained particles. Two different temperatures were used for sample analysis (5 and 300 ^{o}K). The applied magnetic field was varied from 60 000 to −60 000 Oe. Values of saturation magnetization (M_s) and remanence magnetization (M_r) as well as coercive field (H_c) and saturation field (H_s) are reported.

8.3.6 Surface Characterization

8.3.6.1 Detection of amino groups: ninhydrin assay

To confirm and quantify the presence of amine groups on the surface of the functionalized m-PCL microparticles, ninhydrin colorimetric assay was used [27, 39, 40]. Briefly, 10 mg of sample was immersed in 5 mL of 1.0 M solution of ninhydrin in ethanol for 1 minute. The container was then heated at 80 ^{o}C for 5 minutes to accelerate the reaction of the ninhydrin with the amino groups present on the surface of the microparticles. After discarding the suppernatant and allowing the complete evaporation of the ethanol, 5 mL of 1,4-dioxane was added to dissolve the microparticles. After complete dissolution of the sample, 5 mL of isopropanol were added to stabilize the formed blue compound. The sample was filtered to remove the insoluble magnetite material, and the absorbance of the final solution was measured at 570 nm. For quantification purposes, a calibration curve was prepared using solutions of known concentration of 1,6-hexanediamine in a mixture of 1,4-dioxane/ isopropanol (1:1, v:v).

8.3.6.2 X-ray photoelectron spectroscopy (XPS)

X-ray photoelectron spectroscopy (XPS) analysis was performed (ESCALAB 250iXL" spectroscope, VG Scientific, UK) with PISCES software for data acquisition and analysis. XPS measurements were carried out using a monochromatic Al (Kα) radiation (1486.92 eV). Photoelectrons were collected from a take-off angle of 90^{o} relative to the sample surface. The measurement was performed in constant analyzer energy mode (CAE) with 100 eV for survey spectra and 20 eV for high-resolution spectra. Charge referencing was carried out by setting the lower binding energy C 1s photopeak at 285.0 eV. The chemical functional groups identity was obtained from the high-resolution peak analysis of carbon-1s (C1s) and oxygen-1s (O1s).

Overlapping peaks were resolved into their individual components using XPSPEAK 4.1 software. For sample preparation, a suspension of dried microparticles was prepared in ethanol and dripped onto a silicon wafer surface. After the complete ethanol evaporation, the sample was introduced in the XPS pre-chamber for the measurements.

8.3.7 BSA binding experiments

Bovine serum albumin (BSA) was selected as a model protein to study the binding ability of the functionalized m-PCL microparticles. For the NH_2-m-PCL microparticles, a typical carbodiimide (*N*-(3-Dimethylaminopropyl)-*N*'-ethylcarbodiimide hydrochloride, EDC) activation-coupling experiment was carried out [41]. Briefly, 10 mg of dried NH_2-m-PCL microparticles were resuspended in 0.05 M 2-(*N*-morpholino)ethanesulfonic acid (MES) buffer followed by the addition of a freshly prepared EDC solution (40 mg/mL in 0.05 M MES). The suspension was carefully mixed for 15 minutes at room temperature. Subsequently, BSA dissolved in MES buffer was added. The suspension was mixed on an orbital shaker for two different time periods (5 hours and overnight) and at two different temperatures (25 and 37 ^{o}C). After this time, the supernatants were collected to determine protein concentrations. The microparticles were washed and resuspended in MES buffer and stored at 4 ^{o}C for further analysis. When epoxy-m-PCL microparticles were used, the particles were washed in MES buffer and subsequently mixed with BSA solutions, without previous activation of the surface of the microparticles. The experimental procedure was identical to the previously described for NH_2-m-PCL microparticles.

The effect of several experimental parameters on the covalent binding of BSA to the surface functionalized microparticles was studied. The pH was varied in the range of 3.5-7 (MES buffer, 0.05 M). The influence of the ionic strength was investigated by adding different concentrations of NaCl (0.1, 0.5 and 1.5 M) to the buffer solution. In all experiments, BSA concentration in the supernatant was measured at 280 nm in UV spectrophotometer.

To investigate the efficiency of protein covalent binding to the surface groups of the m-PCL functionalized microparticles, the protein-microparticles complexes were immersed in buffer medium containing 1% Tween 20, which removes only the physically coupled (adsorbed) protein [42, 43]. After elution, the released BSA was measured at 280 nm.

8.3.7.1 Confocal laser scanning microscopy (CLSM)

In order to visualize the BSA covalently bound to the surface of functionalized microparticles, confocal laser scanning microscopy (CLSM) (Olympus IX81, Japan) was performed. BSA was labeled with fluorescein isothiocyanate (FITC) prior the binding

experiments [44]. Briefly, FITC solution in DMSO (10 mg/mL) was slowly added to a 10 mg/mL BSA solution in 0.1 M carbonate buffer (pH 9), under moderate and continuous agitation at room temperature. The mixture was allowed to react overnight at 4 ^{o}C in a light protected vessel. The labelled protein solution was then extensively dialysed against PBS buffer (0.01 M, pH 7.4) at 4 ^{o}C and stored as lyophilized powder in a light protected container for further use.

The subsequent binding experiments were carried out following the procedure described above (please see section 8.3.7) using FITC-BSA. After elution of the physically adsorbed FITC-BSA, the labeled protein-microparticles were washed with distilled water, mounted using "Vectashield" mounting medium (Vector Laboratories, USA) and visualized by CLSM.

8.3.8 Cell culture studies in presence of functionalized m-PCL microparticles

Both, a human Osteoblast-like cell line (SaOs-2) obtained from ECACC (UK) and human adipose derived stem cells (ASCs) obtained from the Blood Bank of the upper Austrian Red Cross (Austria) were used in this study. Cells were placed in direct contact with the developed microparticles in order to evaluate their effect on cell viability and cell proliferation. Thus, both cells, SaOs-2 and ASCs, were cultured in 12-well tissue culture plates, at a density of 1 X 10^5 cells/mL having 1.5 mL/well, using Dulbecco's modified Eagle's medium (DMEM; Sigma-Aldrich, USA) supplemented with 10% of heat-inactivated fetal bovine serum (FBS; Biochrom AG, Germany) and 1% of antibiotic/antimycotic solution (Sigma-Aldrich, USA) in a humidified atmosphere with 5% CO_2, at 37 ^{o}C. Twenty-four hours after cell seeding, the cells were approximately 80% confluent. At that time point, the culture medium was replaced by a suspension of the m-PCL microparticles samples to test in DMEM (1 mg/mL). The culture medium was changed every 2 days. In all cases, m-PCL microparticles were sterilized by ethylene oxide (EtO) [45]. After different incubation time (1, 3 and 7 days), the particles were removed by aspiration to perform the further assays.

Cell viability was determined by means of a standard MTS (3-(4,5-dimethylthiazol-2-yl)-5-(3-carboxymethoxyphenyl)-2-(4-sulfophenyl)-2H-tetrazolium) assay [46, 47]. The MTS test was performed according to the manufacturer's instructions (CellTiter 96 One Solution Proliferation Assay Kit, Promega, USA) as well as to previously described protocols [47, 48]. Briefly, the cell monolayer was treated with 200 µL/well of MTS reagent solution (5:1 ratio in serum-free DMEM culture medium without phenol red) and incubated for 3 hours at 37 ^{o}C in a humidified environment containing 5% of CO_2. 100 µL medium from each well were transferred to a 96-well plate and the absorbance at 490 nm was determined (EL 312e Biokinetics microplate reader, BioTek Instruments, USA). The results are normalized to the

positive control (complete DMEM culture medium) for which 100% viability was attributed. The samples were tested in triplicate in three independent assays.

Cell proliferation, after cell contact with the microparticles, was evaluated by quantifying the DNA content using PicoGreen ("dsDNA" quantification kit, Molecular Probes, USA) according to the manufacturer instructions. Before performing the assay, the cell monolayer was carefully washed with PBS buffer (0.01 M, pH 7.4), and then lysed by osmotic and thermal shock. The obtained supernatant was used for DNA analysis. Fluorescence was measured (485 nm excitation and 528 nm emission) in a microplate reader and the DNA amounts calculated according to a standard curve. The samples were tested in triplicate in three independent assays.

Cell morphology was observed by optical microscopy after incubation of ASCs with the microparticles for 3 and 7 days. Each well containing the cell monolayer and the samples was washed with 0.1 M phosphate buffered saline solution and then fixed with 2.5% glutaraldehyde solution in PBS for 30 min at room temperature. This procedure was performed without removing the microparticles from the wells, thus being carefully to avoid the microparticles aspiration. The cells were then stained with 0.4% methylene blue solution in water and examined for microscopic visualization (Axioplan imager Z1, Carl Zeiss, Germany). The analyzed sample was photographed using a high-resolution camera for image acquisition (Leica Microsystems GmbH, Germany).

8.4 RESULTS AND DISCUSSION

Immunomagnetic separation of cells using superparamagnetic particles or beads coated with antibodies against surface antigens has been extensively investigated [8-10, 49]. It has been shown that this procedure is highly efficient for the isolation of several cell types, because the cells immunologically bound to the magnetic particles remain viable and thereafter they can be grown by placing the isolated fraction in suitable culture media.

Particle properties such as size, shape, superparamagnetic behavior and surface functionality determine if they are suitable for immunomagnetic separation.

8.4.1 Preparation of the superparamagnetic m-PCL microparticles

Magnetite (Fe_3O_4) nanoparticles suspension was obtained by adapting a classical co-precipitation method patented by Reimers G. W. et. al [17-19, 35]. Oleic acid was added during the synthesis to provide hydrophobicity and adequate stability to the resulted nanoparticles suspension. The light microscopy images of the obtained magnetite

nanoparticles suspension in water are shown in Figure 8.5 (a) and (b). As can be seen (Figure 8.5 (b)), good suspension stability, defined spherical shapes and narrow size distribution (Figure 8.5 (c)) were achieved for the resulted system. Dynamic light scattering (DLS) measurements showed a mean diameter of 50 nm and a value of polydispersion index (PDI) of 0.210, indicating low polydispersitivity of the obtained nanoparticles.

The obtained magnetite nanoparticles were further entrapped within a poly-ε-caprolactone (PCL) shell to form core-shell microparticles. Particles with spherical shape, smooth surface morphology and particle size in the range 4-135 µm were obtained. Figure 8.6 shows scanning electron microscope (SEM) images of obtained m-PCL microparticles with size 4.2±2.1 µm (Figure 8.6 (c) and (d)) and 52.1±6.9 µm (Figure 8.6 (a) and (b)).

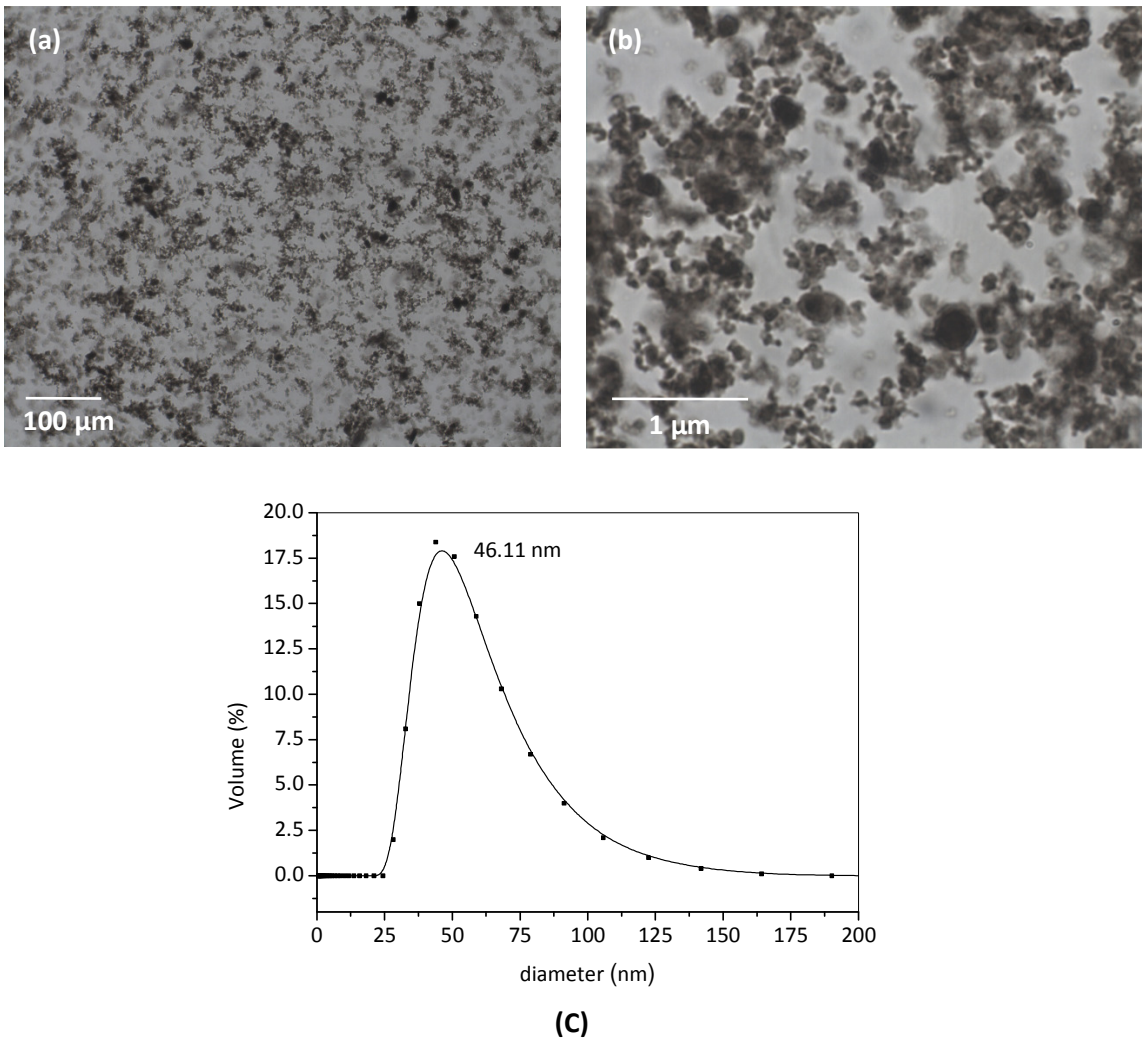

Figure 8.5 Optical micrographs of the synthesized magnetite nanoparticles at different magnifications **(a)** and **(b)**, and their size distribution measured by DLS **(c)** in a mixture water-glycerine (1:1, v:v)

In contrast to the magnetite nanoparticles, the obtained m-PCL microparticles are rather polydisperse with higher value for both, particle size and polydispersion index (PDI) (Figure 8.7). This result was expected because of the different amount of magnetite entrapped inside the microparticles during the encapsulation process. It must be noticed that this process can be controlled by adjusting the experimental conditions and smaller size m-PCL microparticles with narrow size distribution can be obtained (Figure 8.6 (c)).

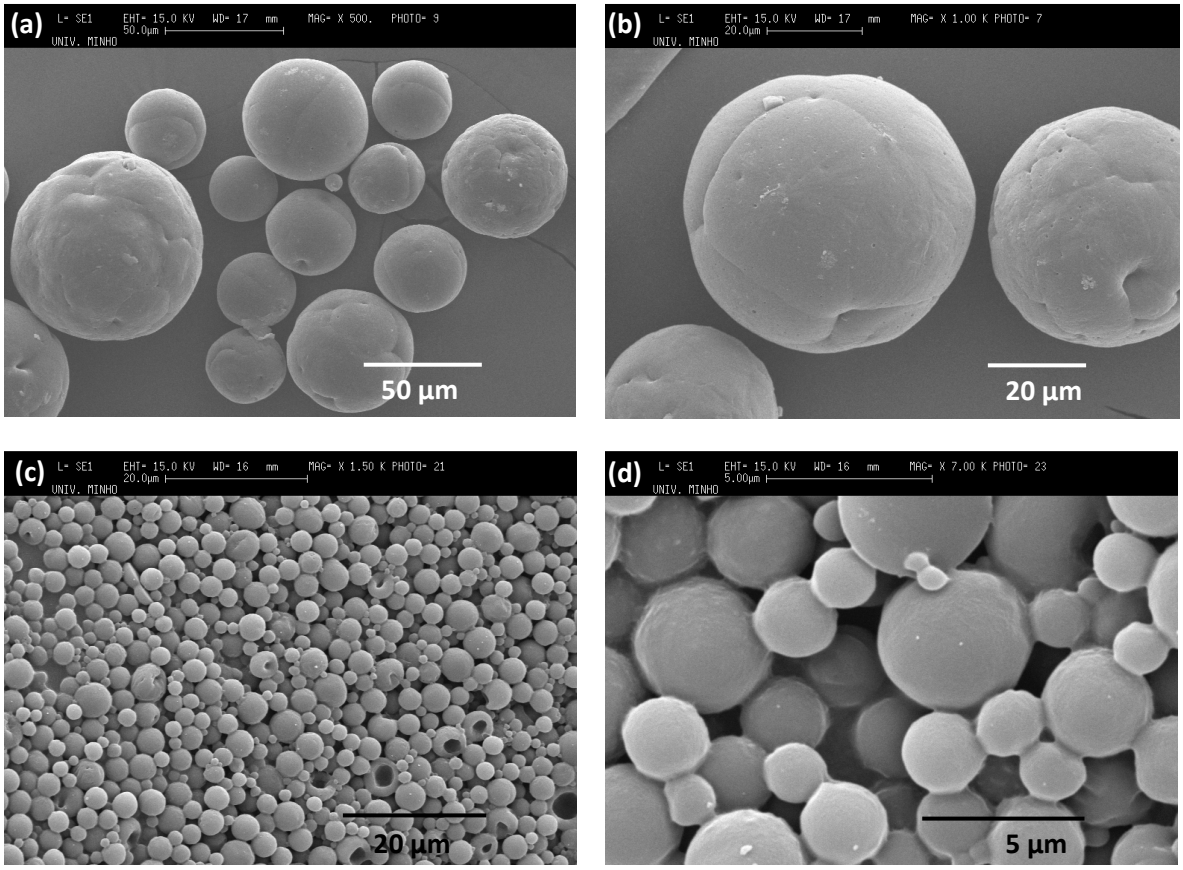

Figure 8.6 SEM micrographs of the magnetic poly-ε-caprolactone (m-PCL) microparticles obtained at different stirring rates. 20 000 rpm **(a)** and **(b)**; 24 000 rpm **(c)** and **(d)**

It is well documented that for applications such as cell isolation, immunomagnetic beads should present adequate particle size [8, 15, 50]. On one hand, particles cannot be excessively small because they can penetrate inside the cells. On the other hand, they cannot be very large because of neglected function. It is reported that the optimal size for cell isolation is about 4 µm [15, 50]. The effect of the experimental conditions on the particle size of the m-PCL microparticles is summarized in Table 8.1. We found that the m-PCL microparticles size and distribution could be controlled by adjusting magnetite to polymer ratio, polyvinyl alcohol (PVA) concentration and stirring rate during their preparation.

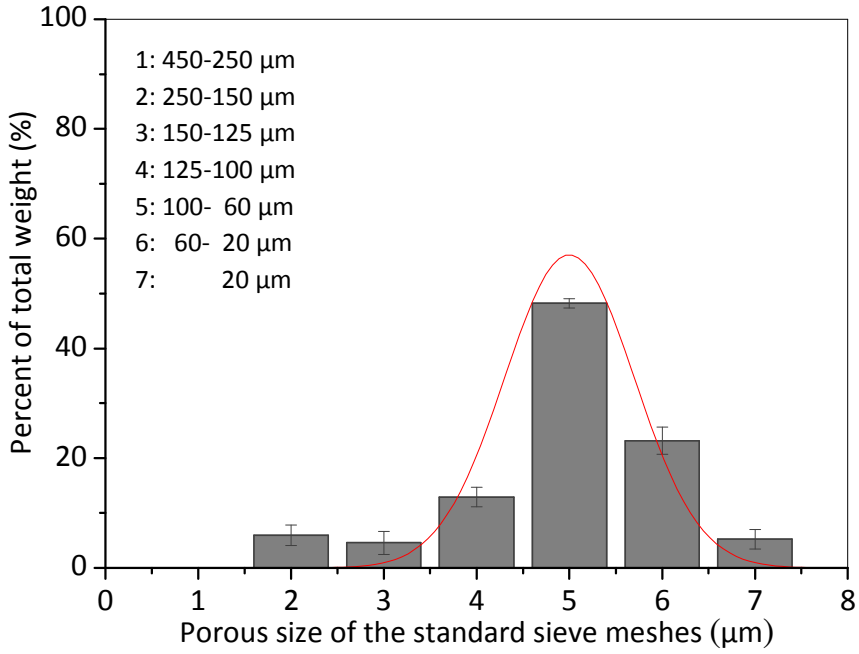

Figure 8.7 Size distribution of the m-PCL microparticles

The magnetite to polymer ratio was varied in the range 0.005-0.15. The increase of the magnetite content resulted in formation of larger and polydispersive particles, but no influence on the surface morphology and spherical shape of the particles was detected. Polyvinyl alcohol (PVA) was used as emulsifier and stabilizer agent during the particle formation. It has been previously reported that for concentrations of PVA higher than 2% the particle morphology is modified and can result in the lost of spherical shape [51]. Therefore, the effect of PVA concentration was also studied by varying its content in the emulsification medium from 0.5 up to 2%. It can be observed (Table 8.1) that the size of the microparticles slightly decreases as the PVA concentration increases, but its effect was not notorious on the particles shape or surface morphology. Hence, PVA concentration up to 2% is suitable for particle preparation by the emulsification method used herein. The stirring rate is the parameter with the more influence on the size of the m-PCL microparticles. The stirring rate of 24 000 rpm resulted in highly monodiserse m-PCL microparticles with a diameter/size of 4.2±2.1 µm (Figure 8.6 (c) and (d)). Once again, it was observed that the stirring rate influences the size and size distribution but not the morphology of the obtained microparticles.

8.4.2 Characterization of the obtained m-PCL microparticles

Fourier transformed infrared (FTIR) spectrum of m-PCL microparticles confirmed the presence of the magnetite entrapped within the PCL shell. The characteristic broad band at 580 cm^{-1} was observed in the spectrum of the synthesized magnetite as well as in the m-PCL microparticles spectrum (Figure 8.8). Characteristic bands of PCL around 1750, 1238, and 1172 cm^{-1}, which corresponds to C=O, asymmetric COC, OC-C and symmetric COC stretchings respectively, are present in both PCL microparticles with and without magnetite.

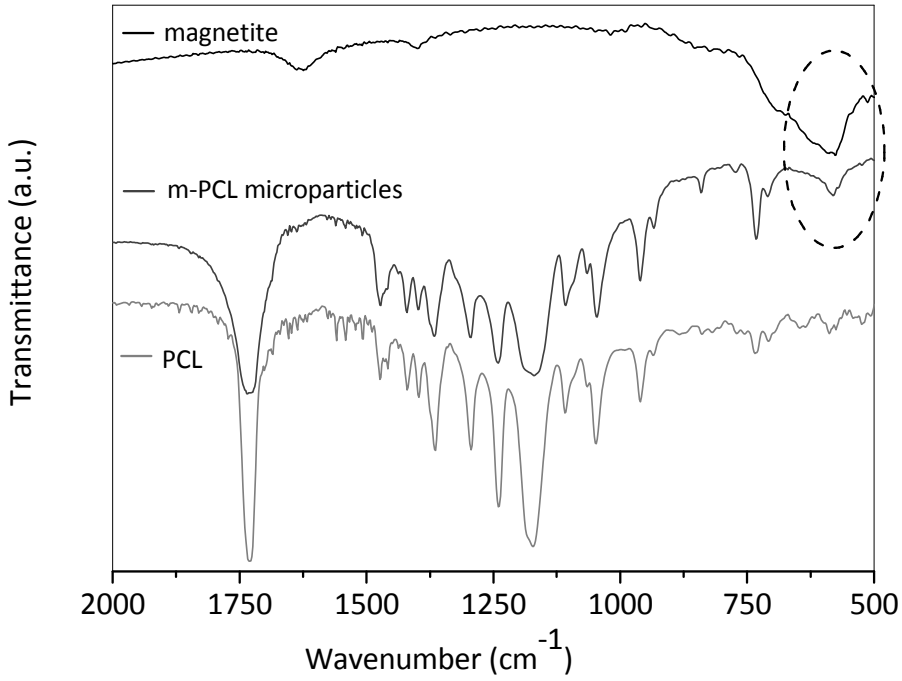

Figure 8.8 FTIR spectra of the obtained magnetic m-PCL microparticles and the respective controls. The characteristic band of magnetite is marked with a circle

To confirm the crystalline structure of the obtained magnetite nanoparticles X-ray diffraction (XRD) was used. XRD patterns obtained for the magnetite nanoparticles and m-PCL microparticles are presented in Figure 8.9. XRD pattern confirmed the magnetite (Fe_3O_4) structure for the nanoparticles (Figure 8.9 (a)) with the detected peaks at 29.94, 35.4, 43.01, 53.4 and 56.96 2theta degree (consistent with the standard data for magnetite JCPDS card 19-0629). The XRD pattern of m-PCL microparticles (Figure 8.9 (b)) shows identical peaks confirming the quite successful entrapment of the magnetite in the PCL shell. Moreover, this result indicates no changes in the magnetite structure during the entrapment process. The

broadening of the peaks observed in the pattern of the m-PCL microparticles is consistent with the composite nature of the microparticles.

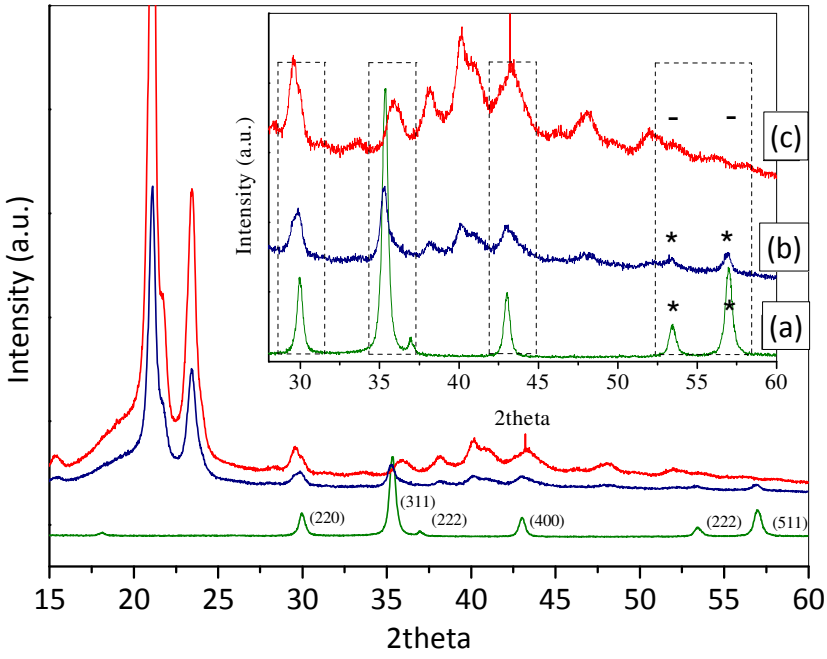

Figure 8.9 X-ray diffractograms for magnetite nanoparticles **(a)**, m-PCL microparticles **(b)** and PCL microparticles **(c)**. The insert graph shows the XRD pattern from 30-60 2theta degree. Characteristics peaks of magnetite phase (JCPDS card 19-0629) (*)

The amount of the magnetite loaded in the m-PCL microparticles was studied by using thermogravimetric analysis (TGA). TGA analyzes were performed under N_2 atmosphere to minimize the mass increase due to iron oxidation but allowing the polymer to decomposed thermally. TGA thermograms (Figure 8.10) obtained for the m-PCL microparticles show a continuous weight loss in the range of 300-400 ^{o}C, which correspond to the decomposition of PCL [52]. The remaining mass after this temperature corresponds to the iron content of the sample. As can be seen, the amount of entrapped magnetite coincides with the initial amount of magnetite (Table 8.1) and the highest magnetite content (13.13%) was obtained for the maximum initial amount of magnetite used for the m-PCL preparation.

The magnetic properties of the obtained m-PCL microparticles are of key importance for their future applications. The magnetic properties, such as saturation magnetization (M_s), relative saturation remanence (m_r=M_r/M_s) and coercivity of remanence (H_c) of the synthesized magnetite nanoparticles and m-PCL microparticles are presented in Table 8.1 and Figure 8.11.

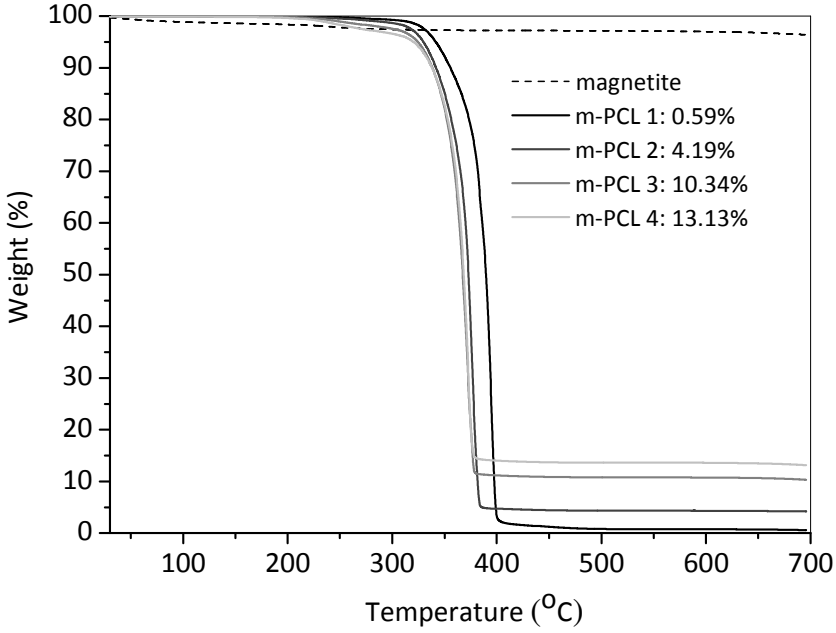

Figure 8.10 TGA thermograms of m-PCL microparticles prepared with different amounts of magnetite

The measurements were performed at room (300 ^{o}K) and at low temperatures (5 ^{o}K) where magnetite presents characteristic magnetic behavior. The obtained magnetite nanoparticles demonstrated superparamagnetic behavior at room temperature with saturation magnetization, M_s=15.7 emu/g (Figure 8.11 (a)). This value of M_s is lower than the reported value for magnetite [53]. This phenomenon has been observed and explained earlier by others authors [17] and can be related with the use of oleic acid (40% related with the amount of produced magnetite) to coat the nanoparticles during their preparation. Lower values were also obtained for m_r (0.0637) indicating a typical superparamagnetic behavior, i.e. absence of magnetic memory of the sample once the applied field is removed. When the temperature was decreased to 5 ^{o}K, the saturation of magnetization increased to values of 51.5 emu/g and the presence of broader hysteresis loop was observed (Figure 8.11 (b): H_c=250 O_e, m_r=0.2544). The increment of the magnetization at low temperature can be related with the correspondent decline of the magnetocrystalline anisotropy. The fact that an incomplete saturation of the magnetization was observed at 5 ^{o}K, can be related with the presence of small grains (due to the nature of the sample), which explain also the gradual increment of M_s value after saturation. Moreover, at lower temperature there are a rearrangement of the Fe^{2+} and Fe^{3+} ions in the unit cell (magnetite crystallizes with spinel structure) with the consequent variation of the configuration of the magnetic moments in the

unit cell. Figure 8.11 (c) presents the magnetization curves of the resulting m-PCL microparticles. A typical superparamagnetic behavior without any hysteresis loop was observed with low values of magnetic remanence, m_r=0.0637. However, the entrapment of the magnetite nanoparticles into the PCL shell resulted in a decrease of the saturation magnetization value to 4 emu/g. The loss of magnetization is due to the fact that the polymer (PCL) has not magnetic properties. Despite the decrease in the magnetization, an excellent isolation of the m-PCL microparticles from the working solution by placing a magnet (external magnetic field) near to the containing vessel was achieved (Figure 8.12). Superparamagnetism was identically observed after removing the external magnetic field.

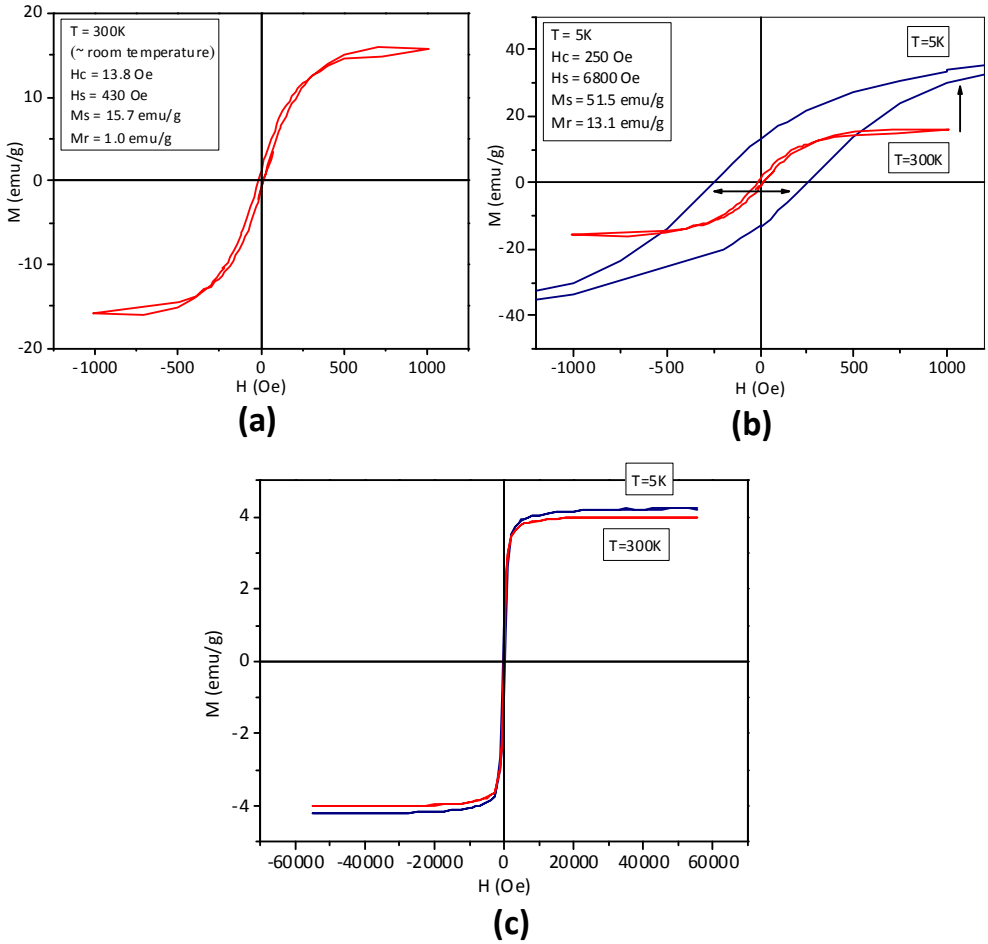

Figure 8.11 Magnetization curves of synthesized magnetite nanoparticles at 300 ^{o}K **(a)**, 5 ^{o}K **(b)** and for the resulting m-PCL microparticles measured at both, 300 and 5 ^{o}K **(c)**

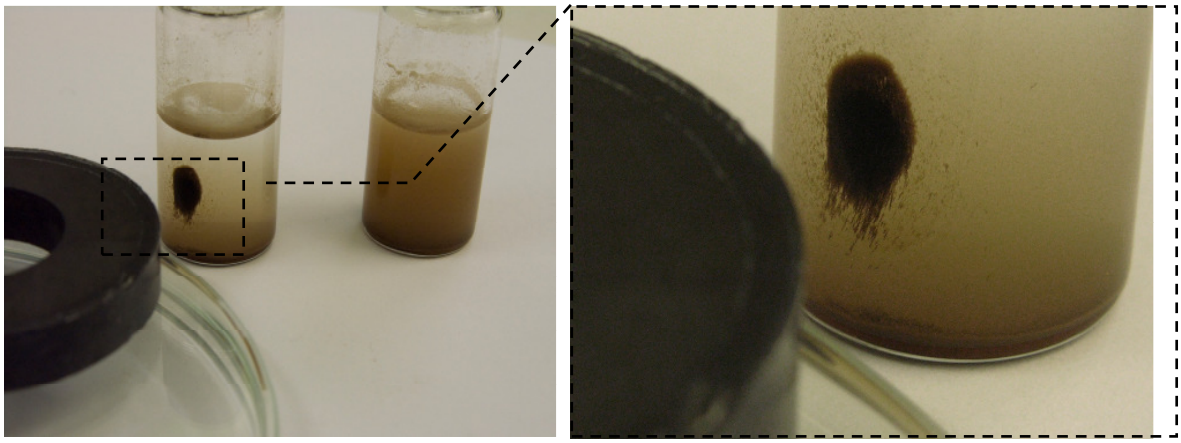

(a) **(b)**

Figure 8.12 Photographs showing the stability of m-PCL microparticles dispersed in water (**(a)**-right vial) and their response to an external magnetic field (**(a)**-left vial and **(b)**)

8.4.3 Surface functionalization of the m-PCL microparticles

The surface of the microparticles were successfully functionalized with amino (through carbodiimide activation) and epoxy groups aiming the covalent binding of protein-like ligands. Amino functionalized m-PCL microparticles were obtained by an aminolysis reaction. Different density of amino groups on the surface (Table 8.2) was achieved by controlling the 1,6-hexanediamine concentration, reaction temperature and time. The quantification of $–NH_2$ groups on the modified m-PCL microparticles (NH_2-m-PCL) was confirmed by a ninhydrin colorimetric assay. The absorbance, determined after functionalization, is significantly higher in comparison with untreated microparticles, clearly confirming the presence of amino groups on the surface. Table 8.2 shows $–NH_2$ density as a function of aminolysis conditions. The amount of $–NH_2$ groups on the m-PCL microparticle surface increases with the aminolysis time and 1,6-hexanediamine concentration. However, for aminolysis time greater than 60 minutes and 1,6-hexanediamine concentration higher than 10%, the density of the $–NH_2$ groups decrease slightly. It was found that the temperature used during the aminolysis reaction does not influence the density of amino groups. The highest density, $5.0\pm0.2 \times 10^{-7}$ mol/mg, was obtained for reaction time of 60 minutes with 10% of 1,6-hexanediamine.

Epoxy functionalized microparticles were analyzed by X-ray photoelectron spectroscopy (XPS). The results from XPS are summarized in Table 8.3. We have observed the presence of Fe in the survey spectra for all the studied materials, evidence of the magnetite entrapped in the m-PCL microparticles and due to the used procedures for the preparation of the microparticles. The detected percentage of Si is due to the silicon wafers which were used as support for the sample preparation. As can be seen from the results, the best coating of the

silicon wafer surface was achieved with the plasma treated sample (only 0.4% Si). Nitrogen was detected only for the $–NH_2$ functionalized m-PCL microparticles, confirming the success of the functionalization. However, XPS results did not show any significant difference between epoxy-modified and unmodified m-PCL microparticles. Previous studies also demonstrated that this technique does not provide clear evidence of the presence of amino and epoxy chemical groups on particles and films surfaces [37, 54]. Hence, additional techniques such as ninhydrin assay, protein adsorption experiments and confocal laser scanning microscopy, were employed in this work for confirmation of both, amino and epoxy functionalization of the m-PCL microparticles.

Table 8.3 Surface chemical composition of functionalized m-PCL microparticles determined by XPS

Sample	%C	%O	%Fe	%N	%Si	%Na
m-PCL	57.4	28.4	0.7	n.d.	12.9	0.7
m-PCL plasma treated	69.1	28.2	0.5	n.d.	1.4	0.7
m-PCL epoxy functionalized	57.8	29.0	0.5	n.d.	10.7	2.1
m-PCL amino functionalized	57.3	27.4	0.7	0.8	13	0.8

8.4.4 Protein coupling experiments onto surface functionalized m-PCL microparticles

Immunomagnetic cell isolation usually involves a series of specific reactions between antigens or antibodies bound onto the surface of the particles, and its correspondent match present in the cells [8]. Hence, antigens (Ag) and antibodies (Ab) can be consider as "intermediate biomolecules" that will define the efficacy of the isolation. Ag or Ab can be covalently bound to the particles surface if there are active sites. Using this approach, a highly stable bioconjugate can be formed, avoiding non-specific attachments and guarantying the proper orientation of the biomolecules on the particles surface. We have performed protein coupling experiments using BSA as a model protein to demonstrate the potential of the developed magnetic microparticles for binding other proteins of interest.

To achieve covalent binding of BSA to the surface functionalized m-PCL microparticles, a carbodiimide coupling procedure was followed in the case of $–NH_2$ functional particles, while direct protein coupling protocol was performed for epoxide activate surface particles. Different conditions in terms of BSA initial concentration, pH, ionic strength and incubation time were studied during the protein adsorption experiments (Figure 8.13).

It must be highlighted that the binding curves in Figure 8.13 correspond to the total amount of BSA coupled onto the surface of different m-PCL microparticles, thus considering both, chemically coupled (covalent bound) BSA and physically coupled (adsorbed) protein.

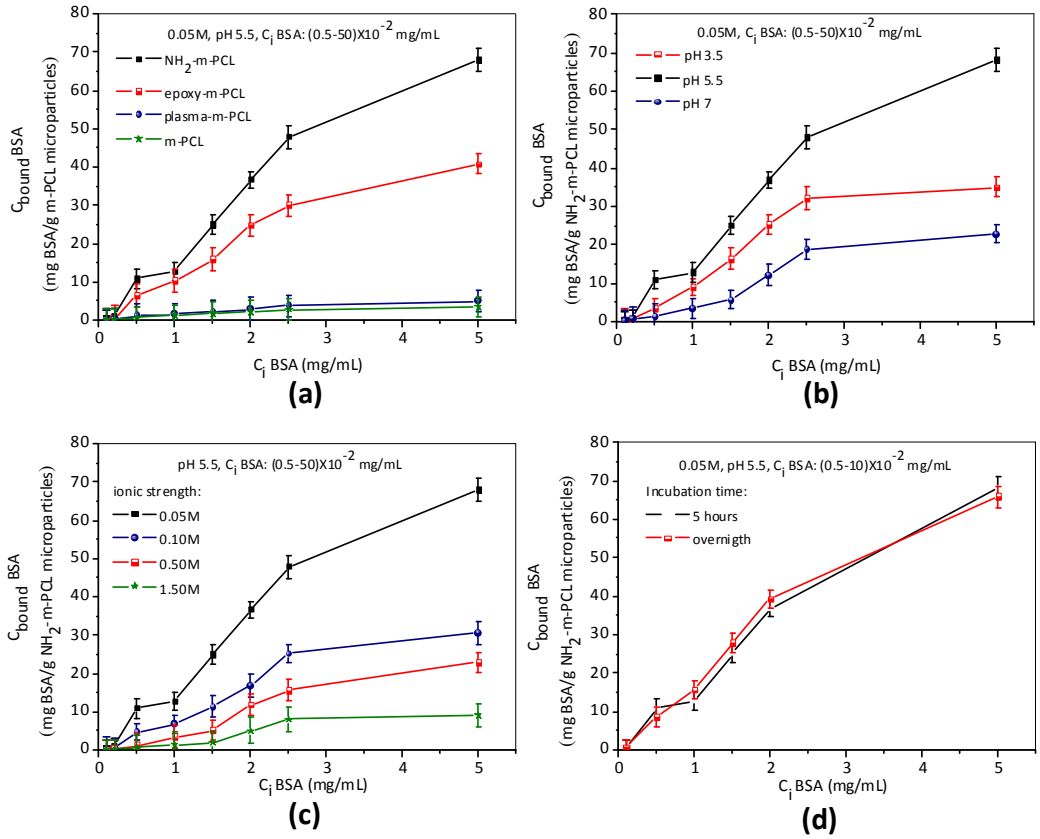

Figure 8.13 BSA binding onto the m-PCL microparticles as a function of surface functionalization **(a)**, pH **(b)**, ionic strength **(c)** and incubation time **(d)**

The introduction of amino or epoxy groups on the surface of the microparticles provide the necessary active sites for immobilization of protein-like molecules via a covalent bond between these groups and the amino/carboxy groups available on protein molecules.

Analysis of the results presented in Figure 8.13 (a) indicates that higher amount of BSA are bound to the surface of both functionalized m-PCL microparticles in comparison with untreated and plasma treated controls. However, highest amount of bound BSA was found when NH_2-m-PCL microparticles (EDC-mediated reaction) were used. This result can be related to a variety of factors. The density of $–NH_2$ and epoxy groups on the surface of the microparticles cannot be compared since a very different chemical processes were used to functionalize and characterize the microparticles surface. For both surface activated microparticles, BSA coupling experiments were carried out at pH 5.5, at which EDC reaction is highly favored. On the contrary, epoxide chemistry is favoured at neutral to alkaline pH. Consequently, BSA bound to NH_2-m-PCL microparticles via EDC is preferential.

Additionally, it can be observed a tendency to achieve a maximum binding plateau by increasing BSA initial amount. Saturation of the surface functional groups by protein molecules

is most probably the reason for this result. Above a certain value of initial protein concentration; there are no more available groups for covalent coupling of additional protein molecules. Consequently, the amount of bound protein remains constant. The observed saturation is directly conditioned by the efficiency of the surface modification and the surface area, thus determining the density of active groups and therefore the amount of coupled protein molecules.

NH_2-m-PCL microparticles were selected to further study the effect of the experimental conditions on the protein coupling.

Figure 8.13 (b) shows the influence of pH on protein binding on NH_2-m-PCL microparticles. The maximum protein binding was obtained at pH 5.5. As previously discussed, pH 5.5 is the optimal one for EDC activity. Consequently, the covalent coupling is highly favored and will control largely the protein binding process. On the other hand, this value is in the range of the isoelectric point (IEP) of BSA (pH 4.7) where the protein carries no net electric charge [41]. Thus at this pH, electrostatic repulsions are minimized since the protein in not charged due to the vicinity to its IEP. By either increasing or decreasing the pH from 5.5, the coupling of BSA to the microparticles surface was drastically diminished.

At lower pH, the amino surface groups are highly protonated (NH_3^+) and therefore not involved in the EDC reaction. Furthermore, at this pH (below BSA IEP) the protein net charge is positive and greater intermolecular repulsion and larger BSA conformational changes occur [55, 56]. The overall result is a decrease on protein binding on the microparticles surface at pH 3.5.

At pH 7 a similar result was observed. The coupling between the microparticles surface and protein molecules drastically diminish. Although it is reported that the EDC-mediated reaction can still take place at pH 7 [41], approaching basic pH this reaction is not favored. Consequently, above pH 7 the covalent coupling of BSA to the microparticles surface via EDC-mediated reaction does not take place.

The effect of ionic strength on protein binding was studied by increasing salt (NaCl) concentration. Figure 8.13 (c) shows the binding isotherms of BSA on NH_2-m-PCL microparticles in MES buffer at pH 5.5 and ionic strength in the range 0.05-1.5 M. A drastic decrease in the bound protein was obtained at higher NaCl concentrations. The interaction between the protein molecules and the ions present in the solutions are most probably the reason for the observed decrease as chloride anions prefer to bind on the surface of the BSA molecules, resulting in changes in the conformation and local charge of the protein macromolecules [57]. These interactions compromise the availability of the protein molecules for the coupling with the microparticle surfaces.

Increasing the incubation time from 5 hours to overnight did not show any significant influence over the amount of bound protein (Figure 8.13 (d)). Therefore, we can state that 5 hours of incubation are enough to allow saturation of the microparticles surface with protein molecules. Similarly, changes of incubation temperature from 25 to 37 ^{o}C resulted in the same amount of bound BSA. This result was expected because temperatures in the studied range do not affect either the EDC chemistry or BSA stability and conformation.

8.4.5 Desorption of the physically adsorbed BSA

Physical adsorption occurs because of the material hydrophobicity and electrostatic interactions between the protein and the material surface [58, 59]. A major problem when working with functionalized surfaces is then to elucidate the amount of chemically (covalent) or physically bound protein. To ensure the separation of these two ways of protein binding, two key methodologies can be followed. Either the protein-particle complex can be treated with buffer solutions containing surfactants or, the surface functional groups that remain free after the protein binding can be quantified.

We have used Tween 20 surfactant to remove the physically adsorbed protein and hence to distinct the covalently bound protein. Table 8.4 summarizes the values of covalent bound protein to both, amino and epoxy functionalized surface. As can be seen, about 70% of the BSA on the amino activated surface was covalently bound. Epoxy superparamagnetic microparticles also show high amount of covalent coupled protein (47%).

Table 8.4 Efficiency of BSA coupling as a result of the surface functionalization

Samples	BSA Totally bound (mg/g)[a]	BSA Covalent coupled (mg/g)	Covalent coupling yield (%)
m-PCL	3.42 ± 2.5	-	-
m-PCL plasma treated	5.00 ± 2.7	-	-
m-PCL epoxy functionalized	40.79 ± 2.6	19.37 ± 3.2	47.49
m-PCL amino functionalized	68.04 ± 3.0	48.92 ± 1.9	71.90

[a]BSA totally bound includes protein physically adsorbed plus covalently coupled

Confocal laser scanning microscopy (CLSM) was used to visualize the covalently coupled BSA (Figure 8.14). Fluorescein isothiocyanate (FITC) labeled BSA was employed during the binding experiments. CLSM results confirmed both: i) successful surface functionalization by the surface treatments proposed in this work (amino and epoxide) and consequently ii) efficient covalent binding of the FITC-BSA onto the microparticles surface. Most intense fluorescence was observed when NH_2-m-PCL microparticles were used. This result again

confirmed a more efficient covalent binding for these microparticles in comparison with the epoxy functionalized ones.

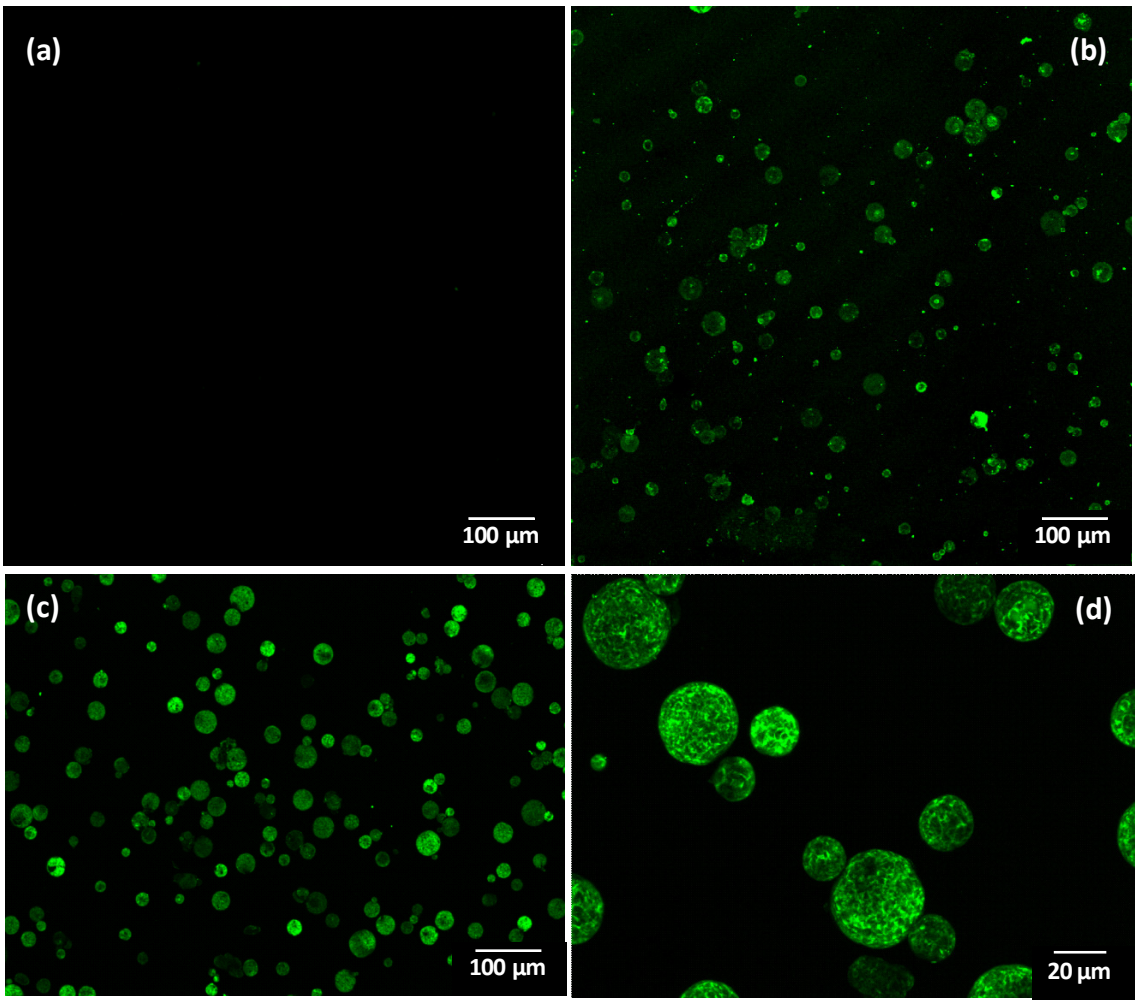

Figure 8.14 Confocal microscopy images of the magnetic microparticles after FITC-BSA covalent coupled at the surface. m-PCL microparticles without binded protein **(a)**, FITC-BSA covalently coupled onto epoxy-m-PCL microparticles **(b)**, NH_2-m-PCL microparticles **(C)** and **(d)**

8.4.6 Cell viability and proliferation as result of the contact with m-PCL microparticles

The effect of the superparamagnetic microparticles on cell viability and proliferation was followed up to 7 days by using MTS and DNA assays respectively. Human Osteoblast-like cells (SaOs-2) were placed in contact with epoxy and amino magnetic microparticles (1 X 10^5 cells/mL). m-PCL and plasma treated m-PCL microparticles were used as controls for evaluation of the effect of functionalization, while DMEM culture medium was used as control for 100% cell viability. Figure 8.15 (a) and (b) represent MTS and DNA results, respectively. Increasing values of O.D. were found with increasing culture time, indicating that none of the tested samples is toxic. The cell viability was found to be above 80% when compared to

positive control (100%) after 7 days of culture. Analysis of DNA results, presented on Figure 8.15 (b), showed no detrimental effect on cell proliferation in the presence of the microparticles. Surface functionalization treatments did no influence the cell viability and proliferation. All the tested samples resulted in very similar values of O.D. and quantified DNA amounts.

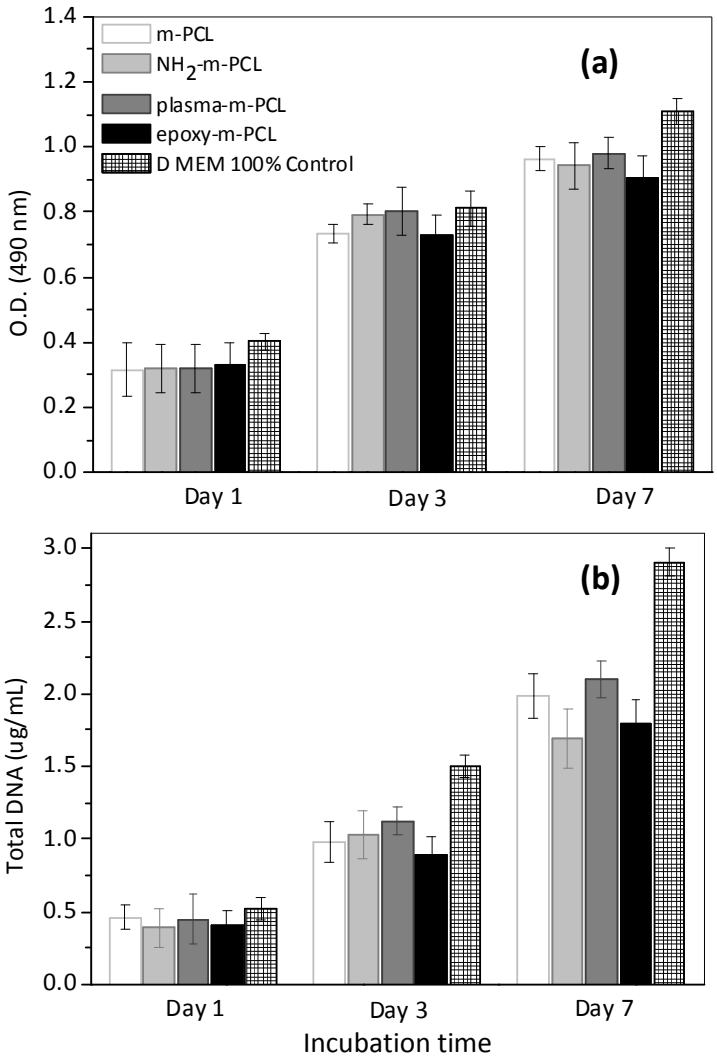

Figure 8.15 Cell viability (MTS) and proliferation (DNA) for osteoblast-like cells (SaOs-2) in direct contact with the studied m-PCL micropaticles after different incubation time

One of the common application of the superparamagnetic microparticles is in the isolation of adipose-derived stem cells (ASCs) [60]. Adipose tissue is very suitable and abundant source of adult stem cells with multipotent properties suitable for tissue engineering and regenerative medicine [60, 61]. Hence, we studied the ASCs response to the presence of

the amino functionalized m-PCL microparticles (Figures 8.16 and 8.17). BSA coupled NH_2-m-PCL microparticles (via EDC activation) was also used for comparison.

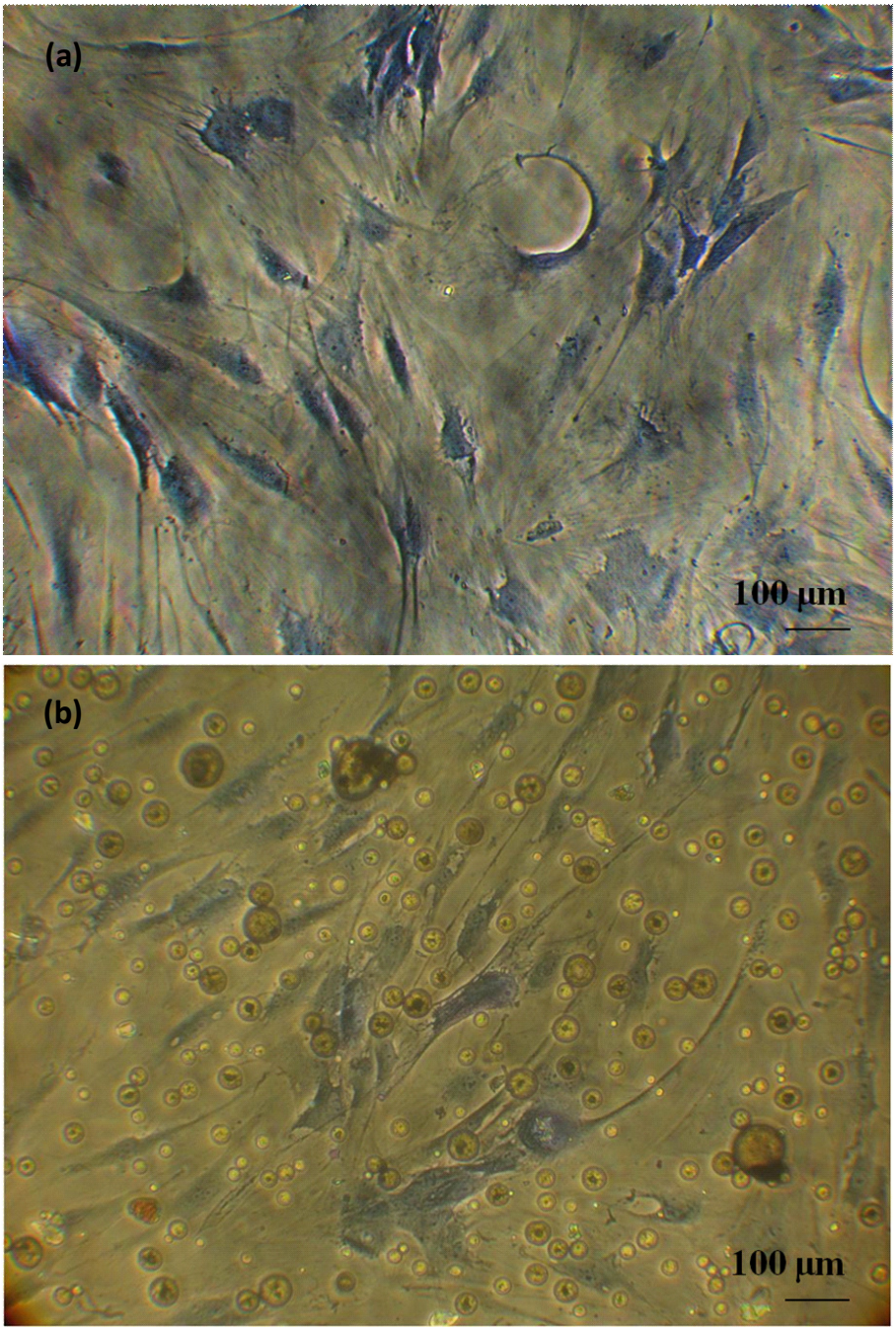

Figure 8.16 Optical micrographs of adipose-derived stem cells (ASCs) in contact with NH_2-m-PCL microparticles (methylene blue staining, 7 days of culture): in DMEM culture medium **(a)** and in direct contact with the NH_2-m-PCL microparticles **(b)**

Characteristic morphology of ASCs was observed when they were cultured in contact with the microparticles (Figure 8.16 (b)) and no morphological changes were identified in comparison with the control (Figure 8.16 (a)). After 7 days of culture, the cells were able to

adhere onto the bottom of the well, spread and proliferate in contact with the magnetic microparticles. The quantification of the DNA indicates good cell proliferation (Figure 8.17). As can be seen, the microparticles did not influence the growth and proliferation of the used cells.

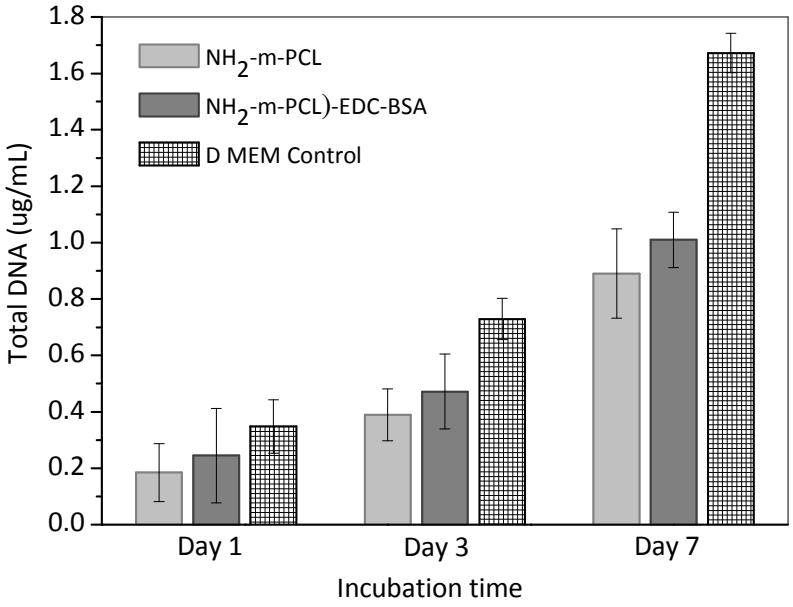

Figure 8.17 DNA assay of ASCs in the presence of the microparticles in comparison with the control

8.5 CONCLUSIONS

Superparamagnetic poly-ε-caprolactone (m-PCL) microparticles were prepared by mixing a magnetite nanoparticle suspension, obtained by co-precipitation from an Fe^{3+}/Fe^{2+} solution, with a poly-ε-caprolactone solution followed by an emulsion solvent extraction/evaporation technique to form core-shell microparticles. m-PCL microparticles presented spherical shape, smooth surface and particle size in the range 4-135 μm. Superparamagnetic behavior was observed for both, magnetite nanoparticles (core-) and m-PCL microparticles (core-shell). Amino groups were successfully introduced onto their surface by aminolysis, whereas epoxy groups were introduced by plasma activation and a vacuum vapor-phase reaction. To ensure the particles' capability for covalent binding of protein-like ligands, bovine serum albumin (BSA) was used as model protein. The high covalent binding capacity for BSA and low physical protein adsorption indicates their capability for covalent binding of protein-like targets. Indeed, that suggests their potential application for isolating cells since this process is mostly based on specific antibody-antigen reactions. From the several experimental parameters investigated on the binding capacity, pH showed the most

pronounced influence. Cell viability, proliferation and morphology were investigated by combining microparticles with osteoblast-like cells (SaOs-2) and human adipose-derived stem cells (ASCs). The developed microparticles presented excellent biocompatibility against both SaOs-2 and ASCs.

8.6 ACKNOWLEDGMENTS

This study was supported by the Marie Curie Host Fellowships for Early Stage Research Training (EST) "Alea Jacta EST" (MEST-CT-2004-008104) for providing E. R. Balmayor and T. Rada a PhD Fellowship and was partially supported by the European NoE EXPERTISSUES (NMP3-CT-2004-500283).

8.7 REFERENCES

1. Bahar, T.; Celebi, S. S. *Journal of Applied Polymer Science* **1999**, 72 (1): 69-73.
2. Gao, X.; Yu, K. M. K.; Tam, K. Y.; Tsang, S. C. *Chemical Communications* **2003**, (24): 2998-2999.
3. Schultz, N.; Metreveli, G.; Franzreb, M.; Frimmel, F. H.; Syldatk, C. *Colloids and Surfaces B-Biointerfaces* **2008**, 66 (1): 39-44.
4. Johnson, A. K.; Zawadzka, A. M.; Deobald, L. A.; Crawford, R. L.; Paszczynski, A. J. *Journal of Nanoparticle Research* **2008**, 10 (6): 1009-1025.
5. Safarik, I.; Safarikova, M. *BioMagnetic Research and Technology* **2004**, 2 (1): 7-24.
6. Franzreb, M.; Siemann-Herzberg, M.; Hobley, T. J.; Thomas, O. R. T. *Applied Microbiology and Biotechnology* **2006**, 70 (5): 505-516.
7. Gu, H. W.; Xu, K. M.; Xu, C. J.; Xu, B. *Chemical Communications* **2006**, (9): 941-949.
8. Safarik, I.; Safarikova, M. *Journal of Chromatography B* **1999**, 722 (1-2): 33-53.
9. Horak, D.; Babic, M.; Mackova, H.; Benes, M. J. *Journal of Separation Science* **2007**, 30 (11): 1751-1772.
10. Gupta, A. K.; Gupta, M. *Biomaterials* **2005**, 26 (18): 3995-4021.
11. Hafeli, U. O. *International Journal of Pharmaceutics* **2004**, 277 (1-2): 19-24.
12. Mornet, S.; Vasseur, S.; Grasset, F.; Duguet, E. *Journal of Materials Chemistry* **2004**, 14 (14): 2161-2175.
13. Schillinger, U.; Brill, T.; Rudolph, C.; Huth, S.; Gersting, S.; Krotz, F.; Hirschberger, J.; Bergemann, C.; Plank, C. *Journal of Magnetism and Magnetic Materials* **2005**, 293 (1): 501-508.
14. Shinkai, M. *Journal of Bioscience and Bioengineering* **2002**, 94 (6): 606-613.
15. Neuberger, T.; Schopf, B.; Hofmann, H.; Hofmann, M.; von Rechenberg, B. *Journal of Magnetism and Magnetic Materials* **2005**, 293 (1): 483-496.
16. Bergemann, C.; Muller-Schulte, D.; Oster, J.; a Brassard, L.; Lubbe, A. S. *Journal of Magnetism and Magnetic Materials* **1999**, 194 (1-3): 45-52.
17. Hamoudeh, M.; Fessi, H. *Journal of Colloid and Interface Science* **2006**, 300 (2): 584-590.
18. Yang, J.; Park, S. B.; Yoon, H. G.; Huh, Y. M.; Haam, S. *International Journal of Pharmaceutics* **2006**, 324 (2): 185-190.

19. Ramirez, L. P.; Landfester, K. *Macromolecular Chemistry and Physics* **2003**, 204 (1): 22-31.
20. Landfester, K.; Ramirez, L. P. *Journal of Physics-Condensed Matter* **2003**, 15 (15): S1345-S1361.
21. Kim, D. H.; Lee, S. H.; Im, K. H.; Kim, K. N.; Kim, K. M.; Shim, I. B.; Lee, M. H.; Lee, Y.-K. *Current Applied Physics* **2006**, 6 (S1): e242–e246.
22. Chen, D. R.; Bei, J. Z.; Wang, S. G. *Polymer Degradation and Stability* **2000**, 67: 455-459.
23. Luong-Van, E.; Grøndahl, L.; Chua, K. N.; Leong, K. W.; Nurcombe, V.; Cool, S. M. *Biomaterials* **2006**, 27: 2042–2050.
24. Pitt, C. G. In *Biodegradable polymers as drug delivery systems*, Chasin, M.; Langer, R., Eds. Marcel Decker: New York, **1990**; pp 71–120.
25. Benoit, M. A.; Baras, B.; Gillard, J. *International Journal of Pharmaceutics* **1999**, 184: 73–84.
26. Nair, L. S.; Laurencin, C. T. *Progress in Polymer Science* **2007**, 32 (8-9): 762–798.
27. Santiago, L. Y.; Nowak, R. W.; Rubin, J. P.; Marra, K. G. *Biomaterials* **2006**, 27 (15): 2962-2969.
28. Carrot, G.; Hilborn, J. G.; Trollss, M.; Hedrick, J. L. *Macromolecules* **1999**, 32: 5264-5269.
29. Sarobe, J.; Molina-Bolivar, J. A.; Forcada, J.; Galisteo, F.; Hidalgo-Alvarez, R. *Macromolecules* **1998**, 31 (13): 4282-4287.
30. Basinska, T. *Macromolecular Bioscience* **2005**, 5 (12): 1145-1168.
31. Forcada, J.; Hidalgo-Alvarez, R. *Current Organic Chemistry* **2005**, 9 (11): 1067-1084.
32. Hong, J.; Gong, P. J.; Xu, D. M.; Dong, L.; Yao, S. D. *Journal of Biotechnology* **2007**, 128 (3): 597-605.
33. Hu, J.; Li, S. J.; Liu, B. L. *Biochemical Engineering Journal* **2005**, 23 (3): 259-263.
34. Duracher, D.; Veyret, R.; Elaissari, A.; Pichot, C. *Polymer International* **2004**, 53 (5): 618-626.
35. Khalafalla, S. E.; Reimers, G. W. Production of magnetic fluids by peptization techniques. US Patent Specification 3843540, **1974**.
36. Lewis, D. H. In *Biodegradable Polymers as Drug Delivery Systems.*, Chasin, M.; Langer, R., Eds. Marcel Dekker, Inc.: New York, **1990**; pp 1-42.
37. Zhu, Y. B.; Gao, C. Y.; Liu, X. Y.; Shen, J. C. *Biomacromolecules* **2002**, 3 (6): 1312-1319.
38. Larson, B. J.; Helgren, J. M.; Manolache, S. O.; Lau, A. Y.; Lagally, M. G.; Denes, F. S. *Biosensors & Bioelectronics* **2005**, 21 (5): 796-801.
39. Moore, S.; Stein, W. H. *The Journal of Biological Chemistry* **1948**, 176 (1): 367-88.
40. Sun, S. W.; Lin, Y. C.; Weng, Y. M.; Chen, M. J. *Journal of Food Composition and Analysis* **2006**, 19 (2-3): 112-117.
41. Hermanson, G. In *Bioconjugate Techniques*, 1st ed.; Academic Press, Inc.: San Diego, CA, **1996**; pp 114-116.
42. Ortega-Vinuesa, J. L.; Bastos-González, D.; Hidalgo-Álvarez, R. *Journal of Colloid and Interface Science* **1995**, 176 (1): 240-247.
43. Peula, J. M.; Hidalgo-Alvarez, R.; Nieves, F. J. D. *Journal of Colloid and Interface Science* **1998**, 201 (2): 132-138.
44. Hungerford, G.; Benesch, J.; Mano, J. F.; Reis, R. L. *Photochemical & Photobiological Sciences* **2007**, 6 (2): 152-158.
45. Reis, R. L.; Mendes, S. C.; Cunha, A. M.; Bevis, M. J. *Polymer International* **1997**, 43 (4): 347-352.
46. Zeltinger, J.; Sherwood, J. K.; Graham, D. A.; Mueller, R.; Griffith, L. G. *Tissue Engineering* **2001**, 7 (5): 557-572.
47. Salgado, A. J.; Coutinho, O. P.; Reis, R. L. *Tissue Engineering* **2004**, 10 (3-4): 465-474.
48. Marques, A. P.; Reis, R. L.; Hunt, J. A. *Biomaterials* **2002**, 23 (6): 1471-1478.

49. Olsvik, O.; Popovic, T.; Skjerve, E.; Cudjoe, K. S.; Hornes, E.; Ugelstad, J.; Uhlen, M. *Clinical Microbiology Reviews* **1994**, 7 (1): 43-54.
50. DynalBiotech: The principle of dynabeads. www.dynalbiotech.com (2008).
51. Balmayor, E. R.; Tuzlakoglu, K.; Azevedo, H. S.; Reis, R. L. *Acta Biomaterialia* **2009**, 5 (4): 1035-1045.
52. Mohamed, A.; Gordon, S. H.; Biresaw, G. *Polymer Degradation and Stability* **2007**, 92 (7): 1177-1185.
53. Yang, T. I.; Brown, R. N. C.; Kempel, L. C.; Kofinas, P. *Journal of Magnetism and Magnetic Materials* **2008**, 320 (21): 2714-2720.
54. Shi, Y. Superparamagnetic nanoparticles for magnetic resonance imaging (MRI) diagnosis. Master of Engineering Science Thesis, The University of Adelaide, SA, Australia, **2006**.
55. Peng, Z. G.; Hidajat, K.; Uddin, M. S. *Colloids and Surfaces B-Biointerfaces* **2004**, 33 (1): 15-21.
56. Li, Y.; Lee, J.; Lal, J.; An, L.; Huang, Q. *Journal of Physical Chemistry B* **2008**, 112 (12): 3797-3806.
57. Su, Y. L.; Li, C. *Reactive & Functional Polymers* **2008**, 68 (1): 161-168.
58. Andrade, J. D. In *Surface and Interfacial Aspects of Biomedical Polymers*, Andrade, J. D., Ed. Plenum Press: New York, **1985**; Vol. 2, pp 1-80.
59. Ortega-Vinuesa, J.; Hidalgo-Álvarez, R. *Biotechnology and Bioengineering* **1995**, 47 (6): 633-639.
60. Park, B. H.; Jung, J. C.; Lee, G. H.; Kim, T. J.; Lee, Y. J.; Kim, J. Y.; Kim, Y. W.; Jeong, J. H.; Chang, Y. M. *Colloids and Surfaces a-Physicochemical and Engineering Aspects* **2008**, 313: 145-149.
61. Rodriguez, A. M.; Elabd, C.; Amri, E. Z.; Ailhaud, G.; Dani, C. *Biochimie* **2005**, 87 (1): 125-128.

Chapter 9

Summary, final remarks and future work

The overall goal of the work presented in this thesis was to develop novel microparticulate materials for the controlled release of bioactive agents for bone repair and regeneration. The materials were characterized and evaluated for their biological response *in vitro*. The preceding chapters described the work that was performed to achieve this goal and this chapter summarizes the significant findings in the experiments presented and describes how the conclusions address the aforementioned hypotheses.

9.1 Summary and final remarks

Nano- and microparticles have been extensively used in biomedical applications mainly as drug delivery systems. These microparticle systems can also be of utility in tissue engineering applications, where they can serve as carriers for the encapsulation and release of growth factors or they can be used to isolate cells from heterogeneous populations [1-4]. Moreover, particles can be combined with hydrogels or scaffolds to modify and improve their mechanical properties [5-9].

It was objective of this dissertation research to develop and characterize new microparticulate systems with potential application in bone tissue engineering. To accomplish this aim, a group of materials was selected with starch being the base material used in the formulation of developed particulate systems. In order to produce the particles, several preparation methods, mainly based on emulsion technology, were used. All the tested procedures generated very stable emulsions, allowing control the drop size and homogeneity by varying reaction conditions (polymeric concentration, composition of emulsification medium, stirring rate, reaction time, type of crosslinker). Several analytical and microscopic techniques were used to characterize the physicochemical properties of the developed microparticles in terms of particle size and size distribution, shape and morphology, porosity, and chemical structure. By changing the reaction parameters, microparticles with different surface morphologies (from smooth to porous), well defined spherical shapes and particle size in the micron-scale (4-900 μm) were obtained. Stirring rate was found to be the most important parameter affecting the particle size, whereas the polymer concentration and emulsification medium showed the largest influence on surface morphology. Thus, the first objective proposed in this thesis was accomplished since particulate systems based on

different materials (starch-poly-ε-caprolactone, SPCL; chitosan-starch, CHT-ST; poly-ε-caprolactone, PCL) and exhibiting diverse properties were successfully prepared.

In order to apply these particulate systems *in vivo*, biodegradability is a desired property. Medical devices with the ability to degrade inside the body have a major advantage since they are designed to perform their function and subsequently degrade without need for surgical removal. Therefore, a subsequent objective of this work was to investigate the biodegradation properties of the developed CHT-ST and SPCL microparticles (Chapter 4 and 6). The PCL microparticles were not considered for degradation studies since they are proposed for cell isolation where material degradation is unlikely to happen. Physiological conditions were mimicked by incubating the materials in phosphate buffered saline (PBS) solution serving as an isotonic solution. To understand the effect of enzymes present in the human blood plasma on the materials degradation, PBS solutions supplemented with α-amylase and/or lipase at physiological concentrations were also used. As a result of incubating the microparticles with these enzymatic solutions, the particle size decreased, the spherical shape was lost and their structure became more porous. Increasing percentages of weight loss and concentration of sugars in solution indicated the progress of the degradation process. The degradation rate was found to be more rapid in the initial 15 days. At the end of the degradation period, about 83% of original weight was lost for SPCL and 67% for CHT-ST. The concentration of reducing sugars released into the solution as result of starch hydrolysis catalyzed by amylase ranged from 10-20 mg/mL for SPCL and CHT-ST. For the SPCL microparticles incubated with lipase, a decrease in pH over time was observed due to the release of carboxylic acids as a consequence of PCL hydrolysis present in the SPCL blend.

Although the biodegradability of the proposed polymeric systems was demonstrated *in vitro*, a major concern related with the *in vivo* use of biodegradable polymers is the possible toxicity of their degradation products. During the course of their degradation, polymeric materials may release toxic products which may compromise their biocompatibility. Hence, the developed microparticles described in this thesis were screened *in vitro* for their possible cytotoxicity using either mouse skeletal myoblast cell line (C2C12) or human osteoblast-like cell line (SaOs-2). In general, the microparticles were found to be non-cytotoxic but in some cases some toxicity was observed when SaOs-2 cells were incubated with extracts from SPCL microparticles. It was postulated that the observed toxicity could be caused by the presence of residual methylene chloride (organic solvent used for the polymer dissolution) which was leached out during the incubation of the microparticles with the cells. To test this hypothesis, the SPCL microparticles were subjected to extensive dialysis to ensure the removal of possible leachable compounds used in their processing. In a subsequent cytotoxicity assay, cell viability

values higher than 80% were obtained for both SaOs-2 (results not shown) and C2C12 cells (Chapter 7). Furthermore, for CHT-ST microparticles comparable results were found. In this case, the crosslinking chemicals used during the particle preparation were found to influence their cytotoxicity. When glutaraldehyde (GA) was used as a crosslinking agent, no more than 55% of cell viability was obtained. This result confirmed the known toxic character of GA and its influence impairing the biocompatibility of its crosslinked products. Different modifications in the microparticle processing, such as reduced concentrations of GA, alternative crosslinking agents (e.g. sodium tripolyphosphate (TPP) and oxidized starch), increased amount of starch and repeatedly washing steps, were investigated to overcome this problem.
In the situations in which toxicity was observed, an extensive washing step is required to reduce toxicity from residual solvents or other chemicals used during the microparticles processing.

Once biodegradability and non-toxicity was demonstrated for the developed particulate systems, the next step in the thesis included testing their potential as carrier of important factors in bone repair strategies. Gentamicin (GTM) a heat-stable antibiotic particularly useful in orthopaedics, was encapsulated in CHT-ST microparticles to be used as an injectable formulation. Dexamethasone (DEX) and bone morphogenetic protein 2 (BMP-2), two known osteogenic agents, were encapsulated into SPCL microparticles. DEX and BMP-2 were individually loaded into the microparticles by direct incorporation in the SPCL matrix.

Subsequently, the capability of the microparticles to act as carriers for those molecules was evaluated by analyzing the loading efficiencies and the release behavior from each carrier system. In addition, the loaded systems were also tested *in vitro* to investigate the activity of released molecules. The activity of released antibiotic was analyzed against bacteria and the osteogenic potential of DEX and BMP-2 encapsulated into SPCL micropartices was assessed using *in vitro* cell differentiation assays.

Encapsulation of GTM into CHT-ST microparticles was achieved with an EE in the range of 55-67%. A burst release was observed followed by a sustained release. Due the hydrophilic nature of CHT-ST matrix and consequent matrix swelling, a significant amount of GTM was released. The drug release mechanism was found to be influenced by a close contribution of both polymer relaxation and drug diffusion, indicating that degradation of the matrix also contributes for controlling the release kinetics. Antibacterial activity of encapsulated GTM was confirmed, since the released antibiotic (up to 30 days) was able to inhibit the growth of *Staphylococcus aureus*. This result indicated that GTM stability and bactericidal properties were clearly not affected by the encapsulation process and release.

Encapsulation efficiencies (EE) of about 93% were obtained for DEX, whereas for BMP-2 only 24% of the protein was encapsulated. This low efficiency obtained for BMP-2 incorporation is related directly with the encapsulation methodology. BMP-2 was co-encapsulated with bovine serum albumin (BSA) as a carrier protein in a ratio 1:20 000, causing a reduced amount of BMP-2 incorporated. However, BSA as carrier protein was indispensable for the preservation of the stability and bioactivity of the growth factor during loading and *in vitro* release. *In vitro* release studies indicated the presence of a burst release for both DEX and BMP-2, mainly during the first 24 hours. This was followed by a slow and steady release, which is typically observed for biodegradable polymers. Released BMP-2 was able to maintain its bioactivity during encapsulation and upon release, as shown by the osteogenic effect in C2C12 cells. Interestingly, the same effect was not observed in the case of DEX. Tested DEX standard solutions and DEX loaded SPCL microparticles were not able to induce osteogenesis in C2C12 cells, as indicated by absence of ALP activity and OCN-promotor activation. On the contrary, DEX loaded SPCL microparticles were capable of inducing osteogenesis in human ASCs, which are primary cells and therefore with more clinical relevance.

This set of experiments and data show that several aims proposed in this thesis were satisfactorily achieved. Starch, in combination with other materials, was processed to obtain non-toxic and biodegradable microparticles with adequate properties for the incorporation and release of a wide group of bioactive agents, including antibiotics, steroids and growth factors.

Besides soluble factors, the use of isolated cells is an essential aspect in tissue regeneration strategies. Therefore, much attention has been given to cell sorting for applications in cell research and therapy. Magnetic cell separation methods are among some of the most efficient methods for bulk cell separation. Although much is now commercially available, the development of new types of magnetic particles and their surface modification are still an area of ongoing research. Magnetic PCL (m-PCL) microparticles were, therefore, developed for cell separation and isolation purposes. Superparamagnetism, uniform and adequate size distribution and functionalized surface are considered the most important characteristics in the design and formulation of microparticles for cell isolation. An optimal superparamagnetic behavior was obtained by the creation of a magnetite nanoparticulate core and a PCL shell. A suitable magnetic response, able to perform particle separation from a solution, was observed by the application of an external magnetic field. Moreover, no significant residual magnetism could be measured when removing the field. Protein binding studies on functionalized m-PCL microparticles using BSA showed high coupling yields with low levels of non-specific adsorption, thus suggesting the successful attachment of antibodies to

microparticle surfaces in isolation experiments. Additionally, the developed magnetic PCL microparticles showed excellent biocompatibility in cell-based assays (cell morphology, viability, and proliferation) using both SaOs-2 and ASCs.

Materials in particulate form have gained increased importance in tissue engineering strategies having into account their enormous potential to deliver within the cellular microenvironment bioactive molecules that are able to regulate cell activities. All of the carrier systems presented in this thesis represent novel forays into the fields of biomaterials, drug delivery and tissue engineering. In the process of developing these systems, an attempt was made to better understand the fundamental aspects of their formulation on their resulting functionality and biocompatibility. The obtained results are promising, since the benefits of delivering bioactive molecules within a carrier material to mediate cellular processes were clearly shown, and can enhance the applicability of delivery systems in tissue engineering applications

9.2 Future work

A number of valuable results were obtained in this research project which will hopefully be of utility in future investigations. The development of an efficient and controlled system for the delivery of BMP-2 and new methods for the surface functionalization of magnetic microparticles used in cell isolation are the most significant contributions of this thesis. Much work remains, however, to be done. The next logical steps may include the following studies:

- To develop bioactive osteoconductive systems by combining the microparticulate systems with bioactive glasses or incorporating functional groups (e.g. silanol groups) to induce the formation of apatite on the surface of the microparticles.

- To optimize the developed starch-based microparticles to be used in dynamic cell culture conditions, using for example the High Aspect Ratio Vessel bioreactor or other appropriate bioreactors.

- To undertake *in vivo* studies to assess the potential of BMP-2 loaded SPCL microparticles to induce new bone formation in critical size defects in animal models.

- To explore the developed systems as carriers in gene delivery therapies using non-viral vectors for bone and cartilage regeneration.

- To finalize the work related with the development of magnetic PCL microparticles, including experiments to prove the efficient isolation of specific cells and hopefully to apply the system as a cell separation method.

9.3 REFERENCES

1. Hoshino, A.; Ohnishi, N.; Yasuhara, M.; Yamamoto, K.; Kondo, A. *Biotechnology Progress* **2007,** 23 (6): 1513-1516.
2. Jing, Y.; Moore, L. R.; Williams, P. S.; Chalmers, J. J.; Farag, S. S.; Bolwell, B.; Zborowski, M. *Biotechnology and Bioengineering* **2007,** 96 (6): 1139-1154.
3. Munoz, N. M.; Leff, A. R. *Nature Protocols* **2006,** 1: 2613-2620.
4. Stuckey, D. J.; Carr, C. A.; Martin-Rendon, E.; Tylera, D. J.; Willmott, C.; Cassidy, P. J.; Hale, S. J. M.; Schneider, J. E.; Tatton, L.; Harding, S. E.; Radda, G. K.; Watt, S.; Clarke, K. *Stem Cells* **2006,** 24 (8): 1968-1975.
5. Schexnailder, P.; Schmidt, G. *Colloid and Polymer Science* **2009,** 287 (1): 1-11.
6. Hoare, T. R.; Kohane, D. S. *Polymer* **2008,** 49 (8): 1993-2007.
7. Agrawal, S. K.; Sanabria-DeLong, N.; Tew, G. N.; Bhatia, S. R. *Langmuir* **2008,** 24 (22): 13148-13154.
8. Malafaya, P. B.; Santos, T. C.; van Griensven, M.; Reis, R. L. *Biomaterials* **2008,** 29 (29): 3914-3926.
9. Malafaya, P. B.; Reis, R. L. *Acta Biomaterialia* **2009,** 5 (2): 644-660.